Advances in Neurosurgery 16

Modern Methods in Neurosurgery

Edited by
W. Walter M. Brandt M. Brock M. Klinger

With 136 Figures and 51 Tables

Springer-Verlag
Berlin Heidelberg New York
London Paris Tokyo

Proceedings of the 38th Annual Meeting of the Deutsche Gesellschaft für Neurochirurgie Münster, May 3–6, 1987

Prof. Dr. Wendelin Walter
Prof. Dr. Mathias Brandt
Neurochirurgische Universitätsklinik
Albert-Schweitzer-Straße 33, D-4400 Münster

Prof. Dr. Margareta Klinger
Neurochirurgische Klinik der Universität Erlangen-Nürnberg
Schwabachanlage 6 (Kopfklinikum), D-8520 Erlangen

Prof. Dr. Mario Brock
Neurochirurgische Klinik und Poliklinik
Universitätsklinikum Steglitz, Freie Universität Berlin
Hindenburgdamm 30, D-1000 Berlin 45

ISBN-13: 978-3-540-18708-0 e-ISBN-13: 978-3-642-73294-2
DOI: 10.1007/978-3-642-73294-2

Library of Congress Cataloging-in-Publication Data. Deutsche Gesellschaft für Neurochirurgie. Tagung (38th: 1987: Münster in Westfalen, Germany) Modern methods in neurosurgery/edited by W. Walter ... [et al.]. p. cm. – (Advances in neurosurgery; 16) "Proceedings of the 38th Annual Meeting of the Deutsche Gesellschaft für Neurochirurgie, Münster, May 3–6, 1987"–T.p. verso. Includes bibliographies and index. ISBN 0-387-18708-1 (U.S.) 1. Nervous system–Surgery–Congresses. 2. Lasers in surgery–Congresses. 3. Magnetic resonance imaging–Congresses. 4. Ultrasonics in surgery–Congresses. 5. Evoked potentials (Electrophysiology)–Congresses. I. Walter, W., 1925- . II. Title. III. Series. [DNLM: 1. Neurosurgery–methods–congresses. W1 AD684N v. 16/WL 368 D4865 1987m] RD593.D47 1987 617'.48–dc 19

2122/3130-543210

List of Contributors*

Albert, F.K. 250
Anagnostopoulos-Schleep, J. 23, 152, 243, 278
Ascher, P.W. 3, 7, 52
Auer, L.M. 52
Bailes, J.E. 20
Baseler, H. 263
Baumann, H. 94
Bennefeld, H. 234
Bien, S. 187
Birg, W. 179
Blanckenberg, P. 44
Bock, W.J. 10, 28, 143, 211, 263
Bockhorn, J. 135
Böcher-Schwarz, H.G. 166
Bongartz, E.B. 39
Brandt, M. 152, 269
Brassel, F. 114, 201
Braun, W. 127
Braunsdorf, W.E. 222
Brock, M. 286
Buchfelder, M. 162
Cedzich, C. 83
Cerullo, L.J. 20
Delank, W. 229
Demirel, T. 127
Dieckmann, G. 130
Diemath, H.E. 241
Dietz, H. 20
Ebhardt, G. 257
Eggert, H. 174
Elger, C.E. 291
Faensen, M. 286
Fahlbusch, R. 83
Fahrendorf, G. 152
Felix, R. 147
Firsching, R. 108, 196
Freiwald, M. 143
Friedburg, H. 179
Friedmann, G. 275
Fritsch, H. 211
Frowein, R.A. 108, 196, 275, 281
Gaab, M.R. 100
Gahlen, D. 143
Gilsbach, J. 57, 67
Grote, E.H. 206
Grüninger, W. 135
Gruß, P. 216
Hansen, K. 156, 183
Harders, A. 57, 57
Heidegger, W. 241
Hense, J. 62
Heppner, F. 3, 52
Herter, Th. 152, 234, 269
Hey, O. 166
Hoch, A. 250
Hoffmann, B. 62
Holzer, P. 52
Hopf, H.C. 94
Huk, W. 162
Iglesias-Rozas, J. 147
Jensen, H.-P. 222
Jungmann, D. 13
Just, M. 166
Kaden, B. 286
Kazner, E. 147
Kern, A. 147
Kiwit, J.C.W. 211
Kleider, A. 94
Knöringer, P. 73
König, H.-J. 23, 152, 243, 278, 291
Köning, W. 275, 281
Kollmann, H.G. 241
Koschorek, F. 222
Krähling, K.H. 23, 243, 278, 291
Kurthen, M. 105
Laborde, G. 67
Lang, G. 98
Laniado, M. 147
Lanksch, W.R. 211
Lindner, R. 216
Linke, D.B. 105
Lins, E. 143, 211

*The address of the senior author is indicated below the relevant contribution heading

Lorenz, M. 100
Maier-Hauff, K. 156, 183
Manicke, Ch. 156
Marguth, F. 211
Mauersberger, W. 201
Mehdorn, H.M. 62
Mewe, R. 23, 291
Michael, T. 156
Milios, E. 179
Mohadjer, M. 57, 179
Mundinger, F. 179
Nanassis, K. 196
Nicola, N. 10
Nistor, R. 162
Nittner, K. 123
Obletter, N. 216
Oldenkott, P. 250
Ott, D. 174
Palmbach, M. 206
Penkert, G. 94
Petersen, D. 206
Pozo, J. 44
Quigley, M.R. 20
Reuter, B.M. 105
Rey, G. 216
Rommel, O. 90
Rommel, Th. 90, 257
Roosen, N. 143, 211, 263
Saad, A. 127
Samii, M. 94
Sander, Th. 31
Sander, U. 44
Sanker, P. 196
Schalow, G. 98
Schirmer, M. 143, 211, 263
Schlegel, W. 243
Schmalohr, B. 105
Schneider, Th. 229
Schober, R. 28, 31
Schönmayr, R. 13
Schörner, W. 147, 156, 183
Schramm, J. 83
Schreiner, S. 263
Schroth, G. 206
Schürmann, K. 166
Schulz, B. 147
Schumacher, M. 174, 187
Seifert, V. 20
Sepehrnia, A. 94
Sigmund, E. 250
Smedema, R. 44
Solymosi, L. 114
Sprung, Ch. 156, 183
Steinmetz, H. 206
Steudel, A. 201
Stork, W. 143, 211
Strauss, C. 83
Szuwart, U. 234, 269
Thun, F. 275
Tronnier, V. 250
Ulrich, F. 10, 28, 31
Volk, B. 187
Walter, W. 269
Wappenschmidt, J. 114
Watanabe, E. 83
Weber, U. 263
Wiese, U.H. 135
Wiesmann, W. 291
Wildförster, U. 229
Wünsche, N. 135
Zanella, F. 196
Zieger, A. 44
Zierski, J. 13

Preface

This 16th volume of *Advances in Neurosurgery* contains a selection of papers presented at the 38th Annual Meeting of the German Society of Neurosurgery, held in Münster on 3-6 May 1987. The program committee had to choose these contributions from a total of 161 presentations. I am very much obliged to the members of the committee who contributed their experience and effort to the organization of the scientific program: Prof. Dr. R.A. Frowein, Prof. Dr. W.J. Bock, Prof. Dr. E. Kazner, Prof. Dr. G. Lausberg, Prof. Dr. M. Klinger, and Prof. Dr. M. Brandt.

The aim of the Meeting was to exchange experiences regarding modern diagnostic and therapeutic achievements. The first main topic was new technical methods in neurosurgery. Refinements in laser technology were introduced; different laser devices have been recognized as useful tools in microsurgery and some peripheral nerve problems. The Cavitron ultrasonic aspirator has proven its value in a great variety of intracranial and spinal tumors within a few years. Its technical advance is impressively demonstrated by some of the papers in this book. With growing experience we have recognized the great value of these additional instruments in limited surgical fields and learned not to overestimate them in the hands of a skilled neurosurgeon.

Intraoperative monitoring by registration of evoked potentials as well as open and transcranial sonographic methods may contribute to safety and increasing perfection of neurosurgical procedures. A number of excellent presentations deal with these subjects. Regarding surgical and monitoring devices, rapidly increasing expense is frequently accompanied by little increase in clinical effectiveness. Some contributors have emphasized this problem and recognized it as a growing challenge to physicians' responsibility.

The second main topic was neurosurgical indications for MRI. Interesting papers document its superiority to conventional neuroradiological methods. The location and extent of lesions may be documented more precisely than by CT scan. Nevertheless, many questions concerning differential diagnosis remain unsolved.

In the final section a large number of remarkable contributions are presented on different aspects of experimental and clinical neurosurgery, such as cerebrovascular disorders, brain perfusion, brain edema, hydrocephalus, histopathology, the role of prostaglandins, the value of interferon and chemotherapy, operative technique, lumbar disc and other spinal disorders, and stereotactic disorders.

On behalf of the organizing committee I would like to thank all those who contributed to the great success of the Meeting in Münster by their

scientific work and discussions. I would like to express my gratitude to Prof. Dr. Margareta Klinger for her outstanding efforts in preparing this publication, and to Springer-Verlag for their excellent cooperation, which has enabled the volume to be presented within a short time.

Wendelin Walter

Contents

Laser

F. Heppner and P.W. Ascher: Eleven Years' Experience with Lasers in Neurosurgery 3
P.W. Ascher: Current Research Projects in Laser Neurosurgery 7
F. Ulrich, W.J. Bock, and N. Nicola: Modified Nd:YAG Laser Operations 10
R. Schönmayr, J. Zierski, and D. Jungmann: Evaluation of Intraoperative Application of Lasers and Cavitron in Neurosurgery 13
J.E. Bailes, V. Seifert, M.R. Quigley, L.J. Cerullo, and H. Dietz: The Development and Future of Microsurgical Tissue Welding with Low-Power CO_2 Laser 20
H.-J. König, K.H. Krähling, J. Anagnostopoulos-Schleep, and R. Mewe: Regeneration of Peripheral Nerves Following Nd: YAG Laser Transection - Experimental Observations 23
F. Ulrich, R. Schober, and W.J. Bock: Laser-Assisted Microanastomoses 28
R. Schober, F. Ulrich, and Th. Sander: A Histological Evaluation of Experimental Nerve Anastomoses with the 1.32-μm Nd:YAG Laser 31

Ultrasound

E.B. Bongartz: Experiences with the Ultrasonic Surgical Aspirator 39
A. Zieger, P. Blanckenberg, J. Pozo, U. Sander, and R. Smedema: Surgical Ultrasonic Aspiration of Brain Tumors 44
L.M. Auer, P. Holzer, P.W. Ascher, and F. Heppner: Ultrasound-Guided Neuroendoscopy 52
J. Gilsbach, A. Harders, and M. Mohadjer: The Microvascular Doppler - An Intraoperative Tool for Aneurysm Surgery 57
H.M. Mehdorn, J. Hense, and B. Hoffmann: Applications of Transcranial Doppler Sonography in Neurosurgery 62
A. Harders, J. Gilsbach, and G. Laborde: New Aspects of Vasospasm Evaluated in 100 Patients with Aneurysm, Subarachnoid Hemorrhage, and Acute Operation: A Transcranial Doppler Study 67
P. Knöringer: Intraoperative Doppler Sonography During Surgery of the Cervical Spine 73

Evoked Potentials

J. Schramm, E. Watanabe, C. Strauss, C. Cedzich, and R. Fahlbusch: Useful Parameters in Intraoperative Monitoring of Evoked Potentials 83
O. Rommel and Th. Rommel: Somatosensory Evoked Potentials of the Trigeminal Nerve Derived Pre- and Intraoperatively in Patients with Trigeminal Neuralgia, from the Point of View of Microvascular Decompression 90
A. Kleider, M. Samii, A. Sepehrnia, H. Baumann, G. Penkert, and H.C. Hopf: Reliable Electrophysiologic Localization of Levels in Cervical Radiculopathy? 94
G. Lang and G. Schalow: Experiences with the Intraoperative Single Unit Potential Recording of Spinal Cord and Cauda Equina Disorders 98
M. Lorenz and M.R. Gaab: Neurophysiological Investigations and ICP Monitoring: An Aid in the Treatment of Head Injury . 100
B.M. Reuter, D.B. Linke, M. Kurthen, and B. Schmalohr: Brain Electrical Activity Mapping (BEAM) of Event-Related Potentials in Coma 105
R. Firsching and R.A. Frowein: The 40-Hz Middle Latency Auditory Evoked Potential in Comatose Patients 108
J. Wappenschmidt, F. Brassel, and L. Solymosi: Interventional Neuroradiology for Neurosurgical Diseases 114

Pain Treatment

K. Nittner: Stimulation of the Sympathetic Trunk Instead of Resection 123
A. Saad, W. Braun, and T. Demirel: Long-Term Results of Facet Denervation 127
G. Dieckmann: Intraventricular Morphine Application by Means of Implanted Pump Systems in Paraneoplastic Pain Syndrome .. 130
U.H. Wiese, W. Grüninger, J. Bockhorn, and N. Wünsche: Intrathecal Administration of Baclofen for Treatment of Spasticity: Neurobiological Principles and First Clinical Results 135

Magnetic Resonance Imaging

N. Roosen, E. Lins, M. Schirmer, M. Freiwald, W. Stork, D. Gahlen, and W.J. Bock: 0.35-T Proton Nuclear Magnetic Resonance Imaging of the Central Nervous System: Clinical Review of 2909 Patients 143
B. Schulz, A. Kern, M. Laniado, W. Schörner, J. Iglesias-Rozas, R. Felix, and E. Kazner: Comparison of CT and MRI, with and without Contrast Enhancement in the Detection of Brain Tumors 147
M. Brandt, J. Anagnostopoulos-Schleep, H.-J. König, G. Fahrendorf, and Th. Herter: Advantages of MRI in the Surgical Strategy for Brain Stem Tumors 152
Ch. Sprung, K. Maier-Hauff, K. Hansen, T. Michael, W. Schörner, and Ch. Manicke: Tumors of the Skull Base and Posterior Fossa in Children - Comparison of CT and MRI 156
W. Huk, M. Buchfelder, and R. Nistor: The Diagnostic Value of CT and MRI in Lesions of the Sella Turcica 162
H.G. Böcher-Schwarz, O. Hey, M. Just, and K. Schürmann: Imaging of Pituitary Tumors in CT and MRT: A Comparative Study 166

D. Ott, M. Schumacher, and H. Eggert: RARE Hydrography as a New Diagnostic Tool with Special Respect to Its Value in Preoperative Examinations 174
M. Mohadjer, W. Birg, H. Friedburg, E. Milios, and F. Mundinger: MRI Stereotaxy for Intracerebral Lesions 179
K. Maier-Hauff, K. Hansen, W. Schörner, and Ch. Sprung: Magnetic Resonance Imaging in Diagnosis and Operative Planning of Cerebrovascular Malformations 183
S. Bien, M. Schumacher, and B. Volk: Neuroradiological and Neuropathological Findings in Intracranial Cavernous Angiomas 187
P. Sanker, R. Firsching, R.A. Frowein, K. Nanassis, and F. Zanella: Clinical, CT, and MRI Findings in Spinal Space-Occupying Lesions 196
W. Mauersberger, F. Brassel, and A. Steudel: Value of Magnetic Resonance Tomography in Diagnosing Intraspinal Space-Occupying Lesions 201
H. Steinmetz, G. Schroth, M. Palmbach, D. Petersen, and E.H. Grote: Magnetic Resonance Imaging in Syringomyelia: Pre- and Postoperative Results 206
J.C.W. Kiwit, W.R. Lanksch, H. Fritsch, E. Lins, W. Stork, N. Roosen, M. Schirmer, W.J. Bock, and F. Marguth: Magnetic Resonance Tomography of Solid Spinal Cord Tumors with Extensive Secondary Syringomyelia 211
P. Gruß, R. Lindner, N. Obletter, and G. Rey: Noninvasive Diagnosis of Lumbosacral Lesions with Special Reference to Magnetic Resonance Tomography 216
W.E. Braunsdorf, F. Koschorek, and H.-P. Jensen: MRI in Complications of Neurosurgical Spine Surgery 222

Computer Tomography

U. Wildförster, Th. Schneider, and W. Delank: Brain Edema - Tumor Quotient in Cranial Computer Tomography as a Preoperative Factor in Histological Prognosis 229
U. Szuwart, H. Bennefeld, and Th. Herter: Ergometric Achievement Tests in Young Hydrocephalus Patients 234

New Research

H.G. Kollmann, W. Heidegger, and H.E. Diemath: Biophysical Differences in Cells of Brain Tumors, Brain Edema, and Normal Glial Tissue 241
J. Anagnostopoulos-Schleep, W. Schlegel, K.H. Krähling, and H.-J. König: Prostaglandin $F_{2\alpha}$ and E_2 as Possible Mediators of Peritumoral Brain Edema 243
F.K. Albert, V. Tronnier, A. Hoch, P. Oldenkott, and E. Sigmund: Interferon-Beta Therapy for Malignant Gliomas (Systemic and Intralesional Administration): First Results of an Ongoing Clinical Study 250
G. Ebhardt and Th. Rommel: Morphological Findings in Malignant Gliomas Before and After Interferon Therapy 257
N. Roosen, S. Schreiner, U. Weber, H. Baseler, M. Schirmer, and W.J. Bock: Electroretinographic Recordings After Intra-arterial Infusion of the Rabbit's Retina with 1,3-bis(2-chloroethyl)-1-nitrosurea (BCNU) Suggesting Retinal Toxicity of BCNU 263
Th. Herter, W. Walter, M. Brandt, and U. Szuwart: Problems of Fibrin Adhesion to Nerves 269

Neurosurgical Operations

R.A. Frowein, W. Köning, G. Friedmann, and F. Thun: Meningioma of the Tentorium 275
K.H. Krähling, J. Anagnostopoulos-Schleep, and H.-J. König: CSF Fistula Occlusion by Ethibloc: Clinical Experiences with 62 Surgically Treated Cases 278
W. Köning and R.A. Frowein: Tumor Growth of Recurrent Meningiomas 281
B. Kaden, M. Faensen, and M. Brock: Transpeduncular Stabilization with the Fixateur Interne in Cases of Spinal Instability 286
R. Mewe, H.-J. König, K.H. Krähling, C.E. Elger, and W. Wiesmann: States of Psychomotor Epilepsy Following Different Kinds of Brain Disease and Trauma 291

Subject Index 295

Laser

Eleven Years' Experience with Lasers in Neurosurgery

F. Heppner and P. W. Ascher

Universitätsklinik für Neurochirurgie der Karl-Franzens-Universität, A-8036 Graz/LKH

On 28 July 1976 HEPPNER removed a cerebral glioma for the first time (1) using a CO_2 laser, after ASCHER had finished extensive biophysical studies into the properties of this new medium (2). This date marks the beginning of laser technique as a routine method in neurosurgery.

By 1 April 1987 we had performed 830 operations with the CO_2 laser, 253 operations with the Nd:YAG laser, and 2 operations with the Ar laser, making a grand total of 1085 operations (Table 1). It could be confirmed that a wavelength of 10.6 µm was best suited for precise incisions, while with a wavelength of 1.06 µm optimal coagulation could be achieved. The power output governing penetration depth and width of the CO_2 laser, especially when superpulsed, can be extremely well controlled, which is imperative when operating within the brain stem (98 times) or on intramedullary spinal tumors (19 times). We have hesitated to use the Nd:YAG laser in these regions, as the low absorption in nervous tissue results in both coagulating and scattering effects, so that its penetration is approximately 10 times that of the CO_2 laser. However, at 1.32 µm the ND:YAG laser's absorption is about 10 times greater than at 1.06 µm, which means more efficient energy conversion to heat in tissue.

Figure 1 shows the effect after a 1-s exposure with 1.32 µm, 12 W power, focused, CW, 200 µm glass fiber. Some scattering effect resembling a halo is visible in the surrounding tissue, separated from the laser-induced lesion by a ring of apparently intact cells. This phenomenon is not clearly understood, but it is obviously due to an inadequate amount of energy. Its electron microscopic appearance is currently under investigation.

These findings, as well as the investigations by FRANK et al. (3), confirm (a) that laser incisions with a wavelength of 1.32 µm can be executed with a precision near to that achieved using a wavelength of 10.6 µm (CO_2 laser) and (b) that the coagulation properties almost equal those with a wavelength of 1.06 µm. As energy emitted at 1.32 µm is only about one-quarter of the emission at a wavelenth of 1.06 µm, it becomes necessary to increase the exposure time to achieve equal cut and coagulation effects on nerve tissue. The high absorption rate of 1.32 µm in Ringer's solution makes it advisable to refrain from the usual irrigation of the operating field.

Trials with the argon laser (4) conducted at our clinic to disobliterate thrombosed carotid arteries, similar to routine operations with the Nd:YAG laser at 1.06 µm conducted by ASCHER on obliterated arteries of the leg, have been most promising.

Advances in Neurosurgery, Vol. 16
Ed. by W. Walter, M. Brandt, M. Brock, and M. Klinger

Table 1. Laser operations carried out at the Universitätsklinik für Neurochirurgie in Graz, Austria, 28 July 1976-1 April 1987

Glioblastomas	243
Astrocytomas	183
Meningiomas	141
Metastases	115
Others	126
Tumors of the pineal gland	10
Adenomas of the pituitary gland	12
Plexus papillomas	4
Medulloblastomas	17
Craniopharyngiomas	6
Acoustic nerve tumors	10
Angiomas and AVMs	28
Ependymomas	33
Tumors of the corpus callosum	1
Others, nonclassified tumors	26
Other intracranial processes	48
Hemorrhagic cysts	18
Arachnoidal cysts	8
Abscesses	8
Tuberculomas	1
Procedures on epileptics	13
Operations on the spinal cord	75
Extramedullary tumors	38
Intramedullary tumors	19
Functional surgery	6
Nucleus pulposus vaporization	12
Operations on peripheral nerves	33
Surgery on the sympathetic nervous system	2
Craniostenosis	7
Operations on vessels	33
Miscellaneous	56
Total number of operations with laser	1085
Operations with CO_2 laser	830
Operations with Nd:YAG laser	253
Operations with the Ar laser	2

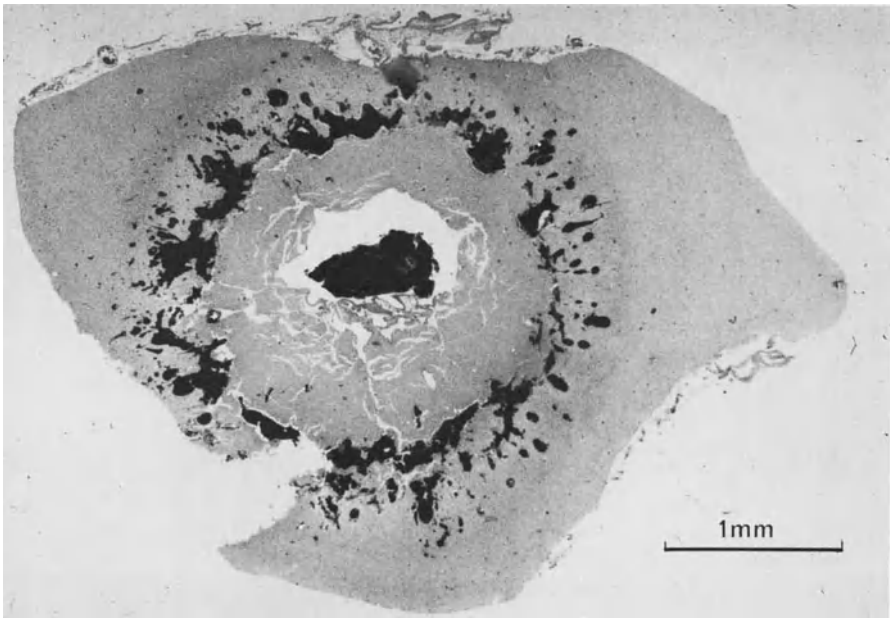

Fig. 1. After a 1-s exposure of the brain tissue with the Nd:YAG laser at a wavelength of 1.32 μm, 12 W power, focused, CW. A scattering effect like a halo is produced, separated from the laser-induced lesion by a ring of apparently intact cells. (x 7)

Cerebral endoscopy opened new fields for the use of the Nd:YAG laser at 1.06 μm, which proved curative in 108 large intracerebral hemorrhages and palliative or diagnostic in 21 deep-seated cystic tumors of the brain. Credit is due to ASCHER, AUER and HOLZER for the development of this method (5). Laser was used to seal the source of bleeding, to remove tissue for biopsy, or to achieve confluence of subdivided cysts. This method, too, has become routine procedure, and is especially successful in spontaneous and traumatic hemorrhages of the cerebellum. In ten patients with a lumbar discopathy, the nucleus pulposus was interstitially coagulated by ASCHER employing an Nd:YAG laser at 1.06 μm. Special clinical criteria and exact radiographic studies were used to determine whether this method was indicated. Hyperhidrosis of the hands, drug-resistant forms of migraine, and postapoplectic thalamic pain can be treated by blockage of the stellate ganglion. If the desired effect is thus obtained, permanency can be achieved by a thoracoscopic preganglionic sympathectomy. Two operations have demonstrated the safe use of the 1.06-μm Nd:YAG laser for this purpose.

Bearing in mind all reports and our own observations, we feel that the following statement is warranted: Good neurosurgery does not necessarily require laser operation, which explains the hesitancy of some neurosurgeons to use the technique. Increasing experience has shown that lasers, dependent on their specific wavelengths, have extended the indications for neurosurgery into areas either hitherto closed, such as the pons and midbrain, or needing improvement, such as the recanalization and anastomosis of blood vessels. For these reasons we feel it is justified that laser surgery was awarded a central position within this

congress. We hope that our observations and discussions will stimulate interest in laser surgery on the central nervous system: an interest indeed richly deserved.

References

1. Heppner F, Ascher PW (1976) Über den Einsatz des Laserstrahls in der Neurochirurgie. Acta Medicotechnica 12:424-426
2. Ascher PW (1977) Der CO_2-Laser in der Neurochirurgie. Molden, Wien
3. Frank F, Beck OS, Hessel S, Keiditsch E (1985) Comparative investigations of the effects of the Nd:YAG laser at 1.06 µ and 1.32 µ in tissue. 6th Congress of the International Society for Laser Surgery and Medicine. Jerusalem, 12-19 October
4. Heppner F (1986) Neurosurgery: the state of the art. Lasers in surgery and medicine 6:415-422
5. Heppner F, Auer LM, Ascher PW, Holzer P (1986) Endoskopische Eingriffe am Gehirn. Acta Chir Austriaca 3/18:70-71 (Kongr. Band)

Current Research Projects in Laser Neurosurgery

P. W. Ascher

Universitätsklinik für Neurochirurgie der Karl-Franzens-Universität, A-8036 Graz/LKH

Introduction

Eleven years ago we introduced first the CO_2 and later the Nd:YAG laser into the neurosurgical treatment of various diseases (1). After initial difficulties, we have performed almost 1100 procedures with the lasers (2, 3). In all these cases, and in our current projects, we used the laser's thermal effect, while other medical specialties are already using its light and pressure effects. Photochemical applications of lasers are also gaining in importance, while as yet we have no experience with their electromagnetic effects.

In contrast to other authors, some of them inexperienced with the laser, I feel that intensive research into applications of the existing lasers will open up enough new possibilities for their use. As long as the potential of the current devices has not been realized, I do not consider the ambitions of some scientists (both physicians and engineers) to develop new lasers for established indications economically justified. Of course, the dye lasers, Excimer laser, and free-electron laser offer interesting possibilities but they are still technically immature, not adapted to medical purposes, and extremely expensive. Better and cheaper versions will soon be at our disposal (e.g., as a by-product of SDI research).

New Applications

Recanalization of the Carotid Artery and Peripheral Vessels

Following a suggestion by CHOY et al. (4, 5), we began in 1985 with the then available argon laser to eradicate arteriosclerotic plaques in the carotid artery. We demonstrated the feasibility of this technique in ten cadavers and three patients. However, this series showed that the argon laser was not the ideal instrument for this purpose. Thus we began a second series using Nd:YAG lasers (1.06 µm, 1.32 µm) in combination with different sapphire tips (different sizes according to the 200- to 600-µg fiber diameter) introduced through a femoral artery catheter. Since the fall of 1986 we have recanalized peripheral arteries with obstructions between 2 and 25 cm long in over 30 patients. In this series only one artery was perforated; one procedure was interrupted because of danger of peripheral circulatory collapse. There were no cases of peripheral embolization and all recanalized vessels are at present still open. Currently, we are improving the angiography catheters and hope then to begin a new series in patients with obstructive disease of the carotid artery.

Advances in Neurosurgery, Vol. 16
Ed. by W. Walter, M. Brandt, M. Brock, and M. Klinger

Vaporization of the Nucleus Pulposus of Protruding Disks

In 1980 we began treating patients with protruding intervertebral disks with chymopapain with the idea of dehydrating the nucleus pulposus. This method - with the proper indication - produced excellent results. However, three reasons kept it from being introduced into clinical routine: (a) the limitation to patients with an intact longitudinal ligament, (b) the theoretical possibility of an anaphylactic reaction to chymopapain, and (c) the cost of the agent, which is not registered in Austria.

A discussion with CHOY (6) led to the idea of reducing the water content of the nucleus by vaporizing it with the laser. Our first series, begun in the spring of 1986, used only the 1.06-μm Nd:YAG laser because only its 200-μm fiber was passable through our 18-G puncture needles. The first 12 patients all spontaneously reported alleviation of their pain symptoms during the procedure (which was done under local anesthesia). Three of these patients remained pain-free, and their neurological symptoms disappeared. The remaining nine had to undergo conventional surgery 3 days to 3 months later because of recurrence of symptoms and persisting protrusion. This is not surprising considering the poor absorption of the Nd:YAG in water and white-colored tissue.

After designing appropriate puncture needles and improving absorption by dying the disk with methylene blue, we are testing the 1.32-μm Nd:YAG laser in a second series of patients. So far, medial protrusions with typical ischiadic symptoms seem ideal indications. However, we feel that the technique will become established only when it can be done with the CO_2 laser.

Sympathectomy in Patients with Hyperhidrosis

Clammy hands are not a serious neurosurgical problem, but for a young person they can be a psychological burden. Thus we began 15 years ago to perform endoscopic transthoracic sympathectomies. Today we use the 1.06-μm Nd:YAG laser with specially designed thoracoscopes to denature and transect the sympathetic cord. The procedure is simple and we have had no complications yet.

Interstitial Thermotherapy of Benign (and, Later, Malignant) Central Tumors

The interstitial irradiation of central tumors is an elegant method to treat benign but absolutely inoperable central tumors. After stereotactic localization, a predetermined amount of radioactive seeds is deposited in the precisely calculated center of the tumor. Naturally, only tumors of firm consistency can be thus approached, because the seeds must remain at the proper location. The irradiation of a thalamic astrocytoma in 1984 with a naked Nd:YAG fiber endoscopically from the ventricle, and a talk with Geza Jako, who told us that the denaturation of tumor protein could be followed by NMR in animal experiments, led us to attempt the denaturation of tumor tissue in patients with inoperable benign central lesions.

Using the Nd:YAG laser with a sapphire tip, we can work in contact with the tumor tissue (interstitially) without overheating of the fiber. The glass fiber itself and the sapphire tip are made of nonmagnetic material. We are constructing stereotactic probes out of carbon fibers and plastics. The laser itself is outside the magnetic

field; its light is transmitted through a 10-m glass fiber. Preliminary results leave us optimistic about the future of this technique.

Conclusion

Despite the widening spectrum of laser applications, we still use only its thermal effect. The laser's light, pressure, photodynamic, and electromagnetic effects promise exciting new vistas in the treatment of neurosurgical diseases.

References

1. Ascher PW (1977) Der CO_2-Laser in der Neurochirurgie, 1st edn. Molden, Wien
2. Ascher PW, Heppner F (1984) CO_2 laser in neurosurgery. Neurosurg Rev 7:123-133
3. Ascher PW (1986) Ten years of laser neurosurgery - a review. In: Joffe SN, Parrish JA, Scott RS (eds) Lasers in medicine, vol 712. SPIE, Washington, pp 228-230
4. Lammer J, Ascher PW, Choy DSJ (1986) Transfemorale Katheter-Laser-Thrombendarteriektomie (TEA) der Arteria carotis. Dtsch Med Wochenschr 111:607-610
5. Choy DSJ, Stertzer SH, Rotterdam HZ, Sharrock N, Kaminow IP (1982) Transluminal laser catheter angioplasty. Am J Cardiol 50:1206
6. Choy DSJ, Ascher PW, Zickel R, Case RB, Kaplan M, Eron L, Di Giacinto G (1987) Percutaneous laser ablation of lumbar disks. Clin Orth Rel Research (to be published)

Modified Nd:YAG Laser Operations

F. Ulrich, W. J. Bock, and N. Nicola

Neurochirurgische Universitätsklinik, Moorenstraße 5, D-4000 Düsseldorf 1

OPMILAS 1.06-μm Nd:YAG Laser Operations

The coagulation and tumor-shrinking properties of the Nd:YAG laser make it a useful tool in the treatment of vascular intracranial tumors, in particular meningiomas. The resection of many tumors, such as base of skull meningiomas, inevitably involves limited access, making precision work with the hand-held laser difficult.

For operations with an extremely narrow access the OPMILAS YAG is helpful in removing small pieces of the tumor without the need to elevate the tumor mass against the normal tissues. No additional safety goggles are needed for the surgeon as long as he looks through the OPMI. It was possible with the OPMILAS YAG to destroy tumor areas in the cranial base with a high degree of precision.

The Nd:YAG laser has proved especially useful for treating highly vascular tumors near the base of the skull, in particular media and lateral sphenoid wing meningiomas, meningiomas infiltrating the olfactory groove or the planum sphenoidale, tumors of the cerebellopontine angle or tentorium, and tumors infiltrating major venous sinuses. In these cases, detachment of the tumor from its bony base as well as the layers of the tentorium can be carried out without difficulty by using a laser power of approximately 20 W in 1-s pulses. Also, using short, intermittent pulses of light focused upon blood vessels, damage to the surrounding tissue is minimized, allowing the Nd:YAG laser to be used safely as an adjunctive measure to achieve hemostasis.

The surgical procedure was always the same. Keeping anatomical structures intact, the tumor capsule was irradiated through a small opening and the tumor excised after shrinkage of the bloodless capsule as already described by BECK et al. (1).

OPMILAS 1.318-μm Nd:YAG Laser Operations

As with other solid-state lasers, the Nd:YAG laser can be made to emit various wavelengths by means of suitable resonator configurations. Following a nonradiating transition from the pumpband, the Nd:YAG laser exhibits transition at 1.06 μm and 1.32 μm, at room temperature, which emits radiation. Because of the short distance to the ground level, the transition at 1.06 μm is considerably more efficient. With the help of dispersion prisms in the resonator or highly selective dielectric resonator mirrors it is possible to suppress the 1.06-μm transition and create optimal conditions for the 1.32-μm transition, so that light of this wavelength is emitted. In the usual clinical

Advances in Neurosurgery, Vol. 16
Ed. by W. Walter, M. Brandt, M. Brock, and M. Klinger

systems the efficiency at 1.06 µm is about 2%, while at 1.32 µm an efficiency of 0.5%-1% can be attained. Using a system designed for a power output of 120 W at a wavelength of 1.06 µm, laser light with a power of about 30 W can therefore be produced at 1.32 µm.

The desired focal diameter of 200 µm can be attained with a 600-µm light conductor and a 1:3 optical system, but the depth of field is very much less and the working distance is reduced to one-third. For this purpose, a special 200-µm focusing light conductor was developed which results in sufficient depth of field at a focal diameter of 200 µm with a 1:1 optical system. However, the maximum output power of the 1.32-µm Nd:YAG laser had to be restricted so that the laser power in the focus was a maximum of 15 W.

By changing the wavelength of the Nd:YAG laser and by also changing the beam geometry, markedly different tissue effects could be achieved.

In an experimental study with the new Nd:YAG laser focused beam irradiation with power values of 12-14 W in 0.1-1 s was applied to the cerebral hemispheres, ischiadic nerves, and carotid arteries of adult rats. Circumscribed lesions of heterogeneous nature with a variable three-dimensional pattern occurred.

The optical instrumentation used for successful aneurysm shrinkage has also been a special micromanipulator, 200-µm fiber, and a 1.32-µm Nd:YAG laser. Although aneurysm clipping is commonly done now, there are aneurysms with a broad base where clipping, wrapping, or coating may not be possible. Laser-assisted aneurysm shrinkage seems to be an effective method for obliterating broad-based aneurysms by application of approximately 12.5 W in 0.1-s pulses. By using these parameters (12.5 W/0.1 s), the 1.32-µm Nd:YAG laser with a 200-µm light conductor also has a good welding effect.

The reaction of the common carotid artery of the rat was tested by irradiation with the 1.32-µm Nd:YAG laser. Transverse and longitudinal slits were made and could be closed by a few exposures of 12.0 W/0.1 s.

In addition it was also possible to carry out laser-assisted vascular and nerve anastomoses with the modified Nd:YAG laser.

Discussion

The use of microsurgical techniques with an operating microscope is now considered the treatment of choice for removing tumors of the base of the skull from surrounding vital structures. These operations inevitably involve an extremely narrow access route. In these circumstances, the OPMILAS YAG micromanipulator is helpful in removing small pieces of the tumor without the need to elevate the tumor mass against the normal tissue. The surgeon can forego the use of the usual goggles by mounting a protective filter on the operating microscope. Blood loss is minimal and shrinkage of the tumour facilitates dissection from vital structures.

In the case of the 1.06-µm wavelength the penetration into brain tissue is essentially dependent on the laser power and less dependent on the exposure time. Macroscopic aspects of brain necroses in 20 rats produced with the modified Nd:YAG laser by application of 8-14 W in 1-3 s were essentially similar to those produced by conventional irradiation. However there appears to be a certain time-depth relation for 1.3-µm laser light, as is typical for the CO_2 laser (1,2).

In could be recognized that the modified Nd:YAG laser can be used as a special coagulative and ablative instrument in the brain. First clinical applications with the new wavelength have shown that it is especially useful for treating tumors near the optic nerve and the brain stem. Moreover, experimental studies have indicated that the modified Nd:YAG laser is useful for tissue welding.

Summary

For operations with an extremely narrow access, an operating microscope adapter - the OPMILAS YAG - is available, even for the 1.06-µm and 1.32-µm Nd:YAG lasers. The high-power Nd:YAG laser has proved especially useful for treating highly vascular meningiomas, as well as hypophysomas and pinealomas. With conversion of the beam geometry, experiments with the modified 1.32-µm Nd:YAG laser have indicated that the OPMILAS YAG is also helpful in the treatment of RG_2 gliomas of adult rats and experimentally produced aneurysms. Moreover, pilot studies have shown that is possible to carry out laser-assisted vascular anastomoses as well as laser-assisted nerve anastomoses using a 1.32-µm Nd:YAG laser.

References

1. Beck OJ, Frank F, Keiditsch E, Wondrazek F (1985) Klinische und experimentelle Untersuchung zur Erweiterung der Nd:YAG Laseranwendung in der Neurochirurgie. Laser in der Medizin und Chirurgie 1:13-18
2. Schober R, Ulrich F, Sander Th, Dürselen R (1986) Laser induced alteration of collagen substructure enables microsurgical tissue welding. Science 232:1421-1422

Evaluation of Intraoperative Application of Lasers and Cavitron in Neurosurgery

R. Schönmayr, J. Zierski, and D. Jungmann

Neurochirurgische Universitätsklinik, Klinikstraße 37, D-6300 Gießen

CO_2 and Nd:YAG lasers and the Cavitron ultrasonic aspirator (CUSA) are regarded as valuable adjuncts in the surgery of intracranial and intraspinal tumors (3-7). Reduction of damage to the surrounding tissue, ability to dissect around delicate adjacent structures, and the possibility of removing the offending mass through a limited exposure are recognized advantages of application of these instruments. Considering the relatively high cost of these devices it seemed justified to review our experience regarding the practice of application, frequency of use, and effectiveness of these advanced technologies in a neurosurgical unit.

Material and Methods

Over a period of 3 years (1.1.1984-1.1.1987) two laser sources (CO_2 lasers, Sharplan 733 and 734; Nd:YAG laser, Medilas) and CUSA were available for all neurosurgical procedures. The surgeons using the devices had had laboratory and operating theater experience with laser prior to this period. The usefulness of the instruments was scored by the surgeon immediately after the operation; they were classified as helpful if they were thought to add to the precision, rapidity, completeness of tumor removal, or hemostasis, even when used only for a short period. In cases where the use of the instrument was abandoned after the first trial it was regarded as not helpful. Site, consistency, and vascularization of the tumor were considered in this assessment.

Results

Out of the total of 4871 neurosurgical procedures, 976 cases were patients with CNS tumors. Lasers and CUSA were used in 472 patients (48%) (Fig. 1). The frequency of application has increased every year, suggesting that with growing experience one is inclined to use the instruments more frequently. In this case the term experience is applied to mean correct indication and timing of application and not manual or technical dexterity.

Eighty-six percent of patients with meningiomas and 98% of patients with cerebellopontine neurinomas were operated using laser and/or CUSA. The devices were much less frequently used for surgery of glial tumors (40%).

CUSA appeared clearly to be the most suitable instrument for surgery of glial tumors. The duration of application of CUSA during operation

Advances in Neurosurgery, Vol. 16
Ed. by W. Walter, M. Brandt, M. Brock, and M. Klinger

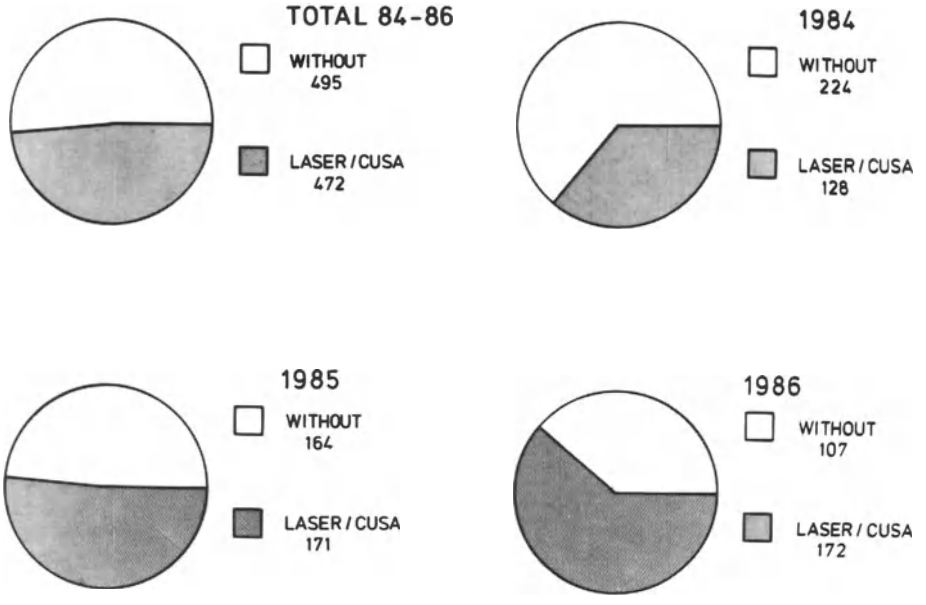

Fig. 1. Laser/CUSA in neurosurgery

ranged from 1 min to 74 min, with an average of 12 min. CO_2 laser was used mainly in surgery of basal tumors (78%), while Nd:YAG laser was used if the mass appeared to be highly vascularized. Combined application of lasers and CUSA was helpful in 32% of cases.

There were no intraoperative complications connected with the use of laser or CUSA. The mortality in the series of patients operated on using this technology was 2.7%. It would be unsound to claim that the morbidity was reduced thanks to use of these instruments as comparisons are not possible.

Discussion and Conclusions

Given permanent availability of laser and CUSA for intracranial and intraspinal tumor operations, the devices were required for 48% of operations. In the total of 4871 operations covering all fields of neurosurgery, the instruments were applied in 9.5% of cases. ASCHER and HEPPNER (1) report that in their 7 years' experience with CO_2 laser surgery they have used it in 6.5% of all neurosurgical procedures and found it indispensable in 15% of cases. BECK (3), who has extensive experience with Nd:YAG laser, used it in approximately 350 cases over a period of 7.5 years.

There is no special "laser neurosurgery" and there are essentially no procedures which could not be performed without these devices. Each of them covers different fields of application: The CO_2 laser is of advantage for debulking "hard", fibrous tumors; CUSA appears to be an excellent instrument for softer ones; and the Nd:YAG laser can be used for coagulation and shrinking of vascularized masses but should not be employed in the immediate vicinity of important structures or in intramedullary surgery. The great majority of neurosurgi-

cal services cannot, of course, acquire all these instruments because of their high price. Thus, some kind of priority should be established. According to our experience the first choice should be the CUSA device, as it will cover the widest range of applications. The choice between the two types of laser is more difficult and at the present stage of commercially available technology it would certainly be false and misleading to recommend to neurosurgeons only one type.

Illustrative Cases

Illustrative cases are shown in Figs. 2-5.

References

1. Ascher PW, Heppner F (1984) Laser in neurosurgery. Neurosurg Rev 7:123-133
2. Bartal AD, Heilbronn YD, Avran J, Razon N (1982) Carbon dioxide laser surgery of basal meningiomas. Surg Neurol 17:90-95
3. Beck OJ (1984) Use of the Nd:YAG-laser in neurosurgery. Neurosurg Rev 7:151-158
4. Edwards MSB, Boggan JE, Fuller TA (1983) The laser in neurological surgery. J Neurosurg 39:555-566
5. Epstein F (1984) The cavitron ultrasonic aspirator in tumor surgery. Clin Neurosurg 31:497-505
6. Fasano VA (1986) Laser neurosurgical techniques. In: Fasano VA (ed) Advanced intraoperative technologies in neurosurgery. Springer, Wien New York, pp 107-139
7. Tew JM Jr, Tobler WD (1984) The laser: history, biophysics and neurosurgical application. Clin Neurosurg 31:506-549

a

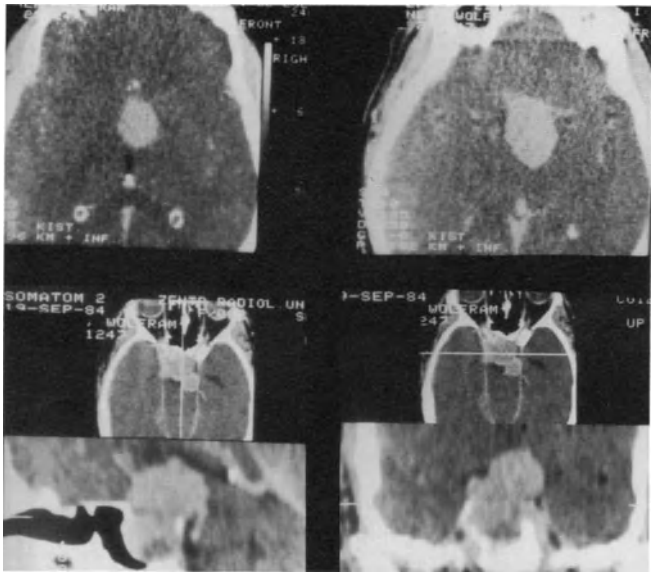

b

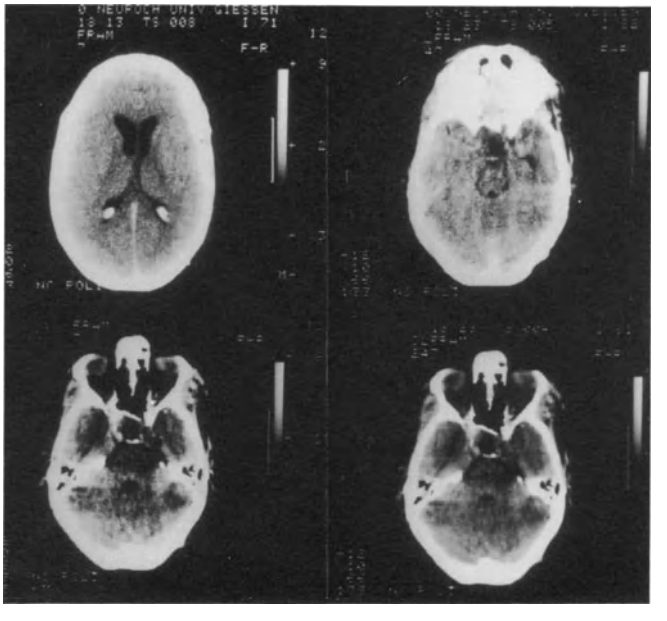

Fig. 2a,b. Giant pituitary adenoma. Supra- and retrosellar extension with compression of the hypothalamus and the upper brain stem.R. pterional approach. CUSA was used to debulk the rostral parts of the tumor. Pulsed low-power CO_2 laser was used to dissect tumor parts and capsule adherent to the hypothalamus. Radical removal was performed with complete preservation of pituitary stalk. CT before (a) and after (b) operation

a

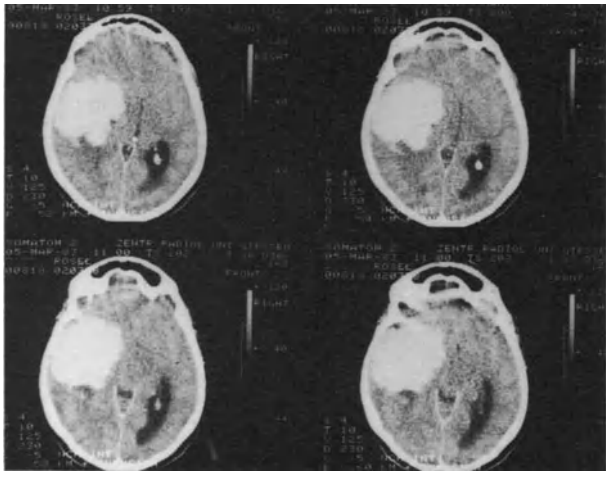

b

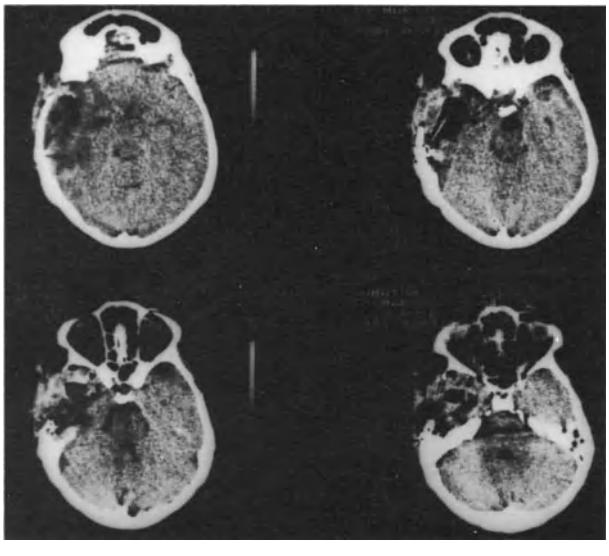

Fig. 3a,b. Malignant parotid tumor. Neck dissection in 1977. Left temporal mass resected in 1983. Two years later there was recurrence with destruction of the skull base; an infratemporal and retropharyngeal extracranial tumor was present with huge intracranial infiltration. The patient's general condition was excellent although there were speech disturbances. Radical resection was performed. Alternating use was made of CUSA and CO_2 laser. CT before (a) and after (b) operation. There was no intracranial recurrence after 2 years

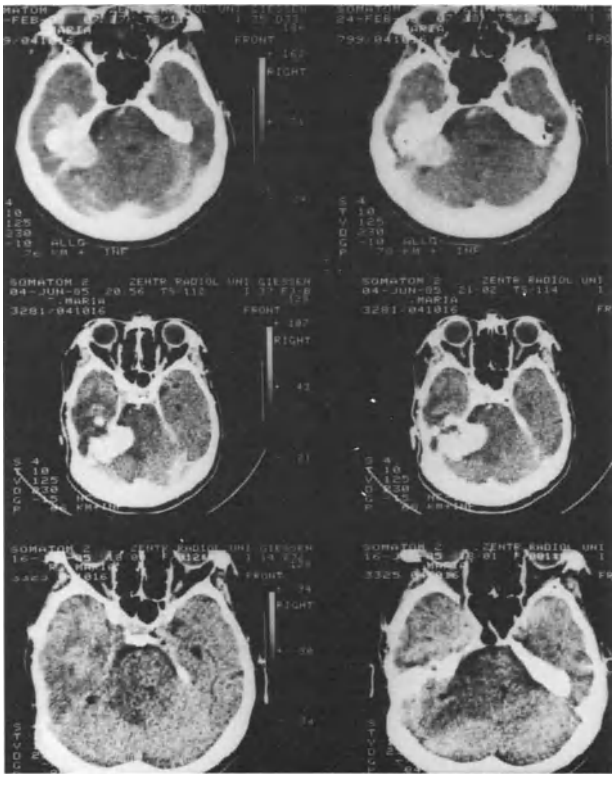

Fig. 4. Petrous ridge meningioma with supra- and infratentorial extension. Radical removal was performed in two stages using Nd:YAG laser. The *bottom row* shows CT scans 2 years after the operation

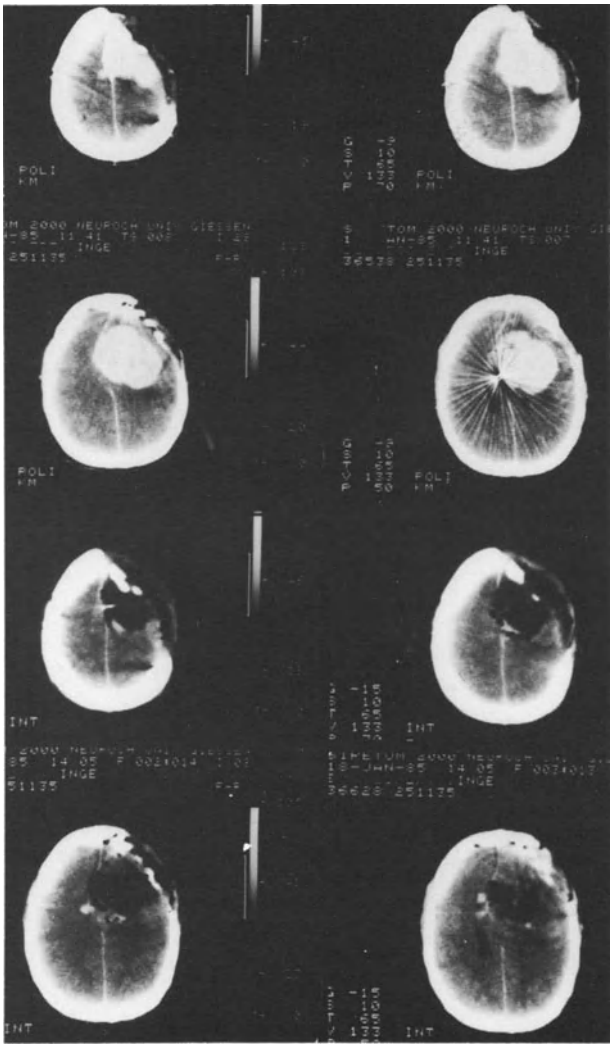

Fig. 5. Recurrent meningioma with involvement of the sagittal sinus. Pre- and postoperative CT scans

The Development and Future of Microsurgical Tissue Welding with Low-Power CO_2 Laser

J. E. Bailes, V. Seifert, M. R. Quigley, L. J. Cerullo, and H. Dietz

Division of Neurosurgery, North-Western University Medical School, Chicago, IL, USA

For some years neurosurgeons have used laser energy for ablative or destructive purposes, and the CO_2 laser has emerged as the workhorse in the removal of central nervous system neoplasms. Recently, investigators have explored the use of CO_2 laser energy for constructive purposes to bond tissues. This technique has become known as "tissue welding."

The first attempt to bond tissues with the laser was with microvascular anastomosis. Jain reported successful coaptation of small arteries using an Nd:YAG source (1). Others experiment with the CO_2 laser because of its desirable properties of low penetration and limited spread in tissue. However, it was not until the milliwatt CO_2 laser was developed that tissue welding became feasible. Because of its low power range (down to 50 mW) and small delivery system (150 µm spot size), accurate application of very small amounts of laser energy was possible through the operating microscope. Neblett was instrumental in the development and preliminary investigations of the use of this laser for bonding different tissues of the nervous system (2).

In our laboratory, we began by performing and analyzing laser-assisted vascular anastomoses (LAVA). We utilized a CO_2 laser (Bioquantum Microsurgical Laser, Bioquantum Technologies, Inc., Houston, Texas, USA) with 60-80 mW continuous mode to perform LAVA in rat femoral and carotid arteries in both end-to-end and end-to-side anastomoses. With considerable practice, it was found that LAVA could be successfully performed with virtually a 100% patency rate in roughly one-third the time that conventional suture anastomoses required (3-5). The animals recovered without ill-effects clinically, and there was no development of delayed thromboses. Histological analysis revealed that the laser caused a transmural thermal change in vessels, with complete vaporization of the tunica adventitia and coagulation necrosis of the tunica media and tunica intima at the zone of impact. The area of tunica media involvement extended approximately 400 µm along the longitudinal extent of the vessel wall, and this layer appeared to constitute the strength of the anastomosis provided by nonspecific bonding after thermally induced denaturation and cooling (6). However, further analysis and follow-up of LAVA specimens revealed a considerable incidence (29.8%) of late aneurysm formation in these vessels. This was deemed as resulting from a failure to fully reconstitute a healthy tunica media with an intact internal elastic lamina in the arteries postoperatively (7). This phenomenon was observed by other investigators using both CO_2 (8) and argon sources (9). Whether this problem is technically surmountable remains to be seen, as it has not been found by all observers (10, 11). More than being related to the number and position of stay sutures, it may be in some degree a func-

Advances in Neurosurgery, Vol. 16
Ed. by W. Walter, M. Brandt, M. Brock, and M. Klinger

tion of the amount of tension on the anastomotic site. Regardless of the etiology of aneurysm formation, it has limited the clinical applicability of this technique until the problem can be overcome. QUIGLEY et al. have utilized this phenomenon to create a modified technique for the production of a new and effective aneurysm model (12).

After extensive work with vascular anastomoses, we attempted to repair peripheral nerves with the CO_2 laser. In preliminary work in adult rats, both end-to-end repairs and interposition grafts were performed in sciatic nerves. Sutureless anastomosis of peripheral nerves was possible using 80-100 mW in continuous mode. In morphological analysis, the laser-anastomosed nerves appeared to have better regeneration than conventional suture anastomoses. Electrophysiological studies showed that laser repairs caused no detrimental effect upon fiber conduction (13). Similar work was undertaken utilizing primates, and the early results were encouraging in laser-anastomosed nerves.

The use of laser to bond nerves may be beneficial in that it creates a complete tissue seal at the repair site. This sealing may prevent escape of sprouting axons, thus improving the orientation of fibers into the endoneurial tubules of the distal nerve segment. The sealing effect may also be beneficial in preventing the ingrowth of fibrous scar tissue from the region surrounding the anastomotic site. Perhaps most importantly, a complete seal, which is "watertight," may provide a more homeostatic local microenvironment that is biochemically favorable for nerve regeneration. In addition to these effects, laser nerve anastomosis prevents the suture foreign body reaction and scar formation which is detrimental to nerve regeneration. Almquist has performed nerve repairs using an argon laser source in both primates and humans (14).

It has been suggested that laser energy may be used to bond other tissues within the central nervous system. Dural closure without cerebrospinal fluid leaks was found to be possible using the milliwatt CO_2 laser. However, poor tensile strength suggested that stay sutures must be used concomitantly (14). Further application of these and other tissue welding techniques, including intracranial use, may be forthcoming to allow the neurosurgeon more potential for constructive surgery.

References

1. Jain KK (1980) Sutureless microvascular anastomosis using a neodymium-YAG laser. J Microsurg 1:436-439
2. Neblett CR (1982) Reconstructive vascular surgery with the use of CO_2 laser. Presented at Cong. on Laser Neurosurg. II. Chicago, Ill, Sept. 25
3. Quigley MR, Bailes JE, Kwaan HC, Cerullo LJ (1985) Histologic comparison of suture versus laser-assisted vascular anastomosis. Surg Forum 36:508-510
4. Bailes JE, Quigley MR, Kwaan HC, Cerullo LJ, Brown JT (1985) Fibrinolytic activity following laser-assisted vascular anastomosis. Microsurgery 6:163-168
5. Quigley MR, Bailes JE, Kwaan HC, Cerullo LJ (1985) Laser-assisted vascular anastomosis. Lancet I:334
6. Quigley MR, Bailes JE, Kwaan JC, Cerullo LJ, Brown JT, Lastre C, Monma D (1985) Microvascular anastomosis using the milliwatt CO_2 laser. Lasers Surg Med 5:357-365

7. Quigley MR, Bailes JE, Kwaan HC, Cerullo LJ, Brown JT (1986) Aneurysm formation following low power CO_2 laser-assisted vascular anastomosis. Neurosurgery 18:292-299

8. Hartz RS, LoCicero J, McCarthy WS (1984) Microvascular applications of very low power CO_2 laser. Presented at the Cong. on Laser Neurosurg. III, Chicago, Ill, May 7

9. Pribil S, Powers SK (1985) Carotid artery end-to-end anastomosis in the rat using the argon laser. J Neurosurg 63:771-775

10. Sartorius CJ, Shapiro A, Campbell RL, Klatte EC, Clark SA (1986) Experimental laser-assisted end-to-side microvascular anastomoses. Microsurgery 7:79-83

11. Neblett CR, Morris JR, Thomsen S (1986) Laser-assisted microsurgical anastomosis. Neurosurgery 19:914-934

12. Quigley MR, Heiferman K, Kwaan HC, Vidovich D, Nora P, Cerullo LJ (1987) Laser sealed arteriotomy: a reliable aneurysm model. J Neurosurg (to be published)

13. Bailes JE, Quigley MR, Cerullo LJ, Kline DG, Shagal V (1986) Sutureless CO_2 laser nerve anastomosis: histological and electrophysiologic analysis. Lasers Surg Med 6:248

14. Heiferman KS, Quigley MR, Cerullo LJ, Block SJ (1986) Dural welding with CO_2 laser. Lasers Surg Med 6:248

Regeneration of Peripheral Nerves Following Nd:YAG Laser Transection - Experimental Observations

H.-J. König, K. H. Krähling, J. Anagnostopoulos-Schleep, and R. Mewe

Neurochirurgische Klinik der Westfälischen Wilhelms-Universität, Albert-Schweitzer-Straße 33, D-4400 Münster

Introduction

Reports about the effect of laser beam on peripheral nerve regeneration are still controversial in their conclusions. ASCHER and HOLZER (2, 3) postulated the suitability of CO_2 laser for treatment of amputation neuromas, while FISCHER et al. (4) and HURST et al. (6) found no evidence that CO_2 laser is less likely to result in neuroma formation than is conventional scalpel neurectomy. Moreover, FISCHER et al. (5) thought the CO_2 laser a useful tool for microepineurial anastomoses, while ALMQUIST et al. (1) favored the argon laser.

Animal Study

The influence of the 1.06-µm Nd:YAG laser on peripheral nerve regeneration was investigated in rat sciatic nerves. Twenty-three nerve trunks were divided by scalpel and 23 by focused laser beam (35 W; pulse duration: 2 s; focus diameter: 0.6 mm). After survival periods between 3 and 240 days, light and electron microscopic findings were evaluated.

Terminal swellings of proximal amputation stumps could be observed in both series, but the average diameter of the divided fascicles was significantly higher after scalpel than after laser transection (Fig. 1). Amputation neuromas with extrafascicular axonal sprouting and proliferation of connective tissue occurred in 8% of laser and 78% of scalpel cases.

Within 3 weeks after transection, regenerative activity is high at the proximal stump of divided rat sciatic nerves (7-9). During that period morphological studies revealed all signs of degeneration after laser radiation and axonal and Schwann cell proliferation after sharp division. Regressive changes of nerve fibers with degradation of the myelin sheath and numerous phagocytes predominated in the light microscopic findings during the first 20 days after operation. These findings were confirmed by transmission electron microscopy. There was no regenerative activity in laser stumps up to 20 days' survival. Myelin lamellae seemed to be wrinkled and distorted. The myelin and fiber system was marked by loss of cohesion and fragmentation. In contrast, regenerating units were present after sharp division. Those microfascicles consisted of Schwann cells, unmyelinated and small myelinated axons differing in diameter, and two or three layers of perineurial cells and collagen fibers.

Advances in Neurosurgery, Vol. 16
Ed. by W. Walter, M. Brandt, M. Brock, and M. Klinger

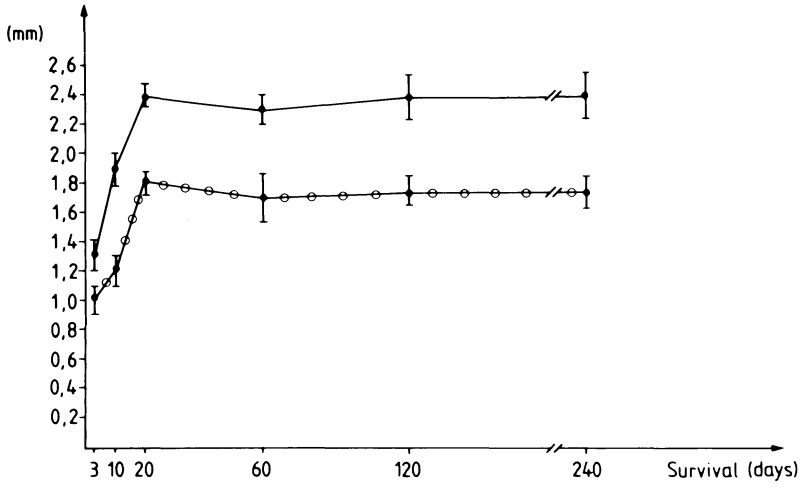

Fig. 1. Average fascicle diameter after Nd:YAG laser and scalpel transection according to different survival periods. ———, scalpel transection; —o—o—, laser transection; n = 46

After survival periods up to 240 days, no regrowing of the severed nerve fibers could be observed outside the dome of the laser stumps, except small terminal swelling (Fig. 2). After scalpel transection, terminal and collateral axonal sprouting and proliferation of Schwann cells and collagen fibers extending into the surrounding tissue were evident (Fig. 3).

In a second series 12 nerve trunks each were reanastomosed by initial microsurgical epineurial suture repair following (a) laser and (b) scalpel transection. In all cases the repair side was crossed by regenerating units 30 days after operation. Proximal and distal to the suture line a microfascicular pattern was restored. Compared with normal nerve structure the percentage of unmyelinated fibers was about 20% higher in laser and scalpel cases. There was no difference in axonal sprouting activity (Fig. 4).

Morphological studies revealed a higher degree of epineurial scar tissue formation and constriction in the anastomotic zone of nerves joined together after scalpel division than was present in laser-treated animals. When nerve trunks were evaluated after survival periods between 30 and 90 days, better coaptation without fusiform thickening by proliferation of epineurial fibroblastic tissue was achieved by laser. There was compression of microfascicular pattern neither by epineurial scar tissue nor by interfascicular collagen fibers.

Conclusion

Nd:YAG laser action on peripheral nerve regeneration is dependent on a variety of central, local, and peripheral influences (7). Neuroma formation seems to be reduced by a temporary sealing of the epineurium (9). Derived from a mesodermal origin, the epineurium usually carries a high fibroblastic activity (7, 8). On the other hand, reduction of fibroblastic activity may support the restoration of microfascicular pattern after reanastomosing of divided stumps.

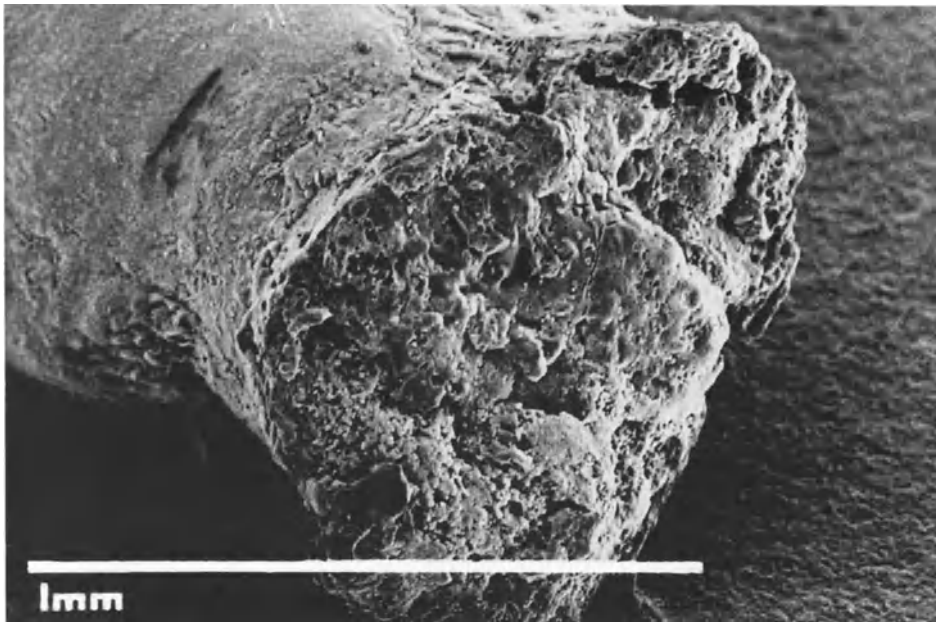

Fig. 2. Amputation stump 60 days after Nd:YAG laser transection: sealed dome of the fascicle without regrowing nerve fibers or proliferation of connective tissue. SEM, x 53

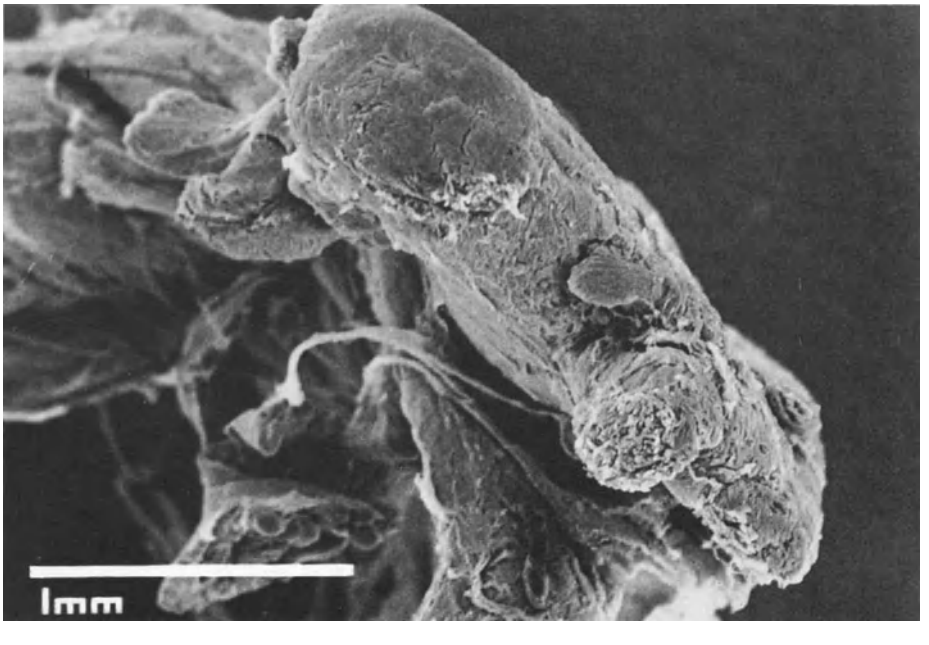

Fig. 3. Neuroma formation 60 days after scalpel division: small "nerve fascicles" are arranged in a chaotic fashion. SEM, x 27

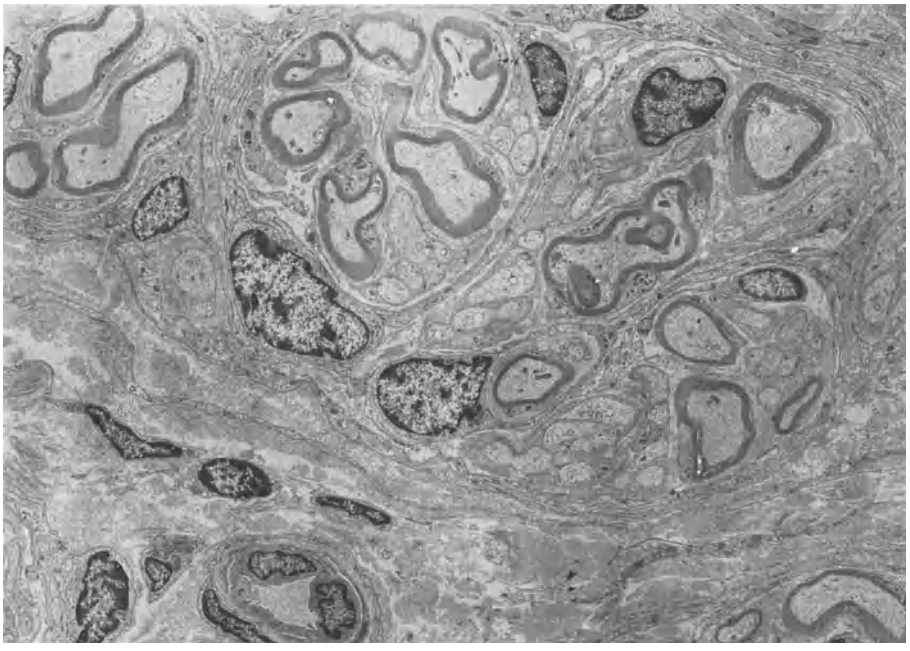

Fig. 4. Nerve trunk 30 days after Nd:YAG laser transection and epidural repair: microfascicular pattern restored, no constriction of fibers by epineurial scar tissue in the anastomotic zone. TEM, x 2000

References

1. Almquist EE, Nachemson A, Auth D, Almquist B, Hall S (1984) Evaluation of the use of argon laser in repairing rat and primate nerves. J Hand Surg (Am) 96:792-799
2. Ascher PW (1979) Newest ultrastructural findings after the use of a CO_2 laser on CNS tissue. Acta Neurochir Suppl 28:572-581
3. Ascher PW, Holzer P (1980) Chirurgie der peripheren Nerven mit dem CO_2 Laser verglichen mit herkömmlichen Instrumenten. Zbl Neurochir 41:37-42
4. Fischer DW, Beggs JL, Shetter AG, Waggener JD (1983) Comparative study of neuroma formation in the rat sciatic nerve after CO_2 laser and scalpel neurectomy. Neurosurg 13:287-294
5. Fischer DW, Beggs JL, Kenshalo DL, Shetter AG (1985) Comparative study of microepineurial anastomoses with the use of CO_2 laser and suture techniques in rat sciatic nerves: Part 1. Surgical technique, nerve action potential and morphological studies. Neurosurg 17:300-308
6. Hurst LC, Badalamente MA, Blum D (1984) Carbon dioxide laser transection of rat peripheral nerves. J Hand Surg (Am) 9:428-433
7. Lundborg G, Dahlin LB, Danielsen N, Hansson HA, Johannesson A, Longo FM, Varon S (1982) Nerve regeneration across an extended gap: a neurobiological view of nerve repair on the possible involvement of neuronotrophic factors. J Hand Surg 7:580-587

8. Morris JH, Hudson AR, Weddell G (1972) A study of degeneration and regeneration in the divided rat sciatic nerve. Z Zellforsch 124: 76-203

9. Sunderland S (1978) Nerves and nerve injuries, 2nd edn. Churchill Livingstone, Edinburgh

Laser-Assisted Microanastomoses

F. Ulrich, R. Schober, and W. J. Bock

Neurochirurgische Universitätsklinik, Moorenstraße 5, D-4000 Düsseldorf 1

Introduction

Pilot studies have indicated that it is possible to carry out laser-assisted vascular anastomoses (LAVAs) with different laser sources. However, thromboses and aneurysmal sacs could not be excluded in long-term follow-ups.

The environment of the anastomotic region of a severed nerve plays an important role in the degree of functional regeneration. Although microsurgical techniques in the past two decades have significantly improved functional recovery following nerve repair, there is still a need to evaluate new procedures that may enhance nerve regeneration. In the past decade, the laser has been used in a number of neurosurgical procedures and reportedly has several potential advantages over conventional techniques (1).

Owing to technical improvements the complication rate has been reduced; such improvements include suitable adjustment of the severed stumps during laser welding with stay sutures using a 1.319-µm Nd:YAG laser, OPMILAS YAG micromanipulator, and a flexible 200-µm fiber.

Materials

Twenty-five end-to-end LAVAs of the carotid artery of adult rats were performed with the modified 1.32-µm Nd:YAG laser (MBB-Medizintechnik, Munich) completed with a flexible 200-µm fiber and a micromanipulator (OPMILAS YAG, Zeiss, Stuttgart). In arteries less than 1 mm in diameter it is necessary to make three additional stay sutures. When fusion points of 12.5 W on a focus of 0.2 mm in 0.1 s are applied there should not be any tension on the vessel wall. At this moment the vessel ends have to be slightly elevated with two microtweezers. LAVAs can withstand pressures up to 300 mmHg.

Laser-assisted nerve anastomoses (LANAs) of the left sciatic nerve were carried out in 25 albino rats, again with the 1.32-µm Nd:YAG laser, in the following way: The nerves were cut through with microscissors. The proximal and distal nerve stumps were adapted by two lateral epineural sutures. The epineurium, adapted by means of tweezers, was welded together on the upper side and the lower side by a few laser fusion points with 12.5 W in 0.1 s, and thus the epineural tube was closed.

Advances in Neurosurgery, Vol. 16
Ed. by W. Walter, M. Brandt, M. Brock, and M. Klinger

Results

Of the 25 LAVAs, 22 were optimally functional and without aneurysmal sacs several weeks following removal. On the other hand, formation of aneurysms was shown in two cases, one after 65 days and the other after 84 days. These two cases had only two functional holding sutures, since one holding suture had been damaged intraoperatively by the laser irradiation. However, the vessels were sealed and had good patency. In a further case with a vessel diameter less than 0.8 mm, a vascular thrombosis was present after 69 days. All remaining 22 LAVAs and all LANAs showed continuity without sacculation and could be identified only on the basis of the sutures left behind. The patency of the microanastomoses could be demonstrated with the method after O'BRIEN in all cases.

Histological findings up to several months later have shown the feasibility of laser-induced tissue welding. Special histological and electrophysiological findings will be presented elsewhere.

Conclusion

Besides the shortening of the operation time with LAVAs, an improvement of vascular integrity could be achieved compared to the conventional technique. In addition, the simplification of the surgical technique made reproduction of laser-assisted microanastomoses more easy and caused fewer complications than was previously the case.

It is expected that in the future laser-assisted anastomosis will be of interest not only in the case of microvessels and nerves but also for fusing other collagen-containing tissue in cardiac surgery, neurosurgery, urology, gynecology, and abdominal and plastic surgery in order to optimize tissue adaptions.

Summary

Laser-assisted microvascular anastomoses and nerve anastomoses can be performed with the most diverse types of laser (1-16). However, postoperative complications in the form of thromboses and aneurysmal sacs as well as neuromas could be detected in 17%-29.8% of cases in longitudinal investigations. By conversion of the beam geometry (1.32-µm Nd:YAG laser, 200-µm light conductor) and use of two or three concentrically applied 10.0 stay sutures, early and late complications could be markedly reduced (12%) in 25 end-to-end anastomoses of the common carotid artery of adult albino rats and of the sciatic nerve, 1 mm in diameter. Histological and fine structural analysis revealed a homogenizing change of collagen with interdigitation of altered individual fibrils that appeared to be the structural equivalent of the welding effect (12).

Acknowledgment. This work was supported by the Ministry of Science and Research of the Federal State of North-Rhine Westphalia, West Germany, IV B5-40205587.

References

1. Beggs JL, Fischer DW, Shetter AG (1986) Comparative study of rat sciatic nerve microepineural anastomoses made with carbon dioxide laser and suture techniques: part 2. Neurosurgery 18/3:266-269

2. Dujovny M, Diaz FG, Ausman J, Diazu J, Cnevas P, Berman K, Malik G (1986) Lasers in advanced neurosurgical technologies. 4th Annual General and Scientific Meeting, LANSI, Venice, Italy, March 11-22

3. Godlewski G, Pradal P, Rouy S, Charras A, Dauzat M, Lan O, Lopez FM (1986) Microvascular carotid end-to-end anastomosis with the argon laser. World J Surg 10:829-833

4. Gomes O, Macruz R, Armelin E (1982) Anastomose vascular com laser de argonio. Rev Hosp Clin Med S Paulo 37:255

5. Quigley MR, Bailes JE, Kwaan HC, Cerullo LJ, Brown JT, Lastre C, Monma D (1985) Microvascular anastomosis using the milliwatt CO_2 laser. Lasers Surg Med 5:357-367

6. Quigley RM, Bailes JE, Kwaan HC, Cerullo LJ (1985) Laser-assisted vascular anastomosis. Lancet 1:334

7. Quigley MR, Bailes JE, Kwaan HC, Cerullo LJ, Brown JT (1986) Aneurysm formation after low power carbon dioxide laser-assisted vascular anastomosis. Neurosurgery 18/3:292-299

8. Jain KK (1980) Sutureless microvascular anastomosis using a neodymium-YAG laser. J Micro Surg 1:436-439

9. Jain KK (1984) Sutureless extra-intracranial anastomosis by laser. Lancet 2:816-817

10. Krueger RR, Almquist EE (1985) Argon laser coagulation of blood for the anastomosis of small vessels. Laser Surg Med 5:55

11. Neblett CR, Morris JR, Thomson Sh (1986) Laser-assisted microsurgical anastomosis. Neurosurgery 19/6:914-934

12. Schober R, Ulrich F, Dürselen R (1986) Laser-induced alteration of collagen substructures enables microsurgical tissue welding. Science 232:1421-1422

13. Ulrich F, Bock WJ, Schober R, Wechsler W (1984) Repair of carotid artery of the rat with Nd:YAG laser. LANSI, 2nd Annual General and Scientific Meeting, Salzburg-Fuschl, Austria, Sept 27-30

14. Ulrich F, Bock WJ (1986) Laser-assisted repair of small blood vessels with 1.3 µm Nd:YAG laser. In: Waidelich W, Kiefhaber P (eds) Optoelectronics in medicine. Springer, Berlin Heidelberg New York Tokyo, pp 418-423

15. Vance CA, Evans JH, Wheatley DJ (1986) Laser assisted anastomosis in coronary surgery. 4th Annual Conference on Lasers in Medicine and Surgery, London, Jan 22-23

16. Waidhauser E, Baumgartner R, Beck OJ, Unsöld E, Wrobel W (1986) Nd:YAG-Laser-assistierte Mikrogefäßanastomosen. 3. Jahrestagung der Deutschen Gesellschaft für Lasermedizin, Lübeck-Travemünde, June 18-21

A Histological Evaluation of Experimental Nerve Anastomoses with the 1.32-μm Nd:YAG Laser

R. Schober, F. Ulrich, and Th. Sander

Neuropathologisches Institut der Universität, Moorenstraße 5, D-4000 Düsseldorf 1

Introduction

The use of the laser in experimental nerve anastomoses is a procedure already established for various types of instruments (1, 3, 9). In a previous investigation using the 1.32-µm Nd:YAG-laser, the welding property could be attributed to a coagulative alteration of collagen with ultrastructural features of fusion of individual fibrils (7). The formation of suture granulomas is thus avoided while, according to a study with the CO_2 laser (4), laser-induced damage to the nerve can be kept minimal. Although the regeneration potential apparently remains undiminished, the distal myelinated nerve fiber population was found not to be significantly different between CO_2 laser-assisted and traditional suture anastomoses in a quantitative analysis (2). However, a detailed and systematic study of the changes taking place at the site of anastomosis is as yet lacking, probably due to technical difficulties inherent in the histological preparation of longer nerve segments. We have tried to overcome these by use of a new plastic embedding technique.

Material and Methods

Details of the experimental strategy and of operative procedures are described elsewhere (10). The sciatic nerves of 18 rats were examined 1-7 days, 3 weeks, and 2 1/2, 3, and 6 months after severance and anastomosis with the 1.32 µm Nd:YAG laser and with two stay sutures. Fixation was either by perfusion via the abdominal aorta with 2.5% glutaraldehyde buffered to pH 7.4 with 0.1 M sodium cacodylate, or by immersion securing a stretched position of the removed segment. In six further rats serving as controls, the nerves were examined 3 months after anastomosis with sutures only. Each nerve was processed with two different histological methods. First, a 10- to 15-mm long segment containing the site of anastomosis was embedded in methacrylate (Technovit 7100, Fa. Kulzer, Wehrheim/Ts.). The manufacturer's instructions were modified to suit the special tissue characteristics of peripheral nerves. Briefly, this involved dehydration in alcohol, preinfiltration and infiltration for at least 24 h at 4°C and at room temperature in a vacuum container, and stepwise polymerization at 4°C, room temperature, and 37°C. Longitudinal sections 2-3 µm thick were cut with a Reichert-Jung autocut microtome 1140 and stained with hematoxylin and eosin, toluidine blue, and sudan black for myelin. Second, the most distal nerve segment, usually consisting of two or three separate fascicles already, was embedded in Spurr's epoxy medium, and 1-2 µm thick transverse sections were cut with a

Advances in Neurosurgery, Vol. 16
Ed. by W. Walter, M. Brandt, M. Brock, and M. Klinger

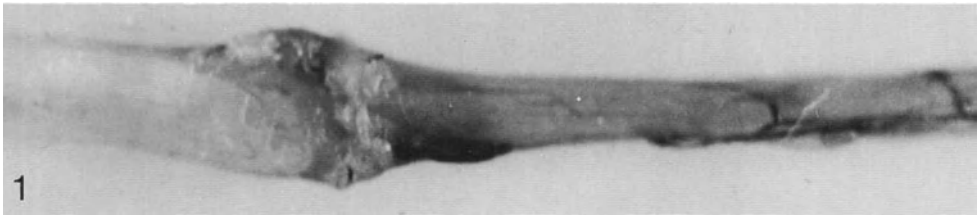

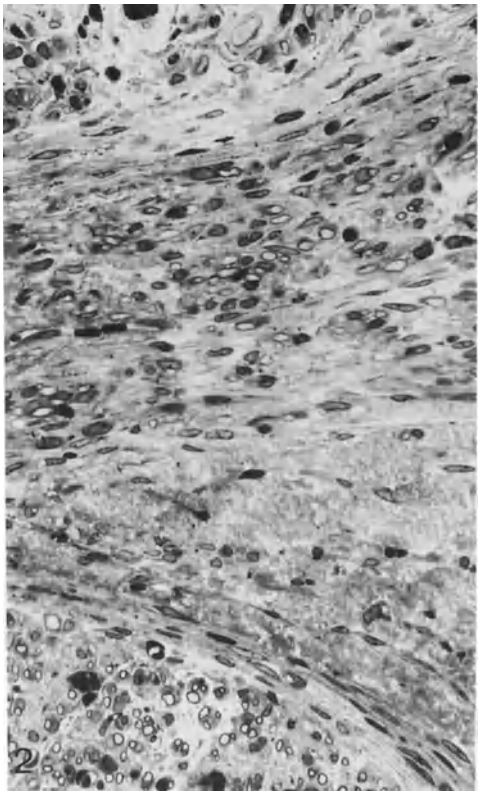

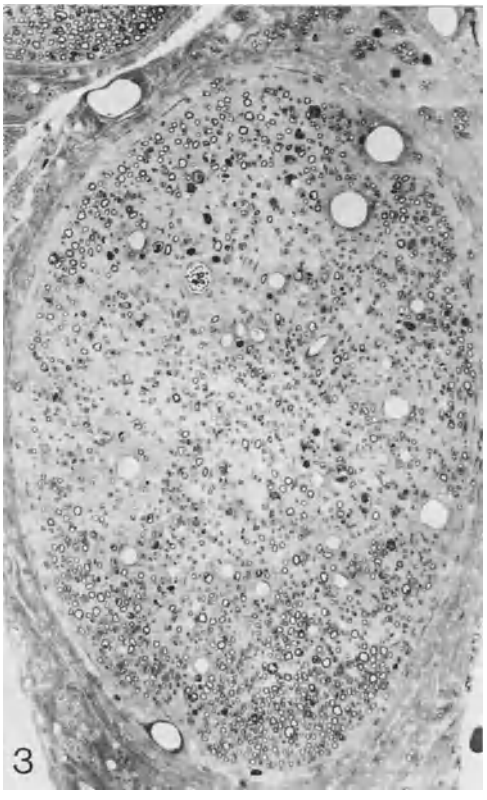

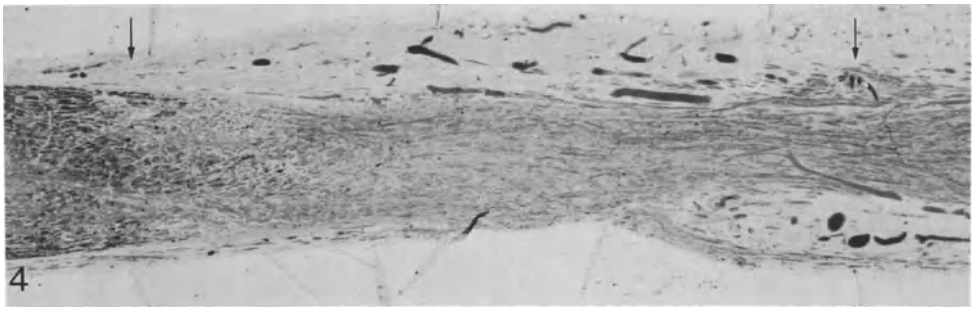

Figs. 1-4

LKB ultratome type III and stained with toluidine blue. In most cases, the removed nerve segment was worked up entirely in serial sections.

Results

In acute preparations, the site of anastomosis could easily be identified macroscopically by the laser-induced epineurial tissue bulging (Fig. 1). Chronic anastomoses, in contrast, were always smoothly contoured except for one case of 3 months with a distinct lateral neuroma. Orientation under the dissecting microscope was facilitated by the persistent knots of suture. The dissection was most difficult in the several-day-old preparations, where the anastomosis was artificially torn apart repeatedly.

Microscopically, the anastomosis in acute preparations showed a gap bridged by coagulated collagen, apparently deriving from the broadly enlarged perineurium. Only in one case was there a persisting close adaptation of the stumps. Cellular ingrowth and capillary sprouting was rapid, and by 1 week, the outer circumference of the anastomosis showed a zone of denser granulation tissue and thus already gave the impression of a new sheath structure. Other areas of the coagulated collagen showed elongated cell formations resembling perineurial lamellae. The endoneurium of both nerve stumps was marked by numerous Schwann cell mitoses and by increasing numbers of mast cells. Wallerian degeneration in the distal stump was accompanied by a vigorous proximal outgrowth of axons. By 3 weeks, many small myelinated fibers were already present in between bands of Büngner and breakdown fragments; others, however, pursued a lateral aberrating course in the broadened nerve sheaths. Although clearly identified as neuromatous by their - at first incomplete - sheath of Henle, they came to follow a strictly longitudinal course within the lamellated compartments of the residual coagulated collagen (Fig. 2). The extent of regeneration in chronic preparations was best assessed in the distal cross sections of the nerve segment. Generally, the endoneurium showed well myelinated regenerated nerve fibers with no appreciable difference between the laser-treated anastomoses and the controls. Although their density was often comparable to that of the normal sciatic nerve, there was a great variation between animals of the same survival time, between the different fascicles of one nerve, and even from field to field within one fascicle (Fig. 3). A similar variation existed in regard to the number of lateral aberrating neuromatous fibers: In 12

Fig. 1. Laser assisted rat sciatic nerve anastomosis, 1 day's survival. Dissecting microscope, ca. x 10

Fig. 2. Cross section of distal nerve segment immediately adjacent to anastomosis, 2 weeks' survival. Note both endoneurial regeneration and interfascicular "neuromatous neurotization" of coagulated collagen. Toluidine blue, x 340

Fig. 3. Cross section of distal nerve branch, 3 months' survival. Endoneurial fiber density is variable, and there are a number of aberrating fibers. Toluidine blue, x 150

Fig. 4. Longitudinal section of anastomosis, 3 months' survival. Proximal stump and suture material are marked by *arrows*. Congested blood vessels are also stained black by this method. Methacrylate, Sudan black, x 20

laser-treated nerves, none were present in 3, occasional ones in 4, and abundant ones in 5; in the 6 controls, none were present in 2, occasional ones in 3, and abundant ones in 1. Reexamination of longitudinal sections of the cases with no neuromas, however, did show lateral aberrating fibers with distal spread in all instances, thus demonstrating the need for application and comparison of more than one technique. The longitudinal sections, furthermore, often showed long distances between the suture granulomas and the proximal stump marked by denser myelin staining, an indication of bridging of a previous dehiscence that would otherwise not have been detected (Fig. 4).

Discussion

The present study shows that use of the 1.32-μm Nd:YAG laser is very feasible in experimental microsurgery of peripheral nerves. The results of laser-assisted anastomoses, however, do not seem to be appreciably superior to those using epineurial suture alone. For two reasons, a general and a specific one, it is advocated that this type of laser be used rather in conjunction with nerve transplantation: First, the occurrence of postoperative dehiscences, probably due to insufficient resistance to tension (6), may be avoided. Second, the laser-specific effect on the collagen of the sheath structures resulting in "neuromatous neurotization" (7, 8) may be favorably exploited. Experimental nerve transplantations using the milliwatt CO_2 laser have already been performed with good gross results (5). The 1.32-μm Nd:YAG laser should be at least as well suited for this purpose because of its superior coagulative capacity. A final evaluation, however, has to rely on a detailed histological examination using both longitudinal and cross sections. Notwithstanding the necessary additional application of physiological methods, this is true especially if one takes the well-known regenerative capacity of the rat sciatic nerve model into account. The newly developed methacrylate embedding technique, allowing the cutting of thin sections of a longer segment of nerve, may be helpful in this respect.

Acknowledgment. The study was supported by the Ministerium für Wissenschaft und Forschung des Landes Nordrhein-Westfalen, West Germany.

References

1. Almquist EE, Nachemson A, Auth D, Almquist B, Hall S (1984) Evaluation of the use of the argon laser in repairing rat and primate nerves. J Hand Surg (Am) 9:792-799
2. Beggs JL, Fischer DW, Shetter AG (1986) Comparative study of rat sciatic nerve microepineurial anastomoses made with carbon dioxide laser and suture techniques. Part 2. A morphometric analysis of myelinated nerve fibers. Neurosurgery 18:266-269
3. Fischer DW, Beggs JL, Kenshalo DL Jr, Shetter AG (1985) Comparative study of microepineurial anastomoses with the use of CO_2 laser and suture techniques in rat sciatic nerves: Part 1. Surgical technique, nerve action potentials, and morphologic studies. Neurosurgery 17:300-308
4. Myers RR, James HE, Powell HC (1985) Laser injury of peripheral nerve: a model for focal endoneurial damage. J Neurol Neurosurg Psychiat 48:1265-1268
5. Richmond IL (1986) The use of lasers in nerve repair. In: Fasano AV (ed) Advanced intraoperative technologies in neurosurgery. Springer, Wien New York, pp 175-183

6. Samii M, Wallenborn R (1972) Tierexperimentelle Untersuchungen über den Einfluß der Spannung auf den Regenerationserfolg nach Nervennaht. Acta Neurochir 27:87-110

7. Schober R, Ulrich F, Sander T, Dürselen H, Hessel S (1986) Laser-induced alteration of collagen substructure allows microsurgical tissue welding. Science 232:1421-1422

8. Schröder JM, Seiffert KE (1970) Die Feinstruktur der neuromatösen Neurotisation von Nerventransplantaten. Virchows Arch (Abt B) 5: 219-235

9. Ulrich F, Sander T, Bock WJ (1986) Anastomosis of the sciatic nerve of the rat with the modified Nd:YAG laser. A preliminary report. In: Waidedelich W, Kiefhaber P (eds) Laser/Optoelektronik in der Medizin. Springer, Berlin Heidelberg New York Tokyo, pp 414-417

10. Ulrich R, Schober R, Bock WJ (this volume) Laser-Assisted Microanastomoses.

Ultrasound

Experiences with the Ultrasonic Surgical Aspirator

E. B. Bongartz

Neurosurgical Department, Slotervaart Municipal Hospital, Louwesweg 6, NL-1066 EC Amsterdam

In clinical neurosurgery there is a need for an instrument capable of removing tumors selectively, without affecting the surrounding blood vessels or brain tissue. At the end of the 1970s the Cavitron ultrasonic surgical aspirator (CUSA) was introduced in Europe. Soon after its introduction the Japanese also developed an ultrasonic surgical aspirator (Sonotec).

I was able to work with both the CUSA and the Sonotec for about 2 years, and for 6 months was able to compare them intraoperatively on the same patient (Fig. 1). Several functions and capabilities were investigated and compared. I will discuss our findings concerning:

Technical aspects
Handling of the apparatus
Preparing the apparatus for use
Handling of the handpiece
Comparison of effectiveness
Operating costs
Reliability
New developments

We also showed the handpieces of the CUSA and the Sonotec to TNO (Toegepast-Natuurwetenschappelijk-Onderzoek, Medisch-technologische dienst, Leiden), a well-known, unbiased, Dutch technical institute.

Technical Aspects

In the CUSA the energy is supplied to a handpiece, where an electric coil and a magnetostrictive transducer convert it into vibration. The amplitude at the beginning of the tip is 300 μm, the same as at the top of the tip.

In the Sonotec the energy is supplied to an electrostrictive transducer, a piezoelectric crystal, which converts it into the mechanical movement. The amplitude at the beginning of the tip is 8 μm and at the top of the tip 240 μm (Tables 1 and 2). The vibration of the tip is longitudinal, meaning that at some places on the tip there is almost no vibration at all, while at other places there is a maximum amplitude, in contrast to the CUSA system, where the whole tip vibrates with the maximum amplitude (Fig. 2). Because of the longitudinal vibration the surgeon is able to grip the tip of the Sonotec directly, but not the top, and a plastic cap around the tip (cf. CUSA) is unnecessary. The longitudinal vibration is the reason for the low amount of heat production and one can work without the irrigation pipe.

Advances in Neurosurgery, Vol. 16
Ed. by W. Walter, M. Brandt, M. Brock, and M. Klinger

Fig. 1. CUSA (*left*) and Sonotec (*right*)

Table 1. Technical details of the CUSA

Power requirement:	240 VAC
Ultrasonic system:	electronic coil magnetostrictive transducer
Beginning amplitude:	300 µm
End amplitude:	300 µm
Frequency:	23 kHz
Energy:	0-75 W
Aspiration:	0-24 mmHg
Irrigation:	1.5-50 cc/min
Produced by:	Cooper Laser Sonics, Inc., Santa Clara, California, USA
Represented by:	Möller-Schwind-Coopervision, Aschaffenburg (W. Germany)

Table 2. Technical details of the Sonotec

Power requirement:	240 VAC
Ultrasonic system:	electrostrictive transducer (PZT)
Beginning amplitude:	8 µm
End amplitude:	240 µm
Frequency:	24 kHz
Energy:	0-100 W
Aspiration:	0-650 mmHg
Irrigation:	0-50 ml/min
Produced by:	Sumitomo Bakelite Co., Ltd., Tokyo, Japan
Represented by:	Söring Comp., Quickborn (W. Germany)

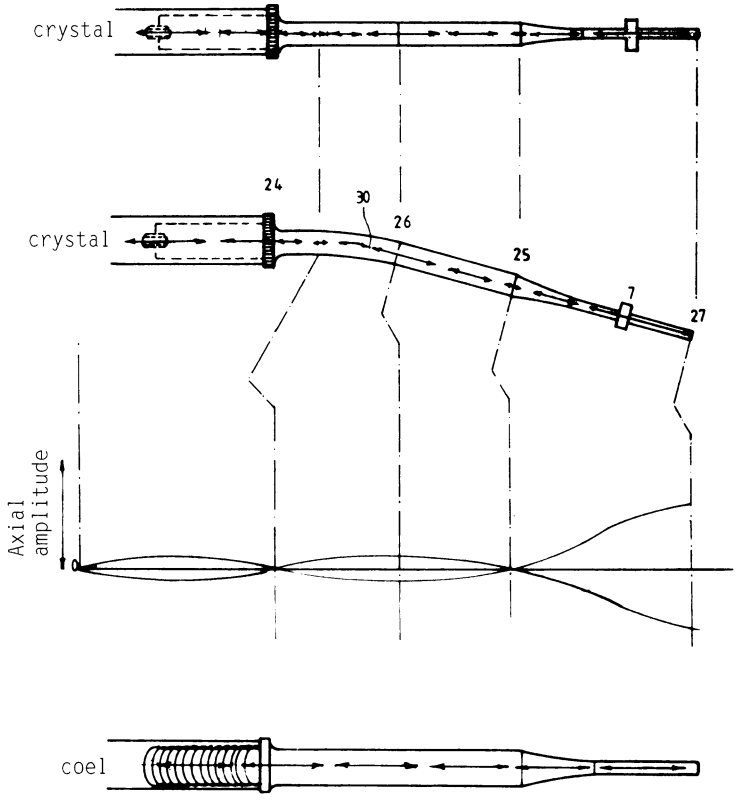

Fig. 2. Vibration waves of Sonotec (*top*) and CUSA (*bottom*)

The handpieces of the CUSA and the Sonotec were examined by TNO and their conclusion was that the design of the Sonotec seemed more advanced.

Handling of the Apparatus

By this is meant not only internal transportation within the hospital, from one operating room to another, but also external transport, for example to another hospital. In the opinion of the nursing staff the Sonotec was easier to transport because it had no protruding parts.

Preparing the Apparatus for Use

The tubes and the different handpieces are, in both cases, stored in a small and handy kit. The Sonotec can be made operational in about 1 min, especially when the irrigation pipe is unnecessary. No difficult instructions are required and no special skill is necessary. The preparation of the CUSA takes longer and is more difficult, so that mistakes were often made.

Handling of the Handpiece

As has already been discussed, the tip of the Sonotec can be gripped directly because of the longitudinal vibration. A disadvantage of the handpiece of the Sonotec is the separate flushing pipe, especially when operating on acoustic neuromas with the patient in a sitting position. The operating neurosurgeon then has to turn the Sonotec system about 180° in his hand. However, we removed the irrigation pipe and the assisting nurse is asked to flush the suction pipe with a saline solution every time the handpiece is given back to her. This prevents blockage of the suction pipe.

The handpiece of the CUSA is more elegant and can, of course, also be gripped at the tip because of the plastic cap around the tip through which the irrigation solution is led.

Concerning the tips, the Sonotec has different tips available. There are short and long straight tips, with either normal, sharp, or angle cut tops. Also there are two curved tips. The CUSA has two straight tips and one slightly curved tip.

Comparison of Effectiveness

Due to the action of vibration energy of ultrasonic waves, emitted from a tip end, it is possible to fragment tissue. Soft tissue is very effectively removed while major blood vessels remain intact. With tumors of hard consistency, where one will need a high amount of energy, every ultrasonic surgical aspirator will also destroy vessels. This means that in regard to the ultrasonic function there is no difference between the systems. Unfortunately, during the investigation no bent tip of the CUSA was available.

Operating Costs

During the time that I was able to compare the instruments on the same patient, the companies substituted the available tips or tubes. The tip of the CUSA had to be removed after one operation or after a couple of hours' use, while the tip with a clock to register the total amount of time the ultrasonic function was used) because the tip fell down. Both tips will break when pressed against bone or metal.

The tube system of the Sonotec was resterilized and used as long as the plastic material lasted. The CUSA tubes were renewed after every operation.

Reliability

Both systems were used for 2 years and during this time there was no need for repair.

New Developments

Both instruments have been altered since this investigation. There is a compact lightweight version of the Sonotec (Sonotec MIC II). A new improved version of the CUSA has also been developed in which a lot of the above-mentioned disadvantages have been resolved (CUSA System 200).

Surgical Ultrasonic Aspiration of Brain Tumors

A. Zieger, P. Blanckenberg, J. Pozo, U. Sander, and R. Smedema

Neurochirurgische Klinik, Evangelisches Krankenhaus, Steinweg 13-17, D-2900 Oldenburg

Introduction

In the last 10 years surgical ultrasonic aspiration has become established as a modern neurosurgical technique (2, 6, 7, 9, 13). The successful use of the ultrasonic aspirator system has suggested that this technique might be applicable for nontraumatic, radical, and time-saving resection of intraspinal and intracranial tumors (1, 2, 5, 7, 8, 12, 13, 14). Using the Cavitron ultrasonic surgical aspirator (CUSA) the tumor can be removed by fragmentation, irrigation, and aspiration. The functional components are regulated at the power and control console (Fig. 1a), whereby the vibration of the emulsifying tip of the handpiece (Fib. 1b) can be activated by the surgeon with a footswitch (2, 6, 9). The aspirated tissue can be used for histological diagnosis (2, 11, 15).

In this study 83 consecutive cases of brain tumors operated on with CUSA are reviewed. This series is characterized by a broad tissue range and partially by deep and critical localizations.

Material and Approach

Between May 1985 and February 1987, 83 consecutive cases of brain tumors were operated on in our hospital using a CUSA Model NS-100 (Cooper Laser Sonics Inc., USA). The tumors were detected by computerized tomography and by cerebral angiography. All tumors were histologically verified.

After craniotomy and opening of the dura mater the tumor dome was prepared by careful bipolar technique. The tumor was then removed as radically as possible, first debulking the center of the tumor intracapsularly and secondly, dissecting the tumor mass layer by layer. Finally the slackened capsule was separated from adjacent structures, avoiding distraction or displacing. An angled and balanced handpiece was used to increase visibility of the operating field, especially under the microscope. If calcified or deeply located parts of the tumor could not be sufficiently removed by CUSA alone, tumor resection followed by hemostasis was achieved by conventional techniques, e.g., laser coagulation.

As demonstrated in Table 1, meningiomas, astrocytomas, glioblastomas, neurinomas, and metastases occurred most frequently. In 64 cases the diameter of the tumor was more than 3 cm. In 34 cases the tumor was located in critical areas such as the speech region and midline and basal structures (Fig. 2). Forty-seven women and 36 men were operated

Advances in Neurosurgery, Vol. 16
Ed. by W. Walter, M. Brandt, M. Brock, and M. Klinger

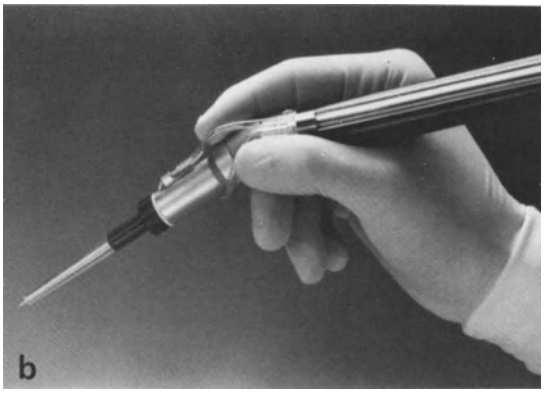

Fig. 1a,b. The CUSA system. a Power and control console. b The new angled handpiece

Table 1. Surgical ultrasonic aspiration of brain tumors

Meningioma	28	Medulloblastoma	2
Astrocytoma	14	Ependymoma	2
Glioblastoma	13	Sarcoma	2
Oligodendroglioma	7	Lymphoma	2
Metastasis	6	Teratoma	1
Neurinoma	6	Pituitary adenoma	1
			n = 83

on. Twenty-one patients were over 60 years old, ranging from 5 to 77 years. Seventy-three patients survived and underwent follow-up within 2-21 months (Table 2).

Results

The efficiency of the CUSA system depended on the consistency and vascularization of the tumor tissue (Table 3). Soft and noncalcified tumors with little blood supply were removed successfully, e.g., endotheliomatous meningiomas, metastases, gliomas, medulloblastomas, and acoustic neurinomas (Fig. 3). Even if the tumors were located in cri-

Supratentorial (n = 53)

Hemisphere (25), Convexity (19), Corpus callosum (1)
Thalamus (1), Falx (5), Intraventricular (2)

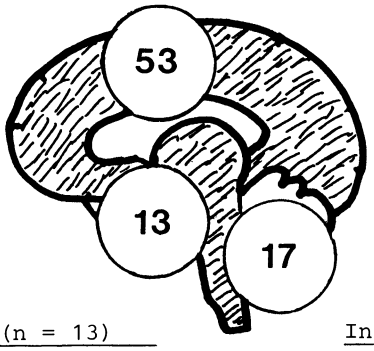

Basal (n = 13)

Frontal base (2)
Sella turcica (4)
Sphenoid wing (2)
Petrosal bone (5)

Infratentorial (n = 17)

Cerebellopontine angle (6)
Hemisphere (5)
Vermis (2)
Tentorial rim (3)
Foramen magnum (1)

Fig. 2. Localization of intracranial tumors (n = 83)

Table 2. Postoperative clinical course and prognosis

Died	10		
Intracerebral cause	3	Hematoma	1
		Edema, infarction	2
Extracerebral cause	7	Cardiopulmonary decompensation	3
		Septic complication	2
		Embolic complication	2
Survived	73		
Quality of life (modified from Karnofsky 1948)			
1 Able to work	24	No functional deficit	3
2 Able to work		Little deficit	21
3 Unable to work	49	Independent	20
4 Unable to work		Needing care	26
5 Unable to work		Bed resting	3
			n = 83

Table 3. Efficiency of surgical ultrasonic aspiration in brain tumor surgery (n = 83)

	Property of tumor tissue
⬆⬆ (n = 56)	Low-grade consistency and vascularization, no calcification e.g. endotheliomatous meningiomas, gliomas, metastases, medulloblastomas, neurinomas, lymphomas, pituitary adenomas
⬆ (n = 16)	Moderate consistency and vascularization and/or calcification e.g. metastases, gliomas, fibroblastic meningiomas, neurinomas, teratomas
⬇ (n = 11)	High-grade consistency and vascularization, extreme calcification e.g. calcified ependymomas and oligodendrogliomas, dermoid cysts, psammomatous meningiomas, sarcomas, angioblastic meningiomas

tical regions of the brain with adherence to basal and functionally important neurovascular structures, tumor resection was successful. The tumor tissue can be skeletonized primarily from blood vessels (carotid and vertebral artery) and neural structures (cortical speech region, brain stem, optic chiasm, hypothalamus, cranial nerves) (Fig. 4). Total tumor resection was done in 55 cases; the angled handpiece provided adequate vision for the neurosurgeon. In 28 cases tumor removal was only performed subtotally because of the extreme attachment of the tumor tissue to key functional structures. As demonstrated in Table 4a, dissection of the tumor tissue was successful in 56 cases (67%), using CUSA alone or in combination with other techniques. The time-saving effect of ultrasonic aspiration depended on the surgeon's ability to work rapidly and precisely in a relatively dry field. Although the average tumor diameter was more than 3 cm, CUSA was used for no more than 10 min in 69 cases (83%) (Table 4b), debulking the tumor mass.

Regarding the early postoperative clinical course and the quality of life of the 73 surviving patients, the bleeding risk was not increased and 44 patients recovered to achieve moderate or complete independence (Table 2). Recurrence of malignant tumors occurred in eight cases (8%).

Discussion

Since the introduction of the CUSA system in neurosurgery by FLAMM et al. (9), this innovative technique has been increasingly applied to brain tumor surgery, e.g., to facilitate access to deeply located brain tumors (6, 8, 13, 14). The benefits of ultrasonic aspiration depend on several unique factors. Laboratory and clinical studies of CUSA have demonstrated that there is no transmitted movement or heat lesion. The blood flow and the neural conduction is not adversely affected more than 1 mm from a lesion generated by the CUSA system (3, 4, 7, 16). The longitudinally vibrating tip favors cellular tissue

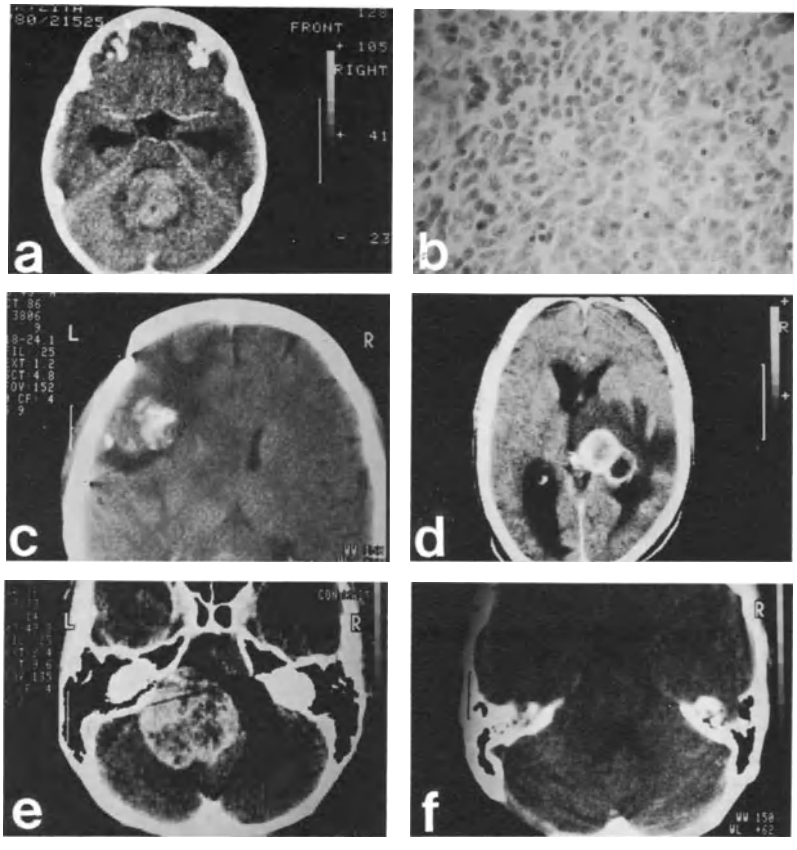

Fig. 3a-f. Brain tumors of a broad tissue range and localization in functionally important regions. a CT scan of a medulloblastoma at the roof of the fourth ventricle. b Histology of the same tumor type: high water content of the tumor cells and a low tumoral density. c Microcalcified recurrent oligodendroglioma of the upper speech region, which was totally removed by CUSA. d Metastasis of an adenocarcinoma of the right thalamic area, which was totally removed by CUSA. e,f CT scans of an acoustic neurinoma with moderate vascularization, which was totally removed by CUSA, preserving the facial nerve

with high water content rather than collagen-rich intracapsular walls and blood vessels (2, 6, 9). Using an angled handpiece, the surgeon's ability to work quickly and precisely is improved, as is the visibility of the operating field, even under the microscope.

The results of our study confirm that the CUSA system is capable of discrete, rapid, nontraumatic, and time-saving removal of a broad range of tumor tissue. The method is most successful if the tumor tissue is soft, noncalcified, and poorly vascularized. Dissection with the CUSA technique can be carried out immediately adjacent to key neurovascular structures with little attendant risk. As stated by PIA (13), CUSA is capable of reducing the operation time, of promoting healing, of shortening recovery, and of minimizing neurological deficits. This point of view corresponds well with the results of our study, i.e.,

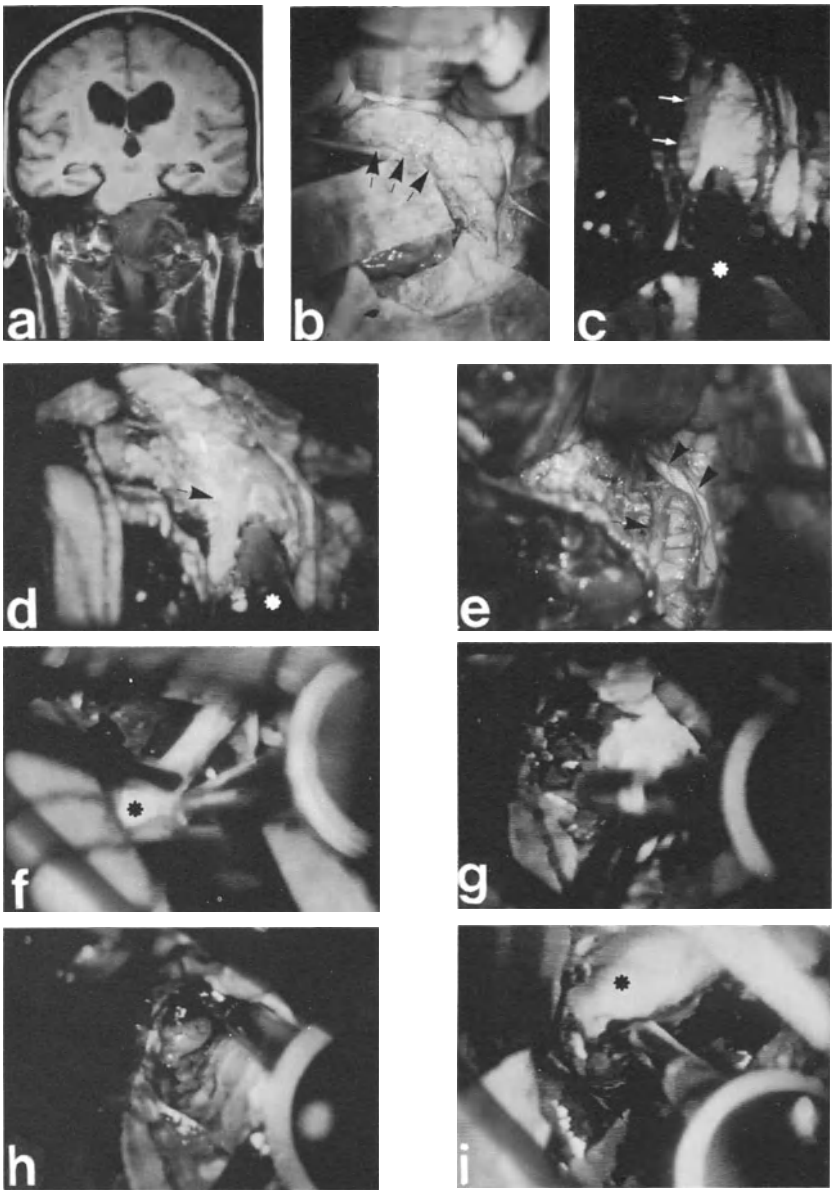

Fig. 4a-i. Surgical ultrasonic aspiration of brain tumors (selected examples; intraoperative video images). a-e Removal of a large meningioma of the foramen magnum: a NMR image of the right-sided meningioma located in the foramen magnum. b Intraoperative view of the tumor mimicking the brain stem and the blood vessels. c,d Skeletonizing the vertebral artery (*arrow*), PICA, and brain stem (*double arrow*) after partial tumor resection. f Resection of a large suprasellar pituitary adenoma (right subfrontal route). Chiasm (*). g Evacuation of a metastatic brain tumor. h Intracapsular removal of an acoustic neurinoma. i Layer-by-layer dissection of a medulloblastoma. Floor of the fourth ventricle (*)

Table 4. Application mode and time of ultrasonic aspiration of brain tumors (n = 83)

a)	Application mode	
	Using CUSA alone	n = 8
	Using CUSA mostly but in combination with other techniques (loop, bipolar laser, etc.)	n = 48
	Equal use of CUSA and other techniques	n = 16
	Little use of CUSA	n = 11
b)	Application time	
	No more than 10 min	n = 69 (83%)
	Between 10 and 20 min	n = 9 (11%)
	More than 20 min	n = 5 (6%)

bleeding problems and disastrous neurological deficits seemed to be prevented by CUSA. A final assessment of the rate of recurrence of brain tumors that were operated on with the CUSA system was not possible, because the follow-up time is too short as yet. Like other high-tech innovations, the CUSA system must be applied with thought. Direct or inadvertent application of the vibrating tip to neurovascular structures may cause laceration. This must be avoided, as must direct mechanical trauma. The CUSA system is of limited value in extremely calcified or dense fibrous tumors. Moreover, it lacks primary hemostatic properties.

Conclusions

As demonstrated in 83 consecutive cases, the CUSA technique is capable of precise, rapid, and nontraumatic removal of a wide variety of brain tumors, in part located in functionally important regions. This technique facilitates the primary separation of tumor tissue from key neurovascular structures without any transmitted movement or heat lesion. The unique properties of the CUSA system might prevent disastrous neurological deficits and therefore might improve recovery time and patient's quality of life. In our opinion the CUSA technique must be favored in brain tumor surgery.

Acknowledgment. We thank Dr. B. Terwey, Röntgeninstitut, Gottorpstraße, D-2900 Oldenburg, for the NMR image.

References

1. Albright AL (1985) Cavitron ultrasurgical aspirator and visual evoked potential monitoring for chiasmal gliomas in children. J Neurosurg 63:138-140
2. Brock M, Ingwersen I, Roggendorf W (1984) Ultrasonic aspiration in neurosurgery. Neurosurg Rev 7:173-177
3. Chopp RT, Shah BB, Addonizio JC (1983) Use of ultrasonic surgical aspirator in renal surgery. Urology 12:157-159

4. Cohen AR, Young W, Ransohoff J (1981) Intraspinal localization with somatosensory evoked potentials. Neurosurgery 9:157-162

5. Epstein F, Epstein N (1982) Surgical treatment of spinal cord astrocytomas of childhood. J Neurosurg 57:685-689

6. Epstein F (1984) The cavitron ultrasonic aspirator in tumor surgery. Clin Neurosurg 31:497-505

7. Epstein F (1986) Spinal cord astrocytomas of childhood. In: Symon L (ed) Advances and technical standards in neurosurgery, vol 13. Springer, Wien New York, pp 135-177

8. Fasano VA, Zeme S, Frego L, Gunetti R (1981) Ultrasonic aspiration in the surgical treatment of intracranial tumors. J Neurosurg Sci 25:35-40

9. Flamm ES Ransohoff J, Wuchinich D, Broadwin A (1978) A preliminary experience with ultrasonic aspiration in neurosurgery. Neurosurgery 2:240-243

10. Karnofsy DA, Abelmann WH, Craver LF (1948) The use of the nitrogen mustards in the palliative treatment of carcinoma with particular reference to bronchogenic carcinoma. Cancer 1:634-656

11. Malhotra V, Malik R, Gondal R, Beohar PC, Parkash B (1986) Evaluation of histological appearance of tissues removed by cavitron ultrasonic surgical aspirator (CUSA). Acta Neurochir (Wien) 81: 132-134

12. Pertuiset B, Farah S, Clayes L, Goutorbe J, Metzger J, Kujas M (1985) Operability of intracranial meningiomas. Personal series of 353 cases. Acta Neurochir (Wien) 76:2-11

13. Pia HW (1986) Microsurgery of gliomas. Acta Neurochir (Wien) 80: 1-11

14. Prakash B (1985) Surgical approach to large thalamic gliomas. Acta Neurochir (Wien) 74:100-104

15. Tamburus RK, Roggendorf W, Stein E, Brock M (1983) Morphologic changes in brain tissue following ultrasonic aspiration. In: Piotrowski W, Brock M, Klinger M (eds) Advances in neurosurgery, vol 12. Springer, Berlin Heidelberg New York, pp 332-337

16. Young W, Cohen AR, Hunt CD, Ransohoff J (1981) Acute physiological effects of ultrasonic vibrations in nervous tissue. Neurosurgery 8:689-694

Ultrasound-Guided Neuroendoscopy

L. M. Auer, P. Holzer, P. W. Ascher, and F. Heppner

Universitätsklinik für Neurochirurgie der Karl-Franzens-Universität, A-8036 Graz/LKH

Introduction

Endoscopic neurosurgical techniques have been used for a variety of intracranial pathological conditions for several decades (3-5, 7, 8, 10-13). Two new technical advances have made a reappraisal of endoscopic neurosurgery worth considering: One is the development of ultrasound imaging for intraoperative use to guide the endoscope to the target area. The other is the development of fiberoptic tubes for the application of Nd:YAG laser energy through the endoscope, and continuous visual control of the target area with the aid of miniaturized TV cameras used under sterile conditions.

Patients and Methods

A "neuroendoscope" (Karl Storz Company, Tuttlingen, FRG) (Fig. 1) has been developed for neurosurgical applications. This rigid-tube endoscope with an outer diameter of 6 mm harbors a suction irrigation system, one channel for a 600- or 400-µm Nd:YAG fiberoptic tube, the optic and light channels, and a separate instrument channel for the alternative use of biopsy forceps, scissors, monopolar coagulation probe, additional suction tube, or other instruments. A detailed description of the instrument has been given recently (1, 2). For the present setup, a Storz endovision 531 Newicon videocamera is used. For the application of Nd:YAG laser energy, a Messerschmitt-Bölkow-Blohm instrument (wavelength 1.06 µm is used.

For laser irradiation only, a second endoscope with an outer diameter of 5 mm and an Alvoran (opening angle 30°) has been developed.

Ultrasound guidance is possible through a 1- or 2-cm burr hole by using a Diasonics intraoperative ultrasound instrument with a 5- or 7.5-mHz intraoperative probe with a 10 mm diameter ultrasound head. For this instrument, a ball joint fixation device is available to focus on an intracerebral lesion as visualized on the ultrasound image. Following fixation of the ball joint mechanism, the ultrasound head can be replaced by a guide for the endoscope, which is introduced into a predefined depth, similar to stereotaxy.

The endoscope is introduced via a 1- or 2 cm burr hole in the frontal temporal or occipital region or on the planum occipitale for cerebellar lesions.

Since 1983, a total of 144 interventions have been performed for various intracranial lesions: Among a total of 112 intracranial hemor-

Advances in Neurosurgery, Vol. 16
Ed. by W. Walter, M. Brandt, M. Brock, and M. Klinger

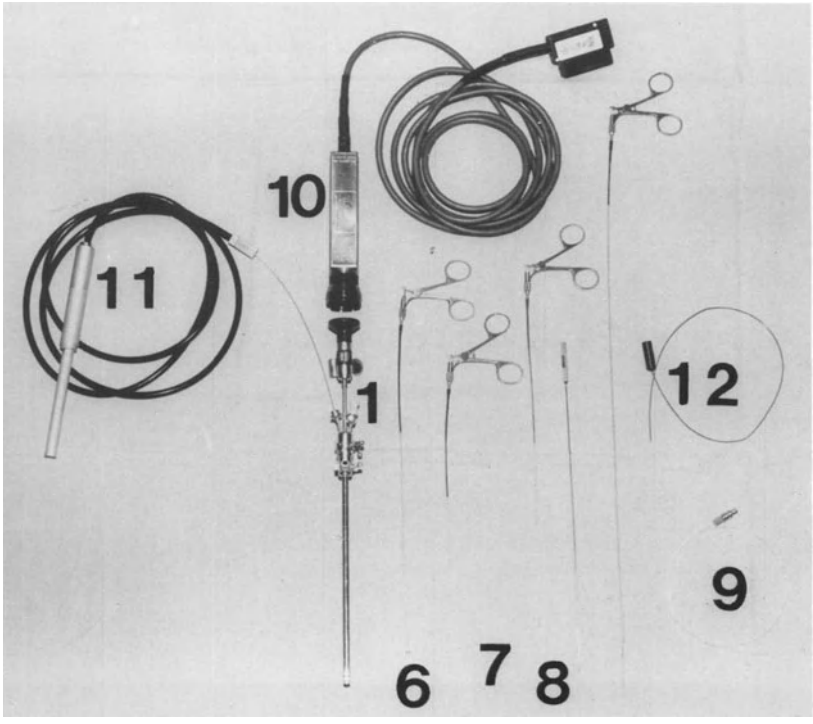

Fig. 1. Endoscopic setup. *1*, mandrin; *6*, biopsy forceps; *7*, microscissors; *8*, forceps; *9*, additional suction tube; *10*, TV camera; *11*, laser; *12*, monopolar coagulation tube

rhages, 79 were spontaneous hypertensive intracerebral hemorrhages, 10 intraventricular clots, 17 traumatic intracerebral hematomas, 5 cerebellar hematomas, and one a brain stem hematoma. In 32 cases, endoscopic biopsy of brain tumors has been performed (6 tumors of lateral ventricles, 6 tumors of the third ventricle, 19 cystic tumors of cerebral hemispheres, 1 tumor of the posterior fossa). In cases of ventricular tumors, an attempt was additionally made to resect as much of the tumor as possible, using biopsy forceps, scissors, and laser irradiation. In several cases of solid thalamic tumors, only laser irradiation from the ventricular surface was done. In cases of cystic tumors of cerebral hemispheres, the inner cyst wall was irradiated with the laser, and an external drainage was inserted at the end of the operation in order to allow the cyst wall to shrink to a small solid mass which was observed on imaging (CT, NMR) controls for its further growth behavior and could eventually be removed with conventional techniques in a second session.

Results and Conclusions

The present endoscopic method has proved to be a low-risk intervention with the advantage of less surgical trauma compared to conventional neurosurgical techniques. There was no surgical mortality, and surgical morbidity was minimal (two patients with intracerebral hemorrhage deteriorated due to rebleeding into the evacuated hemato-

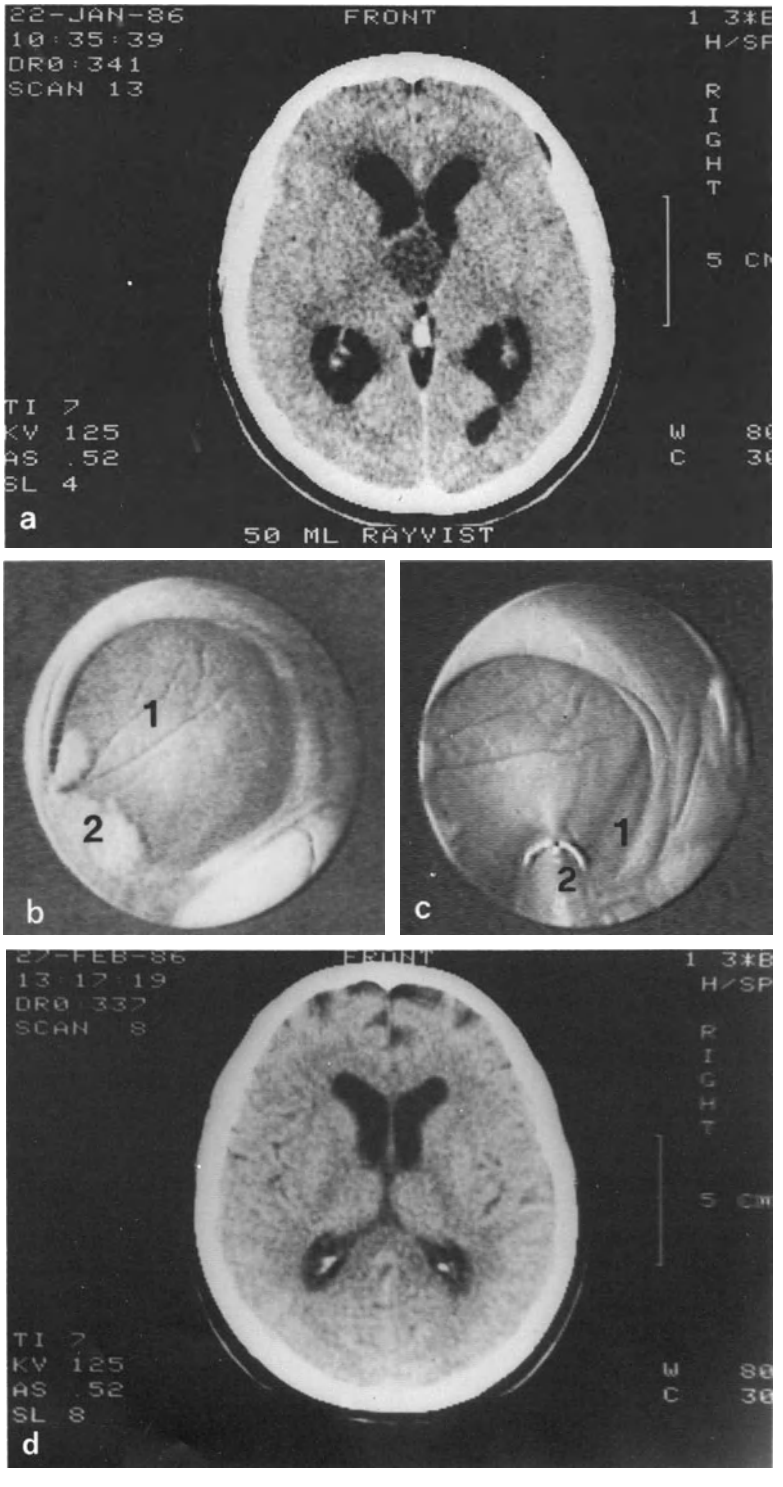
22-JAN-86
10:35:39
DR0:341
SCAN 13
FRONT
1 3*B
H/SP
R
I
G
H
T
5 CM
TI 7
KV 125
AS .52
SL 4
W 80
C 30
a
50 ML RAYVIST
1
2
b
1
2
c
27-FEB-86
13:17:19
DR0:337
SCAN 8
FRONT
1 3*B
H/SP
R
I
G
H
T
5 CM
TI 7
KV 125
AS .52
SL 8
W 80
C 30
d

ma cavity). The major primary concern, that bleeding in the operating field would jeopardize the surgical goal, was found to be unjustified: minor oozing from small vessels either in the wall of a hematoma cavity or in a tumor mostly stopped spontaneously after a few minutes' irrigation of the operating field with the suction irrigation system under pressure control. The laser had to be used in very few instances to stop a hemorrhage; it was mostly used for the denaturation of tumor tissue.

Spontaneous intracerebral hemorrhages were operated on in the framework of a randomized study of medical versus surgical-endoscopic treatment; detailed results of this study will be presented elsewhere. At this time it can be said, however, that endoscopic evacuation of an intracerebral or cerebellar hemorrhage can be done more rapidly and with less surgical trauma than when conventional techniques are used. In cases of massive ventricular hemorrhage with disturbed CSF circulation, endoscopic evacuation may turn out to be the only successful method of surgical treatment, especially in cases of repeated occlusion of external drainages by coagulated blood.

Our experience with the removal of ventricular tumors is still very limited; however, further development of endoscopic techniques for this application seems justified. Figure 2 gives an individual example of a cystic craniopharyngioma, operated endoscopically via a right frontal burr hole. Following removal of the cystic contents, the solid tumor parts could partly be denaturated with the aid of laser coagulation or resected using biopsy forceps and scissors. The patient is fully resocialized; imaging controls 16 months postoperatively showed no signs of tumor recurrence.

In cases of large cystic brain tumors, stereotaxic biopsy may not be successful. Under visual control, several tissue probes can be taken from different parts of the cyst wall through the endoscope. The inner surface of the tumor capsule can be denaturated with the aid of laser irradiation. During postoperative drainage of the collapsing cyst either via an external drain or a subcutaneous reservoir, the further development can be observed using CT or NMR, and if a small solid tumor remains, it can either be removed with conventional techniques in a second session or be treated with other methods.

Fig. 2. a Cystic craniopharyngioma in a 30-year-old patient with blockade of both foramina of Monro admitted due to chronic headache and recent attacks of vertigo and transient paresis and hypoesthesia of the right arm and hand. The tumor was approached endoscopically through a right frontal burr hole. b Endoscopic aspect of enlarged foramen of Monro with vascularized cyst membrane *1* bulging into the right lateral ventricle; *2*, choroid plexus. c Using microbiopsy forceps (*2*), after coagulation with the laser, the capsule was opened and the cystic contents evacuated. *1*, floor of the third ventricle. d Control CT scan 1 month postoperatively. The ventricular size has normalized, and no tumor is visible. The same picture was found on control CT 16 months postoperatively with the patient free of symptoms

References

1. Auer LM (1985) Endoscopic evacuation of intracerebral hemorrhage. Acta Neurochir 74:124-128
2. Auer LM, Holzer P, Ascher PW, Heppner F (1987) Endoscopic neurosurgery. J Neurosurg (submitted)
3. Dandy WE (1922) Cerebral ventriculoscopy. Bull Johns Hopkins Hosp 33:189
4. Fukushima T (1978) Endoscopy of Meckel's cave, cisterna magna and cerebellopontine angle. J Neurosurg 48:302-306
5. Guiot G et al. (1963) Une nouvelle technique endoscopique explorations endoscopiques intracraniennes. La Presse Mêd 71:225
6. Ishiwata Y, Shiozawa T (1985) Ventriculofiberscopic (VF) laser therapy: a new instrument and its possibility. Abstract 8th International Congress of Neurological Surgery, Toronto, No 440, p 262
7. Mixter WJ (1923) Ventriculoscopy and puncture of the third ventricle. Bos Med Surg J 188:277
8. Oppel F, Zeytountchian CH, Mulch G, Kunft HD (1978) Endoscopy of the cerebellopontine angle: its diagnostic and therapeutic possibilities. In: Frowein RA, Wilcke O, Karimi-Nejad A, Brock M, Klinger M (eds) Head injuries. Tumors of the cerebellar region. Springer, Berlin Heidelberg New York, p 269
9. Powell MP, Torrens MJ, Thomson JLG, Horgan JG (1983) Isodense colloid cysts of the third ventricle: a diagnostic and therapeutic problem resolved by ventriculoscopy. Neurosurgery 13:234-237
10. Prott W (1974) Cisternoscopy-endoscopy of the cerebellopontine angle. Acta Neurochir 31:105-113
11. Scarf JE (1935) Third ventriculoscopy as the rational treatment of obstructive hydrocephalus. J Pediatr 6:870

The Microvascular Doppler - An Intraoperative Tool for Aneurysm Surgery

J. Gilsbach, A. Harders, and M. Mohadjer

Neurochirurgische Universitätsklinik, Hugstetter Straße 55, D-7800 Freiburg

Introduction

NORNES et al. were the first to describe the application of a pulsed Doppler system for intraoperative use in aneurysm surgery (8), especially for the patency control of the parent vessels after clipping. The method was improved with the introduction of a high-resolution Doppler system and miniaturized probes developed for microvascular surgery (2, 3). After 6 years of modifications and clinical practice of their application in aneurysm surgery, the system and the probes are now so refined that they can be recommended for routine use, especially in operations which carry a high risk of disturbing the circulation, e.g., in giant aneurysms in calcified necks or in only partially visible vessels.

Method

The investigations were performed with a 20-MHz pulsed Doppler ultrasound velocity meter (EME, D-7770 Ueberlingen) (Fig. 1). The gating system made it possible to move the sample volume stepwise towards and away from the probe and to change its length, i.e., axial resolution. The most recent recordings in aneurysm surgery were all done with a 1-mm probe, which could be fitted in a conventional sucker or in a malleable silver tube that acted as a manipulator (Fig. 2). The acoustic coupling was done with a drop of saline or with CSF.

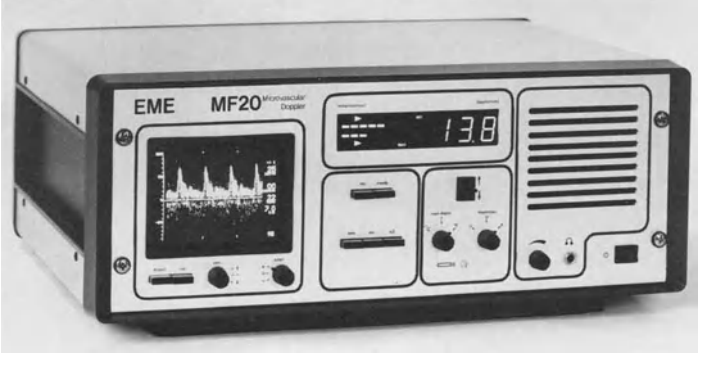

Fig. 1. Microvascular Doppler system with built-in real time spectrum analyzer

Advances in Neurosurgery, Vol. 16
Ed. by W. Walter, M. Brandt, M. Brock, and M. Klinger

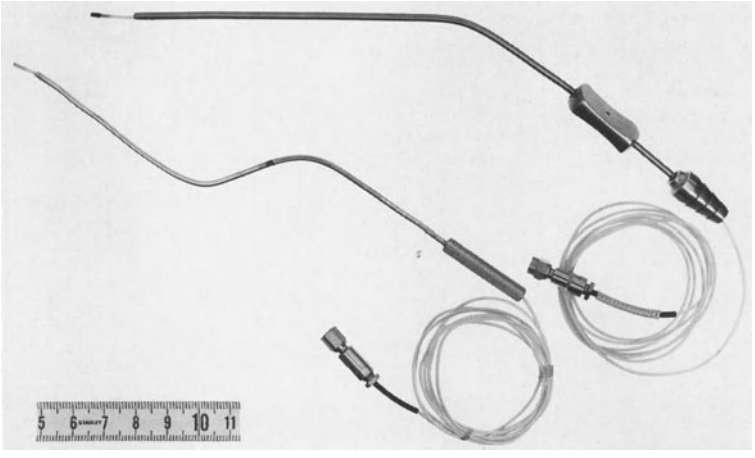

Fig. 2. Sterilizable microprobes for intraoperative use with a diameter of 1 mm. A malleable silver tube or a conventional sucker, into which they fit, serves as a "manipulator"

Results

Since 1980, the microvascular Doppler has been used routinely for large and giant aneurysms, for aneurysms with broad or calcified necks or partially thrombosed sacs, in operations performed by less experienced surgeons, and when the surgeon was not completely convinced of the patency of the parent vessel and exclusion of the aneurysm. The Doppler served as a guide for a hemodynamically proper clip position, as a means of exclusion control of the aneurysm, as an aid in deciding whether the neck was clippable or not, as a means of patency control of sutures after resection of nonclippable aneurysms, and in the case of temporary clipping or unplanned vascular occlusion as an aid in checking the collateral capacity (Figs. 3, 4). Nevertheless, in 5% of our patients operated on early, vessel occlusion with permanent deficits occurred. This was due to technically unclippable aneurysms or surgical injury to perforating arteries, and was already recognized intraoperatively. The inadvertent occlusion of parent arteries recognized only postoperatively no longer occurred.

Discussion

The microvascular Doppler has already proved to be a valuable and sensitive intraoperative tool for repeatable, atraumatic, reliable, and simple assessment of (un)disturbed patency or occlusion (2-6). Animal experiments on microvessels have shown that flow velocity accelerations and changes in the flow pattern as a sign of localized narrowings can be clearly identified by a diameter reduction of as little as approximately 40% (2). That means that a stenosis can be detected long before it becomes hemodynamically effective, which usually does not happen below a diameter reduction of 80% (1). Thanks to the fact that the velocity indicates to the second power the hemodynamic consequences of the diameter reduction, the method is much more sensitive than measurement of the diameter, e.g., by angiography. Fortunately, since the ultrasound emission in microprobes is more or less diffuse, the importance of the incident angle, which between 30° and 60° is already rela-

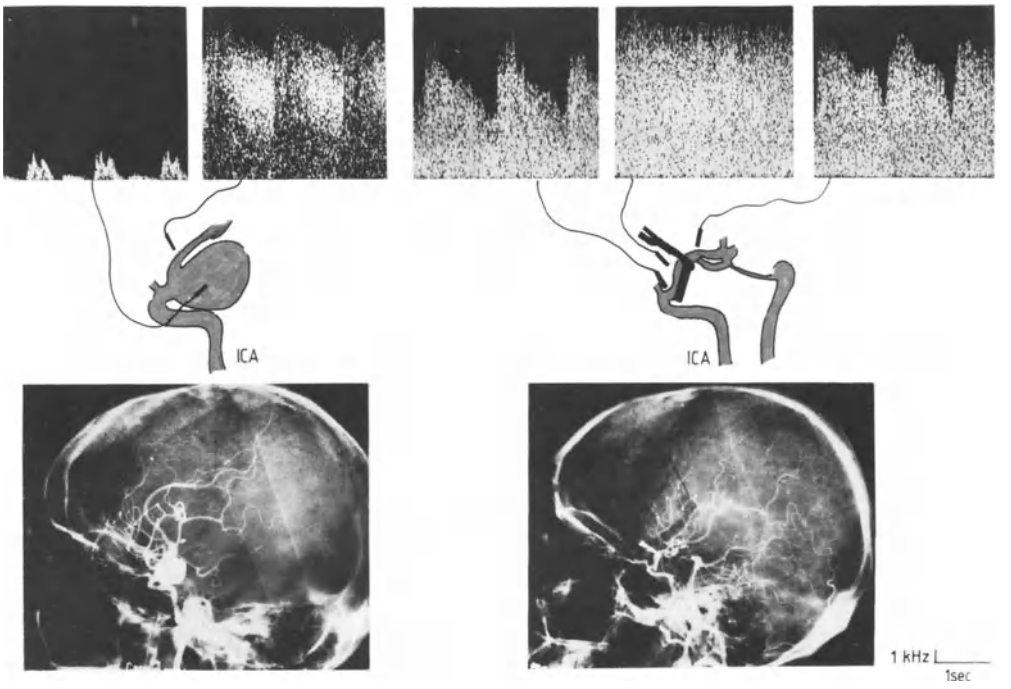

Fig. 3. Flow pattern of a large ophthalmic aneurysm with a preexistent narrowing of the distal internal carotid artery indicated by the flow velocity acceleration. After placement of a fenestrated clip and exclusion of the aneurysm, an additional moderate lumen diameter reduction occurred with a further increase in the flow velocities. The flow velocities of the distal internal carotid artery remain normal as a sign that the stenosis is not hemodynamically effective (6)

tively low, is additionally reduced. That means that there are at least no restrictions for the detection of an (un)disturbed flow or for the exclusion control of the aneurysm.

Comparisons of 140 identifiable vessels of 45 patients who underwent angiography at the end of the operation after the Doppler check showed that there was a clear correlation between the Doppler findings and the angiographically demonstrated diameters (4). In no cases were lumen narrowings overlooked. In 12.5% the intraoperative investigation showed increased velocities without corresponding stenoses in the postoperative angiograms. The possible cause was a release of a mechanical vasospasm or generalized accelerations of the flow velocities due to a dilation of the resistant vessels in patients who underwent early aneurysm surgery.

The influence of the Doppler recordings on the surgical strategy during aneurysm surgery was evaluated in 74 consecutive patients investigated before and after the aneurysm preparation and clipping. In 8 of these 74 patients, the clips appeared to be properly placed, the parent arteries seemed patent, and the aneurysm excluded. The Doppler, however, revealed marked discrepancies between the outer aspect and the intravascular hemodynamics, so that a change in the surgical strategy was necessitated (5).

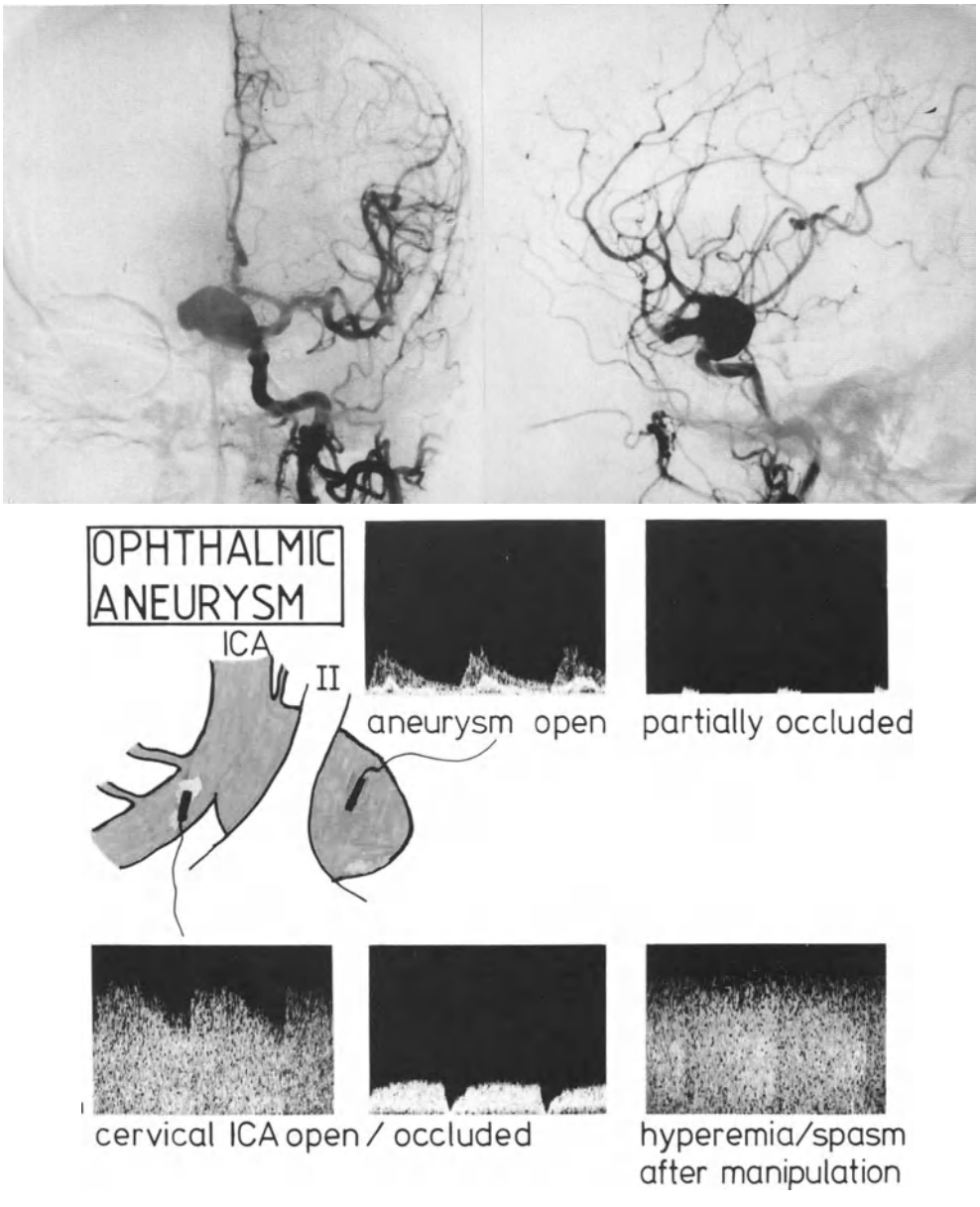

Fig. 4. Giant opthalmic aneurysm with characteristic slow intra-aneurysmal flow velocities. The partially occluded aneurysm is recognizable by residual flow signals. Reduction of the flow velocity and alteration of the pulse curve after temporary occlusion of the cervical internal carotid artery. Reactive hyperemia after restoration of the flow as a sign that the collateral circulation was not sufficient (7)

The Doppler, however, does not prevent rebleeding from a residual aneurysm neck. If there is uncertainty, a cerebral angiography should be performed.

Summary

A high resolution Doppler system with miniaturized probes for intraoperative use and its application in aneurysm surgery are presented. It has proved useful for the evaluation of (un)disturbed patency of the parent arteries and exclusion of the aneurysm.

References

1. Berguer R, Hwang NCA (1974) Critical arterial stenosis: a theoretical and experimental solution. Ann Surg 180:39-50
2. Gilsbach J (1983) Intraoperative Doppler sonography in neurosurgery. Springer, Wien New York
3. Gilsbach J, Harders A (1983) Intraoperative Doppler sonography. In: Jensen H-P, Brock M, Klinger M (eds) Advances in neurosurgery, vol 11. Springer, Wien New York, pp 369-374
4. Gilsbach J, Harders A (1986) Intraoperative Doppler sonography. In: Fasano VA (ed) Advanced intraoperative technologies in neurosurgery. Springer, Wien New York, pp 27-47
5. Gilsbach J, Harders A (1986) Neurosurgical applications of Doppler. In: Spencer (ed) Ultrasonic diagnosis of cerebrovascular disease. De Gruyter, Berlin New York
6. Gilsbach J, Harders A (1986) Comparison of intraoperative and transcranial Doppler. In: Aaslid R (ed) Transcranial Doppler sonography. Springer, Wien New York, pp 106-117
7. Harders A (1986) Neurosurgical applications of transcranial Doppler sonography. Springer, Wien New York
8. Nornes H, Grip A, Wickeby P (1979) Intraoperative evaluation of cerebral hemodynamics using directional Doppler technique. Part 2: Saccular aneurysms. J Neurosurgery 50:570-577

Applications of Transcranial Doppler Sonography in Neurosurgery

H. M. Mehdorn, J. Hense, and B. Hoffmann

Neurochirurgische Universitätsklinik, Hufelandstraße 55, D-4300 Essen

Introduction

When Doppler sonography was applied in the investigation of the extracranial arteries, the intracranial circulation could be examined only incompletely and indirectly. However, transcranial Doppler sonography (TCD) made it possible to insonate the major intracranial arteries through thin-walled parts of the bony structures (particularly the so-called temporal bone window) or through certain bone defects such as the orbital fissure and the foramen magnum. Previous reports from various authors (1, 2) have described techniques of TCD in detail and given normal values of flow velocities in the major arteries of the circle of Willis and its branches. This report deals with our personal experience using this technique in more than 500 selected neurosurgical patients studied over the last 16 months.

The transcranial pulsed Doppler device TC 2-64 from EME (Überlingen, FRG) was used in our department to investigate both the intracranial circulation and the extracranial arteries. Occasionally, in addition the bidirectional continuous wave Doppler device (Debimetre Ultrasonic Delalande) with an emission frequency of 4 MHz was used to study the extracranial arteries.

Patients

One-hundred and ninety patients presented with signs of cerebrovascular insufficiency. Forty-three of them had undergone angiography elsewhere and were referred to us to discuss indications for surgery, while the majority were referred to us to discuss indications for invasive angiographic studies. An additional 158 patients were studied who had already undergone cerebrovascular reconstructive surgery by extracranial-intracranial bypass (EC/IC), 2-9 years prior to this examination. This group of patients was examined with TCD to evaluate the long-term effect of cerebral revascularization.

Further indications for TCD were seen in patients presenting with cerebrovascular accidents produced by arteriovenous malformations or aneurysms, patients with head injury who fulfilled clinical criteria of brain death, and various patients examined prior to major surgery because they were suspected to have intracranial arterial occlusive disease. Since experience gained with the application of TCD in patients with aneurysms and angiomas is reported in this volume by other authors, this paper is mainly concerned with the patients presenting with cerebrovascular occlusive lesions.

Advances in Neurosurgery, Vol. 16
Ed. by W. Walter, M. Brandt, M. Brock, and M. Klinger

Results

Patients with Occlusive Vascular Disease

In 30 patients with internal carotid artery (ICA) occlusion, this lesion could normally be demonstrated by extracranial Doppler sonography or had been shown by angiography. However, additional information could be obtained using TCD on the flow velocity in the middle cerebral arteries (MCA) and the efficacy of collateral circulation: not only through the ophthalmic arteries but also through the anterior and posterior communicating arteries (ACA/PCA). By measuring flow velocities in the MCA, the impact of carotid artery occlusion on the cerebral perfusion could be determined. By measuring flow velocities in the communicating arteries, the functional importance of the circle of Willis could be estimated. Compression of the extracranial arteries such as the common carotid or vertebral arteries helped to define the importance of additional collaterals which may be an important factor in determining the indication for and risks of surgical procedures, particularly in patients with bilateral disease (Fig. 1).

Ten patients were studied who presented with extracranial stenosis; only two of these lesions were severe enough to reduce flow velocities in the carotid siphon and the MCA.

Seven patients presented with a marked increase of flow velocity in the carotid siphon together with a bruit suggestive of ICA siphon stenosis. Because this finding had no surgical implications, angiography was not considered but noninvasive follow-up was suggested.

Seven patients (the youngest aged 4 years) presented with a marked local increase of flow velocity in the proximal MCA and reduced flow in the distal part suggestive of MCA stenosis. After discussion of this finding with the patients, four of them underwent angiography which confirmed the lesion. The others preferred noninvasive follow-up under conservative therapy. An additional three patients presented with MCA occlusion and two with musical bruits suggestive of moyamoya disease.

In all, 59 patients presented with symptoms of vascular occlusive disease in the anterior circulation and significant lesions on TCD. However, in 46 patients who presented with similar clinical pictures, TCD did not show any significant lesions. Some of these patients had undergone inadequate angiography elsewhere which had not shown any lesion. On the basis of TCD findings, indication for further invasive studies was denied and the patients were followed under conservative therapy. Of the total of 105 patients with symptoms attributable to the anterior circulation, only four - who underwent further testing, including CO_2 reactivity test (3) - finally were considered suitable candidates for EC/IC bypass; ten additional patients underwent carotid endarterectomy elsewhere.

Follow-up of the 158 patients after EC/IC bypass surgery showed that the bypass has the highest hemodynamic effect on intracranial circulation in patients with ICA occlusion: a marked long-term contribution to the MCA circulation in this group could be demonstrated in 85% of the patients studied and was most pronounced in those with bilateral ICA occlusion. In contrast, the contribution of EC/IC bypass was lowest in patients with MCA stenosis. Flow values in the proximal MCA on the operated side were only slightly below values obtained on the contralateral side.

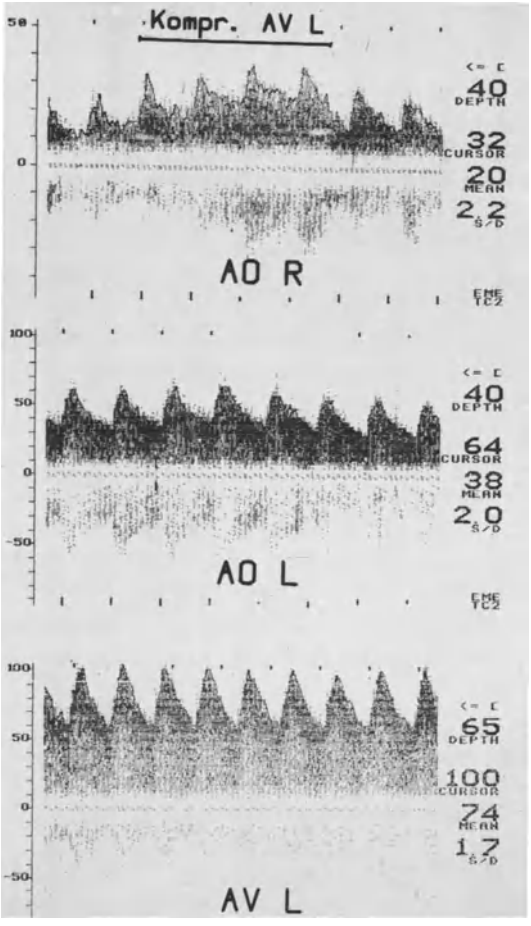

a

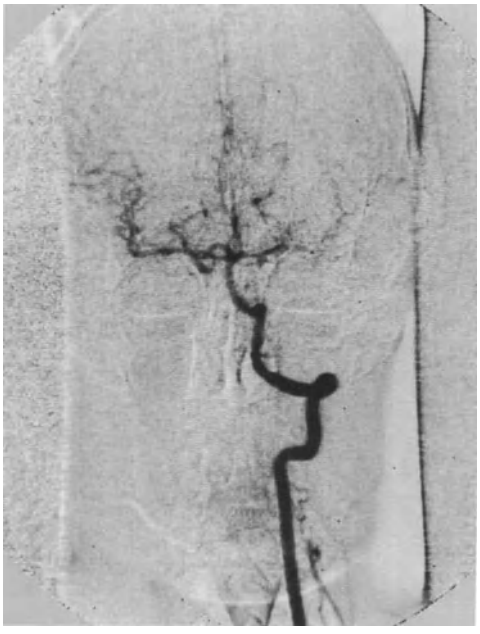

b

Fig. 1a,b. 43-year-old male patient presenting orthostatic TIAs and ischemic retinopathy of the right eye. Bilateral ICA and right vertebral artery occlusion. TCD of both MCAs indicated maximal flow values of about 80 cm/s with circulation maintained through the ophthalmic and the left vertebral artery. a The interaction between both collaterals. Compression of the (high-flow) vertebral artery led to an increase in flow in the right ophthalmic artery; however, this was not enough to maintain MCA flow at sufficient levels as it dropped to below 30 cm/s. b This circulatory pattern was confirmed by angiography: left vertebral angiogram with filling of both MCAs through the vertebral artery

Among 85 patients presenting with clinical signs attributable to the posterior circulation, only 16 presented with pathological findings on TCD. Among them were ten patients in whom no adequate signal of both vertebral arteries or the basilar artery could be detected and six patients with absence of a vertebral artery or stenosis of the distal vertebral or proximal basilar artery. Functional testing of the vertebral circulation was performed in patients who presented with symptoms of vertebrobasilar insufficiency on head turning or tilting. In only one of them could flow reduction to zero in the middle part

of the basilar artery be demonstrated when bending the neck forward; this was accompanied by fainting. This patient and a patient presenting with high-grade subclavian artery stenosis were considered candidates for vascular interventions. In contrast, a patient in whom careful angiographic evaluation had shown a left vertebral artery stenosis at the C4/5 disc level on head tilting had no flow reduction in the basilar artery on TCD when the same maneuver was performed, indicating that this stenosis had little functional importance.

Patients with Vascular Malformations

In 35 patients who presented with symptoms of arteriovenous fistulae (either congenital malformations or spontaneous fistulae), TCD was used to study the circulatory abnormalities caused by these lesions, such as the intracerebral or intracranial steal phenomenon, and the effect of surgery or radiation therapy. The effects of surgical interventions are discussed elsewhere in this volume; the effect of proton beam radiation therapy is demonstrated in Fig. 2.

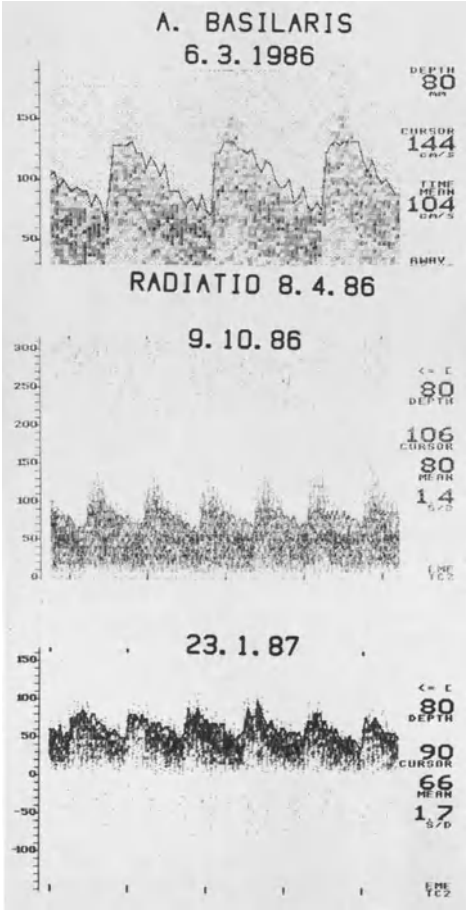

Fig. 2. 38-year-old female patient presenting with focal seizures. Angiography showed an arteriovenous malformation in the right parieto-occipital region that was fed by the ACA and MCA and the vertebrobasilar circulation. TCD demonstrates that a high flow in the basilar artery is reduced following proton beam radiation therapy. (Systolic and mean flow values are given on the *right* of the graphs in cm/s)

Patients with Brain Death

Patients with clinical symptoms of brain death were studied with respect to intracranial circulatory arrest in order to clarify the timing of angiography prior to organ transplant. This helped to avoid unnecessary angiography. It was considered essential to have obtained a previous positive study of the intracranial circulation in order to demonstrate circulatory arrest. If MCA flow could not be obtained later, TCD of the carotid siphon through the orbita and of the basilar artery was helpful in showing either oscillating flow or flow arrest. For flow arrest to be diagnosed, it is considered mandatory that the same experienced observer has performed previous positive studies in this particular patient. Circulatory arrest was confirmed angiographically in all patients who had this finding in TCD.

Discussion

The accuracy of the TCD studies depends on the examiner's experience. In the patients studied with both TCD and angiography, nearly all results were in agreement. Differences could be explained by a time interval and an unstable lesion such as an MCA stenosis. Therefore, confidence in TCD examination increased with time so that it is thought to be a reliable method for repeatable noninvasive investigation of the major intracranial arteries.

The application of TCD in the evaluation of neurosurgical patients helps to reduce indications for angiography and to adjust its timing. From our present experience, it is difficult to estimate the percentage of angiographic studies which could have been replaced or avoided by TCD. In our view, indication for (and timing of) angiography in patients with vascular occlusive lesions and aneurysms should always include indication for subsequent surgery. Therefore, the following protocol for investigation of patients with symptoms of cerebrovascular disease is suggested: Clinical examination is followed by CT scan and complete Doppler examination of extra- and intracranial circulation. If this yields a lesion deemed suitable for surgical intervention, the patient will undergo testing of circulatory reactivity with the CO_2 test (3). If this shows a markedly reduced reactivity, the patient is considered a satisfactory candidate for cerebral revascularization and angiography is performed to delineate the type of revascularization he may need. If no such lesion is found, no angiography is performed and the patient is followed under conservative therapy. This protocol should help to reduce the number of unnecessary angiographies that carry a certain risk to the patient even when performed as DSA studies.

References

1. Aaslid R (ed)(1986) Transcranial Doppler sonography. Springer, Wien New York
2. Harders A (1986) Neurosurgical applications of transcranial Doppler sonography. Springer, Wien New York
3. Widder B (1985) Der CO_2-Test zur Erkennung hämodynamisch kritischer Carotisstenosen mit der transkraniellen Doppler-Sonographie. Dtsch Med Wochenschr 110:1553

New Aspects of Vasospasm Evaluated in 100 Patients with Aneurysm, Subarachnoid Hemorrhage, and Acute Operation: A Transcranial Doppler Study

A. Harders, J. Gilsbach, and G. Laborde

Neurochirurgische Universitätsklinik, Hugstetter Straße 55, D-7800 Freiburg

Introduction

Before the development of the transcranial Doppler machine (3), cerebral arterial vasospasm could only be detected by angiography. Using this method, the incidence of vasospasm was primarily detected in large clinical series. Patients underwent repeated angiography only twice or three times when they showed neurological dysfunctions (7, 11, 14). With the transcranial Doppler machine it is possible to investigate atraumatically the compensatory blood flow velocity increase that is due to arterial vessel lumen narrowing. Thus the individual time course of vasospasm in the different segments of the circle of Willis can be observed (1, 2, 5, 13). The influence of a well or poorly functioning circle of Willis as a result of collateral flow can be measured. Clinical deterioration after subarachnoid hemorrhage (SAH) apart from vasospasm may be caused by intracerebral hemorrhage, edema, infarction, or hydrocephalus. The differential diagnosis of the cause of postoperative delayed neurological deficits can now be carried out using the transcranial Doppler measurements.

Patients and Methods

One hundred consecutive patients who were treated by early aneurysm surgery within 72 h after the SAH underwent transcranial Doppler investigations at least every third day. Blood flow velocities were measured in the middle cerebral artery (MCA), the internal cerebral artery (ICA), the precommunicating segment of the anterior cerebral artery (A_1), the precommunicating segment of the posterior artery (P_1), the siphon, and the basilar artery (BA) (5). All patients prophylactically received nimodipine at intravenous doses of 2 or 3 mg/h (4, 8, 12). During the operation, blood clot evacuation was performed just enough to dissect the aneurysm, but not more. All patients were kept normotensive, but when the Doppler measurements showed a rapid increase in blood flow velocity, induced hypertension therapy was indicated.

Results

The vessel lumen narrowing due to vasospasm revealed by angiography could be correlated in eight patients with the transcranial Doppler measurements. There was an inverse relationship of vessel lumen diameter and the frequencies. In MCA and ICA it was statistically significant, while the compensatory frequency increase in A_1 was much less because there is collateral flow (Fig. 1).

Advances in Neurosurgery, Vol. 16
Ed. by W. Walter, M. Brandt, M. Brock, and M. Klinger

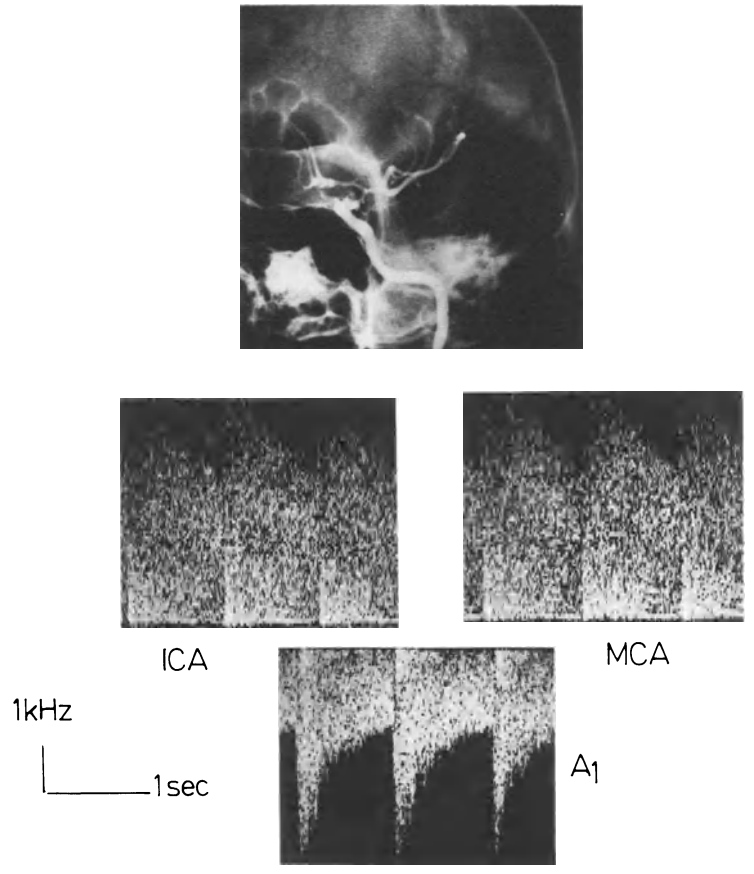

Fig. 1. Angiographically demonstrated vasospasm 11 days after SAH in correlation with the corresponding Doppler findings in the proximal segment of the MCA, the distal part of the ICA, and the precommunicating segment of the anterior cerebral artery on the left side. While angiographically the vessel lumen diameter in all three segments of the circle of Willis is nearly the same, the hemodynamic blood flow velocity increase is lowest in A_1 because there is no need for a compensatory blood flow velocity increase since there is collateralization via the anterior communicating artery

In the first 72 h after the last SAH not one of the 100 patients showed angiographic signs of vasospasm, nor any velocity increase that would correspond to vessel lumen narrowing.

The typical frequency changes after SAH and early aneurysm surgery are shown in Fig. 2. On the side of the transsylvian approach the frequency increase was usually higher than on the contralateral side. There was a frequency increase up to day 10, then a more or less rapid reduction during the next 4 weeks.

Which segments of the circle of Willis showed the greatest vasospasm reaction? The largest hemodynamic changes occurred in the main trunk of the MCA followed by the supraclinoid portion of the ICA. Medium

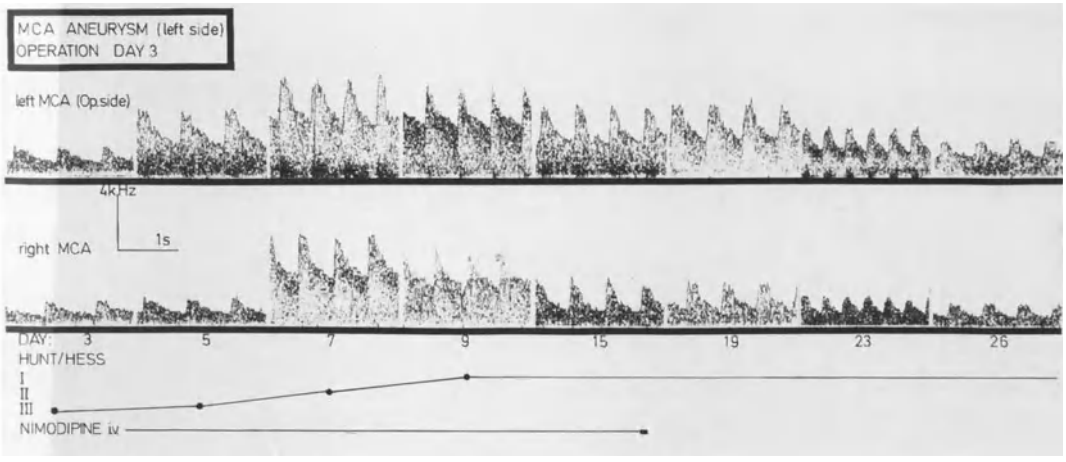

Fig. 2. Time course of frequency changes. Although the frequencies increased up to day 10, the clinical status improved continuously up to day 9. The frequencies were higher on the side on which the sylvian fissure was split. Frequencies decreased slowly up to day 15, then increased from day 15 to day 19 after intravenous administration of nimodipine had been discontinued

hemodynamic changes occurred in A_1 and in the siphon, while the least occurred in the posterior cerebral artery and in the basilar artery. These findings were almost always reproducible, even in those patients who suffered severe subarachnoid hemorrhage with massive blood clots in all basal cisterns.

Nine patients who developed delayed ischemic deficits due to vasospasm showed a rapid increase on the side of the operative approach between day 3 and day 8 after SAH, which was statistically significantly higher than on the contralateral side (Fig. 3). The neurological deficits were transient in eight patients. One patient died due to vasospasm in combination with an unintended hypotonia. The neurological deficits all occurred during the second week and the velocities in the corresponding artery were 3.5 kHz or higher.

Based on this experience we classify the Doppler findings as follows: velocities up to 80 cm/s are in the normal range, velocities between 80 and 120 cm/s are called subcritical spasm, and velocities more than 120 cm/s we call critical vasospasm. A rapid day-by-day velocity increase of about 20 cm/s between the third and seventh day, based on the experience with the DID patients, we call DIDID (Doppler index of delayed ischemic deficits).

The mean values of the highest frequencies in each patient are classified in frequency ranges (Fig. 4). We divided the frequency ranges into six groups: ≤ 80 cm/s, ≤ 120 cm/s, ≤ 160 cm/s, ≤ 200 cm/s, ≤ 240 cm/s, and ≤ 280 cm/s. Only 6% of the patients never exceeded a velocity of more than 80 cm/s in one segment of the circle of Willis. The greatest percentage of frequency increases was in the group of ≤ 160 cm/s and only 4% of the patients showed a rapid increase of velocity in the first 10 days after SAH (≤ 280 cm/s).

The time course of vasospasm is nearly constant and varies only in its severity: between day 0 and day 3 after SAH there is no vasospasm; a

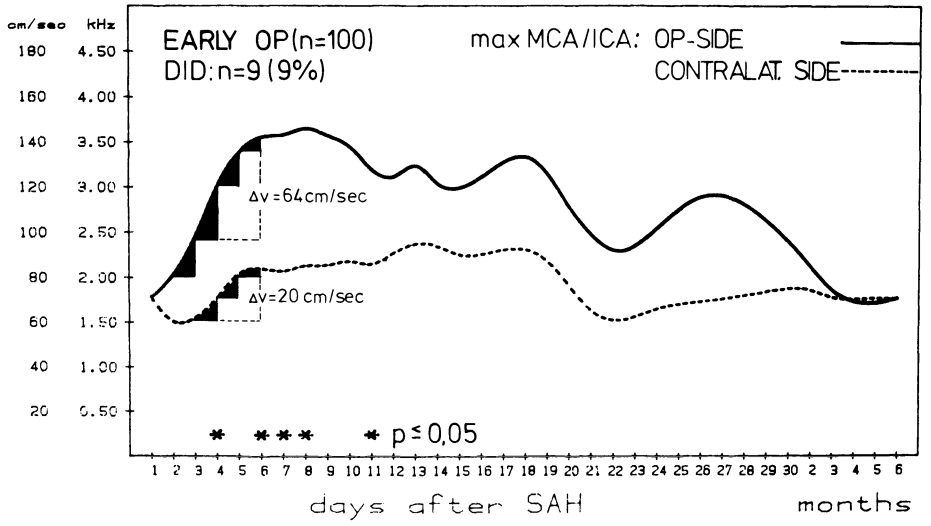

Fig. 3. Patients with transient (8%) and permanent (1%) delayed ischemic deficits due to vasospasm showed a rapid increase of blood flow velocity on the side of the operative approach either in MCA or ICA. The day-by-day increase was about 20 cm/s between day 4 and day 8. This was statistically significant compared with the velocity increase of the contralateral side. This prognostic sign - rapid increase in velocities based on the Doppler findings - is called DIDID (Doppler index of delayed ischemic deficits)

period of increase occurs between day 4 and day 10; the maximum level is reached between day 11 and day 18; and a period of decrease occurs between day 19 and 2 months after the last SAH.

Discussion

Using the transcranial Doppler method it has for the first time become possible to measure atraumatically and repeatedly the blood flow velocities through the skull. Angiography while the patient is suffering vasospasm is 5-10 times more dangerous than in patients who have no cerebral vascular disease (9, 10). There are no reliable clinical signs of vasospasm. Neurological deficits may be caused by infarction, operative trauma, edema, intracerebral bleeding, or hydrocephalus. With the transcranial Doppler method it is possible to measure the individual hemodynamic reaction to the vessel lumen narrowing. In 98% of the patients reliable signals could be obtained postoperatively through the skull. The statistically significant correlation of the inverse relationship of vessel lumen narrowing and the velocity increase was also shown by AASLID et al. (2). Spasm never occurs in the first 3 days after the last SAH and in angiography the arterial lumen seems to be dilated (5, 6). Ninety-four percent of the patients show hemodynamic changes due to vasospasm in one or more segments of the circle of Willis and its maximum is not reached until day 10. Reduction of blood flow velocity lower than the corresponding critical spasm is reached at the latest after the third week following SAH. Prognostic signs of developing neurological ischemic deficits can be measured by a rapid increase in velocity between day 4 and day 10. The patients can be treated with induced hypertension therapy before

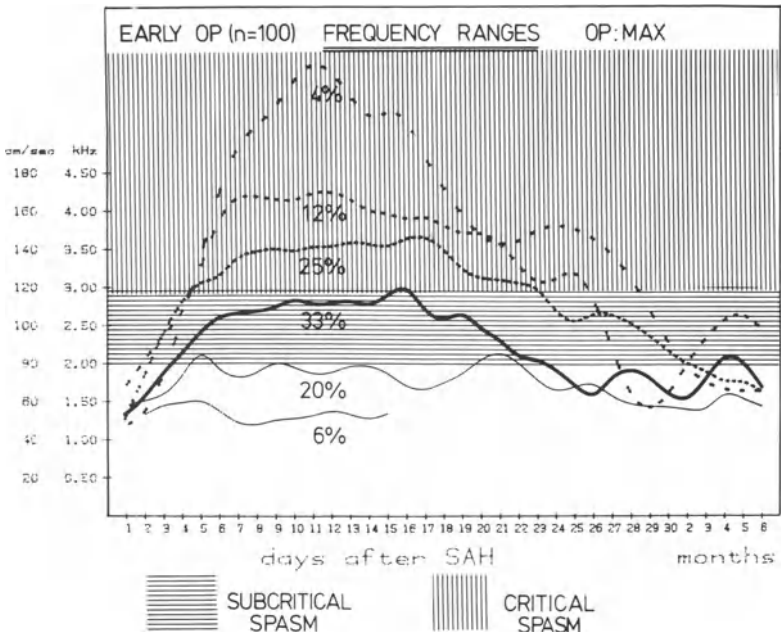

Fig. 4. Frequency ranges of the 100 patients in the time course of the blood flow velocity increases. The ranges are ≤ 80 cm/s, ≤ 120 cm/s, ≤ 160 cm/s, ≤ 200 cm/s, ≤ 240 cm/s, and ≤ 280 cm/s. Only 6% of the patients showed no hemodynamic reaction to the subarachnoid hemorrhage, while 74% were categorized as displaying critical spasm

neurological symptoms start. The time course of the frequency ranges is always the same and varies only in its severity. Even on the side of the transsylvian approach with sylvian fissure splitting and blood clot evacuation, these arteries show more vasospasm than the arteries on the contralateral side. This may be due to the fact that the vasoactive substances which may be the reason for vasospasm can reach the vessel walls more easily. Only 6% of the patients will never show significant velocity increases and therefore no vasospasm on angiography. Twenty percent will show only slight vessel lumen narrowing, i.e., less than 30%.

When the time course of vasospasm is known, delayed aneurysm surgery after severe subarachnoid hemorrhage should not be started until the maximum level of vasospasm is over. This is statistically calculated at the end of the third week after SAH. Delayed angiography and operation at the end of the second week after SAH may be dangerous because the maximum level of vasospasm has just been reached. The different types of vasospasm described in the literature as acute, early, postoperative, late, and chronic are obsolete.

Angiography to demonstrate vasospasm has been made unnecessary by the introduction of transcranial Doppler sonography. The high incidence of neurological dysfunctions as a consequence of vasospasm described in the literature may have other reasons now that we are able to measure the hemodynamic effect of vasospasm. In our series only 8% of the patients showed transient neurological dysfunctions. One patient died due to vasospasm which became symptomatic after 2 h of hypotension.

The overall mortality in the series was 7%. This clinical outcome is the consequence of microsurgery, early aneurysm operation, nimodipine prophylaxis, and transcranial Doppler guided hypertension therapy.

References

1. Aaslid R (ed) (1986) Transcranial Doppler sonography. Springer, Wien New York
2. Aaslid R, Huber P, Nornes H (1984) Evaluation of cerebrovascular spasm with transcranial Doppler ultrasound. J Neurosurg 60:37-41
3. Aaslid R, Markwalder Th-M, Nornes H (1982) Noninvasive transcranial Doppler ultrasound recording of flow velocity in basal cerebral arteries. J Neurosurg 57:769-774
4. Auer LM (1984) Acute operation and preventive nimodipine improve outcome in patients with ruptured cerebral aneurysms. Neurosurgery 15:57-66
5. Fox JL, Ko JP (1978) Cerebral vasospasm: A clinical observation. Surg Neurol 10:269-275
6. Harders A (1986) Neurosurgical applications of transcranial Doppler sonography. Springer, Wien New York
7. Hashi K, Meyer JS, Shinmaru S, Welch KMA, Teraura T (1972) Cerebral hemodynamic and metabolic changes after experimental subarachnoid hemorrhage. J Neurol Sci 17:1-14
8. Kodama N, Mizoi Y, Suzuki J (1980) Incidence and onset of vasospasm. In: Wilkins RH (ed) Cerebral arterial spasm. Williams and Wilkins, Baltimore London, pp 361-365
9. Ljunggren B, Brandt L, Säveland H, Nilsson PE, Cronqvist S, Andersson KE, Vinge E (1984) Outcome in 60 consecutive patients treated with early aneurysm operation and intravenous nimodipine. J Neurosurg 61:864-873
10. Mani RL, Eisenberg RL, McDonald EJ, Pollak JA, Mani JR (1978) Complications of catheter arteriography: analysis of 5000 procedures. I. Criteria and incidence. Am J Roentgenol 131:861-865
11. Mani RL, Eisenberg AL (1978) Complications of catheter cerebral arteriography: Analysis of 5000 procedures. II. Relation of complications rates to clinical and arteriographic diagnoses. Am J Roentgenol 131:867-869
12. Saito J, Sano K (1980) Vasospasm after aneurysm rupture: Incidence, onset and course. In: Wilkins RA (ed) Cerebral arterial spasm. Williams and Wilkins, Baltimore London, pp 294-301
13. Säveland H, Ljunggren B, Brandt L, Messeter K (1986) Delayed ischemic deterioration in patients with early aneurysm operation and intravenous nimodipine. Neurosurgery 18:146-150
14. Seiler RW, Grolimund P, Aaslid R, Huber P, Nornes H (1986) Cerebral vasospasm evaluated by transcranial ultrasound correlated with clinical grade and CT-visualized subarachnoid hemorrhage. J Neurosurg 64:594-600
15. Weir B, Grace M, Hansen J, Rothberg Ch (1978) Time course of vasospasm in man. J Neurosurg 48:173-178

Intraoperative Doppler Sonography During Surgery of the Cervical Spine

P. Knöringer

Bezirkskrankenhaus, Neurochirurgische Abteilung der Universität, Ludwig-Heilmeyer-Straße 2, D-8870 Günzburg

Introduction

In the surgical management of trauma to the cervical vertebrae, rheumatic dislocations or instabilities, and extradural tumors, the artery can be jeopardized during repositioning or tumor removal as well as during stabilization by osteosynthetic measures. It seems appropriate in these cases to determine the position of the artery by means of an intraoperative ultrasound examination, in order to reduce the danger of damage (Table 1).

Table 1. Indications for intraoperative Doppler sonography of the cervical spine

Osteosynthesis
Transarticular screw fixation of C1/2
Transpedicular screw fixation of C2
Tumor resection
Hourglass neurinoma
Tumors of the lateral cervical spine
Removal of the entire vertebra
Luxation and compression fractures
Vascular surgery
Uncoforaminotomy
Vascular surgery for arteriovenous malformations and fistulas
Vascular anastomoses

Transarticular Dorsal C1/2 Screw Fixation According to MAGERL

This procedure is indicated for Jefferson fractures, pseudarthroses of the dens, and atlantoaxial instabilities caused by os odontoideum or rheumatic affection of the transverse atlantic ligament.

The spinous processes and vertebral arches of C1-3 are prepared down to the small vertebral joints using a median incision from occipital to C7 in a seated or prone position. After the subperiosteal prepa-

Advances in Neurosurgery, Vol. 16
Ed. by W. Walter, M. Brandt, M. Brock, and M. Klinger

ration of the roots of C2 in their medial aspects, one Kirschner wire is drilled into each of the lateral masses of C1 a little above the surfaces of the lower joints. This protects the roots of C2. The joints C1/2 can be visualized by lifting the Kirschner wires and their cartilage can then be removed. Fixation with 3.5-mm corticalis screws is done after a hole is predrilled with a 2-mm drill or a 1.8-mm Kirschner wire and thread cutters under lateral X-ray control. The bore hole exists in the caudal region of the transition of the lamina into the joint mass of C2. The direction is sagittal and slanted upwards; orientation is maintained by aiming at the anterior arch of the atlas under lateral X-ray control. The screws then perforate the upper joint surface of C2 between the backward and middle third and enter the lower joint surface of C1. They are to ventrally fix the lateral mass with 1.5 threads of the screw. In the case of Jefferson fractures, spongy bone is inserted between the joint surfaces prior to tightening the screws; an interarcual fusion according to Brooks is subsequently performed for the other indications. The preoperative procedures include lateral and transoral X-rays of the spine as well as axial CTs in 2-mm layers. Variations in the course of the vertebral artery can be recognized on the CT scans. The course of the artery in C2 can additionally be determined by sonography. In old, dislocated Jefferson fractures, where the laterally displaced lateral masses can no longer be entirely repositioned, the screws have to diverge slightly outward instead of into the sagittal plane, so that they do not medially miss the lateral masses. This direction increases the danger of vascular damage, so that the artery should be localized by Doppler sonography in these cases (Fig. 1a-d).

The procedure permits secure stabilization but entails the loss of head rotation. A preoperative CT, exact demonstration of the anatomy, and intraoperative Doppler sonography can securely prevent damage to the vertebral artery.

Transpedicular C2 Screw Fixation According to Judet

The indication for transpedicular screw fixation of C2 is given in Hangman's fractures, where the bony trauma component outweighs the discoligamentous component and conservative treatment is not warranted. Surgical preparation, positioning, and exposure are as for the screw fixation of C1/2. This is also true for the entry point of the screws. The direction of the bore hole and screws converges slightly to the middle and ascends slightly cranially, approximately parallel to the upper margin of the lamina and arch root. The danger of damaging the vertebral artery in this osteosynthetic procedure is greater than when transarticular screw fixation of C1/2 is performed. If the arch root is presented on the medial side and the position of the vertebral artery is demonstrated by sonography, transpedicular screw fixation can be performed between these landmarks without endangering the dura, the spinal column, nerve roots, and, above all, the vertebral artery (Fig. 2a-d).

Tumors

The demonstration of a (usually) ventrally or laterally displaced vertebral artery has been very effective in the removal of hourglass neurinomas. Intraoperative Doppler sonography has been a particularly invaluable aid for the localization of this vessel in recurrent tumors, which often encase the artery.

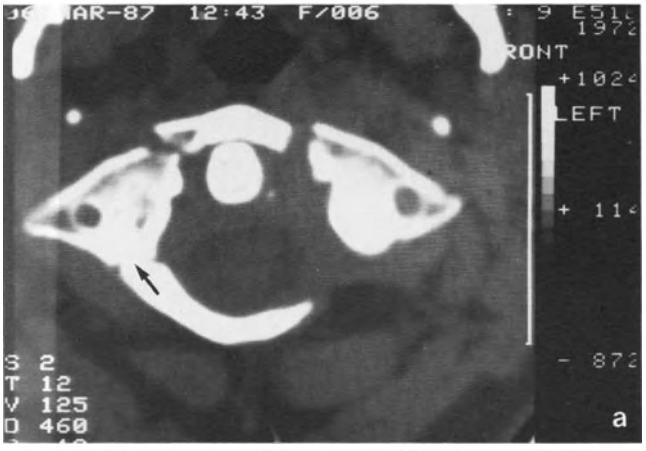

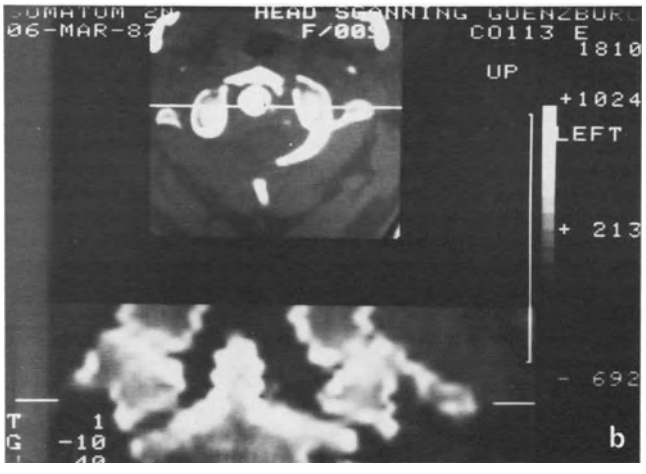

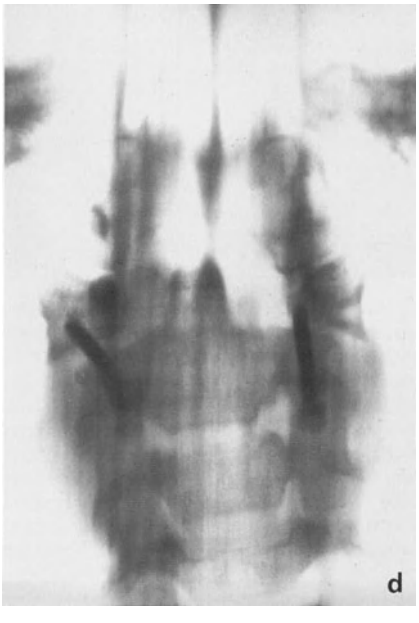

Fig. 1a-d. Roentgenograms and CAT scans of an old unstable healed Jefferson fracture, stabilized by posterior transarticular C1/2 screw fixation. a Preoperative axial CT of the fractured atlas. b Coronal reconstruction in CAT scan showing the dislocation of the lateral masses. c Lateral X-ray after posterior transarticular C1/2 screw fixation. Spongy bone is inserted between the dorsal parts of the joints. A posterior interarcual fusion is not possible because of the fractured posterior arch of the atlas. The right part of the fractured arch of C1 is also screwed. d Coronary X-ray tomogram for demonstration of the transarticular screw fixation of C1/2. The screws diverge slightly outward, so that they do not medially miss the nonreducible laterally dislocated lateral masses

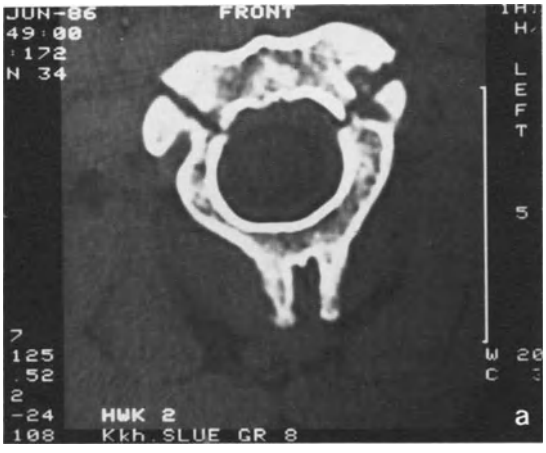

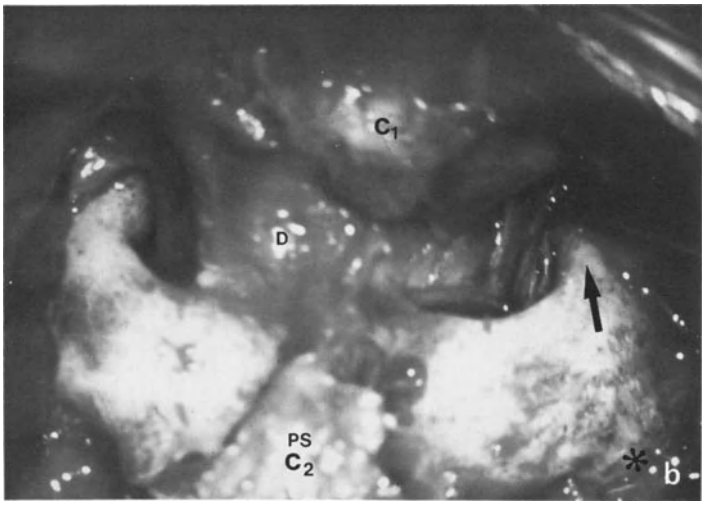

Fig. 2a-d. Transpeducular C2 screw osteosynthesis in a Hangman's fracture. a Axial CT of C2 showing the fracture lines in the arch roots reaching into the body of C2 and on the left into the transverse foramen. b Operative site, C1/2. *C1*, posterior arch of the atlas; *PS C2*, spinous process of C2; *D*, dura. The *star* marks the entry point and the *arrow* the direction of the screw. The arch roots of C2 are prepared subperiosteally. With intraoperative Doppler sonography the position of the vertebral artery can be demonstrated. Between these landmarks the transpedicular screwing can be performed without endangering the dura, spinal column, and vertebral artery. c Axial CT and diagonal reconstruction after transpedicular screwing of C2. The screws compress the fractured parts (*arrows*), passing between the inner margin of the pedicle and the transverse foramen. The screw direction is slightly converging to the middle (axial CT) and ascending cranially parallel to the upper part of the pedicle (reconstruction) without reaching the joints C1/2. d Lateral roentgenogram of the same case

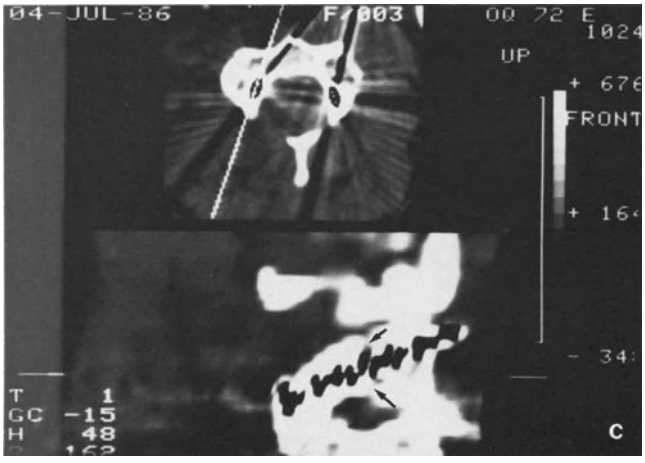

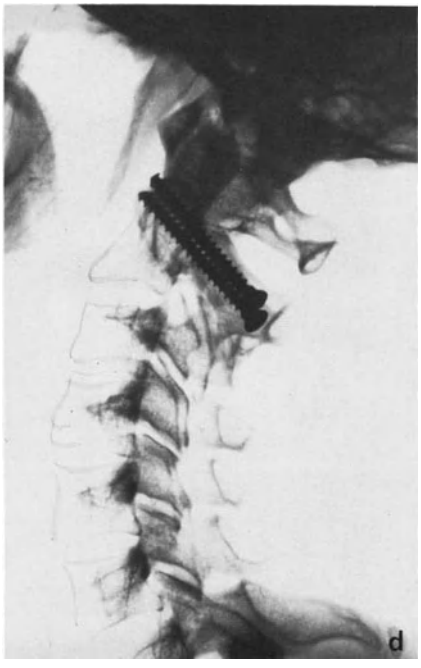

Fig. 2c,d

Extradural tumors extending primarily in a lateral direction cause neurological deficits and unbearable radicular pain by encasing the roots. Radical tumor removal should be attempted to relieve the roots and to prevent a local recurrence. In the dorsal procedure, the tumor masses are removed from the dura and the roots are then decompressed with microsurgical techniques from dorsal until there is healthy tissue. Subsequently, the vertebral artery is localized by Doppler sonography between the roots and the tumor is removed ventrally with the aid of the CUSA instrument. Even larger tumors can be resected in this way between the roots and the vertebral artery (Fig. 3a-c). The ventrodorsal procedure usually becomes necessary for reasons of stability only if the vertebral body is affected.

The combined ventrodorsal access permits the total removal of a vertebra. Intraoperative Doppler sonography, which can be used in the ventral and dorsal portion of the procedure, contributes to the prevention of a lesion of the vertebral artery.

In dorsal osteosyntheses, like plate and hooked plate osteosynthesis, the screws are anchored into the joint masses. If, as proposed by MAGERL, they enter the joint mass in the center between the upper and the lower joint surface near the transition to the lamina, and then run a course 30° outward and parallel to the joint surfaces, then the hardest portion of the vertebra is being fully used for anchoring. When correctly applied, this procedure entails no danger to nerve roots or the vertebral artery, so that intraoperative Doppler sonography is not necessary.

A further indication for intraoperative Doppler sonography is the management of luxation and compression fractures, particularly when

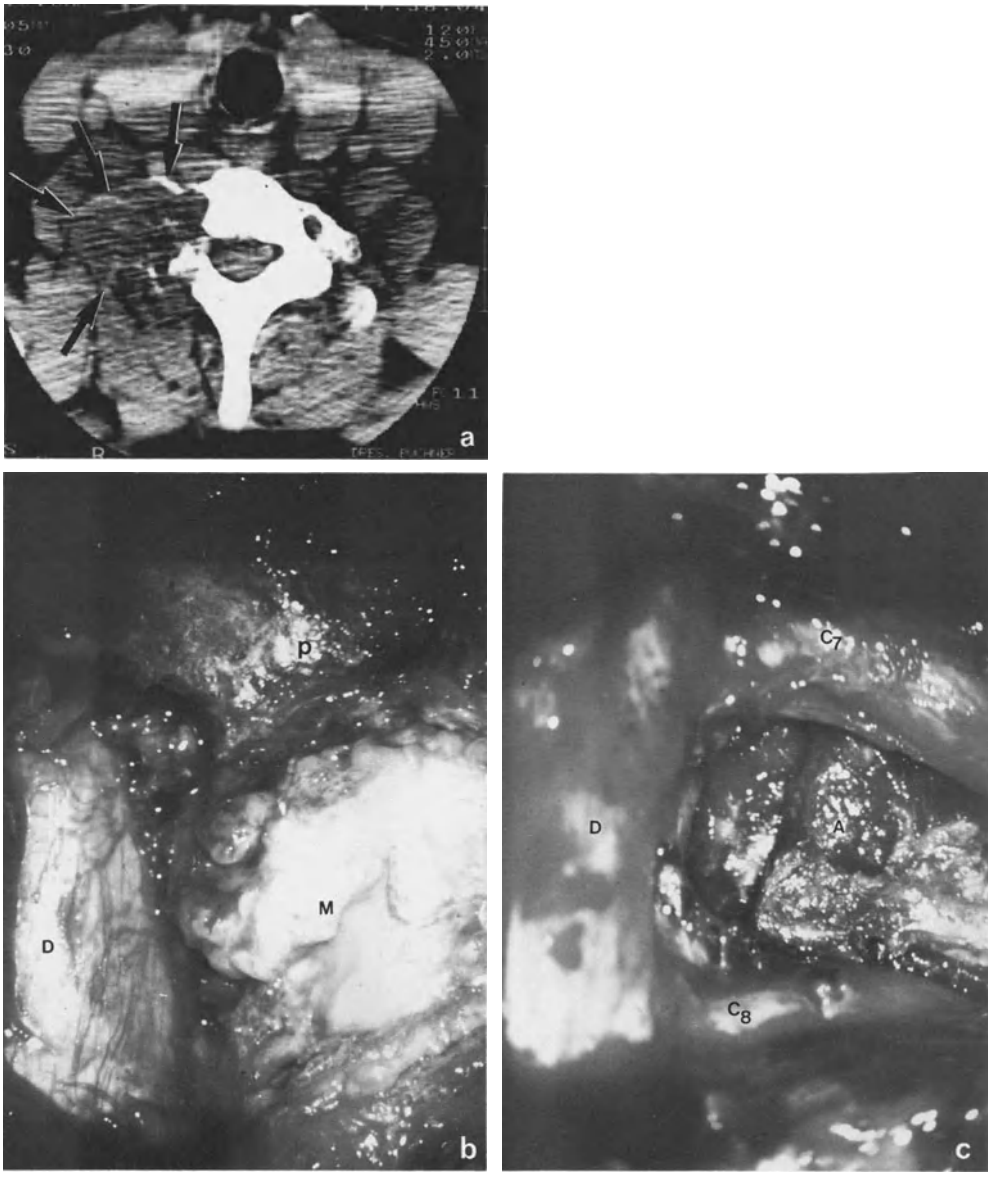

Fig. 3a-c. a CAT scan of C7, showing a metastasis from a hypernephroma *(between arrows)* localized on the right lateral part of the vertebra and causing unbearable radicular pain in the region of C7 and C8 with neurological deficit. The vertebral artery is surrounded by the tumor. b Hemilaminectomy is carried out on the right. *D*, dura; *M*, metastasis surrounding the vertebral artery and compressing the C7 and C8 roots; *P*, right inferior articular process of C6. c Operative site after resection of the metastasis. The roots (C7, C8) are decompressed. The artery vertebral (*A*) and the body of C7 (between dura and artery) are visible. During operation, Doppler sonography was used

there are preoperative signs of vertebrobasilar insufficiency, like rotatory vertigo, nausea, and vomiting. In these cases, the reestablishment of normal blood flow can be ascertained after repositioning and stabilization. If normal blood flow has not been reestablished, angiographic diagnostics should be performed soon, because involvement of the vertebral artery in cervical spine trauma is probably more common than is generally assumed.

Intraoperative Doppler sonography is also of great value in decompression operations of the vertebral artery (uncoforaminotomy) and in the treatment of arteriovenous deformations as well as of traumatic fistulas and vascular anastomoses in the PICA region and the region of the vertebral artery itself.

Conclusion

Doppler sonography constitutes a relatively simple procedure by which the position and the course of the vertebral artery can be demonstrated intraoperatively. One the one hand, this makes surgery of the lateral parts of the cervical spine safer by reducing the risk of damaging the vertebral arteries, and on the other hand the vessels can be more easily and quickly located during vascular surgery.

References

1. Knöringer P (1986) Osteosynthesis in patients with malignant tumors of the cervical vertebral column: indications, technique and results. In: Wenker H, Klinger M, Brock M, Reuter F (eds) Advances in neurosurgery, vol 14. Springer, Berlin Heidelberg New York, pp 125-132
2. Magerl F, Seemann PS (1987) Stable posterior fusion of the atlas and axis by transarticular screw fixation. In: Kehr P, Weidner A (eds) Cervical spine I. Springer, Wien, pp 322-327

Evoked Potentials

Useful Parameters in Intraoperative Monitoring of Evoked Potentials

J. Schramm, E. Watanabe, C. Strauss, C. Cedzich, and R. Fahlbusch

Neurochirurgische Klinik der Universität Erlangen-Nürnberg, Schwabachanlage 6, D-8520 Erlangen

The basic concept of intraoperative monitoring using evoked potentials is based upon the assumption that neuronal tract systems which can be monitored with electrophysiological methods may be saved from permanent functional damage. After having established this difficult technique and having more precisely delineated the range of normal variations (2, 4, 6), we can now try to describe more precisely some possibly useful parameters and the relationship between postoperative neurological findings and intraoperative changes in potential.

Patients and Methods

More than 350 monitoring procedures were done using somatosensory evoked potentials (SEPs), acoustic evoked brain stem potentials (BAEPs) and visual evoked potentials (VEPs). The methods have been described in detail elsewhere (1, 3). We have now monitored over 75 patients with space-occupying spinal lesions, over 50 aneurysm patients, 130 posterior fossa lesions, and 35 space-occupying lesions close to the visual pathways, and we have performed anesthesiological studies in over 100 patients (12, 13). Some of these results have been published (3, 5, 7, 11) or will be published soon (1, 6, 8, 9, 10, 13, 14).

A Summary of Experiences

In applying these techniques two types of learning effect may be differentiated: (a) general effects of learning, which are useful to develop the method and which need not be discussed in detail here (Table 1), and (b) special effects of learning, which may be of great interest to the neurosurgeon thinking of applying this method. There are three special effects of learning (Table 1).

1. Precise Identification of Periods of Functional Danger

We have learned to outline more precisely these periods of endangerment. They are often well enough known without neuromonitoring, as, for example, in aneurysm surgery, but they may be more precisely identified with neuromonitoring, often with surprising results. Two examples will be given: In acoustic neurinoma surgery we learned that AEPs preferably disappear in association with certain surgical maneuvers, e.g., dissection close to or in the meatus or the placement of the brain retractor (Fig. 1). In the second example, a case of spinal cord compression, we detected that the period of decompression may be dangerous. In fact during the removal of the thoracic disk the cortical po-

Advances in Neurosurgery, Vol. 16
Ed. by W. Walter, M. Brandt, M. Brock, and M. Klinger

Table 1. Effects of learning

General effects of learning
1. Optimization of anesthetic and recording technique
2. Effectivity in failure reduction
Special effects of learning
1. Precise identification of periods of possible functional damage
2. Support and guidance in obviously dangerous surgical steps
3. Increase in knowledge about perioperative functional loss by correlation to particular surgical maneuvers

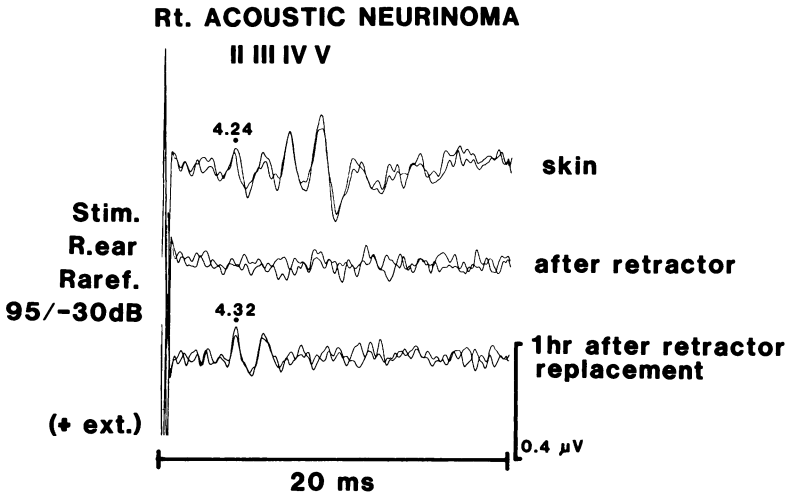

Fig. 1. Potential alteration due to retractor placement in a 44-year-old female with acoustic neurinoma. After reacting to the potential loss by replacing the retractor there was a partial recovery of the BAEP with reappearance of waves II and III. [SCHRAMM et al. (9)]

tential was lost at the very moment at which the sequestered disk was removed from the spinal canal. In this patient there was postoperative neurological deterioration (Fig. 2).

2. Support and Guidance in Obviously Dangerous Steps of Surgery

Apart from the already mentioned dissection of the eighth nerve, two more examples can be given. First, trapping of an aneurysm at a major cerebral artery: in one case with trapping of a PICA aneurysm (Fig. 3) during a period of temporary clipping the normal AEPs and SEPs reassured the surgeon that he could continue with his procedure from temporary to permanent clipping. In the second case (Fig. 4) we initially planned only a partial tumor removal. During a left paramedian occipital approach the tumor was removed starting with the infratentorial portion and then from the pineal region area; encouraged by the constantly good bilateral SEPs and AEPs we proceeded to a nearly total

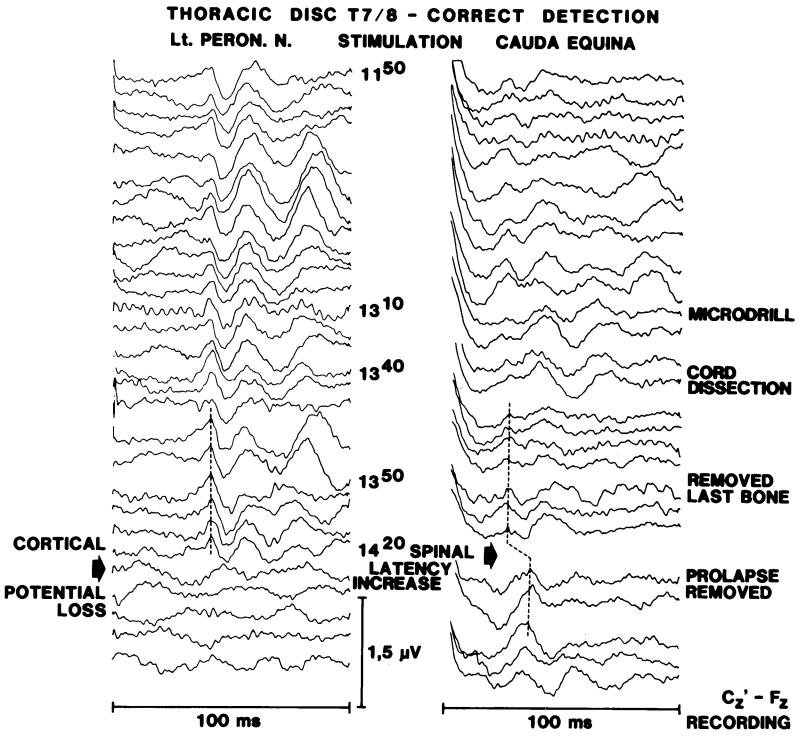

Fig. 2. This patient with a thoracic disk prolapse developed postoperative impairment of function and showed intraoperative loss of cortical potential exactly in the cortical SEP recording completed after the disk fragments were pulled back from the spinal canal into the space created by the microdrill in the vertebral body during the lateral transthoracic approach. Without monitoring SEPs the patient would have been neurologically worse postoperatively and the surgeon would most likely have thought that he injured the spinal cord during another step of dissection like drilling away the vertebral body or dissecting the prolapse off the dural sac. The old clinical saying that decompression may be as harmful as compression is nicely demonstrated in this case. At the same time it is noteworthy that the cortical potentials obtained after stimulation of only one peroneal nerve behaved differently from those obtained after cauda equina stimulation. [WATANABE et al. (14)]

removal (leaving only a 1-cm tumor remnant at the right side of the great vein of Galen into the sinus rectus).

3. Increase in Knowledge About Perioperative Functional Loss

The third group of special effects of learning describes the knowledge we have gained about the pathophysiology of perioperative impairment of neurological function by directly proving the dangerousness of particular surgical maneuvers. One example is the loss of the AEP after the placement of the cerebellar retractor in neurovascular decompression or after coagulation of a vessel in neurinoma surgery (10). Simply by replacing the retractor to another position the potential is recov-

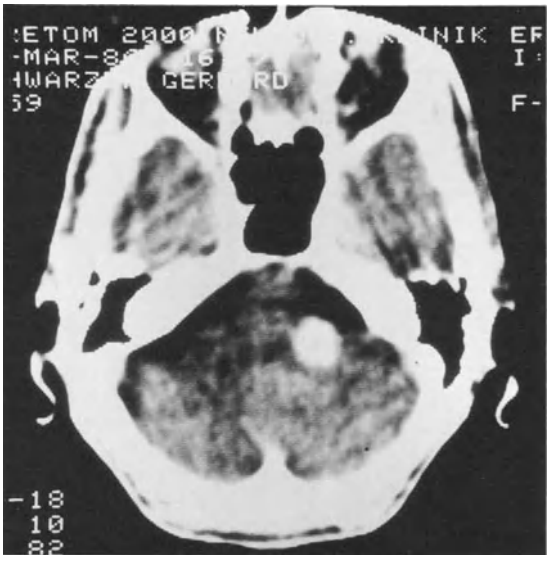

Fig. 3. Giant aneurysm of the PICA in a 35-year-old male patient, where the thrombosed part may be seen on the CT scan. Clipping with preservation of the PICA was not possible; therefore, after temporary trapping without changes in potential, a permanent trapping of the PICA was performed and the aneurysm unpacked and thus the indented brain stem decompressed. There was no postoperative morbidity

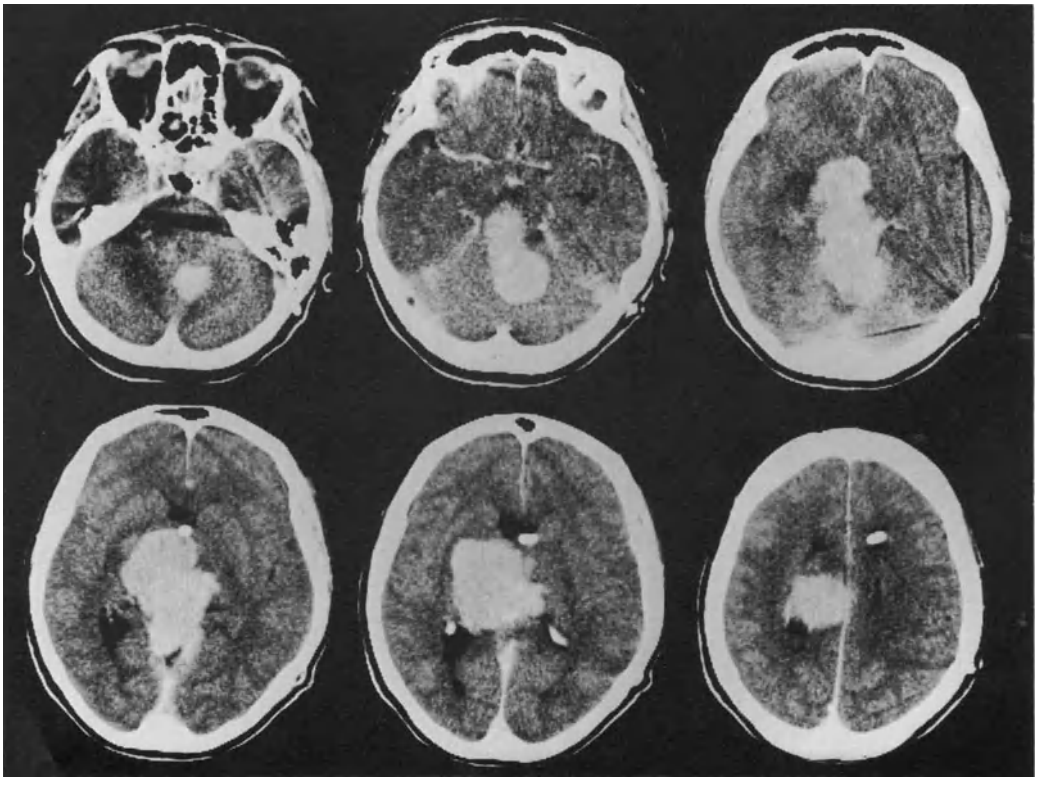

ering quickly. Other examples are seen in spinal tumors, where in our four cases with neurological deterioration the evoked potential impairment was seen twice during decompression. In aneurysm surgery we gained more precise knowledge about the time span between a particular surgical maneuver (i.e., temporary clip placement) and the loss of the potential associated with a neurological deficit.

Useful Parameters

In conclusion there are parameters which have been demonstrated to be useful at our current state of knowledge. Among these parameters are the disappearance of wave I, wave V, or all waves of BAEP, and a marked and sudden increase in central conduction time in aneurysm surgery.

Often enough one is asked in which way changes in potential can influence the surgical procedure. Principally speaking this can happen in two ways (Table 2). The influence on surgical procedure can manifest itself by affecting a single surgical step or by changing the whole approach in a particular case. And the surgeon may be influenced either by the changing of the potential or by the lack of a change in the monitored potential. Again some examples: The surgeon may decide to replace the brain retractor or limit the duration of his temporary clip, or he may even be helped in the decision to perform extra-intracranial bypass surgery in giant aneurysms in cases of permanent evoked potential loss. If a certain change in potential does not happen although it might have happened judging from the invasiveness of a certain surgical step (e.g., occlusion of an artery), the surgeon may feel safe to proceed from probative to permanent vessel occlusion as may be necessary in certain aneurysms.

Table 2. Influence on surgical planning

In particular case
As reaction to EP change
As reaction to lack of EP change
Generally
Principal change in surgical tactics
Cancelling of single surgical steps
Performing riskier surgery
Easier decision for riskier procedure

◀ Fig. 4. 50-year-old female with a large meningioma extending from infratentorially through the tentorial hiatus into the ventricular system. It was either a primary intraventricular meningioma with secondary attachment ot the tentorial notch or a primary notch meningioma. This patient had gaze paralysis and a sensory hemisyndrome on the right side; the main disturbances were, however, psychopathological: slow mentation, acalculia, and dysgraphia. For years the patient had rejected surgery and only 1 year before the current operation had accepted shunt surgery. There was no postoperative morbidity apart from mild transient weakness of the right arm

Negative Experiences

We also, however, have a negative experience to report. In our hands the use of flash evoked visual potentials in the surgery of space-occupying lesions close to the visual pathways was not useful as there were too many false-positive findings, i.e., the incidence of losses in potential without any neurological sequelae was much too large (1). Whether any new techniques will improve this is currently uncertain. We have also seen cases of brain stem morbidity which were not detected by BAEP monitoring (9), as they appeared on the second postoperative day. The reasons for false-negative cases, i.e., cases where there is morbidity of the monitored pathways despite normal EPs, are manifold and have just been started to be discussed in some publications. But there are other possibilities of having postoperative deficits despite monitoring, namely the appearance of a deficit in a pathway system not available for monitoring. It should surprise nobody if SEP and BAEP monitoring in cerebellopontine angle surgery does not detect motor deficits.

A Word of Caution

This summary is based on the combined efforts of a variety of people (doctors, research associates, and graduate students) working in the neuromonitoring group at the University of Erlangen-Nürnberg. This method is not easily introduced into everyday practice and at present in many respects it is still a research tool. The evaluation of the data was time consuming and greatly facilitated by modern computer equipment and application of data management software. So it is quite obvious not only that the introduction of neuromonitoring for clinical purposes is very demanding in terms of personnel, but also that the scientific evaluation of this new procedure needs an even greater number of man-hours.

Conclusions

Neuromonitoring is a complicated and time-consuming technique. There still are and there always will be false-positive and false-negative findings.

With the current state of knowledge the transition from research tool to clinical tool has not yet been completed. But there are clinically useful parameters which may influence surgical procedure in particular cases. It is likely that neuromonitoring will develop into a valuable technique for monitoring nervous function for particular operations under conditions still to be defined more precisely. It will take more time and effort to definitely judge the value of this procedure for clinical practice.

References

1. Cedzich C, Schramm J, Fahlbusch R (1988) Are flash-evoked visual potentials useful for intraoperative monitoring of visual pathway function? Neurosurgery (accepted)
2. Hochstetter A, Schramm J, Fahlbusch R, Mokrusch T (1988) Variability and typical changes of brainstem acoustic evoked potentials monitored in cerebellopontine angle surgery and noncranial surgery. In: Barber C, Blum T (eds) Evoked potentials III. Butterworths, New York London

3. Mokrusch T, Schramm J, Fahlbusch R (1985) Repeatedly reversible alteration of acoustic-evoked brainstem responses with a cystic craniopharyngioma. Surg Neurol 24:571-573

4. Schramm J (1985) Spinal cord monitoring: Current status and new developments. CNS Trauma 2:207-227

5. Schramm J, Mokrusch T, Fahlbusch R, Hochstetter A (1985) Intra- und perioperative akustisch evozierte Hirnstammpotentiale bei Kleinhirnbrückenwinkel-Operationen. HNO 33:495-498

6. Schramm J, Romstöck J, Thurner F, Fahlbusch R (1985) Variance of latency and amplitude in SEPs monitored during spinal cord manipulation. In: Schramm J, Jones SJ (ed) Spinal cord monitoring. Springer, Berlin Heidelberg New York, pp 187-196

7. Schramm J, Romstöck J, Watanabe E (1986) Intraoperatives Rückenmarkmonitoring. Z Orthopädie 124:671-782

8. Schramm J, Romstöck J, Watanabe E (1988) Cortical versus spinal recordings in intraoperative monitoring of space-occupying spinal lesions.In: Barber C, Blum T (eds) Evoked potentials III. Butterworths, New York London

9. Schramm J, Mokrusch T, Fahlbusch R, Hochstetter A (1988) Detailed analysis of intraoperative changes monitoring brainstem acoustic evoked potentials. Neurosurgery (accepted)

10. Strauss C, Fahlbusch R, Schramm J, Hochstetter A (1988) Brainstem auditory evoked potentials after removal of large acoustic neurinomas with preserved hearing and hearing loss. In: Barber C, Blum T (ed) Evoked potentials III. Butterworths, New York London

11. Thurner F, Schramm J (1986) Perioperative Registrierung somatosensorisch evozierter Potentiale bei intrakraniellen Gefäßmißbildungen. Anästh Intensivmed 27:42-46

12. Thurner F, Schramm J, Romstöck J (1985) Effects of fentanyl and enflurane on cortical and subcortical SEP during general anaesthesia in man. In: Schramm J, Jones SJ (eds) Spinal cord monitoring. Springer, Berlin Heidelberg New York, pp 82-89

13. Thurner F, Schramm J, Pasch Th (1988) Wirkung von Fentanyl und Enfluran auf sensorisch evozierte Potentiale des Menschen in Flunitrazepam/N_2O-Basis-Narkose. Anästhesist (accepted)

14. Watanabe E, Schramm J, Romstöck J (1988) Cortical and spinal intraoperative recordings in uneventful monitoring and in cases with neurologic changes.In: Ducker TB, Brown RH (eds) Monitoring of the spinal cord. Springer, Berlin Heidelberg New York

Somatosensory Evoked Potentials of the Trigeminal Nerve Derived Pre- and Intraoperatively in Patients with Trigeminal Neuralgia, from the Point of View of Microvascular Decompression

O. Rommel and Th. Rommel

Neurochirurgische Klinik der Städtischen Krankenanstalten, Ostmerheimer Straße 200, D-5000 Köln 91

Introduction

Only since the cerebellopontine angle has been explored in detail has vascular compression of the trigeminal nerve at the root entry zone into the brain stem proved to be the cause of trigeminal neuralgia in a large percentage of patients with so-called idiopathic trigeminal neuralgia (1, 2). Using neuroradiological methods, symptomatic trigeminal neuralgias can normally be excluded preoperatively. However, the vascular compression that may exist defies the diagnostic procedures applied up to now. Bearing this in mind, in the following study the somatosensory evoked potentials were derived preoperatively and the direct action potentials of the trigeminal nerve were derived intraoperatively.

Materials and Methods

Trigeminal Evoked Potentials Derived Preoperatively

Twenty-eight patients with a typical trigeminal neuralgia were examined in the area of the 2nd and 3rd trigeminal branches. The evoked potentials were derived using standard methods (3). Sensitive nerve endings on the 2nd and 3rd trigeminal branches were stimulated ipsi- and contralaterally. The stimulation was carried out using clip electrodes which were fixed to the upper and lower lips. The somatosensory evoked potential was derived contralaterally using needle electrodes, of which one was localized in position C5/C6 and the other in position F_Z. Amplification, storage, and the formation of mean values were carried out on standard EMG equipment (DA II from Tönnies).

Intraoperative Derivation

In 20 patients derivations of the action potential of the trigeminal nerve were carried out intraoperatively at the root entry zone. Here, after exposing the cerebellopontine angle, the peripheral nerve endings were stimulated using clip electrodes in the labial angle. The derivation was carried out at the root entry zone using neurostimulation forceps. The potentials were presented with a tilting speed of 1 ms/cm and added up a total of 128-256 times. The comparison with the physiological action potential of the trigeminal nerve was made possible by means of an intraoperative derivation on a patient with a small acoustic neurinoma in an intrameatal position; this patient showed no symptoms with respect to the trigeminal nerve.

Advances in Neurosurgery, Vol. 16
Ed. by W. Walter, M. Brandt, M. Brock, and M. Klinger

Results

In the case of 19 patients without antecedent treatment, trigeminal evoked potentials that were easily reproducible on both sides could be derived preoperatively (Fig. 1). In 13 patients the operative findings showed vessel-dependent root compression. In these patients the mean values for the latency of the first positive potential component (P_1) were 20.23 ms on the healthy side and 20.41 ms on the diseased side; consequently, they only showed a slight, statistically insignificant lateral difference (Fig. 2). In six further patients there was no root compression. This group also showed only a slight difference between the symptomatic (P_1:19.95 ms) and the asymptomatic side (P_1:19.47 ms), which was likewise without any statistical significance.

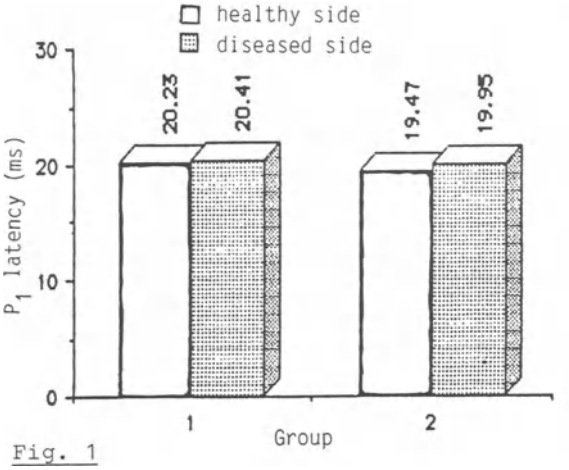

Fig. 1

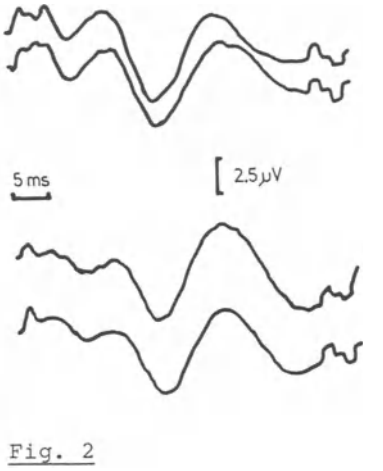

Fig. 2

Fig. 1. Comparison of cortical evoked potentials derived preoperatively between patients with distinct vascular compression (group 1, n = 13) and patients without vascular compression (group 2, n = 6)

Fig. 2. Cortical evoked potentials of the trigeminal nerve derived preoperatively in a patient with distinct vascular compression of the root entry zone

In the case of the control patient the intraoperative derivation of the action potential of the trigeminal nerve at the root entry zone resulted in an easily reproducible multipeak action potential with a distinct upward line after 3.6 ms and an amplitude of 26 V (Fig. 3). In contrast to this, the action potentials in seven patients with trigeminal neuralgia who had not received antecedent treatment, and who had distinct vascular compression, were considerably split up and also clearly reduced in amplitude (2-11.5 V)(Fig. 4). There was, however, no difference with respect to the latency of the beginning of the potential (3.1-3.7 ms) at the follow-up examination.

In six further patients with antecedent treatment for trigeminal neuralgia (thermocoagulation, etc.), a considerably altered action potential likewise appeared with a reduction in amplitude, depending on the extent to which the nerve had already been damaged.

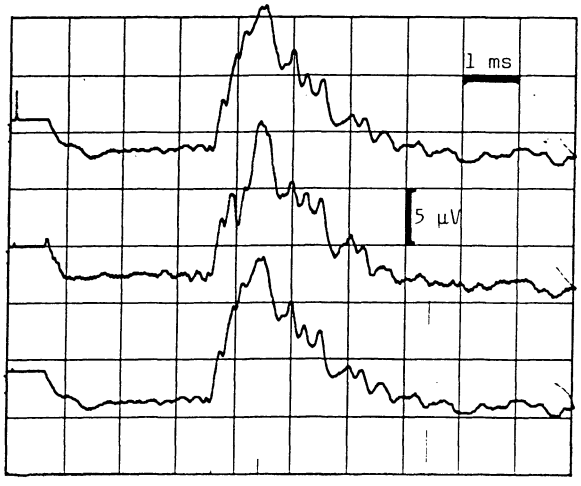

Fig. 3. Intraoperative derivation at the root entry zone in a patient with an acoustic neurinoma in an intrameatal position (control patient)

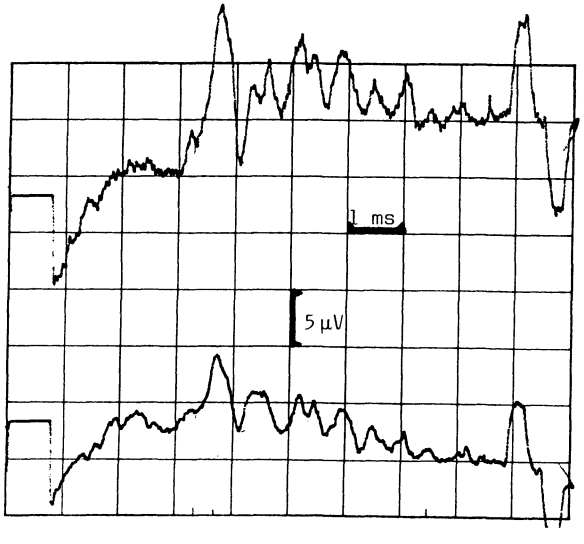

Fig. 4. Intraoperative derivation at the root entry zone in a patient with distinct vascular compression

Discussion

Our examinations could not support the hypothesis, proposed in the literature (4), that vascular compression influences the evoked potentials of the trigeminal nerve. The comparison between the evoked potentials derived preoperatively and the intraoperative findings did not result in any significant latency differences regarding the individual potential components between the symptomatic and the asymptomatic side in the case of existing vascular compression.

In the control subject intraoperative examination of the nerve action potential showed a physiological multipeak potential. This can be explained by the fact that, by means of the electrodes on the upper and lower lips, sensitive nerve endings are stimulated that belong to two different nerve stems with different paths.

The beginning of the potential after a latency of 3.6 ms indicates a nerve conduction velocity of 33-39 m/s with an estimated distance from the stimulus and place of derivation amounting to 12-14 cm. Partial damage to the trigeminal nerve - due to chronic vascular compression - produced an action potential that was distinctly split up and considerably reduced in amplitude. If the trigeminal nerve is not seriously damaged, however, the latency of the beginning of the potential at the root entry zone remains unaffected. Only if the nerve is more seriously damaged, for example as a result of preceding extensive thermocoagulation, can a prolongation in the latency of the beginning of the action potential be proven as well.

Summary

In patients with a typical trigeminal neuralgia, the evoked potentials of the trigeminal nerve that were derived preoperatively did not result in any significant changes in the potential if vascular compression had been determined intraoperatively. However, the intraoperative derivations of the action potentials of the nerve showed typical neurophysiological changes that can be related to the nerve being partially damaged. The cortical evoked potential - as the sum of all potential influences - is not, however, influenced by these changes.

References

1. Dandy WE (1934) Concerning the cause of trigeminal neuralgia. Am J Surg 34:447-455
2. Jannetta PJ, Bennett MH (1981) The pathophysiology of trigeminal neuralgia. In: Samii M, Jannetta PJ (eds) The cranial nerves. Springer, Berlin Heidelberg New York, pp 312-315
3. Stöhr M, Petruch F (1979) Somatosensory evoked potentials following stimulation of the trigeminal nerve in man. J Neurol 220:95-98
4. Stöhr M, Petruch F, Scheglmann K (1981) Somatosensory evoked potentials following trigeminal nerve stimulation in trigeminal neuralgia. Ann Neurol 9:63-66

Reliable Electrophysiologic Localization of Levels in Cervical Radiculopathy?

A. Kleider, M. Samii, A. Sepehrnia, H. Baumann, G. Penkert, and H. C. Hopf

Neurochirurgische Klinik, Krankenhaus Nordstadt, Haltenhoffstraße 41, D-3000 Hannover 1

Introduction

A major problem in neurosurgery is the precise anatomic localization of lesions. In no area is this more evident than in the diagnosis of cervical radiculopathy. Differential diagnosis has always depended on a careful clinical examination along with help provided by a classical dermatome chart. Indications for operation are derived mainly from the clinical examination supported by radiologic findings. Electrophysiologic studies play only a minor, if any, role in this decision-making process.

For cases in which some doubt remains as to the involved level, a reliable instrument for detecting early or small deficits would be invaluable. TACKMANN and RADÜ (4) demonstrated, in 1983, that the clinical value of EMG and F-waves is probably overemphasized. Only in 11 of their 20 patients was a correlation demonstrated between EMG findings and level of involvement. They felt that this was related to the multidermatomal innervation of extremity muscles as shown earlier by Brendler's intraoperative investigations (1).

More recently sensory evoked potentials (SEPs) have come into use. After disappointing results with median and ulnar nerve stimulation, dermatomal stimulation has become a popular means of investigation. With dermatomal stimulation, either the thumb or radial aspect of the forearm is stimulated to demonstrate C6. When investigating C7, the middle finger is stimulated and with C8 the little finger or ulnar aspect of the forearm. While there are both optimistic and skeptical opinions concerning this method, its actual clinical usefulness has not yet been proven. Critics argue that SEP changes are only found in patients with clear-cut clinical findings, pointing out that segmental sensory innervation, as in the multisegmental innervation of the musculature, usually consists of three or four overlapping dermatomes. This dermatomal overlap led Otfried FOERSTER to postulate that a single root could be transected without producing a clinical deficit (2). Since segmental pain pathways do not overlap to the degree of those conveying touch, one would expect to find only a small area of hypalgesia associated with a single root lesion.

Method

Stimulated by the excellent work of INOUYE and BUCHTHAL (3) published in 1977, we intraoperatively studied 30 cervical roots in 24 patients with cervical radiculopathy by electric finger stimulation. Except for one patient, who was operated on from a posterior approach, all

Advances in Neurosurgery, Vol. 16
Ed. by W. Walter, M. Brandt, M. Brock, and M. Klinger

were operated on through a modified Cloward approach with wide foraminotomies performed bilaterally. The interspace level was identified radiologically. The measurements were made following disk removal and required from 25-40 min to complete.

All the fingers on the clinically affected side were sequentially stimulated using ring electrodes (supramaximal stimuli about 10 mA, stimulation duration 100 μs, stimulus frequency between 5 and 10 Hz). The responses were recorded using needle electrodes. The recording electrode was placed in the postganglionic region of the root while the reference electrode was placed directly ventral to it in the wound margin. Analog filtering was performed with a bandpass from 100 Hz to 2 kHz. Depending on the level of artifact disturbance associated with the operating room, an average of 256-1024 sweeps was necessary. Every recording was reproduced at least once. Eight recordings could not be evaluated, secondary to uncontrollable artifacts.

In all 12 clear recordings of the C6 root, thumb stimulation produced the highest amplitude (Fig. 1, Table 1). A significantly reduced amplitude from index finger stimulation could be demonstrated in eight cases, while in the other four no potential could be found. In only four of the 12 recordings could a potential from middle finger stimulation be evoked in the C6 root again with a significant reduction in amplitude. Stimulation of the ring and little finger never produced a potential in the C6 root.

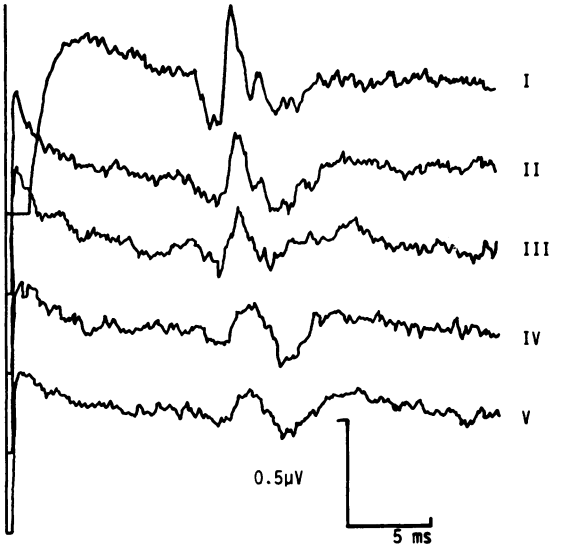

Fig. 1. Nerve root potentials obtained by sequential finger stimulation in a C6 root

The situation for C7 was somewhat more complicated (Fig. 2, Table 2). Of the ten roots, three showed the highest amplitude following stimulation of the thumb, four after stimulation of the index finger, two after stimulation of the middle finger, and only one following stimulation of the ring finger. It is interesting to note that following stimulation of the little finger, a potential on C7 could be recorded in only four patients - and it never produced the highest amplitude.

Table 1. Relationship of response rate and amplitude of response to sequential finger stimulation (n = 12). Mean level of amplitude approximately correlates to height of arrow. Roman numerals represent stimulated fingers

C6 root

			Amplitude		
I	12	–	–	–	–
II	–	8	–	–	–
III	–	–	4	–	–
IV	–	–	–	–	–

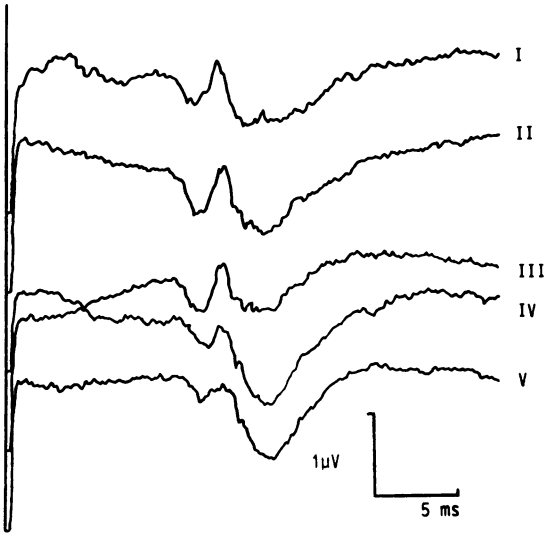

Fig. 2. Nerve root potentials obtained by sequential finger stimulation in a C7 root

Discussion

One of the main axioms of dermatomal SEP diagnostics is the reliability of stimulation points representing specific nerve roots. The goal of our investigation was the reexamination of the segmental innervation of the upper extremity by electrophysiologic means. Our first results show that C6 is clearly represented on the hand by the thumb, with the index and middle finger demonstrating a weaker and less consistent representation.

A dominant sensory distribution for C7 proved more difficult to ascertain. The index and middle finger produced potentials in every case. The thumb produced the highest potential in three of the ten cases, but in two cases it produced no detectable potential. In addition, it would seem that the little finger plays only a very small role in the distribution of C7.

Table 2. Relationship of response rate and amplitude of response to sequential finger stimulation (n = 10). Mean level of amplitude approximately correlates to height of arrow. Roman numerals represent stimulated fingers

C7 root	↑	↑	↑ Amplitude	↑	↑
I	3	-	3	1	1
II	4	4	1	1	-
III	2	5	3	-	-
IV	1	1	1	4	1
V	-	-	1	-	3

The description of dermatomal patterns as reported throughout the literature varies between authors. Our findings are consistent with those of INOUYE and BUCHTHAL (3), who felt that variation was the rule, rather than the exception, with these dermatomal patterns. Perhaps continued work with SEPs can more definitively delineate these tendencies so that the method will be able to play a more important role in the clinical evaluation of patients in the future.

References

1. Brendler SJ (1968) The human cervical myotomes: functional anatomy studied at operation. J Neurosurg 28:105-111
2. Foerster O (1933) The dermatomes in man. Brain 56:1-39
3. Inouye Y, Buchthal F (1977) Segmental sensory innervation determined by potentials recorded from cervical spinal nerves. Brain 100:731-748
4. Tackmann W, Radü EW (1983) Observations on the application of electrophysiological methods in the diagnosis of cervical root compressions. Eur Neurol 22:397-404

Experiences with the Intraoperative Single Unit Potential Recording of Spinal Cord and Cauda Equina Disorders

G. Lang and G. Schalow

Neurochirurgische Abteilung der Ernst-Moritz-Arndt-Universität, Löfflerstraße 23, DDR-2200 Greifswald

We applied the method of recording single unit potentials with wire electrodes to humans. Using two pairs of platinum electrodes it was possible to record extracellular single unit potentials at two different places in nerve root filaments smaller than 1 mm in diameter in the spinal canal and to determine conduction velocities. Afferent and efferent single unit potentials could be distinguished from each other by a reversed conduction time and a reversed potential change. It was also possible to record an activity increase due to skin receptor stimulation (Fig. 1); therefore the method can be used as a diagnostic tool during surgery (1).

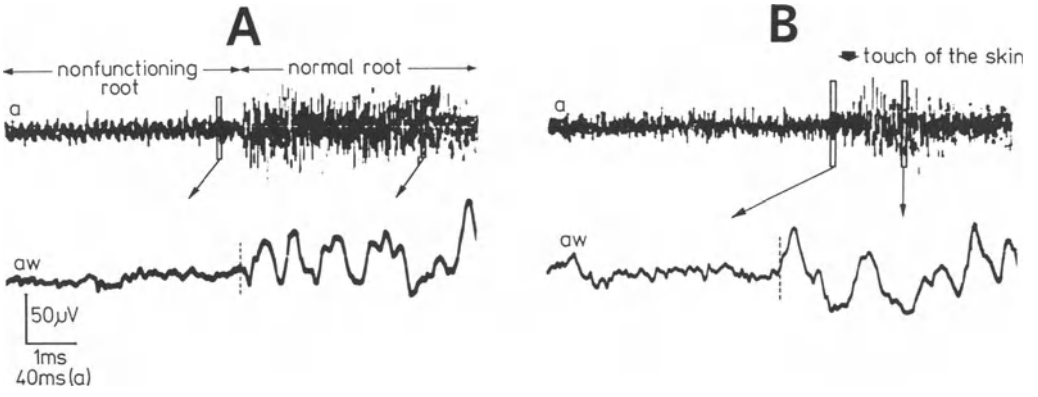

Fig. 1. A Recording of a nonfunctioning nerve root connected to a neurinoma proximally (T5) and of a normal root (T4). B Afferent activity increase in an S3 nerve root filament due to touching the S3 dermatome. The *thick arrow* marks approximately the moment when the skin was touched. To reduce activity, procaine was given locally with cotton plates 5 min before the measurement

The practical aspects of the method are as follows:

1. Examination of the nerve root function and discrimination of afferent or efferent nerve root filaments are possible.
2. To obtain large single unit potential amplitudes clean moist nerve root filaments smaller than 1 mm in diameter should be used and the distance between the recording electrodes and the surrounding tissue should be between 5 and 10 mm to reduce the shunting.

Advances in Neurosurgery, Vol. 16
Ed. by W. Walter, M. Brandt, M. Brock, and M. Klinger

3. If pressure and stretch on nerve fibers gets too high, this can be recognized by a block of conduction in nerve fibers.
4. High single unit potential activity can be reduced by procaine. If reversed potentials occur and the conduction velocities are unrealistically short, then the procaine has most likely been applied too near to the recording electrodes.

The powerfulness of this recording method lies in the second electrode pair, since much more information can be obtained from the measurement, e.g., on the direction of impulse traffic, on conduction velocities of single fibers, and on separation of single unit potentials from artifacts.

Our results were obtained in 29 patients (Table 1).

Table 1. Single unit potential recording during spinal operation (n = 29 patients)

Spinal tumors	14
Traumatic lesion of cauda equina	2
Pain surgery	3
Cervical myelopathy/narrow spinal canal	4
Others	6

Reference

1. Schalow G, Lang G (1987) Recording of single unit potential activity due to receptor stimulation in human nerve roots: a new diagnostic tool. Acta Neurochir 66

Neurophysiological Investigations and ICP Monitoring: An Aid in the Treatment of Head Injury

M. Lorenz and M. R. Gaab

Neurochirurgische Universitätsklinik der Medizinischen Hochschule, Konstanty-Gutschow-Straße 8, D-3000 Hannover 61

Introduction

Advances in the treatment of severe head injury within the last decade have been limited. For further progress, investigative methods are required which allow an objective assessment of patients' status, monitoring of pathophysiological development, and reliable prediction of outcome. In addition to clinical neurological examination and to anatomical investigation by CT scan and MRI, EEG, evoked potentials (EPs), and ICP can provide continuous monitoring of the functional and metabolic conditions of the central nervous system, even if the patient is sedated (3, 4, 11, 13).

Patients and Methods

Between November 1985 and November 1986 48 patients (aged 13-77 years, median 28) with severe substantial head injury were studied. All of them had a Glasgow Coma Score (GCS) ≤ 8 for more than 24 h after trauma. SEPs were measured after stimulation of the median nerve and recorded from the neck and the contralateral scalp in a common way. The somatosensory central conduction time (CCT) and the amplitude ratio of the $N_{20}P_{25}/N_{15}$ (AR) were calculated (Fig. 1) (7, 8, 11). The BAEPs have been classified into four groups: 1, normal; 2, mild decrease of amplitudes of waves III-V or slight increase in interpeak latency I-V; 3, absence of peaks III or V or severe decrease of amplitudes III-V; 4, only wave I or electrical silence (5). The ICP was measured with the epidural microsensor technique (4). The final outcome was classified according to the Glasgow Outcome Scale (GOS) 6-10 months after trauma.

Results

A significance correlation was found between CCT and coma grading (Fig. 2). No clear correlation, however, was seen with the simultaneously measured ICP. The 48 patients, including 25 survivors and 23 deaths (2 not related to head injury - excluded from this series), were divided into two main groups according to outcome: the fully alert and mildly disabled patients (group A) and the severely disabled, the apallic, and dead patients (group B). There are distinct electrophysiological differences between the groups (Table 1). The outcome was significantly worse in patients who had an increase in the CCT to more than 6.6 ms, a decrease of AR to less than 0.3 ($P < 0.001$), or abnormal BAEP (groups 2-4, $P < 0.01$). The mean CCT, too, was significantly different between groups A and B ($P < 0.01$, U-test): in

Advances in Neurosurgery, Vol. 16
Ed. by W. Walter, M. Brandt, M. Brock, and M. Klinger

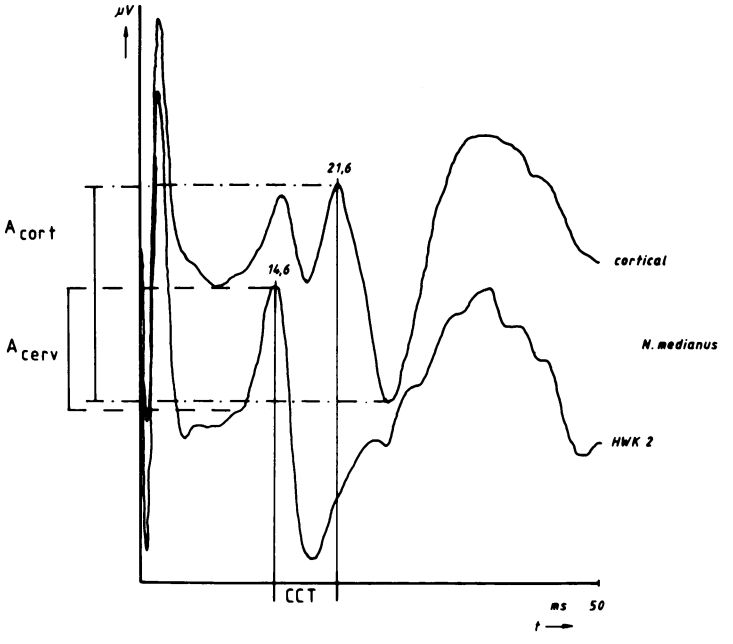

Fig. 1. SEP after stimulation of a median nerve. Recording cortically at C3 or C4 and over the neck (cerv 2 = HWK 2). Amplitude ratio = N_{20} P_{25}/N_{15} = A_{cort}:A_{cerv}. Central (somatosensory) conduction time (*CCT*) = difference of latencies of N_{20} and N_{15}

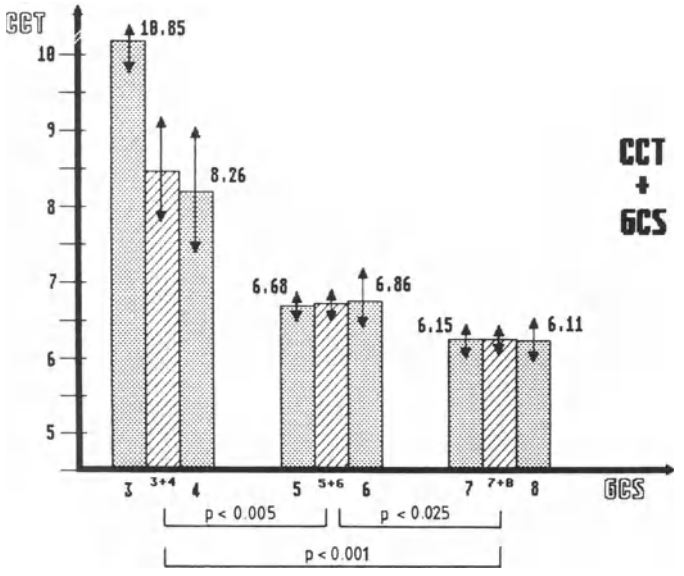

Fig. 2. Glasgow Coma Score (*GCS*) and central conduction time (*CCT*) at time of recording. The CCT increases with worsening of the clinical state. Mean CCT and standard error

Table 1. Prognostic value of evoked potentials. A significant difference in outcome could be shown when SEP and BAEP were markedly abnormal. GOS, Glasgow Outcome Scale; AR, amplitude ratio $N_{20}P_{25}/N_{15}$; CCT, central conduction time

		Outcome (GOS)	I + II	III + V	Significance (χ^2 - test)
Evoked potentials					
SEP	AR	≥ 0.3	14	12	P < 0.001
		< 0.3 or Ø	0	15	
	CCT	≤ 6.6 ms	11	6	P < 0.001
		> 6.6 ms or Ø	3	21	
BAEP		normal	15	13	P < 0.01
		pathol.	1	12	

group A only three patients had a CCT of more than 2.5 standard deviations above mean (5.6 ± 0.4 ms). In one of them we missed a control because of an early transfer to another hospital. Five of the six patients who had demonstrated electrical silence on one or both sides died; the one survivor showed a small N_{20} 3 weeks after injury. This patient, however, remained in a vegetative state. Only one patient of group A showed a slight increase of interpeak latency I-V. Nevertheless, in group B 14 patients were found to have normal responses, even if CCT was pathologically high or ICP was increased. Only one patient with abnormal BAEP had a really good outcome.

Discussion

Surprisingly, we could not find a clear relation between EPs and ICP, although in animal experiments (with inflation of a supratentorial balloon) a correlation could be shown (10). In patients with increased CCT and normal ICP, lesions of the brain stem or midbrain structures may be an explanation, and the number of patients with critically elevated ICP, on the other hand, was perhaps too small. Secondary deterioration or improvement may alter the predictive validity of EPs (2, 5, 8) (Fig. 3). So repeated recordings within the first 3-7 days after trauma are to be recommended in most patients. Normalization of an increased CCT and decreased amplitude ratio is a favorable sign (2, 11). Persistently bad EPs, however, clearly predict the probability of a poor outcome (7). The absence of cortical waves is a reliable and individual sign of bad prognosis. Most of these patients will die.

Middle ear abnormalities due to different trauma, temporal bone fractures, or changes of middle ear pressure after a longer period of nasal intubation are not uncommon in head injury (2, 6, 13) and may often explain abnormal BAEP without brain stem lesions. There seems to be a poor correlation between BAEP and SEP (2), and the BAEP was found to have less prognostic significance (1, 2, 13). Whereas the loss of BAEP may at an early stage predict a poor outcome, the presence of a good BAEP does not necessarily mean a good prognosis (1, 2, 6).

Therefore, only the combination of SEP, BAEP, and ICP provides a reliable index of the severity of primary brain damage and can be used

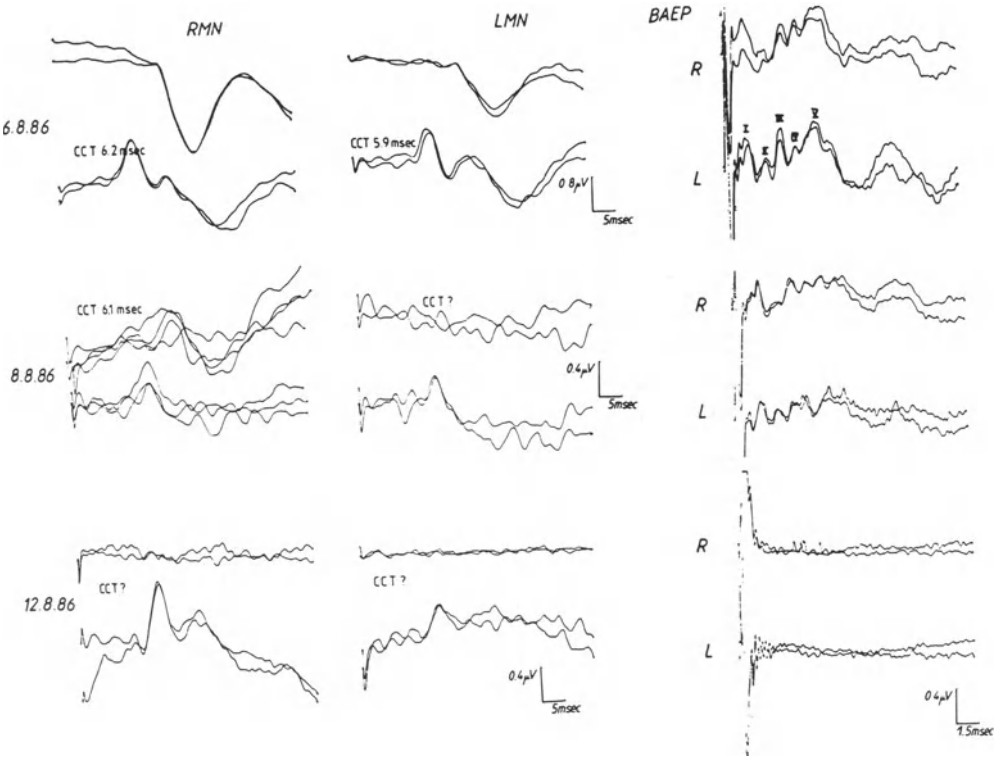

Fig. 3. L.E., male, 53 years old. Right frontal contusion; acute subdural hematoma. EPs quite normal 1 day after injury (GCS6, *upper traces*). Deterioration of clinical state and EPs; loss of cortical responses of the right hemisphere (GCS4, *middle traces*). Progression to brain death with electrical silence (*lower traces*). *RMN*, right median nerve; *LMN*, left median nerve

to assess patients and to monitor the development of secondary brain damage (2). We found a close correlation of CCT and coma grade. Although EPs are powerful prognostic indicators (1, 2, 3, 8, 11, 13), it has to be emphasized that this represents only statistical and not individual information. EPs, however, do improve the reliability of clinical monitoring and ICP and CT findings and are very helpful in the management of patients with critical head injury (5, 9, 12).

References

1. Anderson OC, Bundlie S, Rockswold GL (1984) Multimodality evoked potentials in closed head trauma. Arch Neurol 41:369-374
2. Cant BR, Hume AL, Judson JH, Shaw NA (1986) The assessment of severe head injury by short-latency somatosensory and brain-stem auditory evoked potentials. Electroenceph Clin Neurophysiol 65: 188-195
3. Chiappa KH, Ropper AH (1982) Evoked potentials in clinical medicine. The New England Journal of Medicine 306:1205-1211

4. Gaab M, Ottens M, Busch F, Möller G, Trost HA (1986) Routine computerized neuromonitoring. In: Miller JD, Teasdale GM, Rowan JO, Galbraith SL, Mendelow AD (eds) Intracranial pressure VI. Springer, Berlin Heidelberg, pp 240-247

5. Greenberg RP, Newlon PG, Hyatt MS, Narayan RK, Becker DP (1981) Prognostic implications of early multimodality evoked potentials in severely head injured patients. J Neurosurg 55:227-236

6. Hall JW, Huang-Fu M, Genarelli TA (1982) Auditory function in acute severe head injury. Laryngoscope 92:883-890

7. Hume AL, Cant BR (1978) Conduction time in central somatosensory pathways in man. Electroenceph Clin Neurophysiol 45:361-375

8. Hume AL, Cant BR (1981) Central somatosensory conduction after head injury. Ann Neurol 10:411-419

9. Karnaze OS, Marschall LF, McCarthy CS, Klauber MR, Bickford RG (1982) Localizing and prognostic value of auditory evoked responses in coma after closed head injury. Neurology (NY) 32:299-302

10. Ladds A, Nitta M, Tsutzui R, Symon L (1986) The effect of an acute rise in ICP on the primary somatosensory pathway. In: Miller JD, Teasdale GM, Rowan JO, Galbraith SL, Mendelow AD (eds) Intracranial pressure VI. Springer, Berlin Heidelberg New York, pp 325-330

11. Rumpl E, Prugger M, Gerstenbrand F, Hackl JM, Pallua A (1983) Central somatosensory conduction time and short latency somatosensory evoked potentials in post-traumatic coma. Electroenceph Clin Neurophysiol 56:583-596

12. Symon L, Momma F, Schwerdtfeger K, Bentivoglio P, Costa E Silva JE, Wang A (1986) Evoked potential monitoring in neurosurgical practice. In: Symon L, Brihaye J, Guidetti B, Loew F, Miller JD, Nornes H, Pásztor E, Pertuiset B, Yasargil MG (eds) Advances and technical standards in neurosurgery, vol. 14. Springer, Wien New York, pp 25-70

13. Walser H, Aebersold H, Glinz W (1983) Die Prognose des schweren Schädelhirntraumas mit Hilfe von neurophysiologischen Parametern. Z. EEG-EMG 13:79-83

Brain Electrical Activity Mapping (BEAM) of Event-Related Potentials in Coma

B. M. Reuter, D. B. Linke, M. Kurthen, and B. Schmalohr

Neurochirurgische Universitätsklinik, Sigmund-Freud-Straße 25, D-5300 Bonn 1

Introduction

The large number of publications dealing with the evoked potentials of early and middle latency reflects their diagnostic significance (for review, see 4). In our opinion, the late endogenous components have, however, received too little attention.

The endogenous components are of interest as they may correlate with the state of consciousness in the comatose patient which needs to be evaluated daily in the neurosurgical intensive care unit. The best known of the endogenous components is P300 (11; for review, see 5). In the normal subject P300 (or P3) occurs, for example, on exposure to series of even-pitched tone bursts interrupted by bursts of a differing pitch. The directed attention of the subject is not an absolute requirement. As many investigations have shown, P3 can be elicited even in states of passive attention (e.g., 1, 10). Because P3 is considered a correlate of human cognitive information processing, its study may help in developing a deeper understanding of the states of coma. It is certainly of theoretical interest whether cognitive processes still occur in states of reduced consciousness. Of more practical interest is the measurement of P3 as evidence of the integrity of the involved cortical and subcortical structures of the brain. These include the reticular formation (2), the thalamus (13), the hippocampus (3, 9), and the frontal and parietal cortex.

In this study P3 was measured in several comatose patients with head injuries using the brain electrical activity mapping (BEAM) technique. This technique allows the topographic display of the electrophysiological processes of the brain with an accuracy in the range of milliseconds (7). We used equipment with 28 channels. Figure 1 shows the P3 of a normal awake subject in a state of passive attention (ignoring condition). The cortical P3 reaction consists of two components: the so-called frontal P3a and the more parietal P3b. From a psycho-physiological viewpoint the frontal component is associated more with an orienting response whereas the weaker parietal component correlates more with cognitive interpretation.

Methods

We exposed 31 comatose patients with closed head injuries to the P3 paradigm. We chose to use alternating tone bursts with high and low pitch tones intermingled at a ratio of 1:10. The burst frequencies were 1000 and 1500 Hz. The loudness was 85 dB SPL for both. We chose a long interstimulus interval (ISI) of 2.3 s because we expected the

Advances in Neurosurgery, Vol. 16
Ed. by W. Walter, M. Brandt, M. Brock, and M. Klinger

occurrence of very late components. Normal BAEP and AEP recordings in these patients demonstrated intactness of the auditory pathways. The patients' states of consciousness were ranked with the Glasgow Coma Scale (12). Additionally, thorough clinical neurological examinations were carried out.

Results

In 4 of the 31 patients, P3 responses with frontal and parietal components could be measured. Their reactions to infrequent stimuli differed significantly from those to frequent ones (t-test, $P < 0.001$). These four patients all had a Glasgow Coma Score of 7; that is, they were not awakable but showed coordinated reactions to pain stimuli. Figure 1 shows recordings from one of these four patients, a 29-year-old male with closed head injury. A marked delay in P3, of more than 50 ms, can be seen. Delays up to 800 ms were seen in the three other patients.

As the clinical status of the patients improved the latency of the measured P3s decreased continuously. The four patients survived their head injuries and 6 months later showed only minor deficiencies according to the Glasgow Outcome Scale (6).

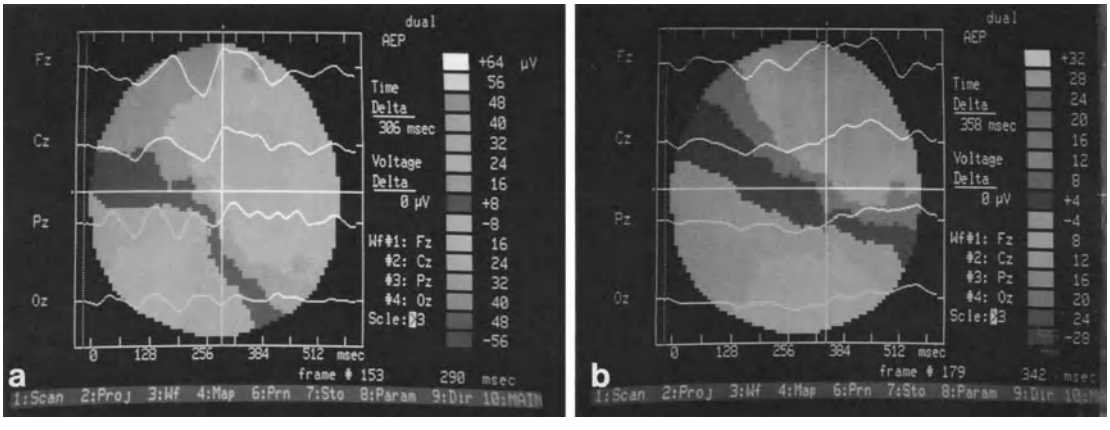

Fig. 1. a P3 in a normal subject with nondirected attention (ignoring condition), frontal component. b P300 in a comatose, nonawakable patient (GCS 7, see text). The frontal P3 is shown

Interpretation

Summarizing, it can be said that the measurement of P3 can aid in evaluating the depth of some states of coma. In addition, through analysis of the structures and their topography, further information can be gained with the BEAM technique. We do not necessarily wish to suggest that the P3 method should be used routinely in the intensive care unit. Our recordings of P3 have shown the importance of the *late* EP components for clinical practice. In agreement with Pfurtscheller et al. (8), we are of the opinion that these are of prognostic value and deserve closer observation. Finally, it appears that elementary cognitive processes, as expressed by P3, certainly occur even in some stages of reduced consciousness.

References

1. Courchesne E (1978) Changes in P3 waves with event repetition: Long term effects on scalp distribution and amplitude. Electroenceph Clin Neurophysiol 45:754-766
2. Desmedt J (1980) P300 in serial tasks; an essential post-decision closure mechanism. In: Kornhuber HH, Deecke L (eds) Motivation, motor and sensory processes of the brain. Electrical potentials, behavior and clinical use. Elsevier, Amsterdam, pp 682-688
3. Halgren E, Squires NK, Wilson CL, Rohrbaugh JW, Babb TL, Crandall PH (1980) Endogenous potentials generated in the human hippocampal formation by infrequent events. Science 210:803-805
4. Halliday AM (1981) Evoked potentials in clinical testing. Churchill Livingstone, London
5. Hillyard SA, Kutas M (1983) Electrophysiology of cognitive processing. Ann Rev Psychol 34:33-61
6. Jennett B, Bond MR (1975) Assessment of outcome after severe brain damage. Lancet 1:480-481
7. Maurer K (ed) (1988) Topographic brain mapping of EEG and evoked potentials. Springer, Berlin Heidelberg New York
8. Pfurtscheller G, Schwarz G, Gravenstein N (1985) Clinical relevance of long-latency SEPs and VEPs during coma and emergence from coma. Electroenceph Clin Neurophysiol 62:88-98
9. Squires NK (1981) Endogenous ERPs recorded from human hippocampus and amygdala. Paper pres. at the Int Conf on EEG correlates of Information Processing, Amsterdam
10. Squires NK, Squires KC, Hillyard SA (1975) Two varieties of long-latency positive waves evoked by unpredictable auditory stimuli in man. Electroenceph Clin Neurophysiol 38:387-401
11. Sutton S, Braren M, John ER, Zubin J (1965) Evoked potential correlates of stimulus uncertainty. Science 150:1187-1188
12. Teasdale G, Jennet B (1974) Assessment of coma and impaired consciousness: a practical scale. Lancet 2:81-84
13. Yingling CD, Hosobuchi Y (1984) A subcortical correlate of P300 in man. Electroenceph Clin Neurophysiol 59:72-76

The 40-Hz Middle Latency Auditory Evoked Potential in Comatose Patients

R. Firsching and R. A. Frowein

Neurochirurgische Universitätsklinik, Joseph-Stelzmann-Straße 9, D-5000 Köln 41

To elicit brain stem auditory evoked potentials (BAEPs), a click delivered at a stimulation rate of 10-11 Hz is usually used. If this frequency is changed to 40 Hz and the analysis time is increased from 10 to 50 ms, two identical responses are elicited, as a click is delivered every 25 ms. If the bandpass filter is reduced to an upper frequency: lower frequency of 1-100 Hz, a sinusoidal reproducible response is obtained, the 40-Hz auditory evoked potential (40-Hz AEP) (see Fig. 1). As GALAMBOS et al. discovered in 1981, this response is maximal if the stimulation rate is increased to 40 Hz and then decreases again at higher stimulation rates (see Fig. 2). The location of the generator of this response is unclear; a midbrain/thalamic generator has been suggested by Spydell et al. As the amplitude of this response depends on the stimulation frequency, a resonance phenomenon has been discussed (9).

In this report 44 comatose patients with various underlying brain lesions have been investigated. The 40-Hz AEP and the BAEP and corresponding CT findings were evaluated to gather more information about the location of the generator of the 40-Hz AEP.

Patients and Methods

Patients

Forty-four comatose patients were examined. Coma grade ranged from I to IV (FROWEIN 1976). Seven patients were in coma grade I, 17 in grade II, 12 in grade III, and 8 in grade IV. Age ranged from 1.5 to 90 years. Causes of coma were: head injury in 19 patients, intracerebral/intracerebellar hematoma in 11, subarachnoid hemorrhage in 4, postoperative courses in 4, and miscellaneous causes (ischemic lesion, postepileptic coma, hypothalamic dysregulation, multiple abscesses, tumor) in 6.

Methods

BAEP. 2 x 1024 unilateral 200-μs alternating rarefaction/condensation 95-dB clicks at 11 Hz and contralateral white noise masking at 65 dB. Montage: Cz to ipsilateral ear lobe. Bandpass settings were 150-3000 Hz. Time base 10 ms.

40-Hz AEP. Same parameters as with BAEP except for a stimulation rate of 40.1 Hz, a bandpass setting of 1-100 Hz, and a time base of 50 ms.

 Advances in Neurosurgery, Vol. 16
Ed. by W. Walter, M. Brandt, M. Brock, and M. Klinger

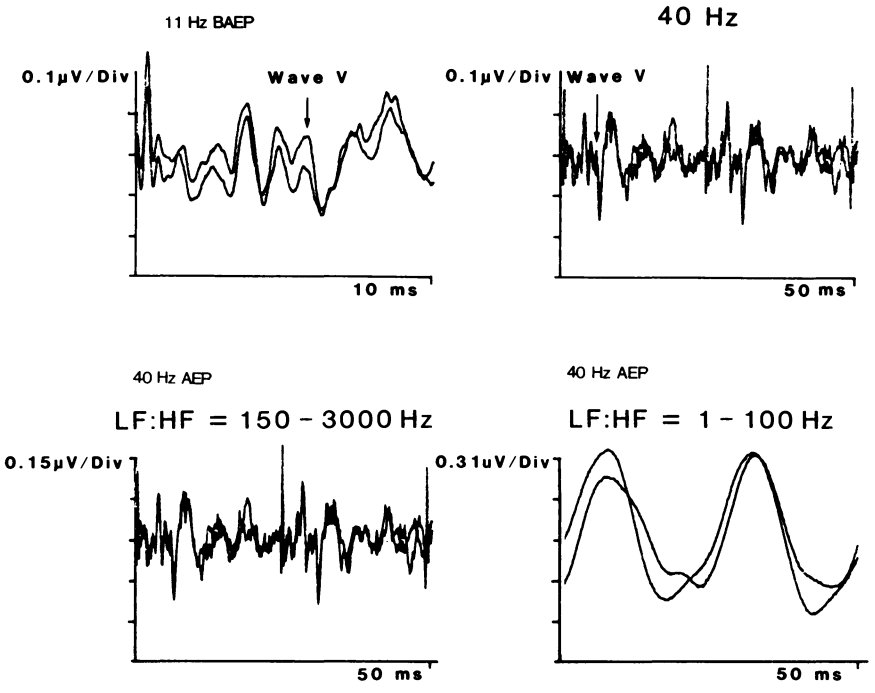

Fig. 1. If the stimulation rate is increased to 40 Hz and the time base is prolonged to 50 ms, a sinus wave-like evoked potential is obtained after reduction of bandpass filter settings

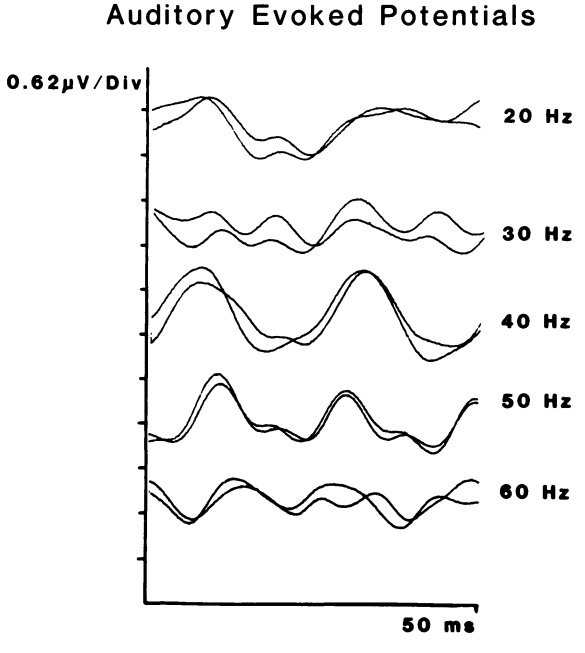

Fig. 2. Increasing the stimulus frequency stepwise, a maximal amplitude of the resulting evoked potential is obtained at 40 Hz

Normative data were obtained from 20 normal controls. The equipment used included a Pathfinder II and a Compact 4 (Nicolet Comp. Madison, Wisc., USA) and a Sensor (Medelec, Old Woking, Surrey, Great Britain). The evoked potentials were graded into three grades:

Grade I: bilaterally normal reproducible evoked responses
Grade II: unilaterally or bilaterally abnormal but at least partly reproducible response and/or unilateral loss of evoked responses
Grade III: bilaterally no reproducible evoked response

For the evaluation of the BAEP, the latency of wave V and the interpeak latency wave III-V were determined. For the 40-Hz AEP, the latency of the first positive peak was determined. Normal latencies were defined to range within the mean value ± 2 standard deviations of the normal controls.

Results

Divergent results of the BAEP and the 40-Hz AEP were found in 3 of the 44 patients. In two patients - a 45-year-old male with pontine hemorrhage (see Fig. 3) and a 71-year-old with intracerebellar hemorrhage - the 40-Hz AEP was lost but the BAEP was partly preserved. In one case - a 39-year-old with intracerebral hemorrhage - the BAEP was preserved on one side (coma grade IV) and the 40-Hz AEP was also preserved on that side, while both the 40-Hz AEP and the BAEP were lost on the other side (see Fig. 4).

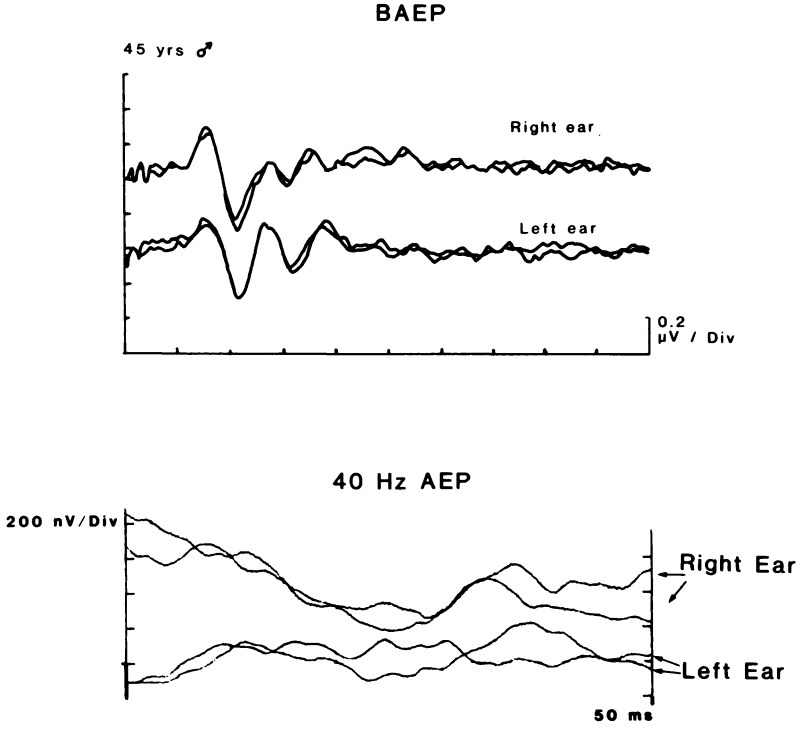

Fig. 3. 45-year-old with pontine hemorrhage. While the BAEP is partly preserved, the 40-Hz AEP is absent

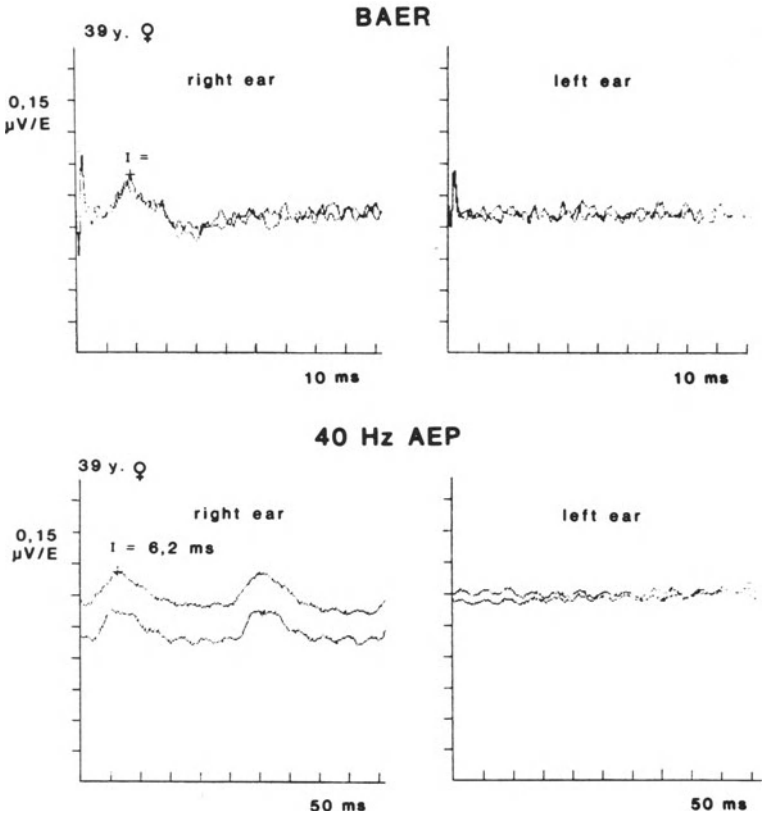

Fig. 4. 39-year-old in coma grade IV. On one side both BAEP and 40-Hz are lost, while on the other side wave I of the BAEP and the 40-Hz are preserved

Two additional cases were remarkable:

Case 1. This 1.5-year-old infant suffered a hemorrhagic contusion in the area of the right cerebellopontine angle. In five serial investigations the BAEP and the 40-Hz AEP were absent on the right side, while they were preserved on the left.

Case 2. This 3-year-old child with massive destruction of the right temporal lobe had a loss of the cortical somatosensory evoked response after stimulation of the left median nerve, while the BAEP and the 40-Hz AEP were normal.

Discussion

The diagnostic and prognostic usefulness of middle and long latency auditory evoked responses in comatose patients is controversial (3-7). So far the 40-Hz AEP has mainly been used to assess hearing levels (9), but it has not been investigated in comatose patients.

The results demonstrated that only in 3 of 44 patients did the 40-Hz AEP differ from the BAEP. The serial investigations proved that this

phenomenon is actually electrical activity from the patient that is being registered, and not an artifact caused by the equipment (case 1). As the 40-Hz AEP was preserved in massive destruction of the temporal lobe, a cortical generator does not seem likely. The loss of the 40-Hz AEP while the BAEP was at least partly preserved was only seen in two patients with infratentorial lesions. It may be assumed that the auditory pathway was interrupted in the upper brain stem, high enough to allow for a partly preserved BAEP but stopping the volley before generating the 40-Hz phenomenon.

The one observation with a preserved wave I of the BAEP and an ipsilaterally preserved 40-Hz AEP is difficult to explain. It may be theorized that the intracerebral part of the auditory pathway was only partly interrupted. The volley passing on was not enough for the registration of the BAEP but enough for the resonance phenomenon.

These findings tend to support the assumption by SPYDELL et al. (8) that midbrain structures play a major role in the generation of the 40-Hz AEP. The use of the 40-Hz AEP seems complementary to the BAEP as it may be the only neurophysiological investigation to indicate functional lesions of midbrain structures. More experience, however, is needed to establish the clinical value of the 40-Hz AEP.

Summary

Using a click administered at 40-Hz a middle latency auditory evoked potential (40-Hz AEP) was registered in 44 comatose patients with defined brain lesions. Corresponding brain stem auditory evoked potentials (BAEPs) and CT findings suggest a midbrain/thalamic generator of the 40-Hz AEP. Thus the 40-Hz AEP appears to be of help in localizing brain lesions and may prove to be complementary to the BAEP.

References

1. Frowein RA (1976) Classification of coma. Acta Neurochir (Wien) 34:5-10
2. Galambos R, Makeig S, Talmachoff PJ (1981) A 40 Hz auditory potential recorded from the human scalp. Proc Natl Acad Sci 78(4):2643-2647
3. Greenberg RP, Mayer DJ, Becker DP, Miller JD (1977) Evaluation of brain function in severe human head trauma with multimodality evoked potentials. J Neurosurg 47:150-177
4. Kaga K, Nagai T, Takamoti A, Matsh RR (1985) Auditory short, middle and long latency responses in acutely comatose patients. Laryngoscope 95:321-325
5. Kraus N, Ozdamar O, Hier D, Stein L (1982) Auditory middle latency responses (MLR) in patients with cortical lesions. Electroencephalogr Clin Neurophysiol 54:275-287
6. Ottaviani F, Almadori G, Calderazzo SB, Frenguelli A, Paludetti G (1986) Auditory brainstem (ABRs) and middle latency auditory responses (MLRs) in the prognosis of severely head-injured patients. Electroencephalogr Clin Neurophysiol 65:196-202
7. Robinson K, Rudge P (1982) The use of auditory potentials in neurology. In: Halliday AM (ed) Evoked potentials in clinical testing. Churchill Livingstone, Edinburgh, London, Melbourne, New York, 371-392

8. Spydell JD, Pattee G, Goldie WD (1985) The 40 Hz event-related potential: normal values and effects of lesions. Electroencephalogr Clin Neurophysiol 62:193-202

9. Stapells DR, Lindon D, Suffield JB, Hamel G, Picton TW (1984) Human auditory steady state potentials. Ear and Hearing 5:105-113

Interventional Neuroradiology for Neurosurgical Diseases

J. Wappenschmidt, F. Brassel, and L. Solymosi

Neuroradiologische Abteilung, Neurochirurgische Universitätsklinik, Sigmund-Freud-Straße 25, D-5300 Bonn 1

The introduction of selective and superselective angiography in diagnostic medicine laid the foundation for interventional therapy. Such therapy includes recanalizing measures, such as intra-arterial fibrinolysis and transluminal angioplasty, for stenosing and occluding lesions and occluding measures for vascular tumors and angiomas.

Recanalization of the cerebral arteries is not a wisely used procedure because the area supplied by these arteries, in contrast to the peripheral arteries, is highly sensitive to hypoxia and the risk of embolism is high. One clear indication for *fibrinolytic therapy* is complete thrombotic or embolic occlusion of the basilar artery. There is virtually no alternative for this therapy. Angioplasty, however, is indicated for surgically inaccessible lesions or when the complication rate associated with operative therapy is high. Surgically inaccessible lesions, that is, high or long-segment carotid stenoses, can be treated by a neurosurgical-neuroradiologic method, that is, by *open angioplasty*. Lesions with a high surgical complication rate include stenoses of the subclavian artery and the origin of the vertebral artery; these processes are accessible only by neuroradiologic methods, that is, by *percutaneous transluminal angioplasty*. Introduction of a dilatation balloon catheter, which occurs under local anesthesia and does not overly stress the patient, leads to an immediately measurable increase in the caliber of the vessel and a rapid improvement in the hemodynamic relations. One of the main indications for the balloon catheter is subclavian steal syndrome. For this syndrome, the balloon catheter is generally considered superior to operative measures and constitutes the method of choice. It is indicated in these cases only when the angiographically demonstrated vascular change is responsible for the symptoms.

Our first example is a 66-year-old man with clinical signs of vertebrobasilar insufficiency. On the angiogram, a high-grade stenosis is seen in the proximal portion of the left subclavian artery with mild poststenotic dilatation. The left vertebral artery is no longer filled orthograde. After two-stage dilatation, the caliber of the vessel is normal with good orthograde filling of the ipsilateral vertebral artery (Fig. 1).

Occluding, devascularizing therapy was initially limited to lesions supplied by the external carotid and the spinal arteries. Today, we will deal only with the spinal lesions. Because of their localization in relation to the circumference of the spinal cord, their extension, and their vascularity, many spinal angiomas are inoperable or cannot be removed in toto. Our first example is a 27-year-old woman with a gradually progressing transverse lesion of the cord accompanied by

Ed. by W. Walter, M. Brandt, M. Brock, and M. Klinger

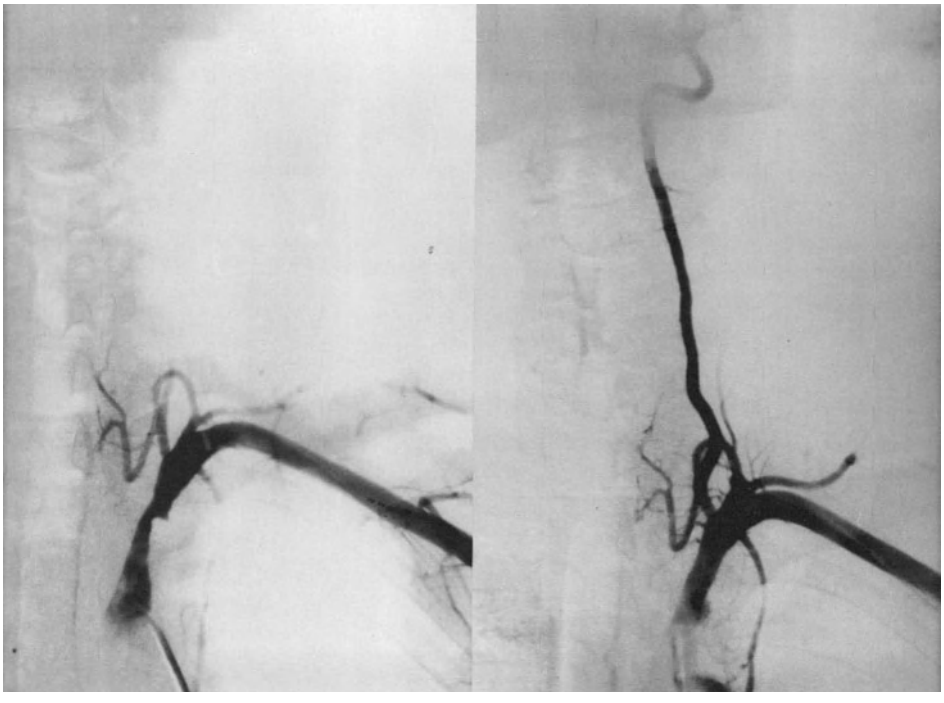

Fig. 1. Subclavian steal syndrome. Arteriogram of the left subclavian artery. Pronounced stenosis in proximal portion of left subclavian artery; caliber is normal after dilatation. Therapeutic success: orthograde filling of ipsilateral vertebral artery

paraplegia and sensory deficits starting T4/T5. On the selective angiogram of the costocervical trunk, the superior thoracic segment of the anterior spinal artery, the inferior end of which supplies the small compartment of an angioma at the level of T4, is visualized over the spinal branch of descending cervical artery. Selective angiography of the 8th intercostal artery on the right side showed an extensive angioma supplied by the spinal branch of the artery and extending over three vertebrae (T5-T7); the dense vascular network occupies the entire posterior, lateral, and part of the anterior circumference of the spinal cord. This angioma seemed at first to be inoperable. Devascularization by embolization is possible only when the spinal branch of the 8th intercostal artery supplies the angioma exclusively and not the spinal cord parenchyma as well. Neuroradiologic clarification is obtained in such cases by passing a balloon into the afferent artery and, under strict neurologic monitoring and derivation of somatosensory-evoked potentials, blocking the blood supply by gradually filling the balloon with contrast medium until the vessel is completely occluded. In our case, total occlusion of the afferent artery was tolerated for 10 min without complications; embolization, therefore, was possible. A control arteriogram made after injection of 16-cm^3 embolizing agent shows the occlusion of the afferent spinal artery; the embolizing agent can be seen in the body of the angioma (Fig. 2). Most of the angioma could then be removed with minimal loss of blood. What appeared initially to be an inoperable angioma was rendered operable

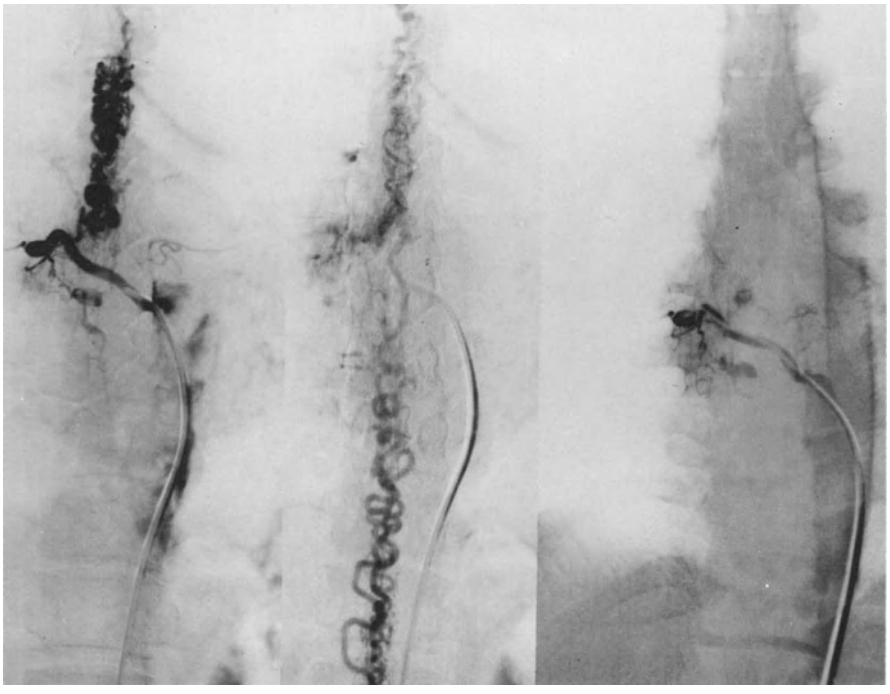

Fig. 2. Spinal angioma. Large angioma supplied by spinal branch of 8th intercostal artery on right side *(left* and *middle)*; supplying vessel occluded after embolization; embolizing agent in body of angioma (*right*)

by neuroradiologic treatment. As exclusive therapy, devascularization of monopedicular angiomas by the application of an embolizing agent, can isolate the angioma from the blood flow.

The extension of superselective angiography to the arteries supplying the cerebral parenchyma and their peripheral branches has facilitated the development of effective new therapeutic measures in interventional neuroradiology, especially for arteriovenous shunts and certain kinds of aneurysm. The main tasks of neuroradiology are to simplify definitive therapy for the neurosurgeon by embolizing devascularization of pathologic lesions and to provide the only alternative therapy for surgically inaccessible lesions. Our discussion today is limited to three examples of surgically inaccessible lesions.

Here you see an inoperable multipedicular angioma in the parietal lobe of the dominant hemisphere. Blood supply is provided by the tributaries of the dilated angular gyri and posterior parietal arteries. In this case, shunt volume was successfully reduced in several sessions by embolization of the supplying vessels. An embolization, however, is safe and effective only when the catheter can be passed electively in a vessel supplying the angioma exclusively and not cerebral tissue as well. The *calibrated leak balloon*, which is attached to a microcatheter, fulfills this requirement: following the flow, the balloon is carried from the carotid into the trunk of the middle cerebral artery and then through the dilated angular gyri artery to the nidus of the angioma. EEG evaluation and clinical neurologic testing revealed no im-

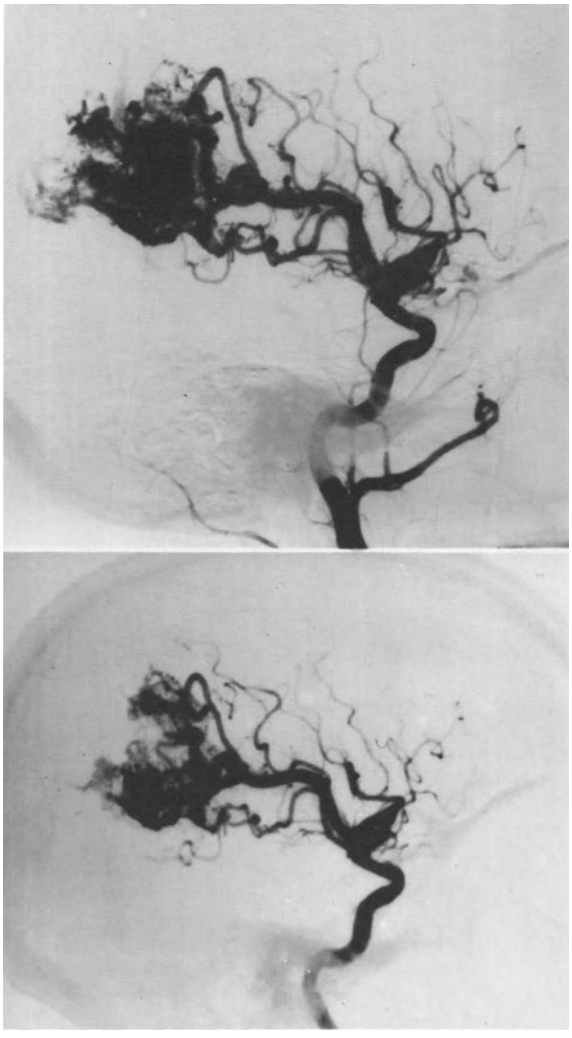

Fig. 3. Inoperable angioma in parietal lobe of dominant hemisphere. Angiogram of left carotid. Large multipeduncular angioma in parietal lobe; blood supply over angular gyri and inferior parietal arteries (*above*). Shunt volume markedly reduced after embolization (*below*)

pairment of cerebral function after the *WADA test*, that is after intra-arterial injection of amobarbital. An embolization, therefore, was possible.

After injection of an embolizing agent, the angioma was considerably smaller than before the start of therapy; the *high-flow compartment*, in particular, was eliminated and shunt volume and risk of hemorrhage, therefore, reduced. After treatment, the course of which was uneventful, the frequency of the patient's attacks decreased sharply and, for the time being, we have not scheduled additional sessions (Fig. 3).

The next example is a *giant aneurysm*. Many giant aneurysms cannot be clamped off because of their wide neck or the high risk for the patient. In our opinion, alternative therapy is indicated only in cases like the following example. This arteriogram of the right carotid shows a giant aneurysm with a pronounced space-occupying character in

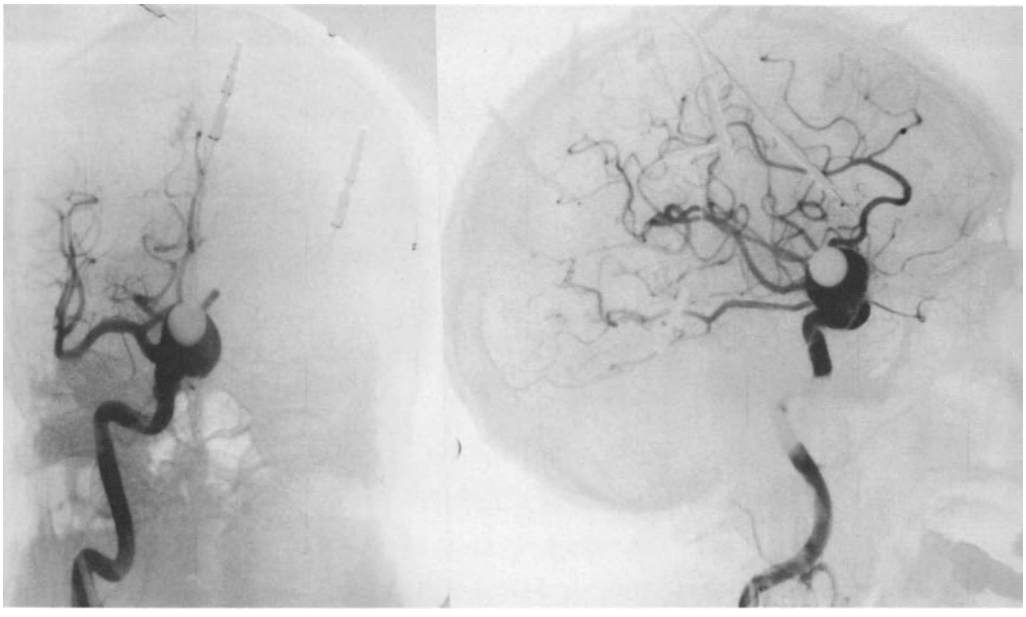

Fig. 4. Giant aneurysm of internal carotid artery at origin of ophthalmic artery. Only superior part of fundus is filled by balloon

the carotid at the origin of the ophthalmic artery. A detachable balloon was easily passed into the aneurysm; after the balloon was inflated with contrast medium, it only partially filled the superior portion of the fundus. Detachment of the balloon here was not possible (Fig. 4).

After complete occlusion of the vessel for 10 min without complications, the balloon detached in the aneurysm-bearing segment of the carotid. A control arteriogram with i.v. DSA 6 months later shows that the aneurysm is still cut off by the occluded supraclinoidal portion of the carotid. The ipsilateral cerebral vessels are supplied over the anterior part of the circle of Willis without neurologic deficits (Fig. 5).

The last example is *carotid artery-cavernous sinus fistulas*. Most of these fistulas are due to trauma. The fistulous opening in the carotid is usually located in the anterior part of the cavernous sinus and sometimes in the posterior part. Two fistulous openings were present in one of our cases: one in the anterior and one in the posterior part. The therapeutic aim, that is, closure of the fistula with preservation of the patency of the carotid, cannot be achieved with the available surgical procedures. Our final example, a fistula in the anterior part of the sinus illustrates the alternative treatment.

The balloon, which is passed transcutaneously from the femoral artery into the intracavernous part of the left carotid, was washed through the fistulous opening and into the cavernous sinus almost immediately. Detachment of the balloon from the catheter was also not difficult. After closure of the fistula, the carotid remained patent and circulation in its cerebral branches was orthograde and unobstructed (Fig. 6).

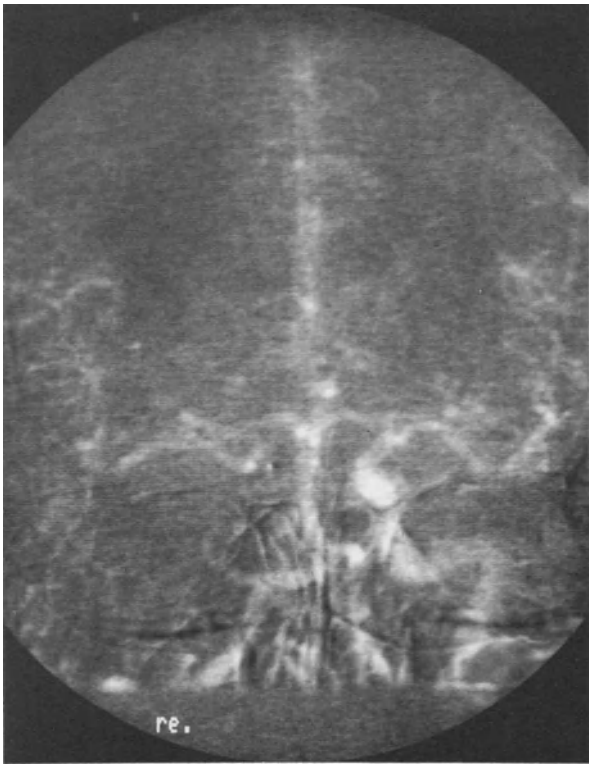

Fig. 5. Control angiography (i.v. DSA). Cerebral vessels on right side demonstrated over anterior circle of Willis; aneurysm-bearing part of right carotid is occluded

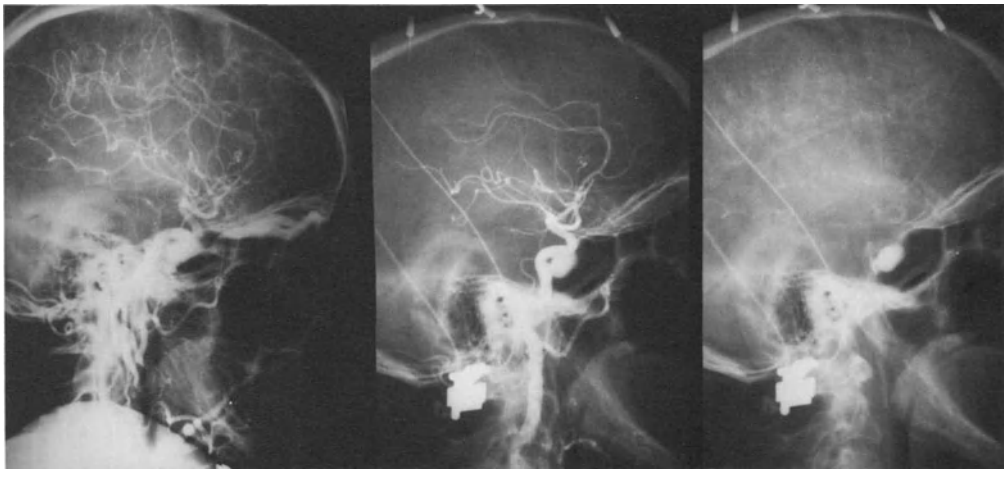

Fig. 6. Carotid artery-cavernous sinus fistula. Arteriogram of carotid. Fistula in anterior portion of cavernous sinus *(left)*. Control arteriogram after balloon detachment (*middle, right*): closed fistula, patent carotid, orthograde demonstration of arteries supplying cerebral parenchyma of left hemisphere

In addition to this case, one balloon was sufficient for fistula closure in four other cases, and four balloons were necessary in one case. Cavernous sinus fistulas are thought to develop spontaneously by rupture of an aneurysm in the intracavernous portion of the carotid. The developmental course of our cases, however, was always paralytic and never apoplectic. By comparison, the spontaneous appearance of a pulsating exophthalmos with its accompanying symptoms is apparently due to angiomas in the dura with shunts into the sphenoparietal or cavernous sinus.

Consequently, the therapeutic aim, that is, complete closure of the fistula with preservation of the patency of the carotid, can be achieved in a high percentage of the patients by transcutaneous balloon embolization using a suitable catheter and balloon. Even complications like dissections, vasospasms of the carotid, and premature detachment of the balloon are extremely infrequent. The method of choice for medium and large fistulas in the cavernous sinus, therefore, should be transcutaneous embolization with detachable balloon. This method, while it should not be considered a competitive measure is, nevertheless, preferable to surgical method because it fulfills Dandy's requirement:

"The simplest and safest thing should be done first."

Pain Treatment

Stimulation of the Sympathetic Trunk Instead of Resection

K. Nittner

Abteilung für Stereotaxie der Neurochirurgischen Universitätsklinik, Joseph-Stelzmann-Straße 9, D-5000 Köln 41

Sympathectomy as a destructive operation at the sympathetic trunk had a favorable effect only for a limited time and its use was therefore soon abandoned.

Indication

Sympathectomy was performed because of pain correlated to the sympathetic trunk. This pain appears as pain in an anesthetic area, hyperpathia, or causalgia. It is known as postherpetic neuralgia following zoster infection, as phantom pain after amputation or exeresis, and as pain in Sudeck's disease.

Employing electrostimulation it is possible to stimulate the sympathetic trunk with variable parameters and at variable intervals. Since 1983 this procedure has been used in our clinic in eight patients, five of them suffering from zoster neuralgia. After paravertebral blocking of the affected segment or of those next to it, the sympathetic trunk was stimulated when the patient reported relief of pain (Fig. 1).

Technical Procedure

The patient is put on the operating table in prone position, if necessary with upholstery under the abdomen or thorax to render the spinal column kyphotic. In local anesthesia under X-ray control a cannula 10 cm in length is directed toward the anterior edge of the vertebral body. When the cannula touches the vertebral body it is moved along it in a ventral direction to the anterior limit of the vertebral body. In the correct position an anchor electrode is placed through the cannula ventrolaterally to the vertebral body.

By means of radiological and electrophysiological testing - electrostimulation - the position of the electrode and its effect on pain is tested; if the result is satisfactory, the electrode is connected to the fascia (Fig. 2). To enlarge the stimulated area a second electrode can be implanted (Fig. 3). After a trial screening period of about 1 week the system is internalized and attached to an RF receiver or a pulse generator.

Advances in Neurosurgery, Vol. 16
Ed. by W. Walter, M. Brandt, M. Brock, and M. Klinger

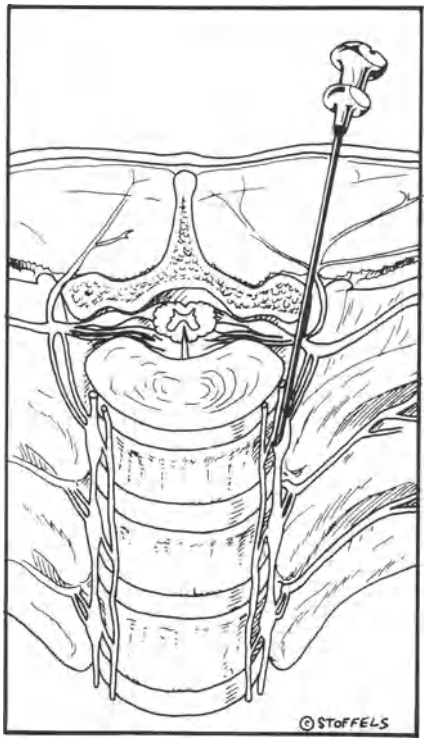

Fig. 1. Position of the puncture needle in relation to the sympathetic trunk (slightly modified from Neurologia repetita, H. Schliack, 1979)

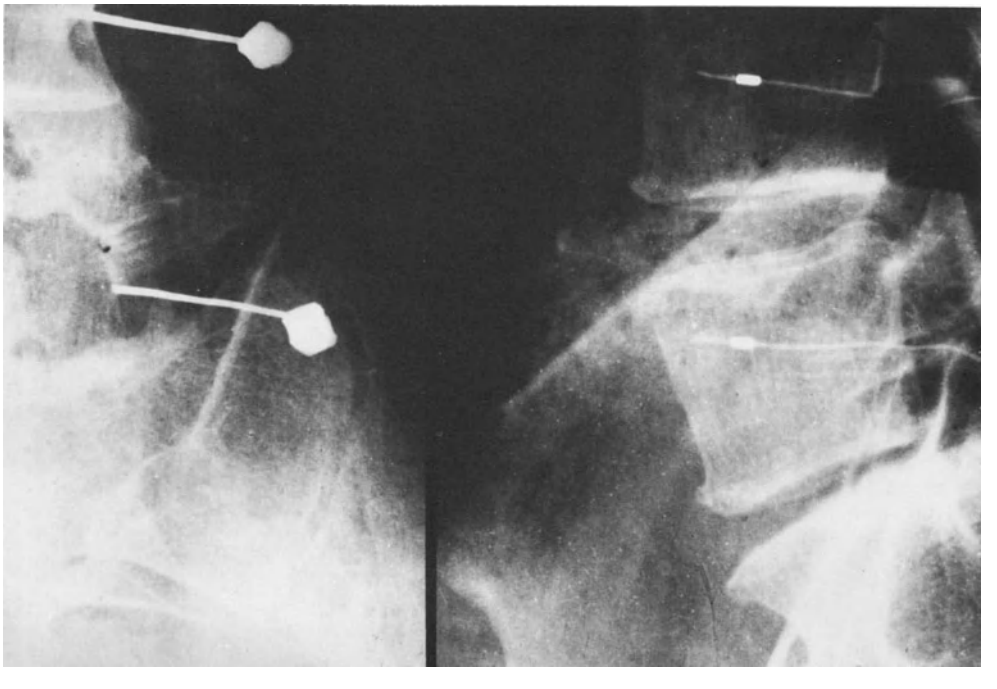

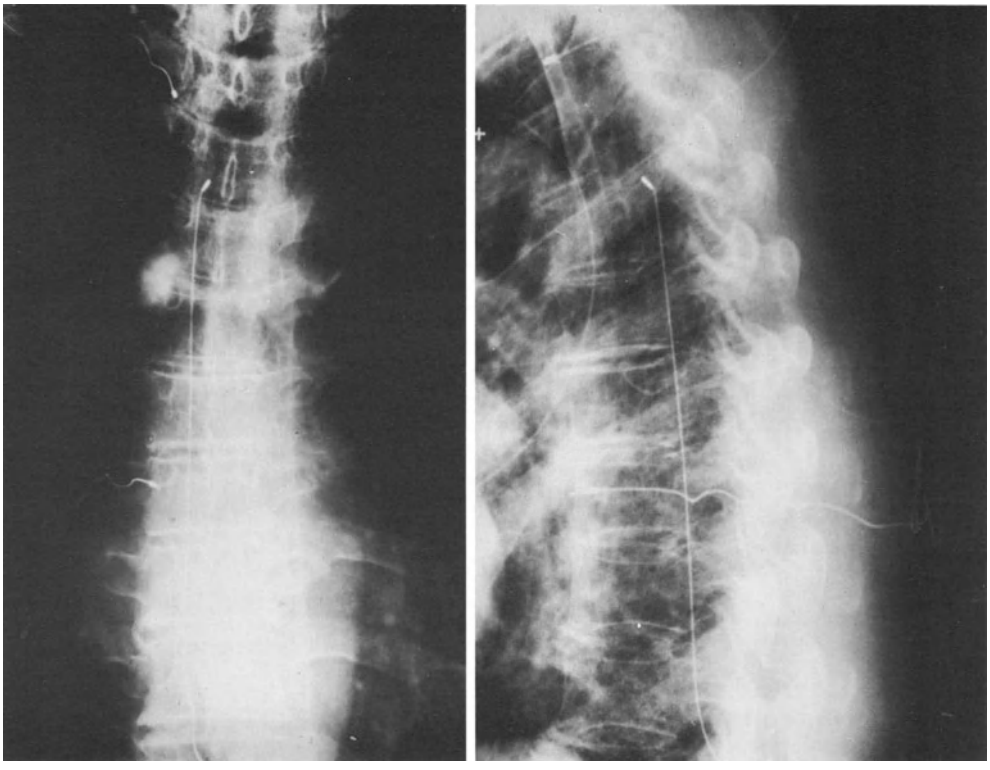

Fig. 3. Two prevertebrally implanted electrodes for stimulation of the sympathetic trunk after epidural electrode implantation without effect. DCS stimulation

Basis

The method is based on the functional anatomy of the sympathetic trunk. To objectify it, additional physiological and pharmacological methods were also considered: the reaction of the arrectores pilorum muscle, skin temperature, dermatographia, secretion of sweat (Minor's test), the behavior of endorphines, and the reaction of opiate antagonists (naloxone).

Results

The method was used in five patients who suffered from severe zoster neuralgia that was resistant to therapy and mainly occurred in the thoracic area. All of them had been treated with drugs, radiotherapy, or TENS (Transcutaneous Electrical Nerve Stimulation); three of them abused drugs.

Fig. 2. *Left:* Position of the puncture needle in relation to the spinal column (anteroposterior). *Right:* Anchor electrodes, inserted through the puncture needle (lateral)

Table 1. Results of the different operative methods in terms of pain relief (n = number of patients)

	n	Postop.				3 months				6 months				>6 months			
		100%	50–80%	30–50%	0–30%	100%	50–80%	30–50%	0–30%	100%	50–80%	30–50%	0–30%	100%	50–80%	30–50%	0–30%
Chordotomy	4		2		2				4				4				4
Epidural stimulation (dorsally)[a]	4			3	1				4				4				4
Prevertebral stimulation	5	1	3		1		4	1			3	1		2 † 1[b]			1

[a] In two patients after previous chordotomy

[b] Removed because of wound infection

The early postoperative results were much better than those of our former methods (Table 1). During the first 6 months all patients reported relief of pain, and some of them were completely free of pain. Two patients died of cancer metastases, and in one patient the system had to be removed because of wound infection. The subsequent follow-up in the remaining five patients with prevertebrally implanted electrodes ranged from about 2 to 3 years; the results were then less favorable.

Experiences up to now allow the following appraisal: In competent hands this operation poses no problems and can just as well be performed on elderly patients. We did not observe any complications after blocking or stimulation of the sympathetic trunk in our patients. Even during the test stimulation, the hyperpathia in the affected skin area disappeared in all patients. Subsequent pain relief remained for a long period. The advantage of the method is the possibility of stimulation of the sympathetic trunk at intervals with variable parameters, avoiding its destruction, because destructive operations are always followed by relapses.

Long-Term Results of Facet Denervation

A. Saad, W. Braun, and T. Demirel

Neurochirurgische Abteilung des Bethesda-Krankenhauses, Hainstraße 35, D-5600 Wuppertal 1

Low back pain and referred leg pain seem to be the result of mechanical alterations in the facet joints (facet syndrome), conservative management of which is unlikely to be of benefit. We took up the suggestion of treating these pains by cutting off the articular nerve supply of the spinal facets in patients whose clinical symptoms and myelography or CT scan did not show any evidence of nerve root involvement. We used the percutaneous technique introduced by SHEALY in 1974. Under fluoroscopic guidance, six cannulae were introduced adjacent to the three lowest facet joints on each side. A radiofrequency thermistor electrode was passed through the needles and the articular nerves were coagulated after testing the electrical stimulation and confirming the position of the electrode by X-ray. This procedure is simple, quick, and of nearly no risk. We only observed complications twice; once a temporary weakness of the quadriceps femoris muscle and once a skin burn caused by defective insulation of the electrode.

Between 1978 and 1984 we treated 311 patients by facet denervation. Of these patients, 128 were suffering from persisting complaints fol-

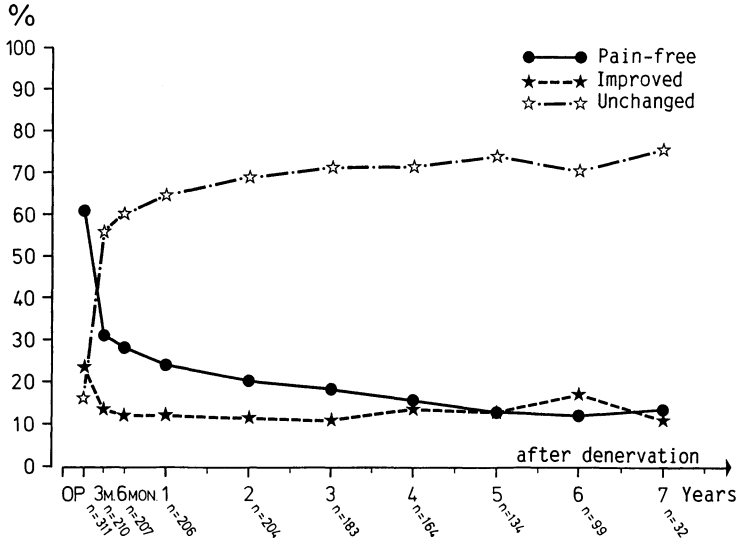

Fig. 1. Long-term results of facet denervation

Table 1. Long-term results of facet denervation

No. of patients	Time after denervation	Pain-free (%)	Improved (%)	Unchanged (%)
311	1st day	61	23	16
210	3 months	31	13	56
207	6 months	28	12	60
206	1 year	24	12	64
204	2 years	20	11	69
183	3 years	18	11	71
164	4 years	16	13	71
134	5 years	13	13	74
99	6 years	12	18	70
32	7 years	14	11	75

Table 2. Results in operated patients

No. of patients	Time after denervation	Pain-free (%)	Improved (%)	Unchanged (%)
128	1st day	59	28	13
73	3 months	25	19	56
73	6 months	22	16	62
73	1 year	18	15	67
73	2 years	16	14	70
59	3 years	15	10	75
50	4 years	12	14	74
47	5 years	11	9	80
29	6 years	7	10	83
14	7 years	7	0	93

lowing disk prolapse surgery and 183, who had not undergone surgery, were suffering from atypical low back pain and referred leg pain.

On the first days after denervation 61% of the patients were pain-free, 23% improved, and 16% unchanged. In 1986, we sent follow-up questionnaires to the 261 successfully treated patients asking about the course of their complaints in the subsequent years. We received 160 evaluable answers. Thus, the results we are now presenting are based on self-evaluation of the patients.

Our long-term results are presented in Fig. 1 and Table 1. It is apparent that after 3 months only 44% of the patients still showed satisfactory results (31% pain-free and 13% improved). After 3 years the rate of success dropped to 25% - 30% and remained much the same in the following years.

Discussion

This is a poor result, in which the postsurgical group (Table 2) experienced a worse course than the previously unoperated group. It remains to be asked whether this procedure is just a placebo therapy, or whether our patient selection was inadequate. It would appear to be the latter, since other authors have reported a better success rate of about 50% or more after 2 - 3 years. The best results are clearly achieved when a temporary nerve block with local anesthesia is carried out to test the effect of denervation prior to coagulation. We did not do this as percutaneous coagulation does not require much more effort than the test block. We have, however, started to make a stricter selection by means of the local anesthesia nerve block and hope to achieve better results in coming years.

References

1. Demirel T (1980) Erfahrung mit der perkutanen Facett-Neurektomie. Med Welt 31 (29/30):1096-1098
2. Lavignolle B (1985) Rhizolysis: Results in Europe. In: Program and Abstracts of the First International Symposium on Alternatives in Spinal Surgery. Paris, France, pp 42-43
3. Ray CD (1985) Facet rhizolysis technique and results in the USA. In: Program and Abstracts of the First International Symposium on Alternatives in Spinal Surgery. Paris, France, p 41
4. Shealy CN (1974) Facets in back and sciatic pain. Minn Med 57:199-203

Intraventricular Morphine Application by Means of Implanted Pump Systems in Paraneoplastic Pain Syndrome

G. Dieckmann

Abteilung für Funktionelle Neurochirurgie, Zentrum für Neurologische Medizin, Robert-Koch-Straße 40, D-3400 Göttingen

Introduction

After the discovery of specific opiate receptors in the brain and spinal cord (8), it was logical to think in therapeutic terms of applying opiates directly in the vicinity of these receptors. Thus spinal opiate administration proved to be highly effective in the treatment of pain (1,9,12). YAKSH (13) provided synoptic information on the pharmacological action of opiates. In the meantime, spinal analgesia has become widespread in the treatment of acute and chronic pain conditions, especially in pain due to carcinoma (3,14). From a technical point of view, the use of implantable application systems with continuous or demand-controlled drug release was helpful, making long-term therapy feasible (3,4). On the other hand, cerebral intraventricular opiate application is less widespread. It is restricted to chronic pain states in the cervicofacial region as well as to such states in disseminated carcinoma metastases and is linked with neurosurgical techniques. There have been communications on this since 1982 (5-7), and BLOND et al. (12) recently reported on experience in a large number of patients. Today, we communicate our own initial experiences with this invasive, but not ablative method in the neurosurgical treatment of chronic incurable pain states.

Materials and Methods

Since August 1984, we have implanted an intraventricular pump system for pharmacotherapy in five patients with paraneoplastic pain syndrome. As shown in Table 1, these patients were in a chronic state of pain owing to disseminated bone metastases in breast cancer, cancer of the head of the pancreas, kidney and bladder cancer, and cancer of the sigmoid colon; there was partial involvement of further parts of the skeletal system in four of the patients. One patient had a recurrent lymphangioma of the tongue and floor of the mouth and had undergone multiple operations and irradiation. The female patients with breast cancer and cancer of the head of the pancreas displayed pain of Pancoast type owing to cervical-osseous metastases with involvement of parts of the brachial plexus.

Technique

We carried out computer-controlled stereotactic application of ventricular catheter into the third ventricle through the foramen of Monro. After arcuate high frontal cutaneous incision over the subdominant hemisphere, stereotactic bore-hole trepanation with a diameter of 3.0 mm

Table 1. Clinical characteristics, daily doses of morphine, and follow-up in five patients with paraneoplastic pain syndrome

Name	Age	Sex	Diagnosis	Morphine		Result	Follow-up
				Dosis (mg)	Duration		
ML	44	f	Breast Ca. Multiple bone metastases	0.5	48 h	+++	2 mo
JM	76	m	Kidney and bladder Ca. Multiple bone metastases	0.2-1.0	24 h	++	6 wk
HS	53	m	Lymphangioma of tongue	0.2	24 h	+++	6 mo
HR	62	m	Sigmoid colon Ca. Multiple bone metastases	0.2	12 h	++	6 mo
UH	58	f	Pancreatic Ca. Multiple bone metastases	1.6	12 h	+++	2 mo

was carried out. A plastic ventricular catheter was introduced by means of a guide mandrin up to the foramen of Monro. The catheter tip was localized by means of contrast medium fluoroscopy and slid through the foramen of Monro into the third ventricle after partial removal of the guide mandrin under fluoroscopic control. The ventricular catheter was shortened to an adequate length at the bore hole. A Silastic reservoir with a conical metal base was inserted via which test doses were given in the subsequent days to determine the morphine concentration required. This subcutaneous reservoir was connected with the distal catheter end of the infusion pump. A subcutaneous skin pouch was applied infraclavicularly. The infusion pump was inserted into this skin pouch. The catheter from the pump was tunnelized upwards to the Silastic reservoir by means of accessory incisions, and the pump catheter was connected with the supporting reservoir.

Technique of Opiate Administration

Injections of the test dose were begun on the first days after the operation by percutaneous injection into the subcutaneous Silastic reservoir, starting with 0.1 mg morphine under intensive care conditions. The dose was slowly raised until the optimal effect as measured by the beginning, quality, and duration of analgesia was achieved in relation to the lower possible dosage. After the correct morphine concentration was attained, the pump reservoir implanted in a pectoral infraclavicular position was filled with the morphine solution in an appropriate concentration. The pump we used was an on-demand pump in which one pump thrust releases 0.1 ml fluid in the desired morphine hydrochloride concentration of 0.1 - 1.0 mg morphine. The patient was instructed in the operation of the two pump buttons which he could feel through the skin; he received a registration card on which he registered the pump thrusts carried out in accordance with the daily-diary adjustment. The time of refilling the reservoir could be calculated from this after a few weeks

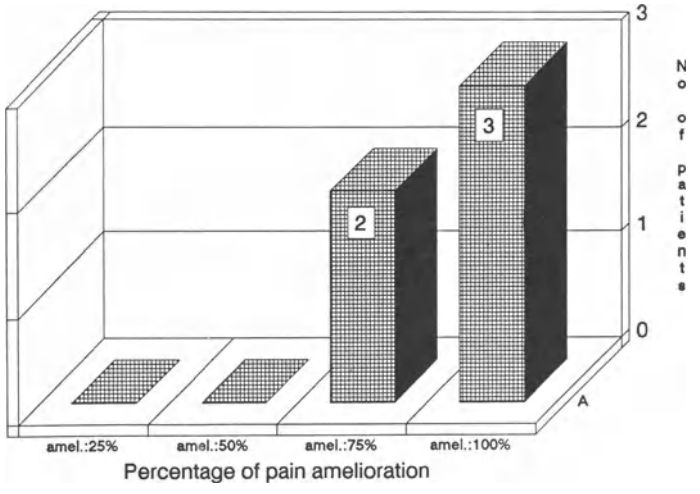

Fig. 1. Results of intraventricular morphine in paraneoplastic pain patients (n = 5)

or months. After this instruction, the patient was discharged home. The opiate application was made demand-controlled by the patient himself under domestic conditions. The reservoir was refilled either at the site of implantation or by the family doctor, who had received appropriate instructions.

Results

All five patients had 75% (two patients) or 100% (three patients) freedom from pain as a result of the demand-controlled intraventricular morphine self-administration (see Fig. 1). The morphine dose and follow-up are shown in Table 1. The freedom from pain commenced after 5 - 10 min and persisted for 12 - 48 h after a single pump thrust. In one patient, the single dose had to be raised in the course from an initial 0.2 mg to 1.0 mg. This patient had previously received large amounts of opiates systemically. In the short period of the follow-up observation of our patients, a significant tolerance phenomenon could not be detected.

Irrespective of the alleviation or freedom from pain attained, all patients reported a decrease in their fear of pain and the occurrence of a feeling of well-being after abolition of the chronic pain. Accordingly, the quality of life improved in all patients. In four of them, the functional daily activity was also markedly improved. Additional administration of analgesic medication was not necessary.

Depending on the concentration of the morphine solution and the frequency of its application, the administration periods were 1 - 3 months. Afterwards, percutaneous refilling of the drug reservoir was necessary.

Side-Effects

In the initial treatment period, two patients temporarily showed vomiting, one patient showed urinary retention, and a further patient developed constipation. One of the five patients was dysphoric even in the further treatment phase. None of our patients had respiratory depression, and none had difficulties due to the implanted system. Operation of the pump buttons through the skin is slightly difficult only in adi-

pose patients. Here, partial resection of the subcutaneous fat layer at the time of implantation of the reservoir has proved effective.

The risk of central respiratory depression is regarded as relatively high in the literature in intraventricular morphine administration even in low doses (5,6,10,11). This could be eliminated by immediate systemic administration of naloxone. We believe that such a risk can be obviated by a deliberately very low, insidiously increased dosage.

Conclusion

The demand-controlled intraventricular self-administration of minidoses of morphine by means of implanted pump systems is a very satisfactory analgesic method for patients with chronic incurable pain states. In accordance with the present state of the art as reported in the literature and our own experience, it is indicated for paraneoplastic pain in malignancies in the head and neck region, in diffuse pain localization owing to disseminated metastases, and in more circumscribed bilateral or midline pain. For this pain, no convincing neurosurgical treatment is available as yet.

The morphine doses necessary are low, and there are no associated toxic phenomena. The method provides a higher quality of analgesia. It can be applied by the patient himself as needed, but it can also act automatically and continuously with implantation of appropriate pumps. The technique is invasive, but not ablative. Besides its analgesic effects, it improves the quality of life of the patient and frequently also his daily general activity.

Summary

Satisfactory improvements in pain were attained in five patients with paraneoplastic pain syndrome by intraventricular administration of 0.2 - 1.0 mg morphine hydrochloride with a fully implanted pump system over 12 - 48 h. Side-effects were transient and negligible. The demand-controlled self-administration of morphine led to a ca. 75% improvement in pain in two patients and a 100% improvement in pain in three patients. This improved the quality of life in all cases. In four patients, daily activity could also be increased. The period of follow-up observation is not more than 6 months.

References

1. Behar M, Magora F, Olshwang D, Davidson JT (1979) Epidural morphine in treatment of pain. Lancet I:527-529
2. Blond S, Meynadier J, Combellas-Pruvot M, Villette C, Dupard T, Christiaens J (1986) Indications et résultats de la morphinotherapie intra-cerebro-ventriculaire dans les algies cancereuses. A propos de 55 patients. Abstr. 2. Int.Symp. The Pain Clinic, Lille 1986:109
3. Coombs DW, Saunders RL, Gaylor MS, Pageau MG, Leith MG, Schaiberger C (1981) Continuous epidural analgesia via implanted morphine reservoir. Lancet II:425-426
4. Lazorthes Y, Gouarderes Ch, Verdie JC, Monsarrat B, Bastide R, Campan L, Cros J (1980) Analgésie par injection intrathécale de morphine. Etude pharmaco-cinétique et application aux douleurs irréductibles. Neurochirurgie 26:159-164

5. Leavans ME, Hill CS jr, Cech DA, Weyland JB, Weston JS (1982) Intrathecal and intraventricular morphine for pain in cancer patients: Initial study. J Neurosurg 56:241-245

6. Lobato RD, Madrid JL, Fatela LV, Rivas JJ, Reig E, Lamas E (1983) Intraventricular morphine for control of pain in terminal cancer patients. J Neurosurg 59:627-633

7. Nurchi G (1984) Use of intraventricular and intrathecal morphine in intractable pain associated with cancer. Neurosurgery 15:801-803

8. Pert CB, Snyder SH (1973) Opiate receptor: demonstration in nervous tissue. Science 179:1011-1014

9. Pilon RN, Baker AR (1976) Chronic pain control by means of an epidural catheter. Cancer 37:903-907

10. Roquefeuil B, Benezech J, Blanchet P, Batier C, Frèrebeau P, Gros C (1984) Intraventricular administration of morphine in patients with neoplastic intractable pain. Surg Neurol 21:155-158

11. Thiebaut JB, Blond S, Farcot JM, Thurel C, Matge G, Schach G, Meynadier J, Buchheit F (1985) La morphine par voie intraventriculaire dans le traitement des douleurs néoplasiques. Med Hyg 43:636-646

12. Wang JK, Nauss LA, Thomas JE (1979) Pain relief by intrathecally applied morphine in man. Anaesthesiology 50:149-150

13. Yaksh TL (1981) Spinal opiate analgesia. Characteristics and principles of action. Pain 11:293-346

14. Zenz M, Schappler-Scheele B, Neuhaus R, Piepenbrock S, Hilfrich J (1981) Long-term epidural morphine analgesia in cancer pain. Lancet I:91

Intrathecal Administration of Baclofen for Treatment of Spasticity: Neurobiological Principles and First Clinical Results

U. H. Wiese, W. Grüninger, J. Bockhorn, and N. Wünsche

Neurochirurgische Klinik und Rehabilitations-Klinik für Rückenmarkverletzte, Hohe Warte, D-8580 Bayreuth

Spasticity

The term "spasticity," as defined by LANCE (7) as "a motor disorder characterized by a velocity dependent increase in tonic stretch reflexes (muscle tone) with exaggerated tendon jerks," includes a clinical phenomenon which is produced by spinal and supraspinal lesions in the central nervous system: The transection of the brain stem at midbrain level, a condition that SHERRINGTON (16) called "decerebrate rigidity," and the condition after spinal cord trauma are combined with clinical and electrophysiological findings identical to the above-mentioned definition. Nevertheless, it certainly cannot be excluded that different mechanisms of neuronal interactions are involved in the formation of spasticity. Although the *imbalance* between the different descending systems, including the reticulospinal and vestibulospinal tracts, could play a major role in the spasticity triggered by supraspinal lesions, the *"sprouting"* theory is gaining more and more importance in the light of growing knowledge of the plasticity of the adult central nervous system. McCOUCH et al. (9) and LIU and CHAMBERS (8) found in monkeys and cats a sprouting of segmental afferent terminals below a spinal cord transection area. It appeared that sprouts and terminals of dorsal root fiber axons in part take over vacated synaptic sites originally occupied by terminations of descending, now degenerated, fibers. Such a process has been suggested to contribute to the spasticity.

Baclofen

Baclofen (beta-4-chlorphenyl-GABA) is as effective a muscle relaxant in patients with complete spinal transections as it is in patients with incomplete lesions (1,5,11), indicating that its site of action is in the spinal cord. It produces a potent and prolonged depression of synaptic transmission in mono- and polysynaptic pathways (6). The reduction of reflexes reflects a reduction in the amplitude of the excitatory postsynaptic potentials (EPSPs) in motoneurons (4), achieved by hyperpolarization of *pre*synaptic nerve terminals (11), which are therefore reduced in their excitability (2,13). Baclofen strongly suppresses the electrically stimulated release of endogenously synthesized glutamic and aspartic acids from slices of guinea pig cortex (14). This information is pertinent, since these excitatory amino acids are believed to be the transmitters released by some primary afferent fibers and interneurons in the spinal cord (15).

It seems very important that after administration of baclofen in high concentrations, e.g., when applied by iontophoresis to single spinal neurons, a reversible depression of neuronal firing occurs (4); this inhibition of cell discharge is a postsynaptic effect (3).

Advances in Neurosurgery, Vol. 16
Ed. by W. Walter, M. Brandt, M. Brock, and M. Klinger

Table 1. Intrathecal administration of baclofen

Patient	V.S./1972/m.	R.F./1942/m.	E.S./1960/m.	G.M./1930/f.	E.K./1927/f.	M.N./1920/f.
Clin. diagnosis	Midbrain lesion	Traumat., C6	Traumat., T2	Cerv. thoracic syringomyelia	ED[b]	ED[b]
Clin. symptoms	Decerebration rigidity	Tetraspastic syndrome	Paraspastic syndrome	Paraspastic syndrome	Paraspastic syndrome	Tetraspastic syndrome
BCF/day	3 × 50 µg	150 µg	300 µg	300 - 330 µg	240 µg	bis 3 × 60 µg
Cath. position	T5	T8	T10	T7	T8	T5
Vol. movement[a]						
Muscle tone[a]						
Spasm[a]						
Clonus						

[a]Before/during intrathecal administration of baclofen
[b]Encephalomyelitis disseminata

Clinical Trials (see Table 1)

Following the methods suggested by MÜLLER and ZIERSKI (10), baclofen was administered initially via a subcutaneous port attached to an intrathecal catheter introduced percutaneously in the lower lumbar region. Several daily bolus injections were used to find out the optimal dosage. After an average of 4 weeks a continuous infusion pump was implanted for continuous administration and to enable patients to be discharged to home care.

Patient 1 (V.S., born 1972; male). Posttraumatic midbrain bleeding. Port implantation. Only slight reduction of the decerebration rigidity (extensor spasticity). An inadvertent overdosage resulted within 3 h in vomiting, blood pressure depression, and breathing insufficiency. Controlled artificial respiration for 24 h; thereafter complete disappearance of the effects of the complication. During the phase of overdosage slightly more reduction of spasticity, no complete suppression.

Patient 2 (R.F., born 1942; male). Traumatic midcervical facet dislocation, complete tetraplegia, tetraspastic syndrome with extensive contractions. Port; pump implantation. Clear reduction of spasticity. After 3 months subcutaneous infection of the pump area, explanation of the pump. Unusually srong effect of oral baclofen administration during the first weeks after finishing the intrathecal baclofen therapy.

Patient 3 (E.S., born 1960; male). Compression fracture of upper thoracic spine, complete paraplegia. Port; pump implantation. Clear reduction of spasticity.

Patient 4 (G.M., born 1930; female). Cervicothoracic syringomyelia; complete paraplegia, paraspastic syndrome. Port; pump implantation. Complete elimination of spasticity. Single catheter disconnection (Fig. 1).

Patient 5 (E.K., born 1927; female). Encephalomyelitis disseminata; paraspasticity in flexion, unable to use the wheelchair. Port; pump implantation. Complete elimination of spasticity; able to use the wheelchair; recreation of voluntary movements. Removal of depressive state.

Patient 6 (M.N., born 1920; female). Encephalomyelitis disseminata; tetraspastic syndrome. Port; during the trial with daily bolus injections (clear reduction of spasticity) infection, growing number of cells in the cerebrospinal fluid, explantation of the port and the intraspinal catheter.

Concluding Remarks

All of the patients with spinal spasticity (patients 2-6) showed a clear reduction of elimination of the spastic syndrome, sometimes combined with a reduction of spasm-induced pain and recreation of voluntary movement. In patient 1 the decerebration rigidity (supraspinal extensor spasticity) could not be influenced sufficiently even after a single inadvertent overdosage. The differing effects of the intrathecal baclofen administration could be based on the different pathophysiological mechanisms, e.g., exertion of an excessive excitatory influence by the disinhibited vestibulospinal system in supraspinal spasticity.

One can only speculate as to whether a hypersensitivity exists based on growing receptor surfaces for baclofen after termination of its intrathecal administration. PENN (12) also reported patients with higher sensitivity for baclofen after interruption of its administration.

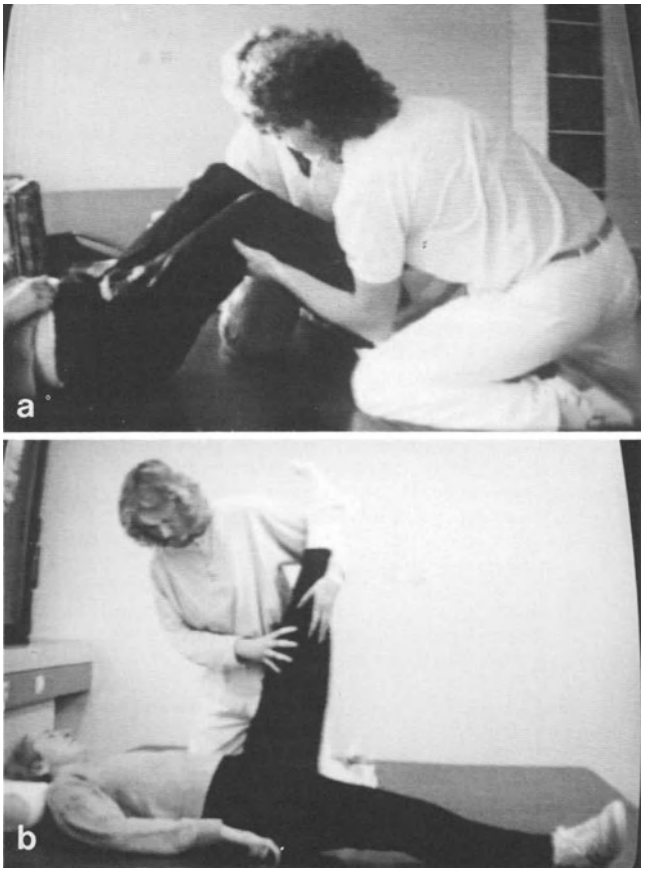

Fig. 1a,b. Patient G.M. before and during treatment with intrathecally administered baclofen

The data presented here with only a small number of patients do not allow any definite conclusion. The multicenter study for examination of the effectiveness of intrathecally administered baclofen, initiated by MÜLLER and ZIERSKI, will yield more detailed knowledge on this new approach in the treatment of spasticity.

References

1. Burke D, Andrews CJ, Knowles L (1971) The action of a GABA derivate in human spasticity. J Neurol Sci 14:199-208
2. Davidoff RA (1980) Effects of baclofen on synaptic activity in the spinal cord. In: Feldman RG, Young RR, Koella WP (eds) Spasticity: Disordered motor control. Yearbook Medical Publishers, Chicago, Illinois, pp 421-432
3. Davidoff RA, Hackman (193) Drugs, chemicals and toxins: Their effects on the spinal cord. In: Davidoff RA (ed) Handbook of the spinal cord, vol 1. Marcel Dekker, New York Basel, pp 409-476
4. Fox S, Krnejevic K, Morris ME, Puil E, Werman R (1978) Action of baclofen on mammalian synaptic transmission. Neuroscience 3:495-515

5. Jones RF, Burke D, Marosszeky JE, Gillies JD (1970) A new agent for the control of spasticity. J Neurol Neurosurg Psychiatry 33: 464-468

6. Kudo Y, Kurachi M, Fukuda H (1976) Action of baclofen on the isolated spinal cord of the frog. Jpn J Pharmacol 26:99P

7. Lance JW (1980) Symposium synopsis. In: Feldman RG, Young RR, Koella WP (eds) Spasticity: Disordered motor control. Year Book Medical Publishers, Chicago, Illinois

8. Liu CN, Chambers WW (1958) Intraspinal sprouting of dorsal root axons. Arch Neurol Psychiat 79:46-61

9. McCouch GP, Austin GM, Liu CN, Liu CY (1958) Sprouting as a cause of spasticity. J Neurophysiol 21:205-216

10. Müller H, Zierski J (1986) Empfehlungen zur Langzeitanwendung von intrathecalem Baclofen bei spinaler und cerebraler Spastizität.

11. Pederson E, Arlien-Soborg P, Mai J (1974) The mode of action of the GABA derivate baclofen in human spasticity. Acta Neurol Scand 50:665-680

12. Penn RD (1986) Vortrag, Symposium local-spinal Therapie der Spastik, Gießen

13. Pierau FK, Matheson GK, Wurster RD (1975) Presynaptic action of beta(-4-chlorophenyl)-GABA. Exp Neurol 48:343-351

14. Potasher SJ (1979) Effects on amino acid release and metabolism in slices of guinea pig cerebral cortex. J Neurochem 32:103-109

15. Puil E (1983) Action and interaction of S-glutamate in the spinal cord. In: Davidoff A (ed) Handbook of the spinal cord, vol 1. Marcel Dekker, New York Basel, pp 105-169

16. Sherrington CS (1898) Decerebrate rigidity and reflex coordination of movements. J Physiol (Lond) 22:319-332

Magnetic Resonance Imaging

0.35-T Proton Nuclear Magnetic Resonance Imaging of the Central Nervous System: Clinical Review of 2909 Patients

N. Roosen, E. Lins, M. Schirmer, M. Freiwald, W. Stork, D. Gahlen, and W. J. Bock

Neurochirurgische Universitätsklinik, Moorenstraße 5, D-4000 Düsseldorf 1

Introduction

The first images using magnetic resonance (MR) were realized in 1973 (12). Clinically useful MR scans of the head were published at the beginning of the current decade (9,11,16), and imaging quality has now attained high standards (3). At present the expensive MR technique is not only used in a research and university setting, but in private clinical practice too (2).

This paper describes the experience of the Röntgeninstitut "Grafenberger Allee" and the Neurosurgical University Clinic, both in Düsseldorf, with clinical MR imaging of the craniovertebral region during the 1984-1986 period.

MR Imaging

All patients were examined at the Röntgeninstitut "Grafenberger Allee" with a Diasonics MT/S MR imager, using a superconductive magnet operating at 0.35 T. Routinely, transverse, coronal, and sagittal scans were obtained with a standard head/neck or body coil; special surface coils were available for high-resolution imaging of the spine, the orbit, and the internal acoustic meatus. Slice thickness was 8 - 10 mm for regular investigations but could be reduced down to 2 mm for high-resolution imaging. The MR studies were performed with the spin-echo (SE) pulse sequence, using repetition times (TR) varying between 550 ms and 2000 ms, and echo-delay (TE) times of 28(30) ms and 56(60) ms.

For the past few months the paramagnetic MR contrast agent gadolinium-DTPA has been at our disposal for use in selected patients. Our personal experience is still limited, and the interested reader is referred to the relevant literature (6,7,19).

Patient Selection

Since the MR imager was operated in private practice, there was no patient selection with regard to special research criteria. Patients were referred for MR imaging by university and nonuniversity medical centers, by practicing neurologists, by internists, and even by primary care physicians. Most patients, however, had been seen by a neurologist or neurosurgeon and had been studied with computed tomography (CT). The results of CT, angiography, neurological examination, etc. were available when evaluating the MR images. Therefore, the diagnosis usually was known or could be obtained by questioning the referring physician.

Advances in Neurosurgery, Vol. 16
Ed. by W. Walter, M. Brandt, M. Brock, and M. Klinger

Table 1. MR findings in 2909 examinations of the head and 953 examinations of the spine (Röntgeninstitut "Grafenberger Allee," 1984-1986)

MR examinations of the head			MR examinations of the spinal region		
Tumor	21.0%		Degenerative vertebral disease	26.8%	
White matter disease (including multiple sclerosis)	16.8%		Tumor	9.5%	
Vascular disease	16.5%	67.3%	White matter disease (including multiple sclerosis)	4.5%	53.9%
Trauma	1.2%		Infection	3.9%	
Hydrocephalus	1.1%		Trauma	2.3%	
Infection	1.0%		Syringomyelia	2.3%	
Orbit and eye	0.8%				
Other conditions	8.9%				
Diagnosis not known, pathological MR scan		4.9%	Diagnosis not known, pathological MR scan		11.1%
Normal MR image		27.8%	Normal MR image		35.0%
		100.0%			100.0%

In a significant proportion of the patient population, however, an exact diagnosis could not be reached, although the MR scans were evidently pathological.

Results (Table 1)

A total of 3862 MR examinations have been performed, comprising 2909 studies of the head, and 953 spinal investigations. In 27.8% of the cranial MR scans no abnormality could be found; in the spinal studies this percentage was even higher (35.0%). Most of these patients nevertheless had some sort of neurological symptomatology, often transient, and on rare occasions they even had a suspicious CT finding.

The diagnosis was not exactly known in 4.9% and 11.1% of MR studies of the head and the spine respectively. In these patients the obviously pathological MR findings were not helpful in reaching a correct diagnosis either. The remaining MR studies were pathological and could be related to known disease entities.

Discussion

We present a retrospective, nonblind review of the case material of the Röntgeninstitut "Grafenberger Allee." Therefore, this series is somewhat biased. However, it demonstrates referral patterns, the relative prevalence of some disease entities, the absence of pathological MR findings in many patients with (transient) neurological symptoms, and the inability to reach a diagnosis in ca. 5% of patients undergoing cranial MR and over 11% of patients undergoing spinal MR.

The importance of MR in the diagnosis and evaluation of cerebral tumors, especially of benign astrocytomas and neoplasms of the middle structures and cerebellum, is well established (4,20,21). The same holds true for white matter disease (1,5) and cerebrovascular disease (18). However, MR is not more efficient than CT in imaging of malignant gliomas (20,21), and its higher efficiency in depicting cerebral infarction (18) has only occasional clinical significance. Therefore, the relative preponderance of white matter disease as well as of benign and midline cerebral tumors in our MR series is understandable.

Due to the excellent noninvasive imaging of the spinal region MR is often the method of choice for studying the spine, especially in syringomyelia, hydromyelia, and spinal cord tumors (8,13), in degenerative vertebral disorders (15,17), and in demyelinating disease (14). MR can obviate the necessity to perform myelography with an X-ray contrast agent that is injected intrathecally (10). Direct sagittal imaging is another advantage of MR over CT of the spine. However, due to the small dimensions of several structures, such as the spinal cord and the nerve roots, imaging quality should be the highest possible in order to obtain adequate MR scans. Scoliosis, too, may degrade image quality because of partial volume effects. Both these reasons may partly explain the higher percentage of normal and of unclear pathological spinal MR scans as compared with cranial MR imaging. Nevertheless, MR seems to be the investigation of choice in spinal disease.

Conclusions

Magnetic resonance imaging is more sensitive to pathological conditions of the central nervous system than is CT, especially in cases of white matter disease. Nevertheless, MR may be normal in the presence of neurological symptomatology. Therefore, the diagnostic yield of MR imaging also depends upon the clinical history, the neurological examination, and the results of CT, angiography, and other ancillary examinations. A complete workup of the patient should be done to obtain all information to enable a correct diagnosis to be reached.

MR can obviate the need for contrast examinations such as myelography in several instances. This, and the lack of ionizing radiation, makes MR imaging very suitable for repeat examinations and for investigation of children.

References

1. Borgel F, Hommel M, Pollak P, Gaio JM, Crouzet G, Lebas JF, Pellat J, Perret J (1986) L'imagerie par résonance magnétique dans la sclérosis en plaques. Sensibilité et corrélations avec la clinique. Rev Neurol (Paris) 142:598-606
2. Bornheim W (1986) Wirtschaftlichkeitsanalysen der modernen bildgebenden Verfahren unter Berücksichtigung von NMR, DSA und CT. In: Vogler E, Schneider GH (eds) Digitale bildgebende Verfahren – Integrierte digitale Radiologie, Medizinisch-wissenschaftliche Buchreihe von Schering. Schering AG, Berlin, pp 28-39
3. Brant-Zawadzki M, Norman D (1987) Magnetic resonance imaging of the central nervous system. Raven Press, New York
4. Chatel M, Darcel F, de Certaines J, Benoist L, Bernard M (1986) T_1 and T_2 proton nuclear magnetic resonance (N.M.R.) relaxation times in vitro and human intracranial tumours. Results from 98 patients. J Neuro-Oncol 3:315-321

5. Edwards MK, Farlow MR, Stevens JC (1986) Multiple sclerosis: MRI and clinical correlation. AJNR 7:595-598

6. Felix R, Schörner W, Laniado W, Niendorf HP, Claussen C, Fiegler W, Speck U (1985) Brain tumors: MR imaging with gadolinium-DTPA. Radiology 156:681-688

7. Gadian GD, Payne JA, Bryant DJ, Young IR, Bydder GM (1985) Gadolinium-DTPA as a contrast agent in MR imaging – theoretical projections and practical observations. J Comput Assist Tomogr 9:242-251

8. Goy AMC, Pinto RS, Raghavendra BN, Epstein FJ, Kricheff II (1986) Intramedullary spinal cord tumors: MR imaging, with emphasis on associated cysts. Radiology 161:381-386

9. Hawkes RC, Holland GN, Moore WS, Worthington BS (1980) Nuclear magnetic resonance tomography of the brain: a preliminary clinical assessment with demonstration of pathology. J Comput Assist Tomogr 4:577-586

10. Hennig J, Friedburg H, Ströbel B (1986) Rapid nontomographic approach to MR myelography without contrast agents. J Comput Assist Tomogr 10:375-378

11. Holland GN, Moore WS, Hawkes RC (1980) Nuclear magnetic resonance tomography of the brain. J Comput Assist Tomogr 4:1-3

12. Lauterbur PC (1973) Image formation by induced local interactions: examples employing nuclear magnetic resonance. Nature 242:190-190

13. Lee BCP, Zimmerman RD, Manning JJ, Deck MDF (1985) MR imaging of syringomyelia and hydromyelia. AJNR 6:221-228

14. Maravilla KR, Weinreb JC, Suss R, Nunnally RL (1984) Magnetic resonance demonstration of multiple sclerosis plaques in the cervical cord. AJNR 5:685-689

15. Modic MT, Masaryk T, Boumphrey F, Goormastic M, Bell G (1986) Lumbar herniated disk disease and canal stenosis: prospective evaluation by surface coil MR, CT, and myelography. AJNR 7:709-717

16. Partain CL, James AE, Watson JT, Price RR, Coulam CM, Rollo FD (1980) Nuclear magnetic resonance and computed tomography. Radiology 136:767-770

17. Roosen N, Dietrich U, Nicola N, Irlich G, Gahlen D, Stork W (1987) MR imaging of calcified herniated thoracic disk. J Comput Assist Tomogr

18. Roosen N, Schirmer M, Lins E, Bock WJ, Stork W, Gahlen D (1986) Nuclear magnetic resonance imaging (MRI) of cerebral ischemia. In: Vogler E, Schneider GH (eds) Digitale bildgebende Verfahren – Integrierte digitale Radiologie. Medizinisch-wissenschaftliche Buchreihe von Schering. Schering AG, Berlin, pp 180-189

19. Runge VM, Clanton JA, Foster MA, Smith FW, Lukehart CM, Jones MM, Partain CL, James AE jr (1984) Paramagnetic NMR contrast agents. Development and evaluation. Invest Radiol 19:408-415

20. Uhlenbrock D, Beyer HK, Grote W (1985) Kernspintomographie bei Hirntumoren. Auswertung von 40 gesicherten Fällen. RÖFO 143:501-507

21. Wende S, Kretzschmar K (1985) Leistungsfähigkeit und Auswirkungen der neuroradiologischen Hirntumordiagnostik. Radiologe 25:497-501

Comparison of CT and MRI, with and without Contrast Enhancement, in the Detection of Brain Tumors

B. Schulz, A. Kern, M. Laniado, W. Schörner, J. Iglesias-Rozas, R. Felix, and E. Kazner

Neurochirurgische Abteilung des Rudolf-Virchow-Krankenhauses, Augustenburger Platz 2, D-1000 Berlin 65

Magnetic resonance imaging (MRI) as a clinical investigation became available in the early 1980s. Since then this method has proven to be a valuable additional diagnostic tool in the recognition and delineation of space-occupying lesions of the brain (1,2,3,5). In the present study the sensitivity and specifity of CT and MRI were compared. The evaluation was done from diagnostic and neurosurgical points of view.

Material and Methods

Between 1984 and 1987, 265 patients (aged 2 - 75 years) with intracranial space-occupying tumors were investigated. Histological confirmation was obtained in 238 cases (89.9%). The classification of the majority of the tumors is given in Table 1.

Computed tomography was done before and after application of intravenous iodinated, nonionic contrast media by use of a third-generation CT scanner. MR images were recorded using a Siemens superconducting whole-body scanner operating at 0.35 and later 0.5 T. The MRI coil used for head imaging (diameter 25 cm) had a nominal spatial resolution of 1 mm in the section imaged.

Table 1. Classification of investigated brain tumors (n = 265)

Diagnosis	No. of patients
Astrocytoma, oligodendroglioma, oligo-astrocytoma	40
Glioblastoma	27
Meningioma	58
Metastasis	35
Schwannoma	10
Medulloblastoma	3
Pituitary adenoma	17
Craniopharyngioma	11
Other tumors (e.g., angioblastoma, lipoma, chordoma, hamartoma, melanoma, lymphoma, epidermoid cysts)	64

Advances in Neurosurgery, Vol. 16
Ed. by W. Walter, M. Brandt, M. Brock, and M. Klinger

Table 2. MRI imaging technique used

Pulse sequence	TI (ms)	TR (ms)	TE (ms)	Number of sections	Measuring time (min)
Spin echo		400	35	2	3.4
Spin echo		800	35.7	4	6.8
Spin echo		1600	35.7	8	13.6
Inversion recovery	400	1400	35	3	13.4

The investigation protocol consisted of several spin echo imaging sequences, including nearly always the spin echo sequences SE 1600/35 and SE 1600/70 and at least one other sequence listed in Table 2.

In 120 patients MRI was done before and after the application of the paramagnetic contrast medium gadolinium-DTPA (Dimeglumin, Schering AG, Berlin) with a dose of 0.1 mmol/kg body weight. T_1-weighted sequences were used in this protocol.

For the evaluation four main groups, consisting of low-grade gliomas, glioblastomas, meningiomas, and metastases, were compiled. In addition midline tumors were investigated separately.

The delineation of tumor vs. edema and edema vs. surrounding brain tissue served as criteria for the evaluation in CT and MRI. In addition the type of contrast enhancement and the demonstration of calcification were considered.

Results

Putting aside histological and topographical classifications, in 47% of cases CT and MRI gave identical results concerning the delineation of the tumor vs. edema or normal tissue. In 34% MRI was superior to CT and in 19% of cases CT gave a better result.

In the following the results are given in more detail with consideration of histological and topographical data.

Low-Grade Gliomas

Neither CT nor MRI allowed differentiation of tumor tissue from perifocal edema in the majority of these tumors (n = 40). In these cases

Table 3. Comparison of imaging techniques in low-graded gliomas (n = 40)

CT	equivalent	to	MRI	20%
MRI	superior	to	CT	65%
CT	superior	to	MRI	15%

Note: After administration of gadolinium-DPTA, no change in percentages occurred

Table 4. Differentiation of tumor tissue from edema and edema from brain tissue in glioblastomas

Glioblastoma: tumor/edema				
Without gadolinium-DTPA (n = 5)				With gadolinium-DTPA (n = 22)
CT	equivalent to	MRI	0%	28%
MRI	superior to	CT	60%	31%
CT	superior to	MRI	40%	41%
Glioblastoma: edema/brain tissue				
Without gadolinium-DTPA (n = 5)				With gadolinium-DTPA (n = 22)
CT	equivalent to	MRI	5%	5%
MRI	superior to	CT	53%	53%
CT	superior to	MRI	42%	42%

Table 5. Differentiation of tumor tissue from edema and edema from brain tissue in meningiomas

Meningioma: tumor/edema				
Without gadolinium-DTPA (n = 19)				With gadolinium-DTPA (n = 39)
CT	equivalent to	MRI	58%	59%
MRI	superior to	CT	11%	23%
CT	superior to	MRI	31%	18%
Meningioma: edema/brain tissue				
Without gadolinium-DTPA (n = 19)				With gadolinium-DTPA (n = 39)
CT	equivalent to	MRI	50%	50%
MRI	superior to	CT	37.5%	37.5%
CT	superior to	MRI	12.5%	12.5%

the delineation of the whole process from normal brain tissue was evaluated. MRI proved to be superior in 65% of cases (Table 3). The superiority of MRI resulted from the high contrast of the lesions vs. the surrounding tissue, which could be shown in the T_2-weighted sequences. No relevant improvement in delineation was possible by the application of iodinated contrast media in CT and paramagnetic agent in MRI, because no contrast enhancement took place. The classification was possible to the same degree with both methods. The diagnosis of oligodendroglioma by CT was facilitated by the proof of calcifications.

Glioblastomas

Computed tomography was done in all 27 patients with glioblastomas before and after application of contrast medium. In the MRI study gadolinium-DTPA was given in 22 cases. CT and MRI with contrast media gave similar enhancement patterns. Both methods were equivalent in the imaging of enhancing tumor tissue and its delineation from the perifocal edema and could be used for the typing of the tumor. T_2-weighted sequences of

MRI allowed better differentiation of the edema from normal tissue compared with CT (Table 4).

Meningiomas

In all 58 patients with meningiomas CT was done with and without contrast medium, whereas MRI with gadolinium-DTPA was performed in only 39 of these patients. When CT with contrast medium was compared with MRI without contrast medium, the imaging of the tumor was comparable in 58%, in 31% CT was better than MRI, and in 11% MRI gave better results than CT. When gadolinium-DTPA was administered in the MRI series the figures changed to 59%, 18%, and 23% (Table 5). Concerning the delineation of edema vs. normal tissue, the methods were equivalent in 50%, while in 37.5% MRI was superior to CT. Due to the characteristic enhancement pattern of meningiomas, CT allows greater precision in the prediction of the histological diagnosis. Furthermore, CT reveals a better relation of the tumor to the bony structures of the skull.

Metastases

In two-thirds of the 35 patients with metastases due to different primary tumors, CT and MRI gave comparable results with respect to delineation of tumor vs. edema. In four cases MRI showed additional tumors at the base of the skull which could not be detected by CT.

Midline Lesions

In this group, tumors in or near the midline of different histological provenience were combined only for topographical reasons. In 55% the tumor demarcation was better with MRI, in 20% CT gave better results, and in 25% the methods were equivalent.

Discussion

This study has shown that for the diagnosis of space-occupying intracranial processes the value of CT and MRI depends on topographical and histological criteria. In low-grade gliomas, T_2-weighted sequences of MRI give better demarcation of the process compared with CT. CT has an advantage by demonstrating calcifications, which are pathognomic for oligodendroglioma.

In accordance with BRADLEY et al. (1) and BYDDER et al. (2), we could not find signs of calcifications in these tumors in MRI. In low-grade gliomas CT and MRI do not allow differentiation between tumor and edema. Histological evaluations of the border zone of these processes reveal that they consist exclusively of tumor tissue with absence of edema. Therefore the excellent picture of the complete process in MRI is valuable as regards indication for surgery.

In many cases of glioblastoma, injection of gadolinium-DTPA give better results than native recordings. Gadolinium-DTPA enhanced MRI gives nearly identical enhancement patterns compared with enhanced CT. Concerning prediction of tumor type and delineation, the two methods are equivalent after application of contrast media (4).

In the diagnosis of meningioma we found major differences. Due to the typical enhancement pattern and the clear relationship to the bony structures, CT gives better results. According to TREISCH et al. (6) in me-

ningiomas MRI depicts a strong homogeneous enhancement after intravenous application of gadolinium-DTPA. This can give hints for tumor typing. MRI has advantages for the diagnosis of meningiomas of the posterior fossa and small meningiomas at the base of the skull, especially meningioma en plaque (3,5).

In midline processes MRI proves better than CT, especially in the diagnosis of small tumors, owing to higher contrast resolution, the multiplanar orientation, and lack of bone artifacts (3,5).

Summary

Computed tomography remains the basic investigation when a space-occupying intracranial process is suspected. MRI is helpful in cases of insufficient tumor imaging and special localizations. For improvement of tumor delineation the application of gadolinium-DTPA is recommended in tumors which already show enhancement in CT scans.

References

1. Bradley WG, Waluch V, Yadley RA, Wycoff RR (1984) Comparison of CT and MR in 400 patients with suspected disease of the brain and the cervical spinal cord. Radiology 152:695-702
2. Bydder GM, Steiner RE, Young IR, Hall AS (1982) Clinical NMR imaging of the brain: 140 cases. AJR 139:215-236
3. Bydder GM, Steiner RE, Thomas DJ, Marshall J (1983) Nuclear magnetic resonance imaging of the posterior fossa: 50 cases. Clin Radiol 34: 173-188
4. Claussen C, Laniado M, Kazner E, Schörner W, Felix R (1985) Application of contrast agents in CT and MRI (NMR): Their potential in imaging of brain tumors. Neuroradiology 27:164-171
5. Han JS, Bonstelle CT, Kaufman B, Benson JE, Alfidi RJ, Clampitt M, Van Dyke C, Huss RG (1984) Magnetic resonance imaging in the evaluation of the brain-stem. Radiology 150:705-712
6. Treisch J, Schörner W, Laniado M, Felix R (1987) Charakteristika intrakranieller Meningeome in der magnetischen Resonanztomographie. Fortschr Röntgenstr 146:207-214

Advantages of MRI in the Surgical Strategy for Brain Stem Tumors

M. Brandt, J. Anagnostopoulos-Schleep, H.-J. König, G. Fahrendorf, and Th. Herter

Neurochirurgische Klinik der Westfälischen Wilhelms-Universität, Albert-Schweitzer-Straße 33, D-4400 Münster

Space-occupying lesions of the brain stem may be documented by CT investigations. More detailed information on their location and extent can be acquired by magnetic resonance imaging (MRI) (1,6). Strategy and operative risk can be better estimated when one knows the growth characteristics, whether cystic or exophytic tumor portions are present, and the relation of the tumor to surrounding structures (3,7).

In 20 patients presenting with brain stem lesions, conventional neuroradiological investigations, including CT scan, were complemented by MRI. Of the above-mentioned cases, 14 were treated surgically. A definite correlation could be found between preoperative MRI findings, surgical condition, and histological diagnosis. The series consisted of eight pilocytic astrocytomas, two ependymomas, two angioblastomas, and two epidermoids. The advantages of MRI are demonstrated by three case reports.

Case Report 1. A 47-year-old male was investigated for signs of cerebellar dysfunction. On the basis of the CT scan an arachnoid cyst was suspected in the area of the cerebellomedullary cistern. MRI showed evidence of a mass growing out of the medulla, which was well visualized on sagittal sections (Fig. 1). Although the Nd-YAG laser may have dis-

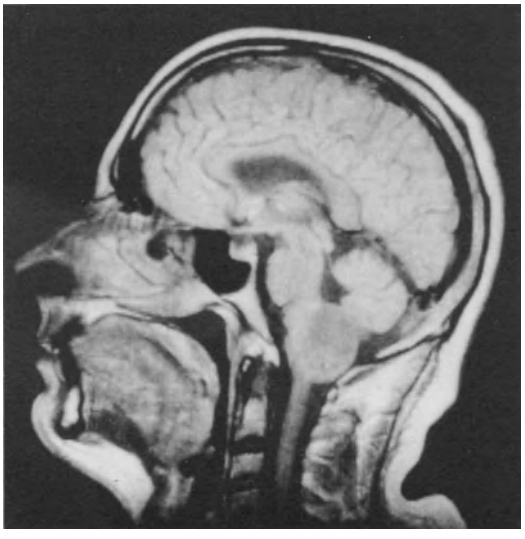

Fig. 1. MRI of a 47-year-old patient with a pilocytic astrocytoma of the brain stem, which was subtotally removed

Advances in Neurosurgery, Vol. 16
Ed. by W. Walter, M. Brandt, M. Brock, and M. Klinger

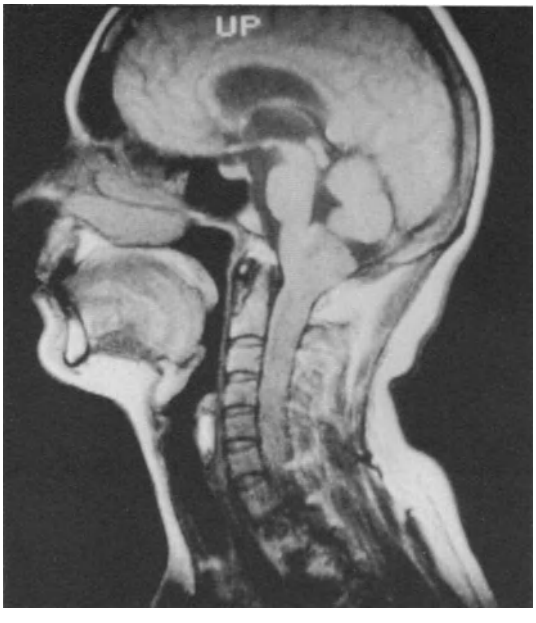

Fig. 2. MRI of a 45-year-old patient with an ependymoma growing out of the brain stem and extending into the upper cervical spinal canal

advantages in the neighborhood of the brain stem, in this case it was successfully used as an additional tool without damaging vital structures. Exact knowledge of the diameter of a mass should be procured. In this case a pilocytic astrocytoma was found. A 2-year follow-up period was uneventful.

Case Report 2. A 50-year-old female patient was treated for multiple sclerosis for more than 25 years. CT scan revealed a right extra-axial hypodense area next to the lower brain stem. Slight enhancement after contrast infusion was observed. MRI sections showed a tumor mass containing two cystic exophytic components. Exact determination of these accessible portions made the microsurgical approach safer and less time consuming. There were no postoperative complications. Histologically a pilocytic astrocytoma was diagnosed.

Case Report 3. A 45-year-old female patient was investigated for paraparesis of the legs. On CT scan symmetrically dilated ventricles were detected. The myelogram showed an intradural extramedullary mass in the upper cervical canal. Sagittal MRI sections demonstrated an exophytic cervicomedullary tumor extending into the spinal canal (Fig. 2). The tumor was removed by CUSA subtotally and was proved to be an ependymoma.

Clinical course seems to be a very important prognostic factor in brain stem tumors. The history of 17 surgically treated patients with brain stem gliomas between 1974 and 1986 was analyzed. Histological findings are shown in Fig. 3. In these cases biopsy or subtotal removal was performed. Postoperative survival was 55% after 11 years. The results may demonstrate the benign biological behavior of the majority of brain stem gliomas (Fig. 4).

From our experience with brain stem tumors we found that MRI gave information unobtainable on CT scan. In the posterior fossa MRI seems to be superior because of the CT artifacts from beam hardening and axial nonuniformity of the sample volume (2,4). CT scan may be suitable

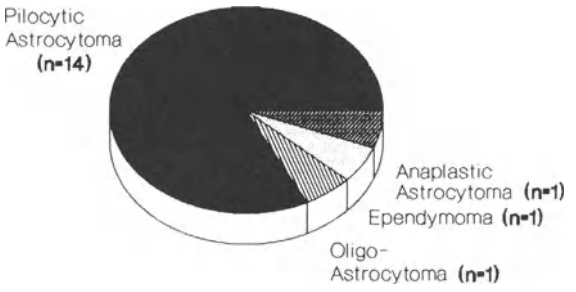

Fig. 3. Histological diagnosis of 17 brain stem gliomas operated on between 1974 and 1976

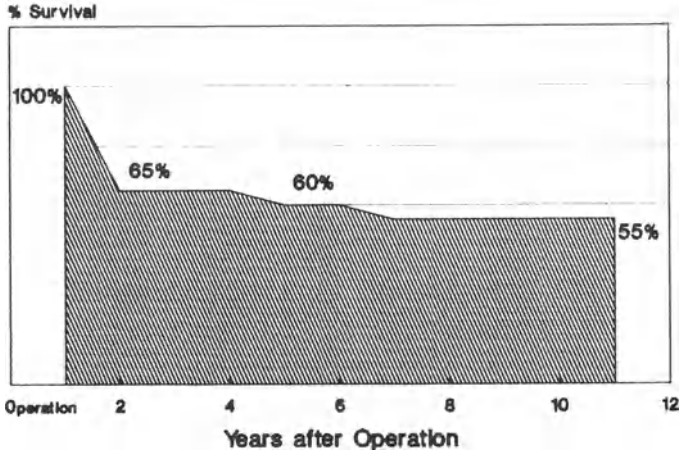

Fig. 4. Postoperative survival of 17 patients with brain stem gliomas operated on between 1974 and 1976

for detecting brain stem lesions. MRI appears to be the investigation to demonstrate the exact extent of the disease (5).

In conclusion, the advantages of MRI from a neurosurgical point of view are as follows:

1. Three-dimensional imaging with few artifacts.
2. Demonstration of tumor growth characteristics (focal, diffuse, cystic, perifocal edema).
3. Additional information concerning preoperative differential diagnosis.
4. Determination of surgical approach (biopsy, total or subtotal removal, cyst evacuation, restoration of CSF pathways).
5. Suitability of additional surgical instruments (laser, CUSA).

References

1. Bradley WG, Waluch V, Yadley RA, Wycoff RR (1984) Comparison of CT and MR in 400 patients with suspected disease of the brain and cervical spinal cord. Radiology 152:695-702
2. McGinnis BD, Brady TJ, New PFJ, Buonanno FS, Pykett IL, DeLaPaz RL, Kistler JP, Taveras JM (1983) Nuclear magnetic resonance (NMR) imaging of tumors in the posterior fossa. J Comput Assist Tomogr 7:575-584

3. Han JS, Huss RG, Benson JE, Kaufman B, Yoon YS, Morrison SC, Alfidi RJ, Rekate HL, Ratcheson RA (1984) MR imaging of the skull base. J Comput Assist Tomogr 8:944-952

4. Lee BCP, Kneeland JB, Deck MDF, Cahill PT (1984) Posterior fossa lesions: magnetic resonance imaging. Radiology 153:137-143

5. Nadjmi M, Ratzka M (1986) Wann ist die NMR-Tomographie in der Diagnostik des zentralen Nervensystems unverzichtbar? In: Walter W, Krenkel W (eds) Jahrbuch der Neurochirurgie 1986. Regensberg und Biermann, Münster, pp 163-176

6. Randell CP, Collins AG, Young IR (1983) Nuclear magnetic resonance imaging of the posterior fossa. AJR 141:489-496

7. Schorner E, Kazner E, Laniado M, Sprung C, Felix R (1984) Magnetic resonance tomography of intracranial tumors: initial experience with the use of the contrast medium gadolinium-DTPA. Neurosurg Rev 7:303-312

Tumors of the Skull Base and Posterior Fossa in Children - Comparison of CT and MRI

Ch. Sprung, K. Maier-Hauff, K. Hansen, T. Michael, W. Schörner, and Ch. Manicke

Neurochirurgische Abteilung im Klinikum Charlottenburg, Spandauer Damm 130, D-1000 Berlin 19

Introduction

Demonstration of brain parenchyma at the base of the skull and in the cerebellum in CT studies is usually rendered difficult by the partial volume effect of adjacent bone structures. As a result, studies by a number of authors have shown the superiority of MRI over CT in demonstrating brain tumors at these locations in adults (8,9,10,15,16,22, 23). Signal enhancement with paramagnetic contrast media has played an important role in this respect (6,7,17). The fact that there is no exposure to X-ray is an additional advantage of MRI in studies of children and adolescents. This important advantage has to be weighed against the long duration of the examination and necessity of sedation or general anesthesia in infants and young children. Since gadolinium cannot be administered to young children, we undertook to compare CT and MRI in children with tumors at the base of the skull and in the posterior fossa.

Patients and Methods

Technically adequate studies are a prerequisite for exact comparison of CT and MRI. For this reason our series was limited to 20 children who had undergone complete CT studies with and without contrast enhancement, including reconstructed images (SOMATOM DR 2), as well as MRI (magneton) with 0.35 and 0.5 T before therapy was instituted.

Our study comprises 20 children and adolescents with tumors at the base of the skull and in the posterior fossa. The frequency of the individual types of tumor corresponds to the incidence of each type in patients of this age group as reported in the literature (1). Table 1 demonstrates the patients and modes of therapy used in our series. There were 12 supratentorial and 8 infratentorial tumors. It was impossible to perform an operation or stereotactic biopsy in 4 of the 20 children; histological diagnosis was made at autopsy in one case. In one additional patient stereotactic biopsy did not provide an exact diagnosis. As a result, histological diagnosis was not possible in four patients in our series.

Direct demonstration of the tumor was the first criterion of comparison between CT and MRI. A second important parameter was the ability of each method to delineate the borders of the tumor. Finally, two independent observers attempted a histological diagnosis on the basis of the images provided by each system. The suitability of each method for evaluation of these criteria was defined on a scale from impossible to excellent (Tables 2 - 4).

 Advances in Neurosurgery, Vol. 16
Ed. by W. Walter, M. Brandt, M. Brock, and M. Klinger

Table 1. Patients and treatment regimes

Case No.	Age	Location	Clinical diagnosis	Histo-logical proof	Operation		Radiation		Chemotherapy	
					Resec-tion	Biop-sy	Alone	Adju-vant	Alone	Adju-vant
1	16	Pineal region	Astrocytoma	+		+	+			
2	15	Pineal region	Astrocytoma	+	+					
3	8	Brain stem	Astrocytoma	+		+	+			
4	6	Brain stem	Pilocytic astrocytoma	+		+	+			
5	14	Fourth ventricle, brain stem	Pilocytic astrocytoma	+	+			+		+
6	10	Vermis of cerebellum, fourth ventricle	Pilocytic astrocytoma	+	+					
7	12	Brain stem	Glioblastoma	+			+		+	
8	10	Brain stem	Glioma ?	Ø			+			
9	13	Brain stem	Glioma ?	Ø						
10	14	Hypothalamic region	Glioma ?	Ø		+				
11	8	L. cerebellar hemi-sphere, brain stem	Medulloblastoma	+	+			+		+
12	7	Parasellar	Craniopharyngioma	+	+					
13	11	Parasellar	Craniopharyngioma	+	+					
14	3	Parasellar	Craniopharyngioma	+	+					
15	14	Parasellar	Craniopharyngioma	+	+					
16	8	Parasellar	Dermoid cyst	+	+					
17	8	Basal medial L. temporal lobe	Hamartoma	+	+					
18	14	Basal medial L. temporal lobe	Hamartoma ?	Ø						
19	15	L. cerebellar hemisphere	Lymphoblastoma	+		+	+			
20	16	Bilateral cerebello-pontile and dorsum sellae	Acoustic neuromas and meningioma	+	+					
			Total	16	11	5	6	2	1	2

Table. 2. Comparison of CT and MRI as regards tumor detection

	CT		MRI
	Plain	Enhanced	
Impossible	1		
Equivocal	7	4	1
Good	5	5	2
Excellent	7	11	17

Table 3. Comparison of CT and MRI as regards delineation of tumors

	CT		MRI
	Plain	Enhanced	
Impossible	1		
Equivocal	6	4	1
Good	6	6	2
Excellent	7	10	17

Table 4. Comparison of CT and MRI as regards specificity

	CT		MRI
	Plain	Enhanced	
Impossible	1		
Equivocal	13	11	14
Good	3	3	4
Excellent	3	5	2

Results

The first criterion considered in our study was the capability of each method to demonstrate the tumor (Table 2). The plain CT scan failed to demonstrate the space-occupying lesion in only one case. MRI provided excellent demonstration of the tumor in 17 cases, as compared to 11 certain diagnoses with contrast-enhanced CT studies and 7 in the plain scan.

The second parameter which we evaluated was the ability of each method to delineate the borders of a brain lesion. Since appreciable brain edema was not present in our patients, delineation of the tumor against brain edema was not evaluated. Table 3 shows that MRI was clearly superior to CT in definition of the extent of the space-occupying lesion and in delineation of the borders of the tumor. This was decisive in establishing an indication for operation and developing a strategy for surgical treatment. The median and paramedian planes have proved especially valuable in demonstration of tumors at the base of the skull and in the posterior fossa.

Two of the authors attempted histological diagnosis using the images obtained with CT and MRI (Table 4). The diagnoses were made without consultation. Enhanced CT scans proved slightly superior to MRI in this regard, which was mainly attributable to failure to demonstrate calcification in cases of craniopharyngioma.

Discussion

In the past few years an increasing number of reports have appeared in the literature comparing CT and MRI in adults (2-5,8-11,15-22) and children (12,13,14,23) with brain tumors and other lesions. However, studies comparing the applicability of the techniques must fulfill certain conditions. One prerequisite is a technically adequate result. For this reason, one of the criteria of inclusion in our series was a technically adequate CT scan made with a third-generation system (Somatom DR 2) including contrast enhancement and reconstructed images. Several authors (2,3,5,12,20) have studied a variety of cerebral conditions of different location and based their evaluation on simple demonstration of the lesion. However, we believe that it is necessary to limit such a study to a single disease entity such as brain tumor, inflammatory disease, or cysts and to analyze a number of parameters such as detection and delineation of the lesion as well as specificity in order to develop a valid comparison of two imaging techniques. Comparison and evaluation of the two methods are difficult, since CT is used as a screening method in most cases. This permits more exact studies with MRI when the lesion has already been identified in the CT scan. It was not possible to avoid this methodological error in our study.

It is difficult to make an objective retrospective analysis of specificity using images from both techniques when the clinical history as well as surgical and histological findings are known (8,11). As a result there are few double-blind comparative studies in the literature (11). We attempted a compromise in our study. Two of the authors evaluated images independently of one another and classified the results in regard to three different criteria on a scale from impossible to excellent. When discrepancies of one step on the scale were found, the poorer rating of the two was included in the evaluation, while a mean value was included when there was a discrepancy of two steps on the scale.

Our analysis of detection and delineation demonstrates the superiority of MRI. The results are comparable to those reported in adults with a variety of brain tumors (2-5,8-11,15-18,20-22) as well as lesions of the posterior fossa (8-10,15,16,19,22,23) and correspond to results reported by other authors in children with brain tumors (12,14,23). The primary disadvantages of MRI reported by most authors are the inability to demonstrate calcification (2-4,12,14,15,17,18,20-22) as well as the lack of osseous landmarks in cases with involvement of bony structures which are detectable on CT scans in most cases (2,4,5,8-10, 15,17,18). This disadvantage has recently been doubted by SARTOR et al. (16).

In contrast to the study published by GENTRY et al. (8) comparing the two methods in demonstration of lesions in the posterior fossa, we did not define specificity according to localization of the tumor. For this reason, the results of our series confirm the superiority of enhanced CT over MRI in establishing a tentative histological diagnosis. Most of the other authors have reported similar conclusions in cases without application of gadolinium (3,11,14,18,20,22,23). Corresponding to our series a number of other investigators (12-14) have reported that sedation was sufficient to allow technically adequate studies, so that the advantages of MRI in children and adolescents are not limited by the necessity of general anesthesia.

Summary

Magnetic resonance imaging does not expose patients to ionizing radiation, and this is particularly important in studies of small children and adolescents. Failure to demonstrate calcification was a major disadvantage of MRI in our series. However, the fact that MRI does not encounter the artifacts which appear in CT studies at the base of the skull and in the posterior fossa renders MRI superior to CT in delineation of tumors from adjacent tissue in this region. The capability of MRI to demonstrate any desired plane is especially advantageous for the neurosurgeon in evaluating the patient for surgical treatment. CT is still superior to MRI in providing a tentative preoperative histological diagnosis, though this may be due to the fact that experience with CT is greater than that with MRI at the present time.

The most important disadvantage of MRI in children is the long duration of the examination. All children in our series were examined under sedation; general anesthesia was not necessary in a single case.

The results of our series show clearly that MRI is not merely a source of additional information complementing the CT study. MRI is the method of choice for demonstrating tumors at the base of the skull and in the posterior fossa in children. As a result, it is our current practice to employ MRI alone in follow-up studies of children and adolescents with tumors in this region.

References

1. Birch JM, Marsden HB, Swimdell R (1980) Incidence of malignant disease in childhood. A twenty-four year review of the Manchester Children's Tumours Registry data. Br J Cancer 42:215-220
2. Bradley WG, Waluch C, Yadley RA, Wycoff RR (1984) Comparison of CT and MR in 400 patients with suspected disease of the brain and cervical spinal cord. Radiology 152:695-702
3. Brant-Zawadzki M et al. (1983) NMR demonstration of cerebral abnormalities: comparison with CT. AJR 140:847-854
4. Brant-Zawadzki M et al. (1984) Primary intracranial tumor imaging: a comparison of magnetic resonance and CT. Radiology 150:435-440
5. Bydder GM et al. (1982) Clinical NMR imaging of the brain: 140 cases. AJR 139:215-236
6. Caille JM, Lemanceau B, Bonnemain B (1983) Gadolinium as a contrast agent for NMR. Am J Neuroradiol 4:1041-1042
7. Claussen C, Laniado M, Kazner E, Schörner W, Felix R (1985) Application of contrast agents in CT and MRI (NMR): their potential in imaging of brain tumors. Neuroradiology 27:164-171
8. Gentry LR, Jacoby CG, Turski PA, Houston LW, Strother CM, Sakett JF (1987) Cerebellopontine angle – petromastoid mass lesions: comparative study of diagnosis with MR imaging and CT. Radiology 162:513-520
9. McGinnis BD, Brady TJ, New PFJ, Buonanno FS, Pykett IL, DeLaPaz RL, Kistler JP, Taveras JM (1983) Nuclear magnetic resonance (NMR) imaging of tumors in the posterior fossa. J Comput Assist Tomogr 7(4):575-584
10. Han JS, Huss RG, Benson JE, Kaufmann B, Yoon YS, Morrison SC, Alfidi RJ, Rekate HL, Ratcheson RA (1984) MR imaging of the skull base. J Comput Assist Tomogr 8(5):944-952

11. Haughton VM, Rimm AA, Sobocinski KA, Papke RA, Daniels DL, Williams AL, Lynch E, Levine R (1986) A blinded clinical comparison of MR imaging and CT in neuroradiology. Radiology 160:751-755

12. Johnson MA et al. (1983) Clinical NMR imaging of the brain in children: normal and neurologic disease. AJNR 4:1013-1026

13. Levene MI, Whitlaw A, Dubowitz V, Bydder GM, Steiner RE, Randell CP, Young IR (1982) Nuclear magnetic resonance imaging of the brain in children. Br Med J 285:774-776

14. Petermann SB, Steiner RE, Bydder GM (1984) Magnetic resonance imaging of intracranial tumors in children and adolescents. AJNR 5:703-709

15. Randell CP et al. (1983) Nuclear magnetic resonance imaging of posterior fossa tumors. AJNR 4:1027-1034

16. Sartor K, Karnaze MG, Winthrop JD, Gado M, Hodges FJ (1987) MR imaging in infra-, para- and retrosellar mass lesions. Neuroradiology 29:19-29

17. Schörner W, Kazner E, Laniado M, Sprung Ch, Felix R (1984) Magnetic resonance tomography (MRT) of intracranial tumors: initial experience with the use of the contrast medium gadolinium DTPA. Neurosurg Rev 7:303-312

18. Uhlenbrock D, Beyer HK, Grotte W (1985) Kernspintomographie bei Hirntumoren. Fortschr Röntgenstr 143:501-507

19. Young IR et al. (1981) Magnetic resonance properties of hydrogen: imaging the posterior fossa. AJR 137:895-901

20. Zimmermann RA et al. (1983) Cerebral NMR imaging: early results with a 0.12 T resistive system. AJR 141:1187-1193

21. Zimmermann RA (1985) Magnetic resonance imaging of midline pediatric cerebral neoplasms. Acta Neurochirurgica 35:60-64

22. Zimmermann RA, Bilaniuk LT, Grossmann RI, Goldberg HI, Edelstein W, Bottomley P, Redington RW (1985) Cerebral NMR: Diagnostic evaluation of brain tumors by partial saturation technique with resistive NMR. Neuroradiology 27:9-15

23. Zimmermann RA, Bilaniuk LT, Packer R, Sutton L, Samuel L, Johnson MH, Grossmann RI, Goldberg HI (1985) Resistive NMR of brain stem gliomas. Neuroradiology 27:21-25

The Diagnostic Value of CT and MRI in Lesions of the Sella Turcica

W. Huk, M. Buchfelder, and R. Nistor

Neurochirurgische Klinik der Universität Erlangen-Nürnberg, Schwabachanlage 6, D-8520 Erlangen

For comparison of CT and MRI in the evaluation of lesions in the region of the sella turcica, the findings of 159 patients (Tables 1 - 3) were analyzed.

Table 1. 159 lesions of the sellar region

100 pituitary adenomas
16 craniopharyngiomas
9 perisellar meningiomas
14 empty sella syndromes
20 nonpituitary lesions

Table 2. 100 pituitary adenomas

34 inactive adenomas
34 prolactinomas
19 GH-producing adenomas
9 ACTH-producing adenomas
3 Nelson tumors
1 TSH-producing tumor

Table 3. 20 nonpituitary lesions

7 gliomas of the optic chiasm
2 germinomas
2 chordomas
2 inflammatory lesions
1 chondroma
1 metastasis
1 ENT carcinoma
1 aneurysm
1 arachnoid cyst
1 encephalocele
1 intrasphenoid meningocele

The diagnosis of *microadenomas* of the pituitary is primarily based on clinical and endocrinological grounds. The visualization of these small tumors of less than 10 mm diameter with modern imaging techniques can only help to confirm the diagnosis and to localize the lesion within the sella more accurately. For this purpose direct and indirect tumor signs can be referred to.

Ed. by W. Walter, M. Brandt, M. Brock, and M. Klinger

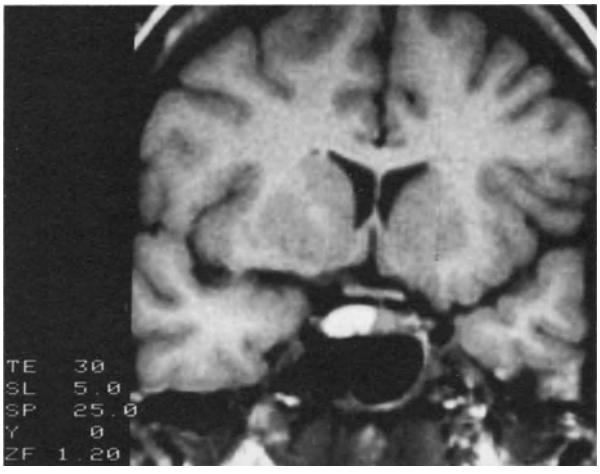

Fig. 1. 31-year-old female with recent hemorrhage into a microprolactinoma. The indirect signs of microadenoma are present. (Coronal scan; SE TR 600 ms/TE 30 ms; 1.0 T)

Direct signs of microadenomas. In CT microadenomas usually appear as a hypodense area within the limits of the gland. More lateral tumors or those with extraglandular growth in the direction of the cavernous sinus, however, are difficult to detect by CT.

In MRI, microadenomas in the majority of cases have prolonged relaxation times; when they are isointense, they may escape detection. Small hemorrhages, which are encountered quite often, can be identified by MRI over a much longer period than by CT (Fig. 1).

Indirect signs of microadenomas include (Fig. 1):
- A convex diaphragm of the sella
- An oblique pituitary stalk
- An oblique floor of the sella

These signs can be detected on direct coronal sections of both CT and MRI. The advantage of MRI can be seen in its greater ability to demonstrate small anatomical details without bone artifacts and its multiplanar facility, which makes possible oblique sections parallel to the pituitary stalk.

In *macroadenomas* the spatial relationship between the tumor and its adjacent structures is of most interest. For this purpose MRI is superior to CT. From the accurate delineation of the shape and extension of the tumor, indications can be deduced as to whether it is encapsulated and thus can be operated by the transsphenoidal route, or whether it grows without a capsule between the perisellar structures, making the transcranial approach more appropriate (Fig. 2).

In tumors with parasellar extension there are no reliable criteria on MR images which enable one to decide whether the adenoma only displaces the wall of the cavernous sinus or whether it has already invaded it. The depiction of larger blood vessels by MRI without the need for contrast media helps one to avoid preoperative angiography in a number of cases. Destruction of the base of the skull by tumor infiltration is more obvious on CT than on MR images.

Treatment with bromocriptine may induce shrinking of prolactinomas in about 30% of cases; the change in size and shape of the tumor can be

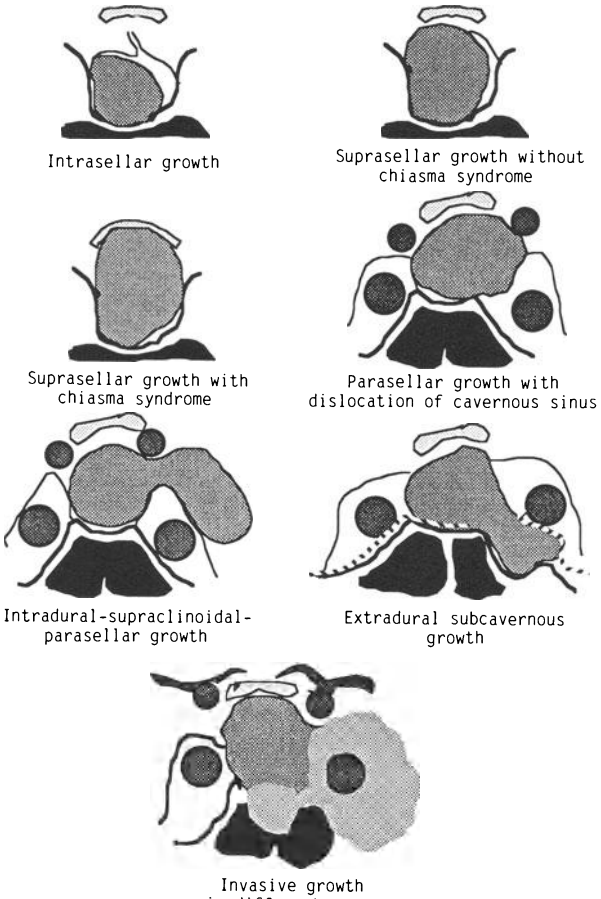

Fig. 2. Scheme of the extrasellar growth of macroadenomas

analyzed better with MRI than with CT. A change in signal intensity as a result of the treatment could be observed only in sporadic cases.

The so-called *empty sella syndrome* is characterized by an intrasellar herniation of the suprasellar cistern and a flat pituitary gland stretched along the floor and the dorsum of the sella. In midsagittal sections the gland appears sickle shaped (Fig. 3), and in coronal scans like an inverted letter T. The pituitary stalk usually rests against the dorsum in the midline. To exclude an intrasellar cyst, cisternography with intrathecal contrast medium may be necessary.

Craniopharyngiomas are partly cystic and/or solid with calcifications. In MRI these calcifications, which are essential for the diagnosis of this kind of tumor, cannot be identified; cysts, however, are evaluated in better detail than by CT.

Meningiomas are difficult to detect without contrast medium in both CT and MRI. Tumors growing en plaque along the base of the skull can be outlined more clearly, and compression of the carotid artery (Fig. 4), which is not seen in adenomas, can be visualized more easily by MRI than CT.

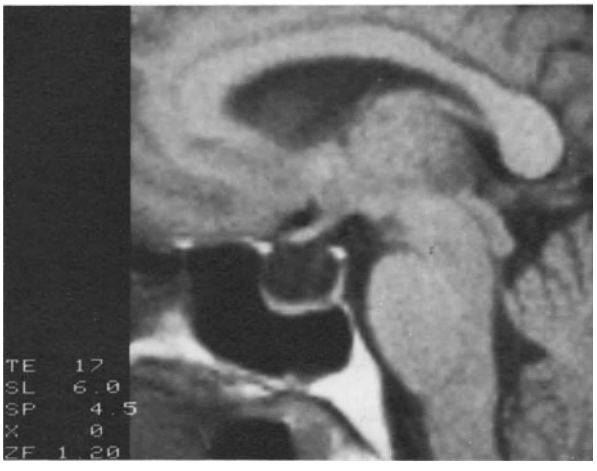

Fig. 3. 57-year-old female with empty sella syndrome. (Midsagittal section; SE TR 500 ms/TE 17 ms; 1.0 T)

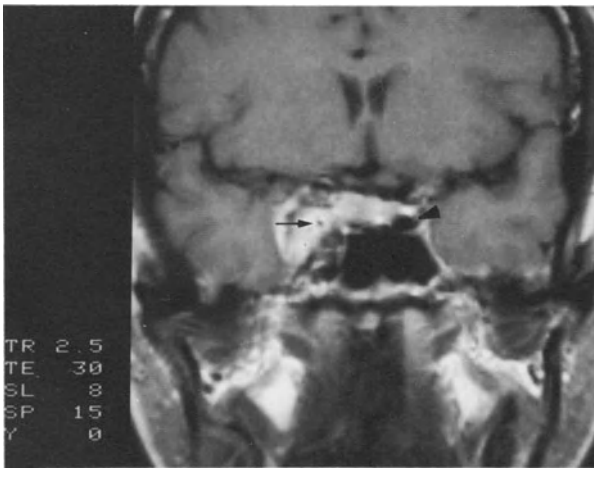

Fig. 4. 42-year-old female with meningioma of the sellar region. Compression of the carotid artery by the tumor on the right side *(arrow)*; compare the normal carotid artery on the left side *(arrowhead)*. (Coronal section; SE TR 2.5 s/TE 30 ms; i.v. gadolinium-DTPA, 0.2 ml/kg; 1.0 T)

Other nonpituitary processes of the sella region – with few exceptions – display prolonged relaxation times T1 and T2; thus they are difficult to distinguish from each other.

In conclusion, MRI makes possible a topographic analysis of the region of the sella, which in many cases renders angiography superfluous. Only for the direct diagnosis of microadenomas and the identification of calcifications does CT seem of equal value or even superior to MRI. MRI therefore is the method of choice for the evaluation of the normal and pathological anatomy of the sellar region.

Imaging of Pituitary Tumors in CT and MRT: A Comparative Study

H. G. Böcher-Schwarz, O. Hey, M. Just, and K. Schürmann

Neurochirurgische Universitätsklinik, Langenbeckstraße 1, D-6500 Mainz

Introduction

When there is clinical suspicion of a pituitary tumor, localization of the tumor and representation of the relation of the tumor to adjacent structures by imaging are prerequisite in establishing the indication for surgery and in planning the operative strategy. Usually, large pituitary tumors do not give rise to problems in CT diagnosis, especially since they will already have led to dilatation of the sella at this stage and will have extended to the suprasellar region (12,15). However, very tiny hormone-producing tumors (ACTH- and GH-producing adenomas, prolactinomas) in the stage of microadenomas, tumor relapses, and tumor remnants cannot always be localized unequivocally in the adenohypophysis or in the former area of operation (3,5,6,8,11,17).

This contribution investigates the following questions:
1. Is the surgeon provided with significant additional information by imaging of pituitary tumors with MRT?
2. Is imaging of microadenomas with MRT feasible in the event of lack of detection or equivocal localization in the CT scans?

Patients and Methods

Fifteen patients (4 male, 11 female) aged from 18 to 64 years with suspicion of pituitary tumors were investigated. In two of these patients, there was suspicion of a tumor recurrence. Fourteen patients were operated on after conclusion of preoperative diagnostics. All the transsphenoidal surgical procedures were preformed by the same neurosurgeon (O.H.). Particular note was taken of the size and exact location of the adenomas in the sella. Those larger than 10 mm were categorized as macroadenomas, those less than or equal to 10 mm as microadenomas. Histological examination was performed in all specimens.

Computer tomography was mostly carried out before admission to the hospital with various tomographs of the newest generation. In 14 cases, the investigations were carried out both without and with i.v. application of contrast medium. The collimation was 2 mm in all cases apart from one exception (4 mm collimation was used in case no. 5). The investigation was carried out six times in the coronal position and nine times in the axial position.

MRT was carried out in ten cases with the Bruker TOMIKON 1100 from the Deutsche Klinik für Diagnostik in Wiesbaden. This tomograph is equipped with a resistance magnet system with a field strength of 0.28 T. The tomograms were carried out in the T_1-weighted sequences with TR between

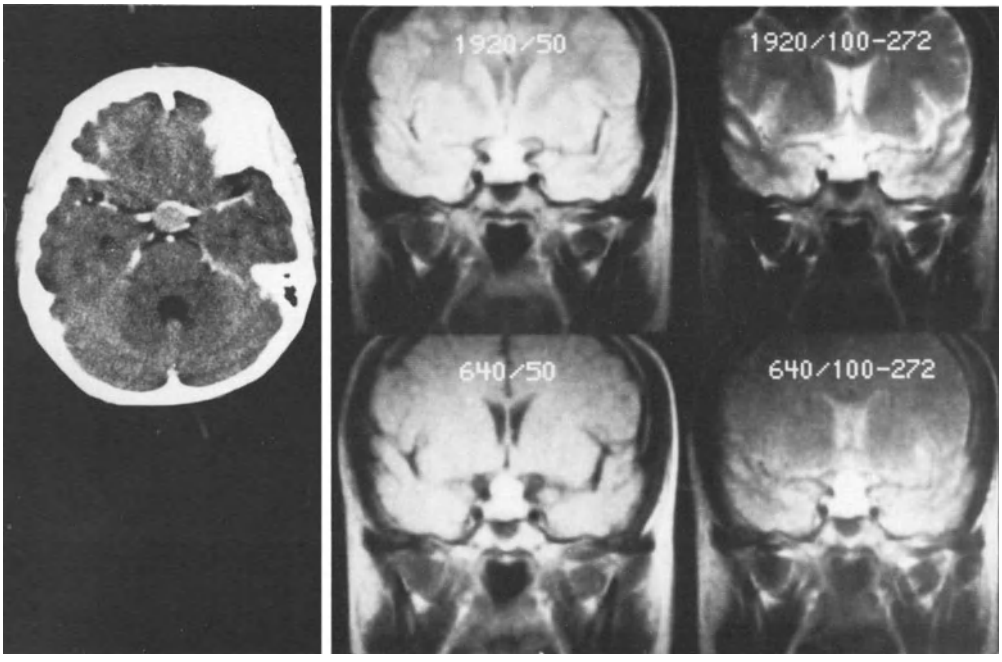

Fig. 1. Fifty-year-old female patient with moderate hyperprolactinemia (prolactin in the serum: 49 ng/ml). A space-occupying lesion appearing to be a solid tumor on contrast-enhanced CT *(left)* and MRT with different TR/TE parameters *(right)* proved intraoperatively to be a cysticercotic cyst

500 and 1400 ms and TE of 50 ms, and in the T_2-weighted sequences with TR of 2000 ms and TE of 100 - 272 ms. Tomogram thicknesses of a minimum of 8 mm could be attained. In two cases, MRT was also performed after administration of gadolinium. Five investigations were carried out with newer instruments equipped with a supraconducting magnet of 1.0 T (tomogram thickness 3 - 5 mm, TR = 500 - 700 ms, TE = 28 - 40 ms and TR = 1800 - 3000 ms, TE = 60 - 120 ms).

Results

The results are presented in detail in Table 1. All of the patients investigated were operated on apart from case no. 2 (empty sella with hyperprolactinemia). Microadenomas (four prolactinomas, two ACTH adenomas, two HGH adenomas) were found in eight patients; macroadenomas were found in two patients (one prolactinoma, one HGH adenoma); macroadenoma recurrences (one prolactinoma, one HGH adenoma) were found in two patients; a craniopharyngioma was found in one female patient, together with one astrocytoma II in the left temporal lobe which could only be detected by MRT; a further female patient had a cysticercotic cyst which looked like a pituitary adenoma on CT and MRT (Fig. 1).

As expected, large pituitary tumors could be detected both by CT and MRT. In contrast to CT, however, excellent imaging of the parasellar structures (especially the relationship of the tumors to the optic chiasm, the third ventricle, the cavernous sinus, and the carotid ar-

Table 1. CT and MRT findings with pituitary lesions (n = 15)

No.	Sex	Age	Diagnosis	Endocrinological findings	CT findings	MRT findings	Surgical findings
1	f	35	Acromegaly	HGH: 2.15 ng/ml Somatomedin C: 34.7 nmol/l	Hypodense lesion, right; Invasion of the right cavernous sinus; No enhancement	T_1: hypointense lesion, right; invasion of the right cavernous sinus and compression of the internal carotid artery T_2: not available	Macroadenoma
2	f	26	Hyperprolactinemia	Prolactin: 149 ng/ml	Empty sella	T_1: hypointense empty sella T_2: hyperintense empty sella No adenoma seen	No surgery
3	f	23	1. Craniopharyngioma 2. Astrocytoma II	Latent insuff. of the anterior lobe of the pituitary	Partial calcified intra- and suprasellar tumor; Enhancement	1. T_1 and T_2: hyperintense intra- and suprasellar structure 2. T_1 and T_2: hyperintense lesion in the left temporal lobe	1. Cystic craniopharyngioma 2. Astrocytoma II
4	f	27	Hyperprolactinemia	Prolactin: 276 ng/ml	Multiple hypodense lesions; Sella floor erosion, right	T_1 (with Gd-DTPA): hyperintense lesion, right lat. T_2: hyperintense lesion, right lat.	Microadenoma
5	f	50	Cysticercosis	Prolactin: 49 ng/ml	Intra- and suprasellar tumor with enhancement	T_1: hyperintense intra- and suprasellar structure T_2: hyperintense intra- and suprasellar structure Elevation of the optic chiasmata	Cysticercotic cyst intra- and suprasellar
6	f	39	Acromegaly	HGH: 6.1 ng/ml Abnormal glucose test	Intrasellar cystic lesion; No enhancement	T_1: hypointense intrasellar lesion T_2: hyperintense intrasellar lesion	Microadenoma
7	f	47	Hyper prolactinemia	Prolactin: 762.3 ng/ml (treatment with 7.5 mg bromocriptine)	Intra-, supra-, and parasellar tumor; Invasion of the left cavernous sinus; Enhancement	T_1 and T_2: isointense intra-, supra-, and parasellar tumor; Invasion of the left cavernous sinus and displacement of the internal carotid artery	Macroadenoma

8	f	30	Hyper-prolactinemia	Prolactin: 125 ng/ml	Cystic hypodense lesion, left	T_1: hyperintense lesion, left T_2: iso/hyperintense lesion, left	Microadenoma
9	m	27	Hyper-prolactinemia (first operation 8 years previously)	Prolactin: 344 ng/ml	Hyperdense intrasellar structure, left; Invasion of the sphenoidal sinus; Enhancement	T_1 and T_2: hyperintense structure left; Invasion of the sphenoidal sinus; Enhancement	Macroadenoma
10	f	18	Hyper-prolactinemia	Prolactin: 24.3 ng/ml	Hypodense lesion, right	T_1: hyperintense lesion, right T_2: hyperintense lesion, right	Microadenoma
11	m	64	Acromegaly (first operation 9 years previously)	HGH: 7.2 ng/ml Abnormal glucose test	No relapse seen	T_1: isointense structure in the frontal part of the sella T_2: hyperintense structure in the frontal part of the sella	Macroadenoma
12	f	18	Hyper-prolactinemia	Prolactin: 56 ng/ml (treatment with 5 mg bromocriptine)	Hypodense lesion, left	No lesion seen	Microadenoma
13	m	55	Cushing's disease	ACTH: 89 pg/ml Abnormal dexamethasone and CRF test	No lesion seen	No lesion seen	Crescent-shaped microadenoma
14	f	38	Acromegaly	HGH: 12.9 ng/ml Somatomedin C: 50 nmol/l	Sella floor bulging, right; Herniation of the diaphragma sellae	T_1: hypointense lesion, right T_2: hyperintense lesion, right, Herniation of the diaphragma sellae	Microadenoma
15	m	31	Cushing's disease	ACTH: 50.1 pg/ml Abnormal dexamethasone and CRF test	No lesion seen	T_1 (with Gd-DTPA): no lesion seen T_2: hyperintense lesion, right	Microadenoma

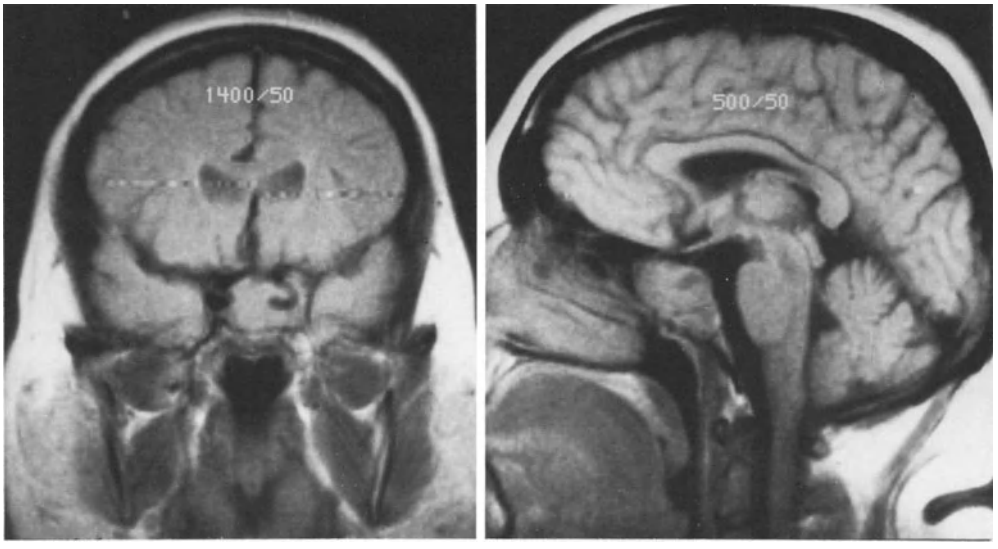

Fig. 2. Coronal and sagittal MR tomograms (T_1 weighted) of a 47-year-old female patient (no. 7) with hyperprolactinemia (prolactin level in the serum: 762.3 ng/ml). On MRT, the ingrowth of the tumor into the cavernous sinus and the displacement of the left internal carotid artery to intrasellar can be clearly discerned (collimation 8 mm, TR/TE 1400 ms/50 ms or 500 ms/50 ms)

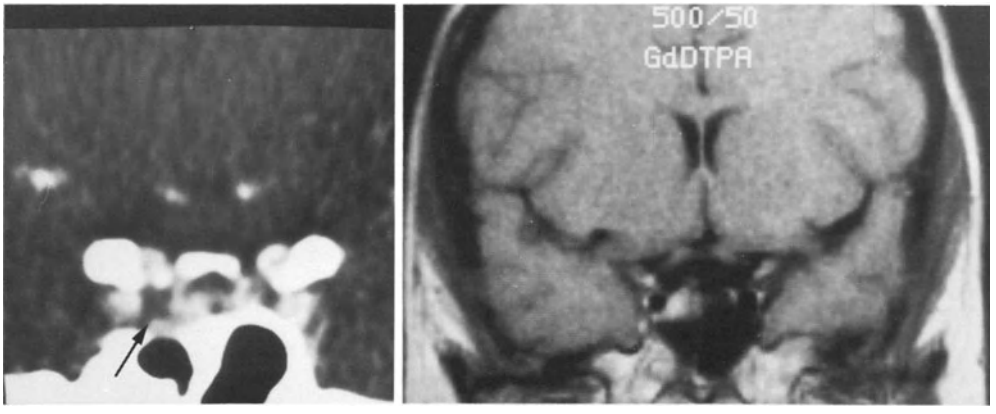

Fig. 3. Coronal CT after administration of contrast medium *(left)* and MRT with TR/TE of 500 ms/50 ms after Gd-DTPA administration *(right)* in a 27-year-old female patient with hyperprolactinemia (276 ng/ml). Several intrasellar hypodense lesions on CT make it difficult to localize the microadenoma unequivocally *(arrow)*. On MRT, unequivocal localization of the microadenoma as the hyperintense structure on the right

teries) was achieved with MRT in these cases. In two cases, the surgeon was provided with important information that the tumor had already infiltrated the cavernous sinus and had walled-in the internal carotid artery (cases no. 1 and 2). Figure 2 shows an example of this: angiography could be dispensed with on the basis of the MRT findings.

In five patients with microadenomas, an intrasellar focal lesion was found on CT, in agreement with the surgical finding. However, appreciable uncertainty as to the exact tumor localization was present in the evaluation owing to hypodense artifacts (Fig. 3). In three patients of the microadenoma group (nos. 13,14,15), no intrasellar focal lesion could be detected on CT.

With MRT, focal pathological signal alterations were shown in six patients; these agreed in terms of localization with the microadenoma found intraoperatively. Of these patients, four had a corresponding finding in CT and two (nos. 14,15) showed a normal CT finding. In patient no. 12, a pathological alteration in the signal could not be detected on MRT despite the positive CT finding. In patient no. 13, a characteristic focal lesion was not shown on CT and MRT (a crescent-shaped cellular hyperplasia in the adenohypophysis at the floor of the sella was found intraoperatively). Two patients with recurrent adenoma (nos. 9,11) were investigated: both relapses were detected with MRT, but only the relapse in patient no. 9 was detected by CT.

Discussion

Compared to CT, MRT makes possible more precise imaging of the parasellar and suprasellar extent of large pituitary tumors and their relationship to the surrounding structures (10,13,14). However, the third ventricle and the optic chiasm are typically impressed or raised. The retraction of walling-in of the surrounding large vessels (internal carotid artery and anterior cerebral artery) or ingrowth of the tumor into the cavernous sinus, which is important for planning the operation, is readily discernible on the coronal sections. Angiography can thus be dispensed with in most cases. These details cannot be represented with the same precision by CT (4,7).

Despite a collimation of 8 mm, six of the eight microadenomas found surgically and confirmed histologically could be detected by MRT in our study. This finding thus contrasts with the investigations of LEE and DECK (14). Other authors were likewise able to demonstrate microadenomas on MRT: KUCHARCZYK et al. (13) in 10 out of 11 cases and POJUNAS et al. (16) in 6 out of 11 cases. Relative to the gray substance of the brain tissue, these adenomas can appear isointense, hyperintense, or hypointense in T_1- and T_2-weighted tomograms. Small tumor hemorrhages or cystic alterations which appear as signal-intensive foci in all image weightings by prolongation of the T_2 time, increase of proton density, and reduction of the T_1 time are excellently delimitable (10). However, as indicated in publications by other authors (13,16,17), microadenomas demonstrated in CT and confirmed surgically cannot always be detected with MRT. In our own patients, this was also the case in one female patient (no. 12). On the other hand, there are also cases of microadenomas which are exactly detected by MRT but which cannot be imaged on CT (two cases in our investigation). For the neurosurgeon, there is thus an unequivocal indication for performance of MRT in some cases so long as direct localization of the microadenomas is not possible with CT or only indirect signs are found. The latter are only relatively nonspecific for the presence of a microadenoma (1,5). In one female patient of our series with hyperprolactinemia (case no. 2), an "empty

sella" without adenoma could be demonstrated on CT and MRT. According to BRYNER and GREENBLATT (2) and JONES et al. (9), this finding alone may be responsible for the hyperprolactinemia demonstrated in this female patient. Finally, it should be mentioned that a comparative study is rendered more difficult by investigations with different tomographs.

Summary

In 15 patients with suspicion of a pituitary tumor, CT and MRT investigations were carried out in parallel. In the patients with macroadenomas (n = 4), excellent imaging of the juxtasellar structures and their relationship to the tumors was possible with MRT. Of eight microadenomas, six could be definitely localized by MRT and five by CT. An adenoma could be definitely demonstrated only by CT, and two other adenomas only by MRT. It can be concluded from this that the abilities of the two modalities to image microadenomas are independent of each other. An ACTH microadenoma could be detected neither by CT nor by MRT. In one female patient with a craniopharyngioma which could be imaged by both procedures, an astrocytoma II in the left temporal lobe was found in addition with MRT. A space-occupying lesion which appeared to be an intrasellar and suprasellar solid tumor on CT and MRT proved intraoperatively to be a cysticercotic cyst.

Acknowledgments. The authors are indebted to Drs. Hentschel, Krüger, Magin and Ludwig, Mainz, and Drs. Halbsguth and Lochner, Frankfurt, for providing the CT images.

References

1. Bruneton JN, Drouillard JP, Sabatier JC, Elie GP, Tavernier JF (1979) Normal variants of the sella turcica. Radiology 131:99-104
2. Bryner JR, Greenblatt RB (1977) Primary empty sella syndrome with elevated serum prolactin. Obstet Gynecol 50:375-380
3. Chambers EF, Turski PA, LaMasters D, Newton TH (1982) Regions of low density in the contrast-enhanced pituitary gland: normal and pathologic processes. Radiology 144:109-113
4. Cohen WA, Pinto RS, Kricheff JJ (1982) Dynamic CT scanning for visualization of the parasellar carotid arteries. AJR 138:905-909
5. Davis PC, Hoffman jr JC, Tindall GT, Braun IF (1985) Prolactin-secreting pituitary microadenomas. Inaccuracy of high-resolution CT imaging. AJR 144:151-156
6. Davis PC, Hoffman jr JC, Tindall GT, Braun IF (1985) CT-surgical correlation in pituitary adenomas: Evaluation in 113 patients. AJNR 6:711-716
7. Hayman LA, Evans RA, Hinck VC (1979) Rapid high dose (RHD) contrast computed tomography of perisellar vessels. Radiology 131:121-123
8. Hemminghytt S, Kalkhoff RK, Daniels DL, Williams AL, Grogan JP, Houghton VM (1983) Computed tomographic study of hormone-secreting microadenomas. Radiology 146:65-69
9. Jones JR, de Hempel PAC, Kemmann E (1977) Galactorrhea and amenorrhea in a patient with an empty sella. Obstet Gynecol 49:9-11
10. Just M, Higer HP, Vahldieck G, Bone D, Kunze S, Hey O, Pfannenstiel P (1987) MR-Tomographie benigner Hirntumoren. Submitted to RöFo

11. Kaplan HC, Baker jr HL, Houser OW, Laws jr ER, Abboud CF, Scheidhauer BW (1985) CT of the sella turcica after transsphenoidal resection of pituitary adenomas. AJR 145:1131-1140

12. Kricheff JJ (1979) The radiologic diagnosis of pituitary adenoma. Radiology 131:263-265

13. Kucharczyk W, Davis DO, Kelly WM, Sze G, Norman D, Newton TH (1986) Pituitary adenomas: high-resolution MR imaging at 1.5 T. Radiology 263-265

14. Lee BCP, Deck MDF (1985) Sellar and juxtasellar lesion detection with MR. Radiology 157:143-147

15. Nadjmi M, Piepgras N, Vogelsang H (1981) Kranielle Computertomographie. Thieme, Stuttgart

16. Pojunas KW, Daniels DL, Williams AL, Haughton VM (1986) MR imaging of prolactin-secreting microadenomas. AJNR 7:209-213

17. Teasdale E, Teasdale G, Mohsen F, Macpherson P (1986) High-resolution computed tomography in pituitary microadenomas: is seeing believing? Clinical Radiology 37:227-232

RARE Hydrography as a New Diagnostic Tool with Special Respect to Its Value in Preoperative Examinations

D. Ott, M. Schumacher, and H. Eggert

Sektion Neuroradiologie der Universität, Hauptstraße 5, D-7800 Freiburg

The advent of magnetic resonance imaging considerably improved preoperative morphological evaluation in neurosurgical patients. The time-consuming examination, which is particularly hampering in severely ill and agitated patients, is still a disadvantage inherent to the standard spin-echo sequences at a tolerable field strength. Of the many fast-imaging procedures that have been tried, we adopted the RARE method (rapid acquisition with relaxation enhancement) for routine examinations. RARE hydrography with selective fluid contrast obtainable in a very short acquisition time (4 - 10 s) can easily be used to visualize CSF spaces, thus producing scans comparable to myelography, cisternography, or ventriculography, all of which are invasive and dependent on contrast media.

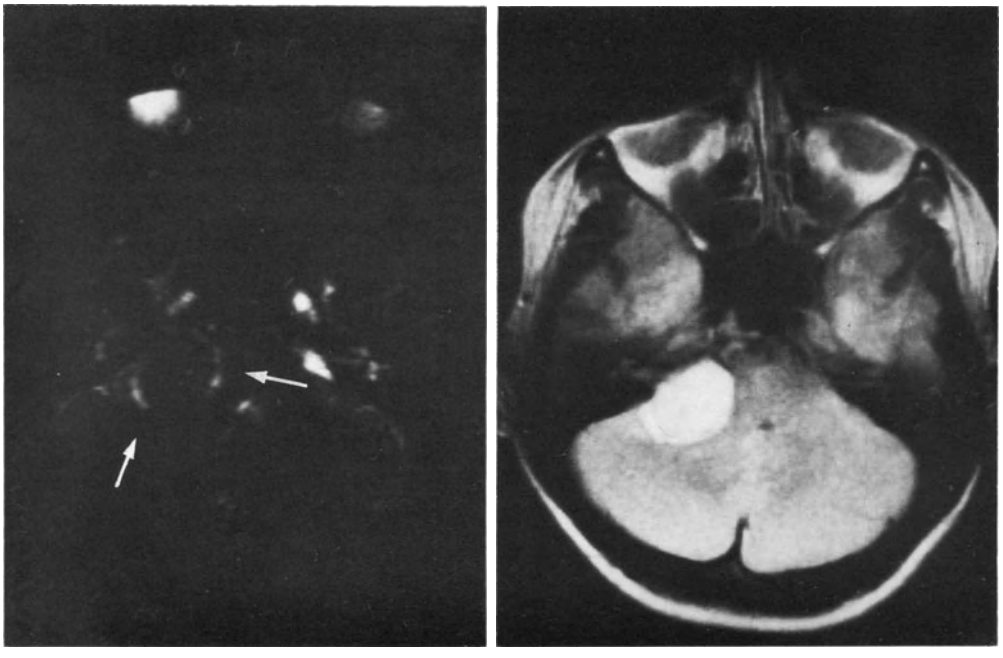

Fig. 1. Acoustic neurinoma. On the *left*, the CSF border is marked by *arrows* (RARE hydrography); on the *right* is a T_2-weighted SE scan

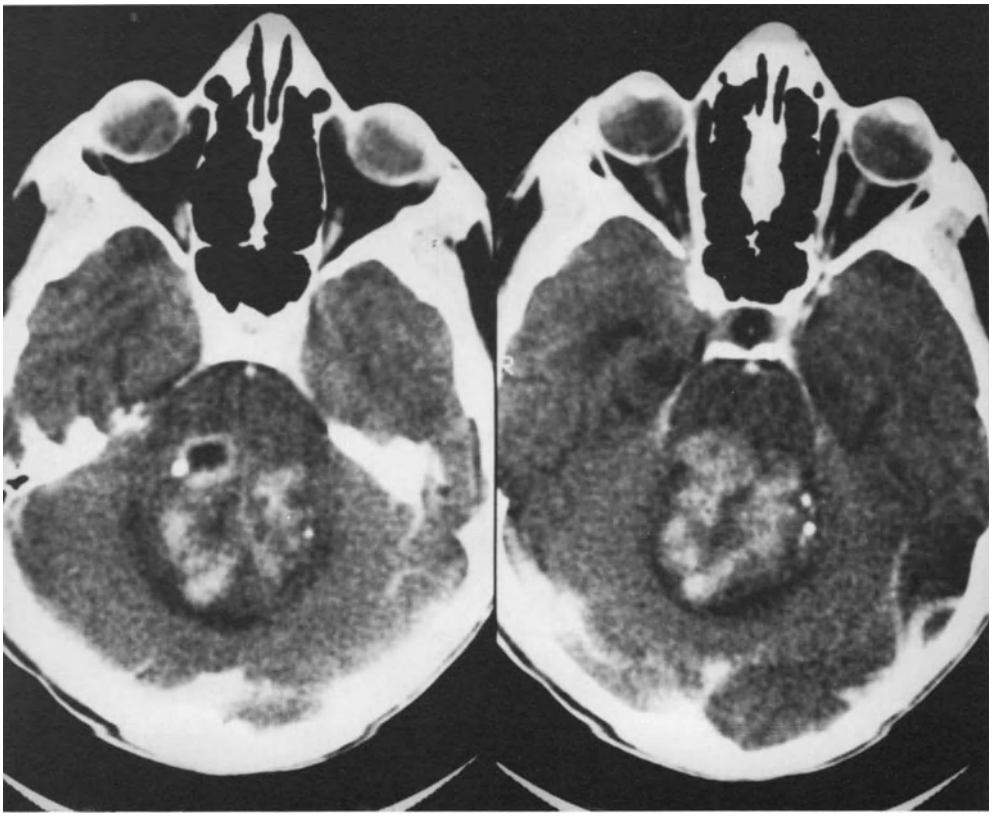

Fig. 2. CT of a pseudocystic tumor within the fourth ventricle

Method

The method described by HENNIG et al. (1,2) is based on the principles of echo imaging with generation of long echo trains, each echo carrying spatial information due to phase encoding. The projections for the 256 × 256 image reconstruction are read out after one or a few excitations. The read out time differs for all projections (causing different T_2 weighting) which produces overall a heavily T_2-weighted image with good spatial resolution and high signal/noise ratio for structures with long transversal relaxation time (T_2). The signal/noise ratio can further be heightened by only a few averaging procedures, not essentially prolonging the acquisition time, which ranges between 4 and 10 s per excitation. The short sampling time also allows a three-dimensional data set to be acquired in less than 15 min with a reconstruction mode for slices of 1 mm thickness. The examinations were performed on a 0.23-T system, Bruker BNT 1100, using a 50-cm body coil or 28-cm and 22-cm head coils.

Material and Results

In more than 200 cerebrospinal examinations we performed RARE hydrography with a slice thickness between 5 and 100 mm, mostly in addition to conventional SE images. Important applications of this method are

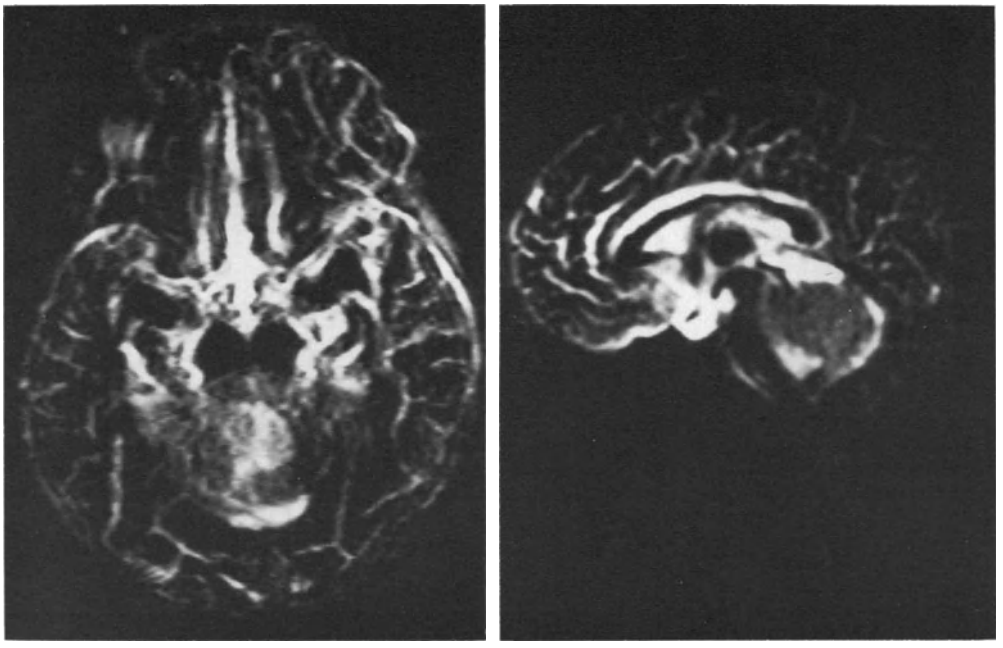

Fig. 3. Corresponding RARE scans to Fig. 2, revealing the intraventricular tumor position

space-occupying lesions close to cisterns or cerebral ventricles. In 15 acoustic neurinomas the exact degree of narrowing of the cerebellopontine angle cistern could be seen, and all cases except one showed a well-described fluid rim at the medial border of the neurinoma, which we interpreted as the subarachnoid layer of the nerve protruded to the brain stem by tumor growth (Fig. 1). In the one patient who did not show this phenomenon, the bilateral tumors, associated with known neurofibromatosis, had an irregular lobular shape.

In infratentorial neoplasms the important topographical relationship to the brain stem and surrounding CSF spaces are not very well shown on CT scans. Figures 2 and 3 show a patient in whom the CT only delineated an irregular, partially cystic mass, not allowing identification of the fourth ventricle and its spatial relationship to the tumor. The SE series, too, did not allow the differentiation of tumor, cyst, and ventricle. The sagittal RARE scan, however, revealed an enormously enlarged fourth ventricle with the tumor inside being adherent to the medulla, pons, and roof of the fourth ventricle and no cyst at all. All topographical details were proven operatively.

In cerebral tumors RARE hydrography always allowed us to judge any ventricular or cisternal compression, and in some cases with isointensity of tumor or edema and related CSF only the combination of the SE and RARE image outlined the exact tumor border.

Subarachnoid cysts are another important application for cerebral RARE hydrography. It offers a quick multiplanar evaluation of the cyst and outlines possible segmentation by arachnoid structures much sharper than do SE scans. The use of 3DFT data sampling in 15 min promises to yield even better information about septa and communication with other

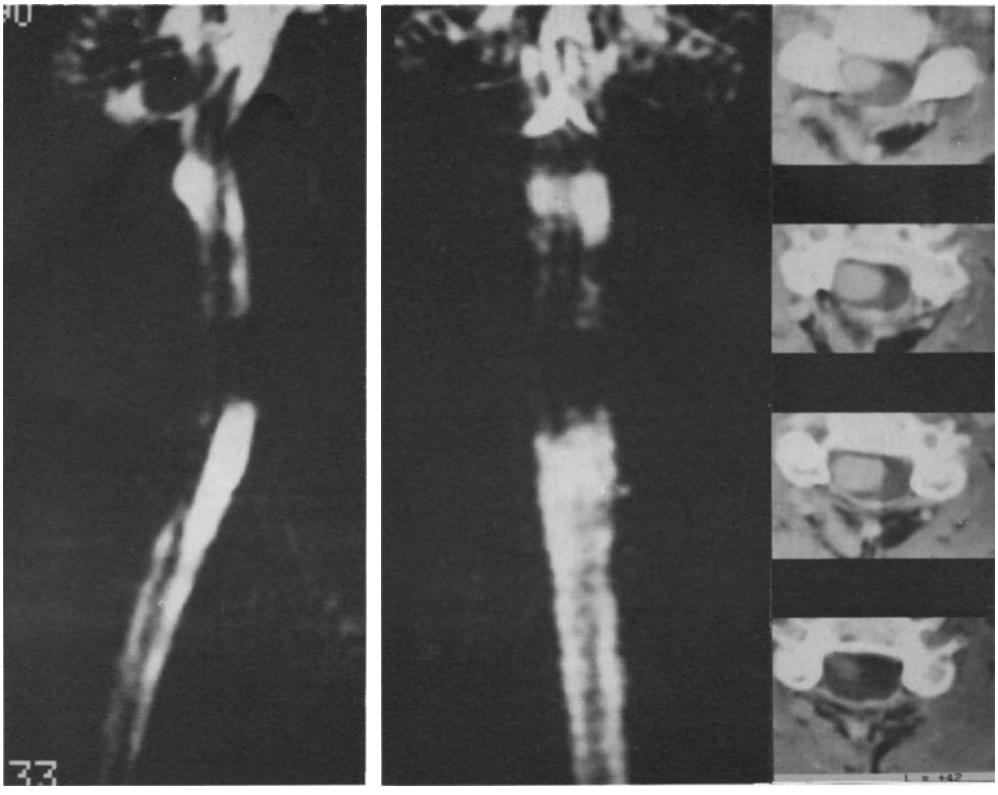

Fig. 4. Cervical meningioma. RARE scans in lateral and frontal views and corresponding CT scans

CSF structures for its reconstruction in 1-mm slices. Spinal RARE hydrography, a particularly fast form of MR myelography, is routinely implemented in our spinal examinations due to its very short acquisition time and the good screening possibilities as regards subarachnoid compression. We feel that conventional myelography can be partially replaced by this method. The localization of spinal tumors gives excellent results, superior to those provided by conventional myelography, in the cervicothoracic and craniocervical regions, particularly in patients with impaired mobility of the cervical spine. Figure 4 shows a cervical meningioma, comparing CT and MR myelography. The latter provides all essential information about tumor size and position and also outlines the displacement of the spinal cord. In syringomyelia the syrinx itself and its occupying effect on the subarachnoid space can be seen in the same experiment within less than a minute. Other cystic tumors, meningoceles, and unnatural CSF deposits due to fistulas or traumatic traction of the root can be visualized in a safe and quick way.

Discussion

The main advantages of RARE hydrography are the very short acquisition time (4 - 10 s on average) and the absence of contrast media. The inherent properties of the method therefore allow its easy application

at all spinal levels as well as its use as ventriculo- or cisternography. Due to the high signal/noise ratio with good spatial resolution, the method is sensitive enough to identify even small lesions, thus increasingly rendering conventional myelography superfluous. There is a further advantage of MR myelography as there are practically no positioning problems; this allows easy panmyelography including the craniocervical junction. The additional information obtained by examination of cerebral CSF spaces is evident in all cerebral lesions with a direct or indirect relationship to cisterns and ventricles. Knowledge of partially open or totally compressed CSF spaces and of the exact tumor relation to surrounding brain parenchyma has a direct influence on the neurosurgical approach, thus stressing the importance of detailed topographical examination.

References

1. Hennig J, Nauerth A, Friedburg H (1986) Rare imaging: A fast imaging method for clinical MR. Magn Reson Med 3:823
2. Hennig J, Friedburg H, Ströbel B (1986) Nontomographic approach to MR-myelography. J Comput Assist Tomogr 10:375

MRI Stereotaxy for Intracerebral Lesions

M. Mohadjer, W. Birg, H. Friedburg, E. Milios, and F. Mundinger

Abteilung Stereotaxie und Neuronuklearmedizin, Neurochirurgische Universitätsklinik, Hugstetter Straße 55, D-7800 Freiburg

Introduction

Some intracerebral lesions, for example low-grade gliomas, particularly those located infratentorially and near the base, are more clearly depicted in MRI examinations than in CT; this has made it necessary for us to integrate this method of examination into our stereotactic procedure (1,2). The method of MRI stereotaxy for the stereotactic device of RIECHERT and MUNDINGER in the computer-compatible form of MUNDINGER and BIRG was developed by us in order to combine both techniques (2,3).

Materials and Method

The production of a highly stable MRI-compatible base ring is required for MRI stereotaxy. Adjustable riders with plastic screws serve as fixation devices on the patient's head. On the inside concentrically arranged, the plastic ring carries a small plastic tube filled with paramagnetic liquid (Fig. 1). On both sides of the sagittal and coronal MR images, this tube appears as a bright point which allows precise lo-

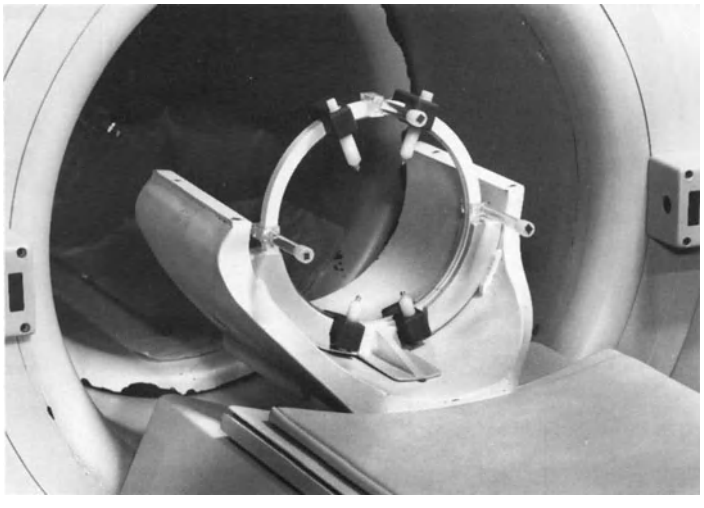

Fig. 1. MRI-stereotaxy ring with ringholder and special head coil

Advances in Neurosurgery, Vol. 16
Ed. by W. Walter, M. Brandt, M. Brock, and M. Klinger

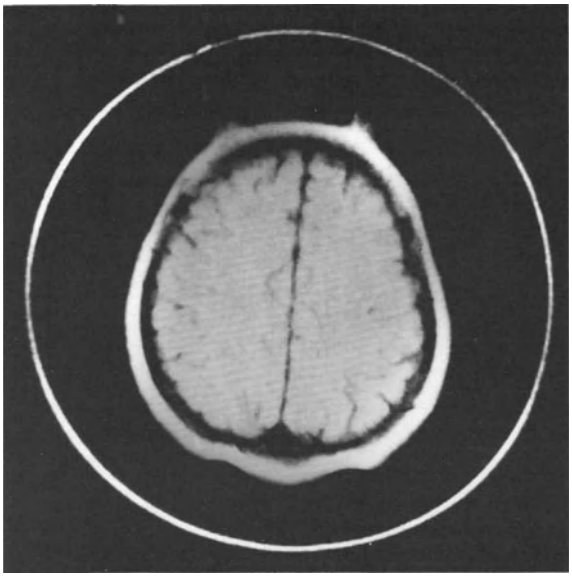

Fig. 2. MR horizontal image through the middle of the plastic ring. The reference ring filled with paramagnetic liquid is clearly visible

calization. A further four plastic tubes are required for location on the axial MR images. The diameters between them coincide with the X- and Y-axes, and the point where they intersect marks the coordinate origin of the stereotactic device (Fig. 2).

An additional ring holder, made of highly stable plastic and fixed to the scanner table, is necessary to fix the ring (Fig. 1). For this scanner, a special head coil with an integrated ring holder has been produced; it permits reasonable images even with relatively low field strength.

The two bright marks on the edge of the image correspond to the sagittal section of the concentric circle (Fig. 3a). Both marked distances are measured directly with the aid of the joystick; the X-coordinate, which is still missing, is taken from the coronal section (Fig. 3b). In order to control the precision of our MRI stereotactic procedure, all the operations performed so far have additionally been followed by a routine CT stereotactic examination. We were able to establish an exact correspondence of the target point coordinates in MRI and CT.

Discussion

In recent years we have performed MRI/CT-stereotactic surgery on a total of 14 patients with intracerebral lesions at different sites. The procedure acquires significance in particular in cases in which the foci are more clearly depicted in the MRI examination, especially those located in infratentorially and near the base (4). Nevertheless, MRI stereotaxy should only be employed in special cases, and perhaps also in functional surgery. The examination may not be carried out on restless patients and those who would require a general anesthetic as both the movement and the incompatible metal produce artifacts.

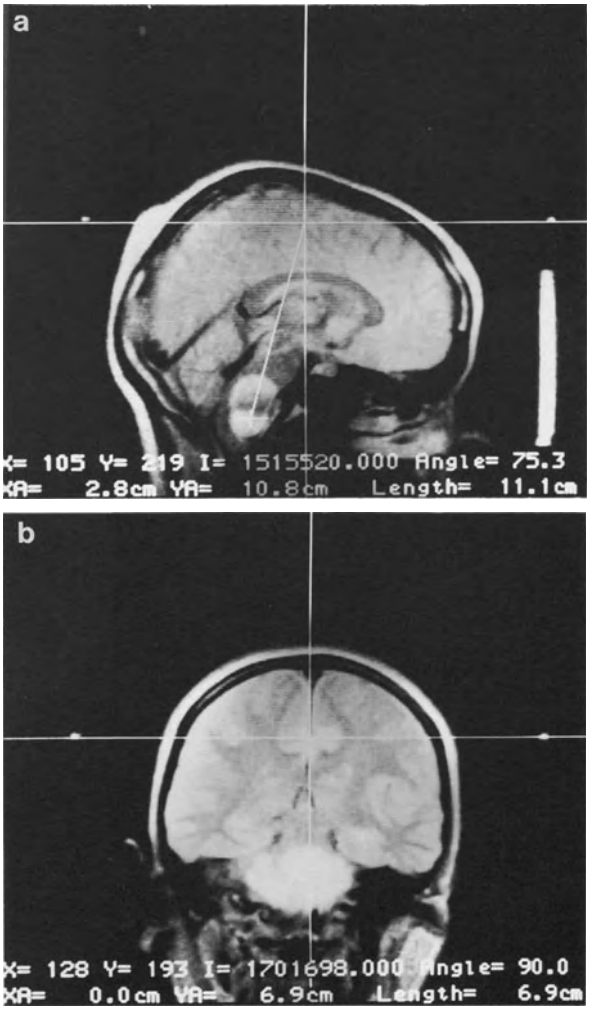

Figs. 3a,b. MRI control and sagittal slices (Brucker): two bright points (from ring rube) allow precise localization

Conclusion

With the aid of a new MRI-compatible stereotactic ring and matching head fixations made of special plastics, the stereotactic operative technique could be combined with MRI; this made it possible to determine the coordinates directly from the MR images. The method was controlled using the proven technique of CT stereotaxy and showed that the target coordinates correspond. Employing this method, structures which are more clearly depicted in MRI are particularly open to stereotactic surgery. Moreover, this procedure will offer advantages for functional therapy, as ventriculography with a contrast medium, which involves certain risks, especially for older patients, is no longer necessary.

References

1. Birg W, Mundinger F, Mohadjer M, Weigel K, Fürmaier F (1985) X-ray and MR stereotaxy for the functional and nonfunctional neurosurgery. Appl Neurophysiol 48:22-29

2. Mundinger F (1982) CT-stereotactic biopsy of brain tumors. In: Voth D, Gutjahr P, Langmaid C (eds) Tumors of the central nervous system in infancy and childhood. Springer, Berlin Heidelberg New York, pp 234-246

3. Riechert T, Mundinger F (1956) Beschreibung und Anwendung eines Zielgerätes für stereotaktische Hirnoperationen (II. Modell). Acta Neurochir 3:308-337

4. Thomas DGT, Davis CH, Ingram S, Olney JS, Bydder GM, Yong IR (1976) Stereotactic biopsy of the brain under MR-imaging control. AJNR 7: 161-169

Magnetic Resdonance Imaging in Diagnosis and Operative Planing of Cerebrovascular Malformations

K. Maier-Hauff, K. Hansen, W. Schörner, and Ch. Sprung

Neurochirurgische Abteilung im Klinikum Charlottenburg, Spandauer Damm 130, D-1000 Berlin 19

The introduction of MRI in the diagnosis of cerebral space-occupying lesions such as brain tumors, cysts, or intracerebral hemorrhages has improved diagnostic results (4,5). As a nonivasive method CT was already successful in identifying cerebrovascular malformations (CVMs) (3,8,10,12,13). In this retrospective study we aimed to assess the value of MRI.

Materials and Methods

Thirty patients suffering from CVMs, 8 females and 22 males aged 13 - 67 years, were examined by CT, MRI, and angiography. Patients with acute hemorrhage were excluded. A synopsis of the data is shown in Table 1. The CT scan was carried out by third-generation units with high definition. MRI scans were performed with a Magnetom Siemens scanner at 0.35 or 0.5 T. Features of the MRI examination are summarized in Table 2. We used T_1- and T_2-weighted sequences as well as a proton density sequence. We evaluated signal intensity, signal homogeneity, and the shape and contours of the lesions, as demonstrated in Table 3.

Results

MRI examination of all patients gave an exact picture of the CVMs and their topographic relation to the surrounding brain structures. As seen in Table 4, all AVMs showed a hypointense signal intensity. Depending on the applied sequence, 67% were inhomogeneous and 33% homogeneous. According to the size of the lesion, angiomas were mostly round or lobulated and sharply outlined. In contrast to these findings, the giant aneurysm of the middle cerebral artery (MCA) presented two different components. The perfused part of the aneurysm showed a hypointense signal character while the thrombosed area was hyperintense in all sequences. The cavernoma was demonstrated as a round inhomogeneous hyperintense lesion.

Discussion

The present study shows a good correlation between the MRI and angiographic findings. In all cases except the cavernoma (case 29), MRI allowed an exact diagnosis. Though up to now CT has been the only noninvasive method for imaging angiomas (7) it was not able to give sufficient diagnostic security in the detection of midline lesions in the posterior fossa or brain stem. Due to blood flow effects in MRI, this method is appropriate for presenting CVMs with high blood flow (1,2).

Advances in Neurosurgery, Vol. 16
Ed. by W. Walter, M. Brandt, M. Brock, and M. Klinger

Table 1. Synopsis of angiographic, CT, and MRI findings in 30 cases of cerebral vascular malformations (CVM)

Case No.	Age/ sex	CT	MRI	Angiography	Size
1	15/m	ps/ce	hi/hg/l/sh	AVM, interhemispheric fissure	1 × 1
2	24/f	ps/ce	hi/ihg/l/sh	AVM, left cerebellopontine angle	3 × 3.5
3	13/m	ps/ce	hi/ihg/l/sh	AVM, right temporal	2 × 3
4	52/m	ps/ce	hi/hg/r/sh	AVM, right parieto-occipital	4 × 4
5	45/m	ps/ce	hi/ihg/l/ush	AVM, left frontotemporal	6 × 7
6	44/f	ps/ce	hi/hg/r/sh	AVM, left parietal	3 × 3
7	51/m	ps/ce	hi/ihg/r/sh	AVM, suprasellar	2 × 3
8	15/m	Ø/Ø	hi/hg/r/sh	AVM, right frontal corpus callosum	1 × 1
9	47/m	Ø/ce	hi/hg/r/sh	AVM, right frontal	2 × 2
10	48/m	ps/ce	hi/ihg/l/ush	AVM, left occipitotemporal	6 × 7
11	21/f	ps/ce	hi/ihg/l/sh	AVM, left temporoparietal	3 × 3
12	44/m	Ø/ce	hi/ihg/l/sh	AVM, medulla oblongata	2 × 3
13	49/m	ps/ce	hi/ihg/l/ush	AVM, left occipitotemporal	6 × 6
14	28/f	ps/ce	hi/ihg/s/sh	AVM, right cerebral marrow	2 × 3
15	49/f	ps/ce	hi/hg/r/sh	AVM, right temporal	5 × 6
16	37/f	ps/ce	hi/ihg/s/sh	AVM, left occiptioparietal	5 × 5
17	55/m	ps/ce	hi/ihg/l/sh	AVM, left occipitotemporal	3 × 4
18	32/m	Ø/ce	hi/hg/s/sh	AVM, left temporal	2 × 2
19	41/m	ps/ce	hi/ihg/r/sh	AVM, pons	3 × 3
20	42/m	ps/ce	hi/hg/r/sh	AVM, left parieto-occipital	5 × 7
21	30/f	Ø/ce	hi/ihg/r/sh	AVM, left frontal	2 × 1
22	58/m	ps/ce	hi/ihg/s/sh	AVM, right posterior fossa	4 × 5
23	19/f	ps/ce	hi/hg/l/sh	AVM, right occipital	3 × 2
24	42/m	Ø/ce	hi/ihg/r/sh	AVM, left temporal	3 × 3
25	48/m	Ø/ce	hi/ihg/r/sh	AVM, left parietal	1 × 1
26	29/m	Ø/ce	hi/ihg/r/ush	AVM, left temporal	2 × 3
27	54/m	Ø/ce	hi/ihg/r/sh	AVM, left temporal	2 × 3
28	59/m	ps/ce	hi/ihg/s/sh	AVM, right cerebellopontine angle	3 × 4
29	32/m	Hyper-dense ce	hyi/ihg/r/sh	Cavernoma, left parieto-occipital	5 × 5
30	67/m	Calci-ficated ce	hi and hyi/ r/sh	Aneurysm of right A. cerebri media	3 × 3

Abbreviations: ps, signs of a pathologic lesion in plain CT; ce, contrast enhancement; hi, hypointense; hg, homogeneous; l, lobulated; sh, sharp; Ø, normal findings; hyi, hyperintense; ihg, inhomogeneous; r, round; s, serpentine; ush, unsharp

Table 2. Features of the MRI examination

Magneton Siemens	
Field strength 0.35/0.5 T	
Sequences	
T_1 weighted	(TR 400/TE 35)
Proton density	(TR 1600/TE 35)
T_2 weighted	(TR 1600/TE 70)

Table 3. Criteria for the evaluation of MRI with CVMs

Signal intensity (hypo-, iso-, hyperintense)
Signal homogeneity (round/lobulated/serpentine)
Contour (sharp/unsharp)

Table 4. Positive findings in identification of AVMs by MRI (n = 28)

Signal intensity	Hypointense	100%
Signal homogeneity	Homogeneous	33%
	Inhomogeneous	67%
Shape	Round	46%
	Lobulated	36%
	Serpentine	18%
Contour	Sharp	86%
	Unsharp	14%

The results of our study demonstrated a high tissue-vessel contrast and the absence of bony artifacts. Therefore the localization of the lesion and its relation to the surrounding tissue can be clearly demonstrated. Though we have little experience with giant aneurysms or cavernomas, MRI gave important diagnostic indications in both cases (cases 29 and 30). The different parts of the aneurysmal sac showed distinct signal intensities, which was very helpful for the operative planning. In contrast the angiography did not show the exact localization of the thrombosed part. This result corresponds to those of ELLER (6) and WORTHINGTON et al. (14). MRI of the operated cavernoma (case 29) was not satisfactory: we suspected a highly vascular tumor with central necrosis. The histological examination proved the lesion to be a cavernoma. It was remarkable that this malformation was characterized by a hyperintense signal in all applied sequences. This might be explained by very slow flowing blood (1).

Conclusions

The advantage of MRI is the simultaneous imaging of the brain structures which we do not receive in angiography and which is less clearly differentiated in CT. MRI supplies the surgeon with exact information concerning the localization, shape, and size of the lesion so that important conclusions can be drawn regarding the indication for surgery and the surgical approach. In some cases (cases 6, 8, 23) we decided upon direct surgical intervention in patients with unfavorably located angiomas. Without MRI we would have hesitated to perform surgery.

Summarizing, from the results of our study we conclude that MRI is very helpful for the diagnosis and surgery of CVMs, but there is no doubt that cerebral angiography is indispensable in such patients.

References

1. Axel L (1984) Blood flow effects in magnetic resonance imaging. AJR 143:1157-1166
2. Bradley WG, Waluch V, Lai KS, Fernandez EJ, Spalter C (1984) The appearance of rapidly flowing blood on magnetic resonance images. AJR 143:1167-1174
3. Brainin M, Omasits M, Seiser A (1984) Angiome des Hirnstamms mit jahrelangem klinischen Verlauf. Nervenarzt 55:659-664
4. Brant-Zawadzki M, Davis PL, Crooks LE, Mills CM, Norman D, Newton TH, Sheldon P, Kaufman L (1983) NMR demonstration of cerebral abnormalities: comparison with CT. AJR 140:847-854
5. Bydder GM, Steiner RE, Young IR, Hall AS, Thomas DJ, Marshall J, Pallis CA, Legg NJ (1982) Clinical NMR imaging of the brain: 140 cases. AJR 139:215-236
6. Eller TW (1986) MRI demonstration of clot in a small unruptured aneurysm causing stroke. J Neurosurg 65:411-412
7. Kretzschmar K, Grumme Th, Kazner E (1980) Möglichkeiten und Grenzen der Computer-Tomographie und Angiographie in der Diagnostik cerebraler Gefäßmißbildungen. Radiologe 20:105-112
8. Kumar AJ, Fox AJ, Vinuela F, Rosenbaum AE (1984) Revisited old and new CT findings in unruptured larger arteriovenous malformations of the brain. J Comput Assist Tomogr 8(4):648-655
9. Schörner W, Bradac GB, Treisch J, Bender A, Felix R (1986) Magnetic resonance imaging (MRI) in the diagnosis of cerebral arteriovenous angiomas. Neuroradiology 28:313-318
10. Schumacher M, Stoeter P, Voigt K (1980) Computertomographische Diagnose und Differentialdiagnose cerebraler Gefäßmißbildungen. Radiologe 20:91-104
11. Servo A, Porras M, Raininko R (1984) Diagnosis of cavernous haemangiomas by computed tomography and angiography. Acta Neurochirurgica 71:273-282
12. Valavanis A, Wellauer J, Yasargil MG (1983) The radiological diagnosis of cerebral venous angioma: cerebral angiography and computed tomography. Neuroradiology 24:193-199
13. Weisberg LA (1978) Computed tomography in the diagnosis of intracranial vascular malformations. Computerized Tomography 3:125-132
14. Worthington BS, Kean DM, Hawkes RC, Holland GN, Moore WS, Corston R (1983) NMR imaging in the recognition of giant intracranial aneurysms. AJNR 4:835-836
15. Young IR, Bydder GM, Hall AS, Steiner RE, Worthington BS, Hawkes RC, Holland GN, Moore WS (1983) NMR imaging in the diagnosis and management of intracranial angiomas. AJNR 4:837-838

Neuroradiological and Neuropathological Findings in Intracranial Cavernous Angiomas

S. Bien, M. Schumacher, and B. Volk

Sektion Neuroradiologie der Universität, Hauptstraße 5, D-7800 Freiburg

Introduction

Intracranial cavernous angiomas, also known as cavernomas, are a rarely diagnosed vascular malformation. They account for approximately 5% - 13% of all vascular malformations (41,55). Cavernomas consist of partly thrombosed vessel convolutions with large cavernous vessel spaces. Direct angiographic confirmation is usually impossible because of the thrombosis and the slow blood flow in cavernomas. In CT and MRI they appear as non- or minimally space-occupying, well demarcated lesions frequently containing calcifications (7,9,67).

Materials and Methods

Neuroradiological and neuropathological findings were obtained in 18 patients with surgically and histologically confirmed intracranial cavernous angiomas. Computer tomograms and cerebral angiograms were carried out in all of the patients. In 14 cases MRI was additionally performed.

Results

In the 18 patients (ten women and eight men), 19 cavernomas were diagnosed. Seventeen of the cavernomas were supratentorially located, two were infratentorial; one patient had two cavernomas. In CT all of the malformations appeared hyperdense prior to contrast medium application. Following intravenous application of contrast material there was slight enhancement. The vessel-like structures which showed up on the contrast-enhanced CT scans were interpreted in three cases as being draining veins. The calcified portions appeared as structures distributed diffusely and in lumps within the lesion (Fig. 1). In every case the space-occupying effect on the surrounding brain tissue was less than expected from the size of the lesions. The borders between the lesions and brain tissue were irregular, but clearly demarcated. In MRI the signal behavior was characteristic: due to a short T_1 relaxation time, high signal intensity in the T_1-weighted images could be confirmed. Since the T_2 time was considerably prolonged, the lesion could also be distinguished in the T_2-weighted images from the surrounding brain tissue. As in CT, the malformations were inhomogeneous. The calcifications in the cavernomas corresponded to zones of slight or absent signal intensity in MRI. The boundary to the surrounding tissue was also irregular, but well demarcated (Fig. 2). An angiographically confirmed enlarged sylvian vein could be identified in MRI by its laminar flow.

Advances in Neurosurgery, Vol. 16
Ed. by W. Walter, M. Brandt, M. Brock, and M. Klinger

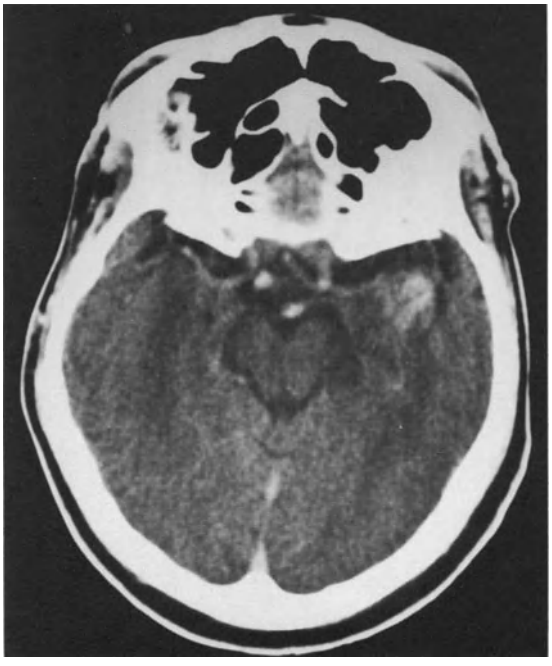

Fig. 1. CT of a temporopolar cavernoma in a 22-year-old woman after contrast medium infusion

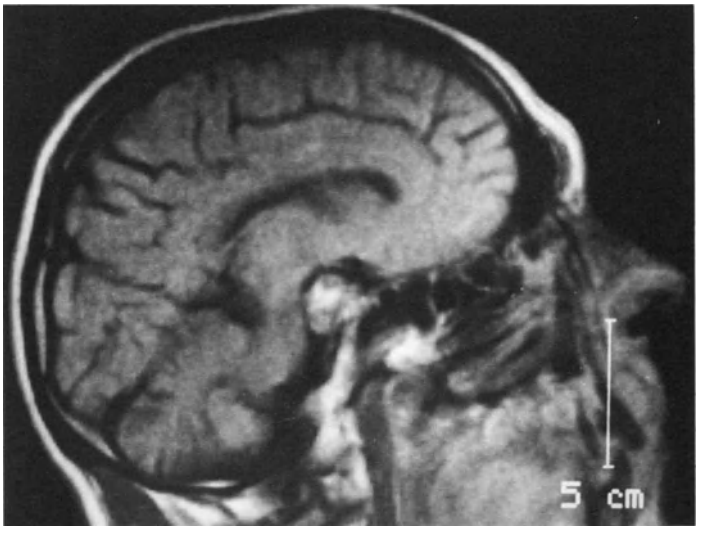

Fig. 2. MRI of a small cavernoma in the left uncus of a 42-year-old man

The angiographic findings were nonspecific: in one case an enlarged sylvian vain could be visualized; in two further cases a wide though still normal vein was assumed to be a draining vein. A displacement of the posterior cerebral artery could be established in one patient with a cavernous angioma in the left uncus. Direct confirmation of the angioma was not possible in any case. The only sign of larger cavernomas in angiography was the appearance of an avascular zone.

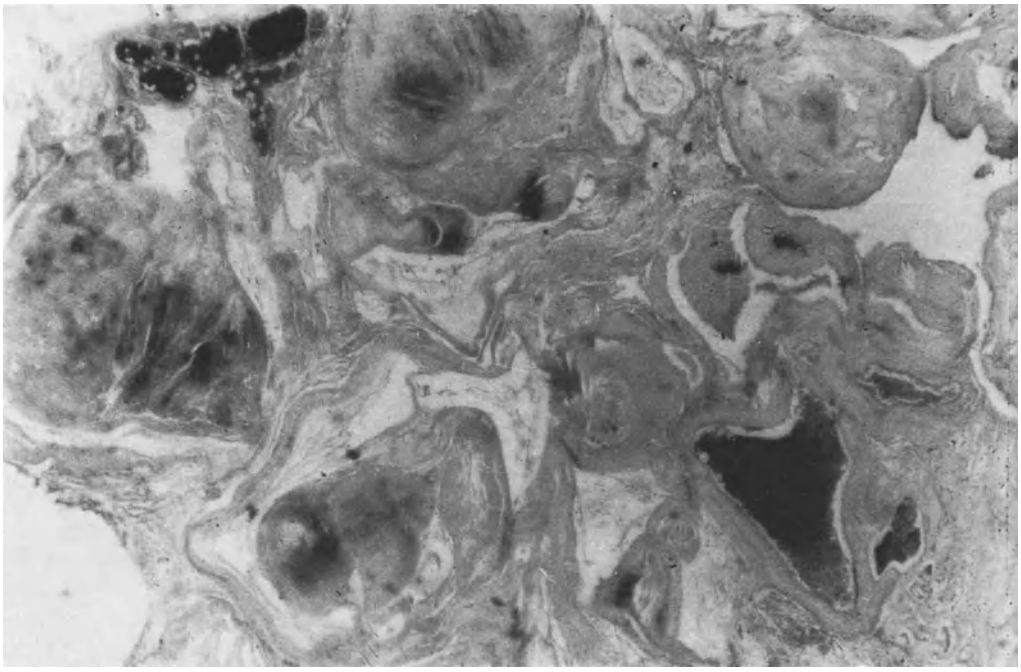

Fig. 3. Cavernoma with varying vessel lumens, regressive changes, and small calcifications (HE, × 120)

Histological examination revealed a convolution of atypical vessels of different diameters lying close together. Some of the multiple, mostly ectatic lumina were filled with blood, some with thrombi attached to the vessel wall. Numerous vessels contained older organized thrombotic material, sometimes with calcifications. Their walls were thin, often split, and displayed hyalinization and sclerosis. With the elastica van Giesen stain, the absence of the elastica interna was characteristic for cavernomas. In the perivascular area siderophages could regularly be found. Macroscopically, the brain tissue in the vicinity of the cavernoma was yellowish owing to siderophages as a sign of recurring bleeding. The surrounding brain tissue showed multiple pigment macrophages, focal capillary proliferations, and pronounced reactive astrocytosis (Fig. 3).

Discussion

Vascular malformations of the brain are usually divided into arteriovenous malformations (AVMs), telangiectasia, cavernous angiomas, and venous angiomas (38,63). Cavernous angiomas are rarely diagnosed. They account for only 5% - 13% of diagnosed intracranial malformations (41, 55). CT and MRI, however, seem to have brought about an increase in the number of cavernous angiomas diagnosed. VOIGT and YASARGIL in 1976 found only 164 cases in the literature up to 1974. In 1986, SIMARD et al. discovered 126 cases reported after 1960.

Cavernomas can occur in any location in the skull (71,78): supratentorial and infratentorial locations in the cerebral parenchyma (3,9,15,

Table 1. Typical appearance of intracerebral cavernous angiomas in neuroradiological and neuropathological investigations

Neuroradiology:

MRI:
- A short T_1 relaxation time causes a high signal intensity in T_1-weighted images
- The T_2 time is considerably prolonged, so that the lesion also manifests itself with a high signal intensity in T_2-weighted images
- There is marked signal intensity in the first echo in series with long T_R

CT:
- Already clearly hyperdense in the plain scan
- Slight or no enhancement after contrast medium infusion
- Recent bleedings or those in resorption occasionally seen in the surrounding tissue

CT and MRI:
- Inhomogeneous structure
- Occasional calcification corresponding to zones of slight or absent signal in MRI and calcified structures in CT
- Irregular but well demarcated boundary to the surrounding tissue
- No perifocal edema

Angiography:
- No direct angiographic visualization because of slow blood flow and/or thrombosis
- Occasional enlarged draining vein

In all neuroradiological investigations:
- No or relatively slight space-occupying effect on the surrounding tissue

Neuropathology:

In the cavernoma:
- Convolution of vessels with different diameters
- Frequent calcifications
- Atypical vessel walls, thin with proliferating intima and no elastica interna
- No normal brain tissue between the cavernoma vessels

In the surrounding of the cavernoma:
- Surrounding tissue yellowish, containing numerous siderophages as a sign of recurrent bleeding
- Marked reactive astrocytosis
- Multiple pigment macrophages

22,43,45,59,67,68,72,76,84), paraventricular and intraventricular (12, 25,27,35,49,56,82), intracranial but extracerebral (30,46,49). Further, cavernomas have been known to occur in the spinal canal inside and outside the spinal cord (5,17,21,39,53,69,75), in the orbit and eye (16, 18,22,24,32,33,37,44,47,54,62,77,80,85,86), and in the body, particularly the liver (1,2,19,42,52,81).

Cavernous angiomas are usually not detected until adulthood, but they can become symptomatic during childhood (31,53,58,74,82,84). They usually occur by chance; however, there are some reports in the literature of increased familial incidence and genetic factors in the development of cavernomas (6,11,13,23,34).

It is not easy to confirm preoperatively the vascular character of cavernomas. Although there are reports of direct angiographic confirmation by the pathological staining of the lesion (28,38,51,58,60,61,70), cavernomas usually escape direct angiographic visualization (4,20,29, 66,67,71,76,79). Frequently, the only sign of the vascular character of the lesion is an enlarged physiological vein representing a draining vein (8,15,66,67,71,83).

In CT cavernomas are visualized as well demarcated, primarily hyperdense, non-space-occupying lesions that can contain calcification. After the application of contrast material there is slight enhancement (73). Bleeding in the vicinity of the lesion in various stages of resorption is occasionally observed. There is usually no perifocal edema (10,14,66,67). A few studies describe a hypodense lesion in the plain CT scan with marked enhancement (26).

Only in a few cases are MRI findings of intracerebral cavernous angiomas mentioned in the literature. The MR images in 11 patients with so-called angiographically occult vascular malformations have been published (36). A shortened T_1 and a prolonged T_2 relaxation time were found in most of the lesions. These findings correlate with our results of shortened T_1 times with a prolonged T_2 relaxation time. In a recently published study (36), a case of a cavernoma of the cauda equina is described. A clearly demarcated signal-intensive lesion was found in MRI. These results are comparable with our MRI investigations in 14 patients with intracranial cavernomas in whom signal-intensive lesions in T_1- and T_2-weighted images with a clear but irregular demarcation to the surrounding tissue could be confirmed (Table 1).

The histological results of our study correspond to those in the literature (3,9,10,11,12,20,26,28,29,45,50,56,59,60,70,71,72,74): convolutions of vessels of different sizes with atypical walls, missing elastica interna, calcifications and thromboses, and the absence of normal brain tissue within the lesion. Recurring hemorrhage in the surrounding brain tissue can often be verified.

Summary

The neuroradiological and neuropathological findings among 18 patients with surgically and histologically confirmed cerebral cavernous angiomas are presented. Seventeen of the angiomas were supratentorial, two were infratentorial; one patient had two cavernomas. In CT the malformations were already hyperdense on the plain scan and showed no substantial contrast enhancement. Direct confirmation of the angioma by angiography was not possible in any case. In MRI the cavernomas were clearly demarcated with zones with high signal intensity. Histological examination revealed vessel convolutions of different sizes, some of which were thrombosed, some open. The vessel walls had a typical structure; the elastica interna was characteristically missing.

References

1. Abrams RM, Beranbaum ER, Santos J, Lipson J (1969) Angiographic features of cavernous hemangioma of the liver. Radiology 92:308-312
2. Barnett PH, Zerhouni EA, White jr RJ, Segelmann SS (1980) Computed tomography in the diagnosis of cavernous hemangioma of the liver. AJR 134:439-447
3. Bartlett JE, Kishore PRS (1977) Intracranial cavernous angioma. AJR 128:653-656

4. Becker DH, Townsend JJ, Kramer RA, Newton TH (1979) Occult cerebrovascular malformations. A series of 18 histologically verified cases with negative angiography. Brain 102:249-287

5. Bergstrand A, Höök O, Lidvall H (1964) Vascular malformations of the spinal cord. Acta Neurol Scand 40:169-183

6. Bicknell JM, Carlow TJ, Kornfeld M, Stovring J, Turner P (1978) Familial cavernous angiomas. Arch Neurol 35:756-749

7. Bien S, Friedburg H, Harders A, Schumacher M (1987) Intracerebral cavernous angiomas in MRI. Acta Radiologica Diagn

8. Bogren H, Salavander C, Wickbom I (1970) Angiography in intracranial cavernous hemangiomas. Acta Radiol (Stockh) 10:81-89

9. Brühlmann Y, Tribolet N de, Bereny J (1985) Les angiomas caverneux intracerebraux. Neurochirurgie 31:271-279

10. Chin D, Harper C (1983) Angiographically occult cerebral vascular malformations with abnormal computed tomography. Surg Neurol 20: 138-142

11. Clark JV (1970) Familial occurrence of cavernous angiomata of the brain. J Neurol Neurosurg Psychiatr 33:871-876

12. Coin CG, Coin JW, Glover MB (1977) Vascular tumors of the choroid plexus: diagnosis by computed tomography. J Comput Assist Tomogr 1:146-148

13. Combelles G, Blond S, Biondi A, Combelles-Pruvot M, Szikala G, Christiaens JL (1983) Formes familiales des hemanigomaes caverneux intracraniens. Neurochirurgie 29:263-269

14. DiTullio MV, Stern E (1979) Hemangioma calcificans. Case report of an intraparenchymatous calcified vascular hematoma with epileptogenic potential. J Neurosurg 50:110-114

15. Diamond C, Torvik A, Amundsen P (1976) Angiographic diagnosis of telangiectases with cavernous angioma of the posterior fossa. Report of two cases. Acta Radiol Diagn 17:281-288

16. Duke-Elder S, MacFaul PA (1974) The ocular adnexa. Vascular tumors. In: Duke-Elder S (ed) System of ophthalmology, vol 13. Mosby, St. Louis, pp 1086-1095

17. Fischer B (1971) Über eine auf kongenitaler Basis entstandene Kavernomähnliche Bildung des Rückenmarks. Frankf Z Pathol 20:37-56

18. Frenkel M, Russe HP (1967) Retinal teleangiectasia associated with hypogammaglobulinaemia. Am J Ophthal 63:215-220

19. Glazer GM, Aisen AM, Francis IR, Gyves JW, Lande J, Adler DD (1985) Hepatic cavernous hemangioma: magnetic resonance imaging. Radiology 155:417-420

20. Giombini S, Morello G (1978) Cavernous angiomas of the brain. Account of fourteen personal cases and review of the literature. Acta Neurochir 40:61-82

21. Hadlich R (1903) Ein Fall von Tumor cavernosus des Rückenmarks mit besonderer Berücksichtigung der neueren Theorien über die Genese des Cavernoms. Virchows Archiv 172:429-445

22. Harris GJ, Jakobiec FA (1979) Cavernous hemangioma of the orbit. J. Neurosurg 51:219-228

23. Hayman LA, Evans RA, Ferrell RE, Fahr RM, Ostrow P, Riccardi VM (1982) Familial cavernous angiomas: natural history and genetic study over a 5 year period. Am J Med Gen 11:147-160

24. Hood J (1970) Cavernous hemangioma of the orbit. Arch Ophthal 83: 49-53

25. Iwasa H, Indei I, Sato F (1983) Intraventricular cavernous hemangioma. Case report. J Neurosurg 59:153-157

26. Ishikawa M, Handa H, Maritake K, Mori K, Nakano Y, Aii H (1980) Computed tomography of cerebral cavernous hemangioma. J Comput Assist Tomogr 4(5):587-591

27. Jain KK (1966) Intraventricular cavernous hemangioma of the lateral ventricle. J Neurosurg 24:762-764

28. Jonutis AJ, Sondheimer FK, Klein HZ, Wise BL (1971) Intracerebral cavernous hemangioma with angiographically demonstrated pathologic vasculature. Neuroradiology 3:57-63

29. Kamrin RB, Buchsbaum HW (1965) Large vascular malformations of the brain not visualized by serial angiography. Arch Neurol 13:413-420

30. Kawai K, Fukui M, Tanaka A, Kuramoto S, Kitamura K (1978) Extracerebral cavernous hemangioma of the middle fossa. Surg Neurol 9: 19-25

31. Khosla VK, Banerjee AK, Mathuriya SN, Metha S (1984) Giant cystic cavernoma in a child. Case report. J Neurosurg 60:1297-1299

32. Kopelow SM, Foos RY, Straatsma BR, Helper RS, Pearlman JT: Cavernous hemangioma of the orbit. Int Ophthalmol Clin 11:113-124

33. Krause U (1971) A case of haemangioma of the orbit. Acta Ophthal 49:221-231

34. Kufs H (1928) Über heredofamiliäre Angiomatose des Gehirns und der Retina, ihre Beziehungen zueinander und zur Angiomatose der Haut. Zschr Neurol Psych 113:651-686

35. Lattermann I (1952) Morgagnis Syndrom bei umschriebenem Angioma cavernosum in der Wand des dritten Ventrikels. Endokrinologie 29: 297-304

36. Lemme-Plaghos L, Kucharczyck W, Brandt-Zawadzki M, Uske A, Edwaeds M, Norman D, Newton TH (1986) MR imaging of angiographically occult vascular malformations. AJNR 7:217-222

37. Lewis RA, Cohen MH, Wise GN (1975) Cavernous haemangioma of the retina and optic disc. Br J Ophthal 59:422-434

38. Lillequist B (1975) Angiography in intracerebral cavernous hemangioma. Neuroradiology 9:69-72

39. Lorenz O (1901) Cavernöses Angiom des Rückenmarkes. Tötliche Blutung. Inaug.-Dissertation Jena

40. McCormick WF (1966) The pathology of vascular ("arteriovenous") malformations. J Neurosurg 24:807-816

41. McCormick WF, Schochet SS (1976) Atlas of cerebrovascular disease. Saunders, Philadelphia

42. Miller JH, Greenspan BS (1985) Integrated imaging of hepatic tumors in childhood. Radiology 154:91-100

43. Mizutani T, Goldberg HI, Herson LA, Murtagh F (1981) Cavernous hemangioma in the diencepalon. Arch Neurol 38:379-382

44. Moss HM: Expanding lesion of the orbit. A clinical study of 230 consecutive cases. Am J Ophthal 54:761-770

45. Mori K, Handa H, Gi H, Mori K (1980) Cavernomas in the middle fossa. Surg Neurol 14:21-31

46. Moritake K, Handa H, Nozaki K, Tomiwa K (1985) Tentorial cavernous angioma with calcification in a neonate. Neurosurgery 16:207-211

47. Mortada A (1962) Unilateral proptosis of unexplained origin. Br J Ophthal 46:369-373

48. Namba S, Ishimitsu H, Nakasone S (1979) Cavernous hemanigoma of the brain. No Shinkey Geka 7:277-283

49. Namba S (1983) Extracerebral cavernous hemangioma of the middle cranial fossa. Surg Neurol 19:379-388

50. Numaguchi Y, Fukui M, Miyake E, Kishikawa T, Ikeda J, Matsuura K, Tomonaga M, Kitamura K (1977) Angiographic manifestations of intracerebral cavernous hemangioma. Neuroradiology 14:113-116

51. Numaguchi Y, Kishikawa T, Fukui M, Sawada K, Kitamura K, Matsuura K, Russell WJ (1979) Prolonged injection angiography for diagnosing intracranial cavernous hemangiomas. Radiology 131:137-138

52. Ohtomo K, Itai Y, Furui S, Yashiro N, Yosikawa K, Iio M (1985) Hepatic tumors: differentiation by transverse relaxation time (T_2) of magnetic resonance imaging. Radiology 155:421-423

53. Ortner WD, Kubin H, Pils P (1973) Ein zervikales kavernöses Angiom. Röfo 118:475-476

54. Pertuiset B, Aron-Rosa D (1975) Extra- and intra-cranial radical surgery in orbital angiomas. Mod Probl Ophthalmol 14:558-561

55. Pool JL, Potts DG (1965) Aneurysms and arteriovenous anomalies of the brain. Diagnosis and treatment. Harper and Row, New York

56. Pozzati E, Padovani R, Morrone B, Finizio F, Gaist G (1980) Cerebral cavernous angiomas in children. J Neurosurg 53:826-832

57. Pozzati E, Gaist G, Poppi M, Morrone B, Padovani R (1981) Microsurgical removal of paraventricular cavernous angiomas. J Neurosurg 55:308-311

58. Prensky AL, Gado M (1973) Angiographic resolution of a neonatal intracranial cavernous hemangioma coincident with steroid therapy. Case report. J Neurosurg 39:99-103

59. Ramina R, Ingunza W, Vonofakos D (1980) Cystic cerebral cavernous angioma with dens calcifications. J Neurosurg 52:259-262

60. Rao VRK, Pillai SM, Radhakrishnan VV, Mathews G (1979) Hypervascular cavernous angioma at angiography. Neuroradiology 18:211-214

61. Roberson GH, Kase CS, Wolpow ER (1974) Telangiectases and cavernous angioma of the brainstem: "cryptic" vascular malformations. Neuroradiology 8:83-89

62. Rowbotham GF, Little E (1966) Haemangioma of the orbit. Br J Ophthal 50:47-49

63. Rubinstein LJ (1972) Tumors of the central nervous system. Armed Forces Institute of Pathology, Washington DC

64. Runnels JB, Gifford DB, Forsberg PL, Hanbery JW (1969) Dense calcification in a large cavernous angioma. J Neurosurg 30:293-298

65. Russell DS, Rubinstein LJ (1971) Pathology of tumors of the nervous system, 3rd edn. Arnold, London

66. Savoiardo M, Passerini A (1978) CT, angiography and RN scans in intracranial cavernous hemangiomas. Neuroradiology 16:256-260

67. Savoiardo M, Strada L, Passerini A (1983) Intracranial cavernous hemangiomas: neuroradiologic review of 36 operated cases. AJNR 4: 945-950

68. Schneider RC, Liss L (1958) Cavernous hemangiomas of the cerebral hemispheres. J Neurosurg 15:392-399

69. Schröder JM, Brunngraber (1965) Über ein intramedulläres cavernöses Angiom (mit einem Beitrag zur Erblichkeit). Acta Neurochir 12:632-641

70. Segall HD, Segal HL, Teal JS, Rumbaugh CL, Bergeron RT (1974) Calcifying cerebral cavernous hemangioma with brain scan and angiographic findings. Neuroradiology 7:133-138

71. Simard JM, Garcia-Bengochea F, Ballinger WE, Mickle JP, Quisling RG (1986) Cavernous angioma: a review of 126 collected and 12 new clinical cases. Neurosurgery 18:62-172

72. Tagle P, Huete I, Mendez J, del Vilar S (1986) Intracranial cavernous angioma: presentation and management. J Neursurg 64:720-723

73. Terao H, Hori T, Matzutani M, Okeda R (1979) Detection of cryptic vascular malformations by computerized tomography. Report of two cases. J Neurosurg 51:546-551

74. Tribolet N de, Kaech D, Perentes E (1982) Cerebellar haematoma due to a cavernous angioma in a child. Acta Neurochir 60:37-43

75. Ueda S, Saito A, Inomori S, Kim I (1987) Cavernous angioma of the cauda equina producing subarachnoidal hemorrhage. Case report. J Neurosurg 66:134-136

76. Vaquero J, Leunda G, Martinez R, Bravo G (1983) Cavernomas of the brain. Neurosurgery 12:208-210

77. Vogelsang H, Werry H, Hoffmann K (1975) Angiographische Diagnostik von Hämangiomen im Orbitalbereich. Klin Mbl Augenheilk 166:477-482

78. Voigt K, Yasargil MG (1976) Cerebral cavernous hemangiomas or cavernomas. Incidence, pathology, localization, diagnosis, clinical features and treatment. Review of the literature and report of an unusual case. Neurochirurgia 19:59-68

79. Wakai S, Ueda Y, Inoh S, Nagai M (1985) Angiographically occult angiomas: a report of thirteen cases with analysis of the cases documented in the literature. Neurosurgery 17:549-555

80. Witschel H, Font RL (1976) Hemangioma of the choroid. Survey Ophthal 20:415-431

81. Wood MW, White RJ, Kernohan JW (1957) Cavernous hemangiomatosis involving the brain, spinal cord, heart, skin and kidney. Staff Meet Mayo Clin 37:249-254

82. Yamasaki T, Handa H, Yamashita J, Moritake K, Nagasawa S (1984) Intracranial cavernous angioma angiographically mimicking venous angioma in an infant. Surg Neurol 22:461-466

83. Yamasaki T, Handa H, Moritake K (1985) Cavernous angioma in the fourth ventricle. Surg Neurol 23:249-254

84. Yoshimoto T, Suzuki J (1986) Radical surgery on cavernous angioma of the brainstem. Surg Neurol 26:72-78

85. Zaubermann H, Feinsod M (1970) Orbital hemangioma growth during pregnancy. Acta Ophthal 48:929-961

86. Zeidler I, Zetterström B (1959) Analysis of cases of venous cavernous angioma of the brain. Acta Ophthal 37:350-354

Clinical, CT, and MRI Findings in Spinal Space-Occupying Lesions

P. Sanker, R. Firsching, R. A. Frowein, K. Nanassis, and F. Zanella

Neurochirurgische Universitätsklinik, Joseph-Stelzmann-Straße 9, D-5000 Köln 41

Introduction

Between 1978 and 1987, 164 patients with intraspinal space-occupying lesions – excluding prolapsed disks – were operated on the Neurochirurgische Universitätsklinik Köln. Since 1984, preoperative magnetic resonance imaging (MRI) has been used in 27 patients (see Table 1).

Table 1. Histology of 164 spinal tumors (27 were investigated by MRI)

Tumor	No.	%	Investigated by MRI No.	%
Ependymoma	13	8	2	7
Astrocytoma	7	4	4	15
Neurinoma	20	12	3	11
Meningioma	41	25	7	26
Chondro-, osteoblastoma	7	4	1	4
Sarcoma	6	4	-	-
Plasmacytoma	9	5	-	-
Lymphoma	6	4	1	4
Metastasis	27	17	3	11
Heterogeneous	28	17	6	22
	164	100	27	100

Advantages attributed to MRI in comparison with other neuroimaging procedures are a superior differentiation of tissue without artifacts and the presentation of a larger part of the spinal cord. In this report MRI is compared with the corresponding clinical findings, other radiological investigations, and the intraoperative findings. Illustrative case reports are presented to demonstrate limitations of MRI.

Ed. by W. Walter, M. Brandt, M. Brock, and M. Klinger

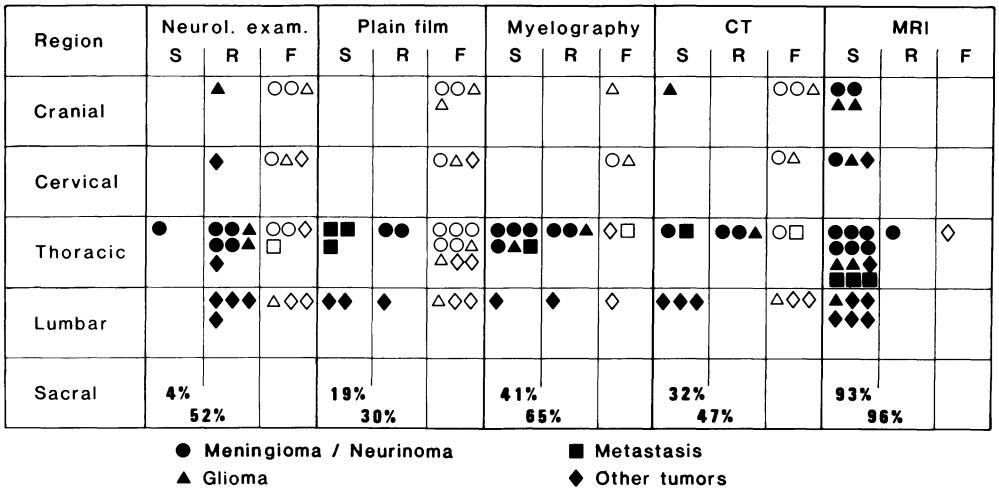

Fig. 1. Demonstration of the upper tumor pole by neurological examination, plain film, myelography, CT, and MRI. Accurate (●) and false (*F*, o) demonstration of the spinal segment (*S*) or spinal region (*R*)

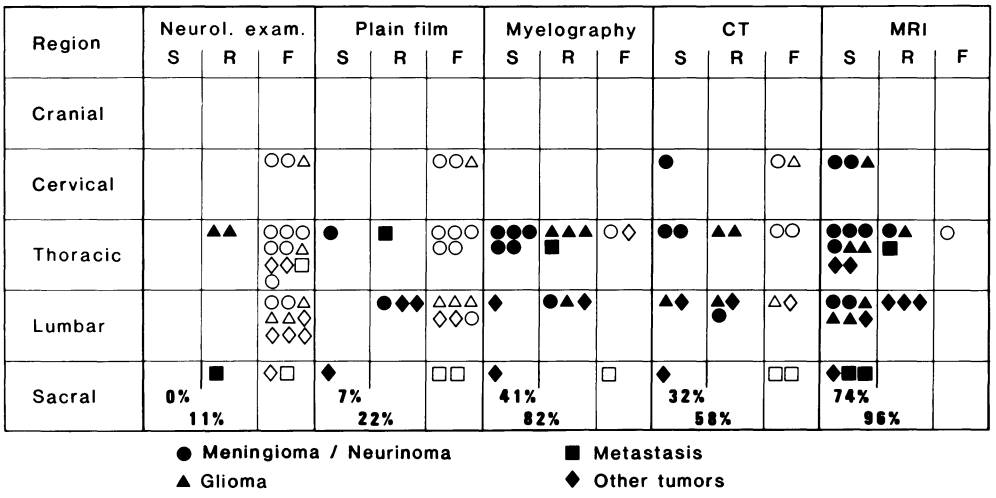

Fig. 2. Demonstration of the lower tumor pole by neurological examination, plain film, myelography, CT, and MRI. Abbreviations as in Fig. 1

Results

Localization of the Extent of the Tumor

In more than half the cases, the upper pole of the tumor could be localized by history and clinical investigation alone, while the lower pole was hardly localized by clinical means only (Figs. 1, 2). Plain X-ray indicated the upper pole in one-third of the patients, giving evidence of osteolytic areas, widened intervertebral foramen, or soft

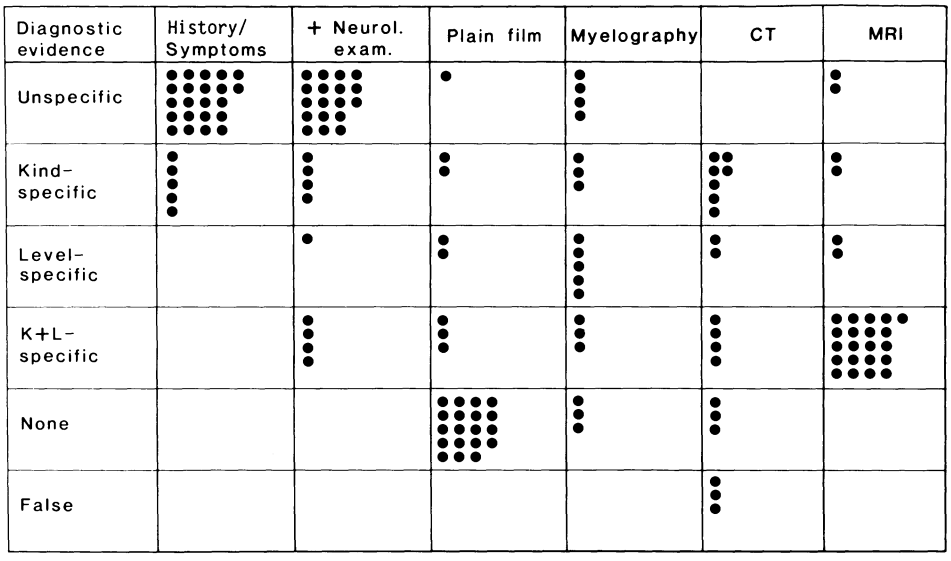

Fig. 3. Diagnostic value of anamnesis, neurological examination, plain film, myelography, CT, and MRI

tissue masses. Myelography identified the upper or lower pole of the tumor in over 80%. CT identified the upper and lower poles in 32% (Figs. 1, 2). Taking CT, history, and neurological findings, the upper and lower tumor poles were accurately identified in 6 out of 14 cases (43%). If a glioma was suspected, usually the CT investigation was interrupted and an MRI was done. With MRI, the upper tumor pole was correctly identified in 25 out of 27 cases (93%), and the lower pole in 3 out of 4 cases.

Preoperative Identification of Kind of Tumor

The histological kinds of tumor are listed in Table 1. Four out of 27 cases were initially treated as a prolapsed disk. Other wrong diagnoses were infections, muscle dystrophy, and meralgia paresthetica. Gliomas were the kind of tumor most often identified by CT. Only one meningioma was diagnosed preoperatively by CT. MRI identified the kind of tumor in 23 out of 27 cases.

Preoperative Localization of Tumor and Identification of Kind of Tumor

Meticulous neurological investigation and history identified the kind and extent of tumor in four patients (15%) (Fig. 3). Myelography was accurate in determining the extent of tumors. CT was accurate in diagnosing the kind of tumor in those cases in which neurological findings suggested the correct level. MRI identified the correct extent *and* kind of tumor in 78% of cases.

Case 1. This 56-year-old female complained of pain of the lumbar and thoracic spine for 9 months, when weakness of both legs and loss of bladder control were observed. Neurological findings included a sensory level at T9 and some weakness of hip and knee movements. Lumbar myelography presented a bloc of contrast medium at T11. MRI (T2) gave

evidence of an intraspinal space-occupying lesion extending from T9 to L1. Thus a laminectomy from T11 to L1 was performed, but there was only a small neurinoma measuring 2 × 1 cm which was completely removed.

Case 2. This 45-year-old male complained of weakness of the left foot for 20 years, which gradually deteriorated to disturbed gait and bladder and sex function. MRI before and after administration of gadolinium gave evidence of an intradural extramedullary tumor with a maximal length of 4 cm at the level of L1, which was interpreted as a malformation tumor (dermoid cyst or lipoma). At operation after laminectomy at L1 and L2 and upon opening of the dura, a cystic tumor was disclosed extending from T12 to L3, calling for an enlargement of the laminectomy. Histology revealed a bronchogenic cyst.

Discussion

The approximate location of the tumor was made likely by the *history and neurological findings* alone in 50% of cases (1,2,8). As could be expected, *plain X-ray* did not contribute much to the identification of the kind and extent of spinal tumors, if they did not cause bony lesions.

Since the advent of modern neuroimaging, *myelography* is used less frequently (9). However, as it is a valuable tool for localizing the tumor, it will certainly remain important for the planning of operative procedures.

CT is useless as a screening measure in unclear spinal conditions (6), but may be helpful if one segment looks suspicious. CT may then contribute to the preoperative identification of the kind of tumor.

MRI disclosed the location and kind of tumor in 23 out of 27 cases. Difficulties reading the MRI were faced in a patient with a large edema and another patient with a cystic malformation tumor.

Conclusion

Although MRI proved to be a superior neuroimaging procedure in spinal tumors, there are misleading findings. If MRI cannot identify the kind of tumor beyond any doubt, the additional use of CT and/or myelography may be advisable, to localize the upper and lower poles of the tumor.

Summary

MRI was used in 27 space-occupying lesions of the spinal canal. When the segment was determined clinically, CT disclosed the correct location in 50%. With MRI, the tumor was localized in 25 out of 27 cases. The perifocal edema of a neurinoma and the large cystic center of a bronchogenic cyst led to misinterpretations of the extent of the tumor.

References

1. Bock WJ (1987) Der Begriff "Fehldiagnose" in der medizinischen Literatur. In: Bock WJ, Schirmer M (eds) Differentialdiagnosen in der Neurochirurgie. Urban & Schwarzenberg, München Wien Baltimore, pp 1-4
2. Frowein RA, Friedmann G, Kunstein-Böhm U (1974) Wahl der Kontrastmittel-Diagnostik bei zervikalen Bandscheibenschäden. Röntgen-Bl 27: 538-548

3. Gallimore GW Jr, Harms SE (1987) Selective three-dimensional MR imaging of the spine. J Comput Assist Tomogr 11(1):124-128

4. Jacobi C, Stichnoth F-A, Knaak G, Neitzel L, Felgenhauer K (1987) Kernspintomographie: Indikationen bei ZNS-Erkrankungen. Dtsch Ärzteb l 84:65-68

5. Lochner B, Halbsguth A, Pia H-W, Fischer P-A (1985) Die spinale Kernspintomographie. Nervenarzt 56:174-185

6. Sandvoss G (1987) Probleme bei der Höhendiagnostik spinaler Prozesse im Computertomogramm. In: Bock WJ, Schirmer M (eds) Differentialdiagnosen in der Neurochirurgie. Urban & Schwarzenberg, München Wien Baltimore, pp 198-202

7. Sartor K (1986) Spinal tumors: magnetic resonance imaging. In: Wenker H, Klinger M, Brock M, Reuter F (eds) Advances in neurosurgery, vol 14. Springer, Berlin Heidelberg New York, pp 72-80

8. Schirmer M (1987) Die Bedeutung der Symptomatik in der Differentialdiagnostik spinaler Tumoren. In: Bock WJ, Schirmer M (eds) Differentialdiagnosen in der Neurochirurgie. Urban & Schwarzenberg, München Wien Baltimore, pp 150-153

9. Wappenschmidt J (1986) Conventional radiologic diagnosis of spinal tumors. In: Wenker H, Klinger M, Brock M, Reuter F (eds) Advances in neurosurgery, vol 14. Springer, Berlin Heidelberg New York, pp 59-68

Value of Magnetic Resonance Tomography in Diagnosing Intraspinal Space-Occupying Lesions

W. Mauersberger, F. Brassel, and A. Steudel

Neurochirurgische Universitätsklinik, Sigmund-Freud-Straße 25, D-5300 Bonn 1

During the last 18 months we have employed magnetic resonance tomography (MRT) to investigate 20 patients with spinal tumors with the following locations and histology:

Intramedullary = 13 (6 ependymomas, 3 syringomyelias, 1 angiolipoma, 1 venous angioma, 1 metastasis from medulloblastoma, 1 spongioblastoma)
Intradural-extramedullary = 4 (3 neurinomas, 1 meningioma)
Extradural = 3 (3 metastases)

The high proportion of intramedullary tumors is striking. Since these lesions are most difficult to diagnose by myelography and computer tomography, we saw an advantage in using MRT especially for these locations.

Pathological processes are visible in MRT as soon as they change or modify the normal anatomy, especially when they cross the border between spinal cord and spinal fluid or when they penetrate the outer border of the spinal canal. This is due to the fact that the MRT shows a high contrast between spinal cord and spinal fluid, in addition to the availability of sliced layers in all three dimensions of the space showing the neighboring bone structures at the same time.

Intramedullary tumors (Fig. 1) show a focal widening of the spinal cord. By slicing in the sagittal direction their vertical extension can be better evaluated by MRT than by myelography. This is especially so with T_1-weighted images, since a myelogram only makes visible those portions already showing a "stop" or a narrowing of the subarachnoidal space (4-6,8-10). This applies particularly to syringomyelia (1-3).

The resolution of spinal computer tomography is not sufficient to evaluate adequately intramedullary tumors with the exception of calcified or fat-containing tumors. The signal intensity of an intramedullary tumor does not distinguish it markedly from the spinal cord. This is not, however, the case with heavily vascularized or cystic tissue portions, where the pathological area attracts attention through its inhomogeneity. Especially in T_2-weighted images, an increase in signal intensity is to be found in solid tumor protions, whereas normal spinal cord tissue, for instance tissue found in the neighborhood of a syringal cavity, does not show a marked increase in signal intensity (5,10).

The diagnosis of syringomyelia (Fig. 2) is made easier by demonstration of a coexisting Arnold-Chiari syndrome, a malformation easily diagnosed in the sagittal image (3).

Advances in Neurosurgery, Vol. 16
Ed. by W. Walter, M. Brandt, M. Brock, and M. Klinger

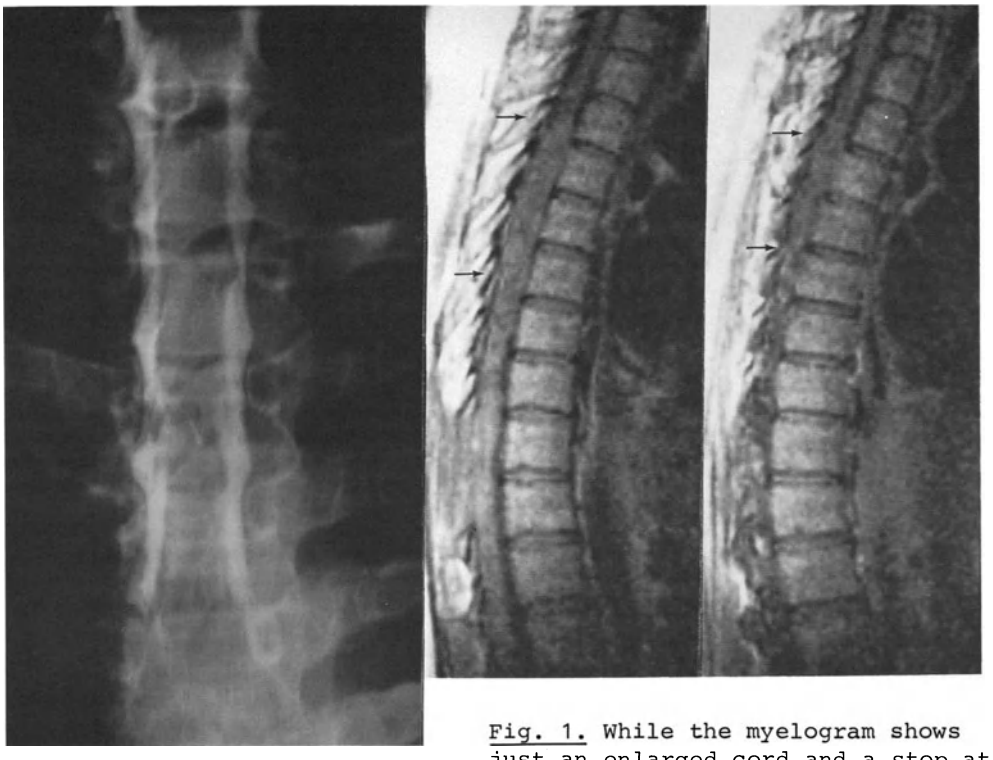

Fig. 1. While the myelogram shows just an enlarged cord and a stop at a certain level, MRT demonstrates, through the expansion of the medulla and the inhomogeneity of the signal behavior, extension of the tumor (an ependymoma) from T4 to T7 *(arrow)*. At the same time the immediate postoperative tumorless segment T10 - T11 is seen

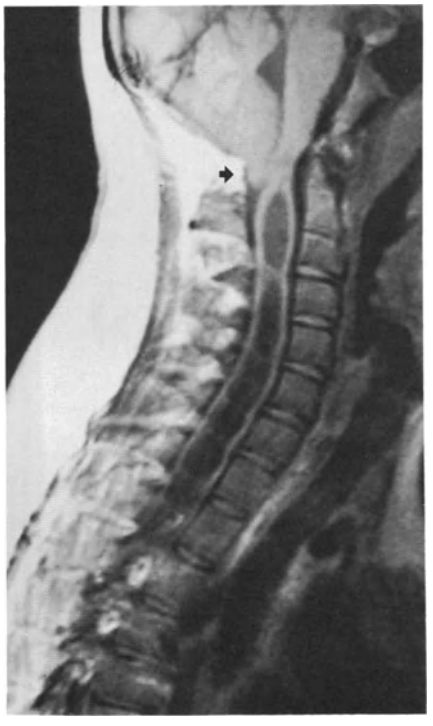

Fig. 2. Marked intramedullary cystic formation with multiple septations in the cervical spinal cord caused by syringomyelia. Due to simultaneous and considerable scoliosis, the affected thoracic segments are not shown. Included is an Arnold-Chiari I malformation with a very low anatomical level of the cerebellar tonsils and the fourth ventricle

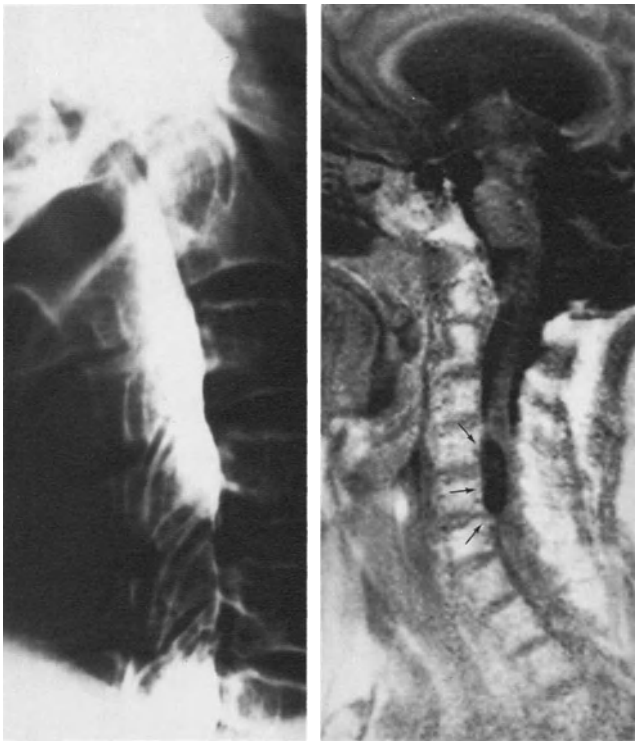

Fig. 3. Intradural-extramedullary tumor (neurinoma) at the level C4-5. In contrast to the myelogram, MRT demonstrates the preponderant ventral location of this tumor *(arrow)*

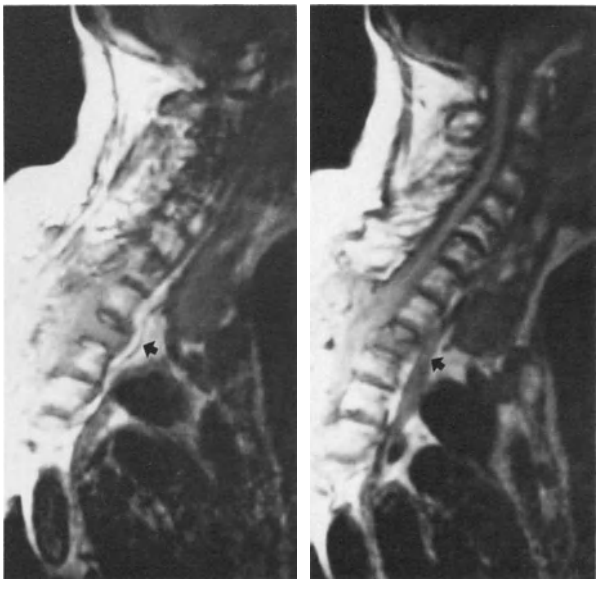

Fig. 4. Vertebral metastasis at T3 *(arrow)*. Because of the diminished signal intensity, it is possible to delimit the afflicted vertebra from the neighboring segments of the vertebral column. Likewise, the epidural and ventral expansion of the tumor can be recognized

Visualization by MRT of tumors in an intradural-extramedullary localization (Fig. 3) is sometimes so poor as to be of no use (4,8,10). This is because the size of the tumor is relatively small and the relaxation times from meningiomas and neurinomas show only a minimal difference from healthy tissue. Several authors point out that these tumors can be made visible only by use of surface coils and that in these cases the extramedullary locations can be better demonstrated in axially sliced layers than in sagittal ones (8-10).

Extradural tumors (Fig. 4), especially metastases and infiltrates from leukemia and lymphomas, are seen in an impressive way because of compression of the dural sheath and diminishing signal intensity of the infiltrated vertebral bodies, particularly in T_1-weighted images. In addition it is possible to demonstrate multiple metastases during a single course of examination (11).

Discussion

Magnetic resonance tomography represents an enrichment of the diagnostic methods presently available, especially in regard to intramedullary and extradural lesions.

The information provided by MRT about the composition of intramedullary tumors, which on myelograms can be diagnosed only through indirect signs, as well as the better demonstration of tumor extension lengthwise, makes it possible to improve the planning of surgery. The excellent visualization of extradural tumor masses gives reason to believe that in the near future MRT will become the diagnostic alternative to myelography for acute spontaneous transverse lesions of the spinal cord.

The disadvantages of the method also need to be mentioned. They lie in the factors of cost and time, but especially in the lack of specificity of the information, so that a pathological finding may represent a tumor as well as a demyelinating disease such as an inflammatory process. In order to interpret MRT images, exact knowledge of the clinical findings is a prerequisite. In addition, the lack of visualization of calcification must be mentioned; this may be of crucial importance in the differential diagnosis. Further disadvantages lie in the relative thickness of the slices, which are done routinely at 10-mm intervals, leading to reduced picture quality. Furthermore the visualization of osseous structures is inferior to that obtained with conventional X-ray films, so that processes with beginning osseous changes cannot always clearly be recognized. In addition, various artifacts, for example metal implants and flowing artifacts due to large blood vessels, may reduce the usefulness of the method. More experience is needed before passing final judgment on the method, its further indications and limitations.

References

1. Aichner F, Gerstenbrand F, Huk W, Pallua A (1984) MRT-Tomographie in der Diagnostik der Syringohydromyelie. Nervenarzt 55:324-327
2. Decker K, Heller H, Petsch R (1985) Syringomyelie in MR. Fortschr Röntgenstr 142:569-570
3. DeLaPaz RL, Brady TJ, Buonanno FS, New PFJ, Kisler JP, McGinnis BD, Pykett IL, Taveras JM (1983) Nuclear magnetic resonance (NMR) imaging of Arnold Chiari type I malformation with hydromyelia. J Comput Asssist Tomogr 7:126-129

4. Gawehn J, Schroth G, Thron A (1986) The value of paraxial slice in MR imaging of spinal cord diseases. Neuroradiology 28:347-350

5. Han JS, Kaufmann S, El Yousef SJ, Benson JE, Bonstelle ChT, Alfidi RJ, Haaga JR, Yeung H, Huss RG (1983) NMR imaging of the spine. AJR 141:1137-1145

6. Heller H, Petsch R, Auberger TH, Decker K (1985) Kernspintomographie der Wirbelsäule. Fortschr Röntgenstr 142:419-426

7. Just M, Higer P, Gutjahr P, Pfannenstiel P (1986) NMR-Tomographie von zerebralen Mittellinientumoren und Halsmarkprozessen im Kindesalter. Fortschr Röntgenstr 145:163-166

8. Lochner B, Halbsguth A, Pia H-W, Fischer P-A (1985) Die spinale Kernspintomographie. Nervenarzt 56:174-185

9. Modic MT, Weinstein MA, Pavlicek W, Starnes DL, Duchesneau PM, Boumphrey F, Hardy Jr RJ (1983) Nuclear magnetic resonance imaging of the spine. Radiology 148:757-762

10. Sartor K (1986) Spinal tumors: magnetic resonance imaging. In: Wenker H, Klinger M, Brock M, Reuter F (eds) Advances in neurosurgery, vol 14. Springer, Berlin Heidelberg New York, pp 72-80

Magnetic Resonance Imaging in Syringomyelia: Pre- and Postoperative Results

H. Steinmetz, G. Schroth, M. Palmbach, D. Petersen, and E. H. Grote

Neurochirurgische Abteilung der Eberhard-Karls-Universität, Calwer Straße 7, D-7400 Tübingen

Introduction

Up until now, none of the numerous hypotheses on the pathogenesis of syringomyelia (SM) have been confirmed. Being the protagonist of hydrodynamic theories, GARDNER (5) explained SM by the prevention of normal CSF flow via the foramina of Luschka and Magendie, which he thought to have failed to open due to an underlying Arnold-Chiari malformation (ACM). As a consequence, the systolic CSF pressure pulse wave generated by the choroid plexus pulsation should be transmitted into a persisting central canal of the spinal cord, thus leading to pathological cavitation ("communicating syringomyelia"). Modified hydrodynamic concepts were reported by WILLIAMS (8), BALL and DAYAN (2), and DU BOULAY et al. (3). All such approaches, however, have in common the assumption of a malformation located at the craniospinal junction and leading to impaired CSF circulation and pathological CSF pulsation. The surgical therapy is therefore often focused on the dorsal decompression of the craniocervical junction besides direct shunting of the syrinx. In the present study 22 SM patients were examined using magnetic resonance imaging (MRI) in order to find indications of hydrodynamic alterations at the level of the foramen magnum and to evaluate the size and shape of the syringes. Pre- and postoperative data were compared.

Material and Method

Twenty-two patients were examined with the Siemens Magnetom (1.5 T, 256 × 256 matrix). Evaluations were done on T_1-weighted spin-echo images (TE 30 ms, TR 400 ms) in the sagittal plane and in axial cuts at the level of the largest syrinx diameter. The thickness of the contiguous slices was 8 mm in 20 patients; the last two patients were studied with 1.3- and 2.3-mm slices using a new gradient arrangement. Of the 22 patients, 4 were examined pre- and postoperatively after insertion of a syringosubarachnoid shunt (7) plus dorsal decompression of the craniospinal junction. All syringes were located cervically with extension into the thoracic region. Mean age in the patient group was 48 years (21 - 69 years), with a female-male ratio of 10 : 12.

Two patients had formerly suffered a trauma with compression fractures of vertebral bodies within the syrinx localization. Two further patients presented accompanying intramedullary tumors: an astrocytoma in one case and multiple hemangioblastomas in the other. As a control group, 15 patients were compiled who had been examined for various reasons but showed normal MRI findings. A quantitative evaluation was performed on the following parameters using a measuring circle and ruler (Rabone-Chesterman Chrome Face No. 27 R): position of the cerebellar

 Advances in Neurosurgery, Vol. 16
Ed. by W. Walter, M. Brandt, M. Brock, and M. Klinger

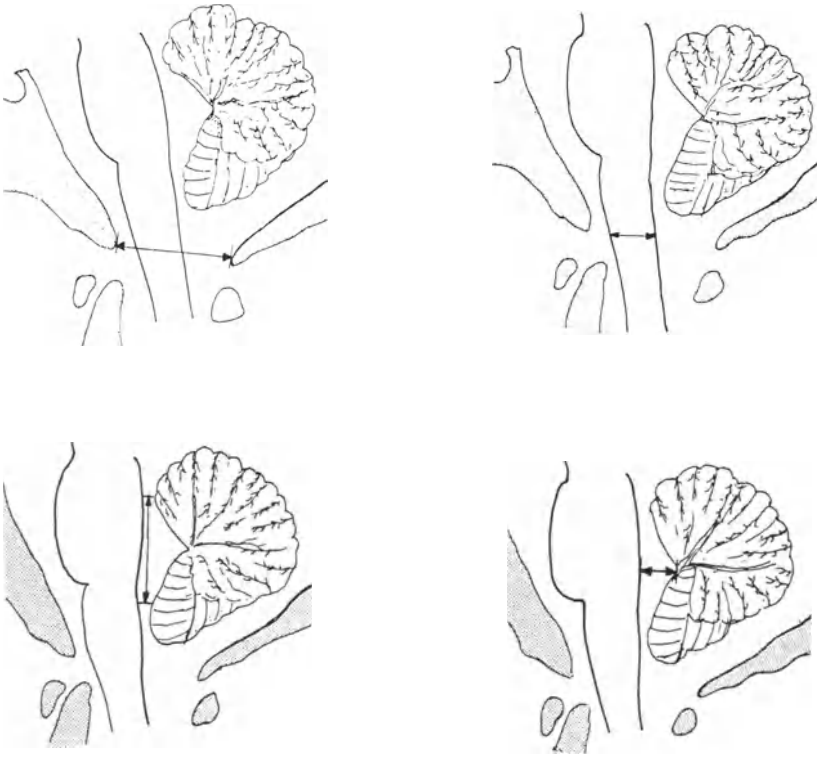

Fig. 1. MRI parameters of the posterior fossa and craniospinal junction measured in 22 SM patients and 15 controls without significant differences

tonsils compared to the level of the foramen magnum, sagittal diameter of the foramen magnum and medulla at the same level, size of the fourth ventricle (median cut), and maximal sagittal and transverse diameters of both syrinx and spinal cord in an axial cut at the level of their largest diameter as seen on the sagittal projection (Figs. 1, 2).

Results and Discussion

1. Only 5 of the 22 patients showed a type I ACM with a pathological caudal position of more than 5 mm below the level of the foramen magnum (1). Thus, ACM is not as frequent as reported by GARDNER (5) from intraoperative evaluation (68 of his 74 cases).
2. Only one patient showed communicating SM with a visible extension of the syrinx into the fourth ventricle. This patient, however, had no ACM, suffered from multiple intramedullary hemangioblastomas, and showed no clinical signs suggestive of SM. Connections between syringes and the ventricular system were in particular not demonstrable in the recent cases studied with 1.3- and 2.3-mm slices. This accords with the histological studies by HUGHES (6) and FEIGIN et al. (4), who also failed to demonstrate communicating syringomyelia.
3. The diameters of the fourth ventricle, foramen magnum, and medulla at this level were normal in all SM patients when compared to the

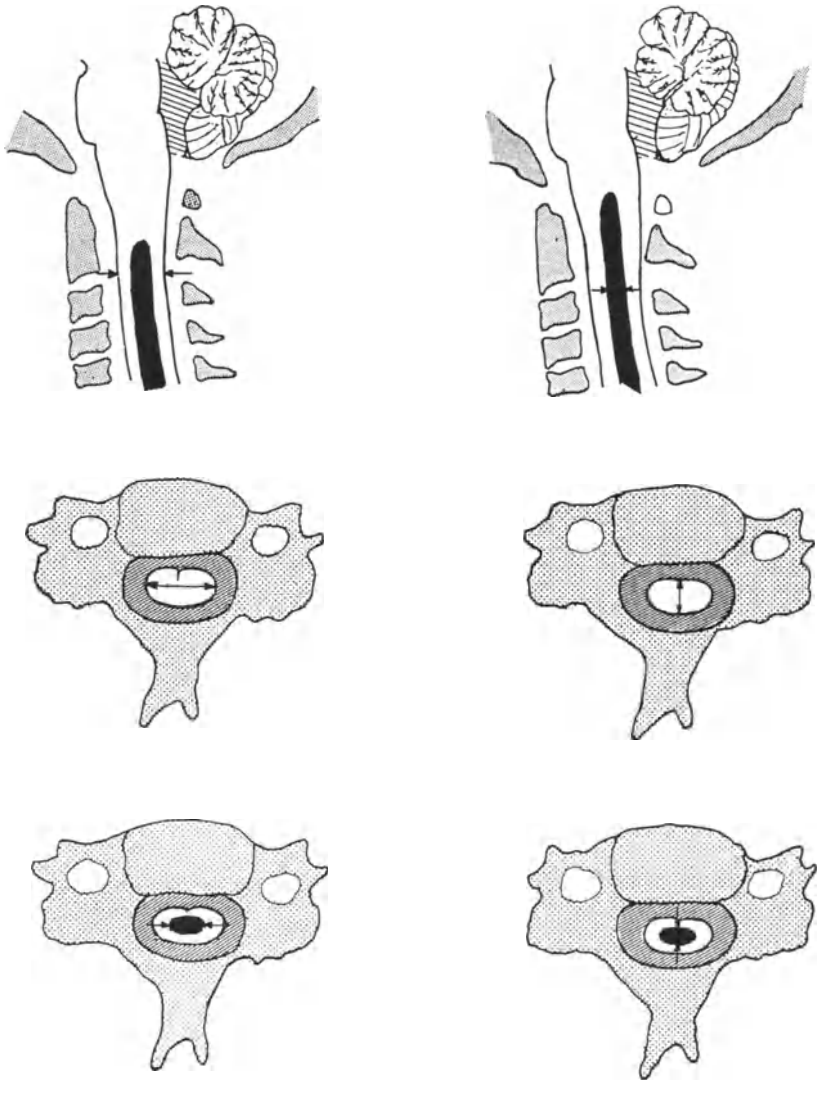

Fig. 2. MRI parameters depicted from axial sections of the spinal cord in 22 SM patients

control group. These data, together with the results given under points 1 and 2, do not confirm hydrodynamic concepts of SM formation implying impaired CSF circulation at the craniocervical junction.

4. Of the 22 SM patients, 10 showed external spinal cord diameters ranging within the normal limits even at the level of the maximal syrinx diameter. As these would most probably present a normal myelogram, MRI is the diagnostic procedure of first choice in clinically suspected SM.
5. Only in about one-third of the patients did the cranial SM extension correlate ± one segment with the most cranial neurological segment.

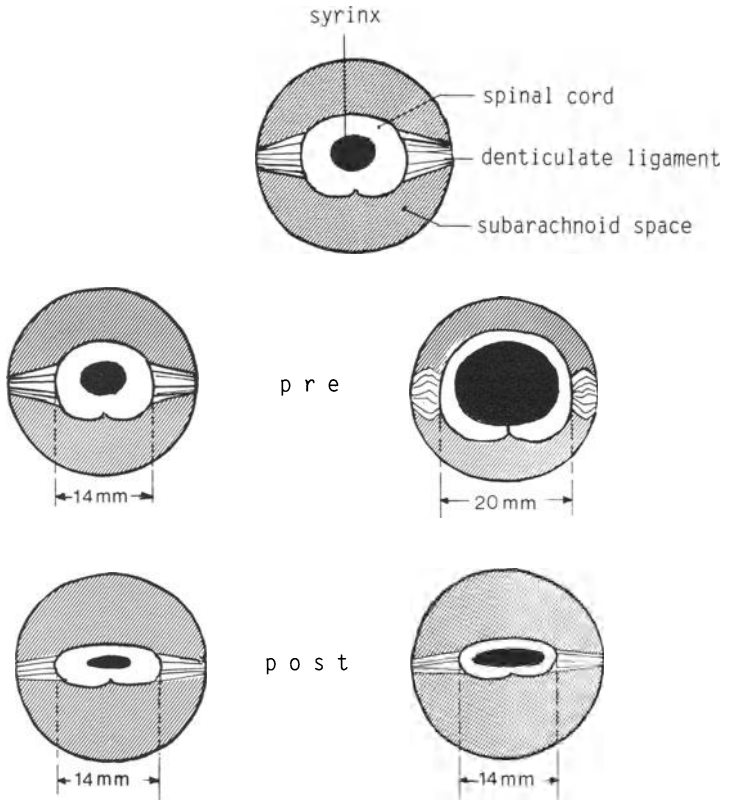

Fig. 3. Typical MRI findings before and after insertion of syringo-subarachnoid shunt: the spinal cord and syrinx collapse in the antero-posterior direction. Postoperatively the syringes take on strongly oval shapes indicating low intrasyringeal pressure

As a rule, the cranial extension on MRI reaches two or three segments above the clinical level.

6. The shape of the syrinx in the axial plane seems to provide valuable information on the presence and degree of intramedullary compression (Fig. 3). This can be concluded from the comparison of pre- and postoperative images in four patients as well as from corresponding postoperative findings in two further patients who had not been studied preoperatively.
   As a rule, the syringes are almost round prior to decompression. After surgery they collapse in the anteroposterior direction and take on transversely oriented, strongly oval shapes. This is explained by the lateral fixation of the collapsing cord by the denticulate ligaments. It is noteworthy that three patients who were not operated on also showed strongly oval cavitations. All of them were most severely and chronically disabled by their disease. Spontaneous perforations of the syringes are conceivable in these cases. Hence, the impression from the data presented is that the shape of the syrinx as visible in the axial projection provides a measure of the syringosubarachnoid pressure gradient and that a transverse oval shape reflects a low intrasyringeal pressure condition. Axial MRI projections should therefore be included in diagnostic studies of

known SM. They might be of relevance in the decision regarding surgery and/or shunt insufficiency.

References

1. Aboulezz AO, Sartor K, Geyer CA, Gado MH (1985) Position of cerebellar tonsils in the normal population and in patients with Chiari malformation: A quantitative approach with MR imaging. J Comput Assist Tomogr 6:1033-1036
2. Ball MJ, Dayan AD (1972) Pathogenesis of syringomyelia. Lancet 2: 799
3. Du Boulay G, Shah SH, Currie JC, Logue V (1974) The mechanism of hydromyelia in Chiari type I malformation. Br J Radiol 47:579-587
4. Feigin I, Ogata J, Budzilovich G (1971) Syringomyelia: The role of edema in its pathogenesis. J Neuropathol Exp Neurol 30:216
5. Gardner WJ (1965) Hydrodynamic mechanism of syringomyelia: its relationship to myelocele. J Neurol Neurosurg Psychiat 28:247-259
6. Hughes JT (1978) Pathology of the spinal cord, 2nd edn. Saunders, Philadelphia
7. Tator CH, Meguro K, Rowed DW (1982) Favorable results with syringosubarachnoid shunts for treatment of syringomyelia. J Neurosurg 56: 517-523
8. Williams B (1969) The distending force in the production of "communicating syringomyelia". Lancet 2:189-193

Magnetic Resonance Tomography of Solid Spinal Cord Tumors with Extensive Secondary Syringomyelia

J. C. W. Kiwit, W. R. Lanksch, H. Fritsch, E. Lins, W. Stork, N. Roosen, M. Schirmer, W. J. Bock, and F. Marguth

Neurochirurgische Universitätsklinik, Moorenstraße 5, D-4000 Düsseldorf 1

Introduction

Space-occupying lesions of the spinal cord and lower medulla oblongata still represent a clinical and diagnostic challenge to the neurosurgeon, and up until very recently a preoperative diagnosis of the tumor's nature was impossible. This was because the conventional diagnostic neuroradiological procedures such as myelography and computed tomography (CT) often fail to establish a diagnosis in the "problem" zones of the neuraxis. These are areas with very close anatomical relations to surrounding bony structures, e.g., the temporobasal structures, the posterior fossa, and in particular the spinal cord. It is in these areas that the technique of magnetic resonance tomography (MRT) has revolutionized the neuroradiological workup and has been particularly helpful in diagnosing syringes and spinal cord tumors of various nature.

Particular neuroradiological and clinical problems arise in cases of small spinal cord tumors that are accompanied by large spinal cysts, so that the syringomyelic changes may dominate the clinical picture and the neuroradiological findings (4,9,10). It is in these cases that MRT in combination with digital substraction angiography (DSA) of the thoracic vessels often enables us to diagnose the underlying tumor preoperatively and to predict its nature.

In the neurosurgical departments of Düsseldorf and Munich University hospitals, during the past 3 years we have had occasion to examine and operate on eight patients with small spinal cord tumors and large secondary syringes: six intramedullary capillary hemangioblastomas and two ependymomas. As we think that this complex disease represents a well defined clinical entity, below we present a typical case from this group.

Case Report

A 54-year-old woman was admitted to the neurosurgical clinic of Düsseldorf's Medical School with a progressive paraparesis and bladder dysfunction. She had experienced excellent health up to 2 years earlier, when she had noticed the onset of therapy-resistant lumbar pain. On two occasions she experienced sudden onset of "weakness" of both legs that caused her to fall to the ground. On such a fall she fractured her right radius. Clinically we saw a severe paraparesis of both legs: the patient could only walk with assistance. There was complete urinary retention combined with anesthesia of the perineum. We thought these findings to be consistent with a diagnosis of a conus/cauda lesion;

Advances in Neurosurgery, Vol. 16
Ed. by W. Walter, M. Brandt, M. Brock, and M. Klinger

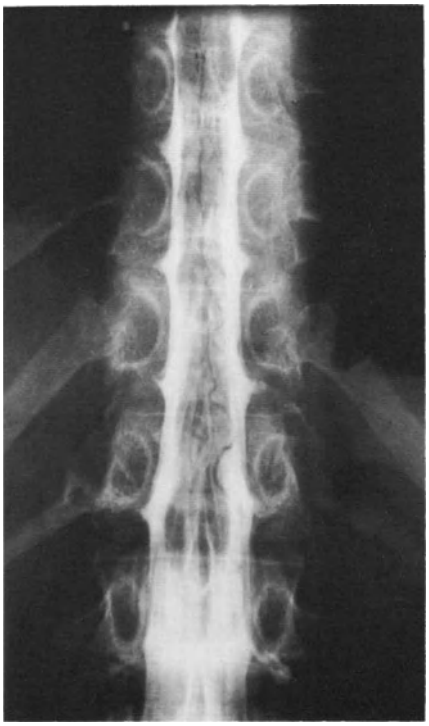

Fig. 1

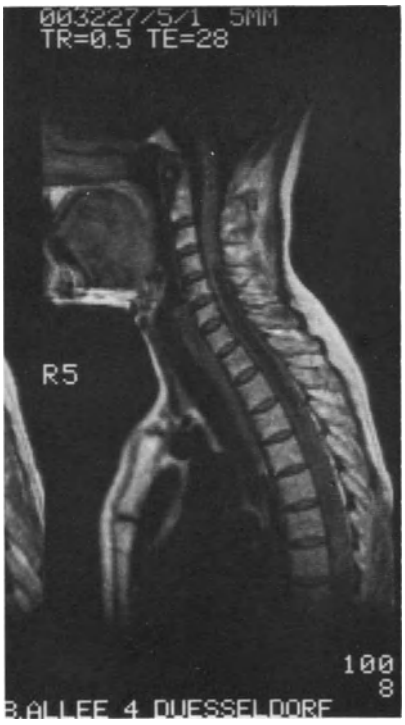

Fig. 2

Fig. 1. Pathological ectatic veins are present on the dorsal surface of the spinal cord and angioma racemosum venosum (Foix-Alajouanine disease) was suspected

Fig. 2. MRT (Diasonic 0.35 T) shows a large cervical syrinx extending from C4 to T4

however, there were cloniform ankle jerks and absent abdominal reflexes. A questionable hypalgesia at the level T8 was elicited as well.

Lumbar myelography showed a space-occupying lesion at the level of the vertebral bodies 8 - 12 (Fig. 1) with narrowing of the subarachnoid space and large pathological vessels in the conus/cauda area. We performed a laminectomy from vertebral body 9 to 12 and resected large ectatic veins that seemed to have compressed the spinal cord from its dorsal surface. There was no indication of any tumor or syringomyelia. We made the diagnosis of angioma racemosum venosum of the spinal cord (Foix-Alajouanine disease). Clinical improvement after this first operation lasted only for 3 months, then the paraparesis worsened. In a second myelogram we saw a complete stop of contrast medium at the thoracolumbar junction and an enlargement of the cervical spinal cord. Cervical MRT revealed a large syrinx extending from C4 to T4 (Fig. 2). In a second operation we performed a syringosubarachnoid shunt at C7 and reexplored the area of the conus medullaris. This time swelling of the lower thoracic cord and conus was found. There was a cystic cavity that contained proteinaceous liquid. A biochemical analysis revealed

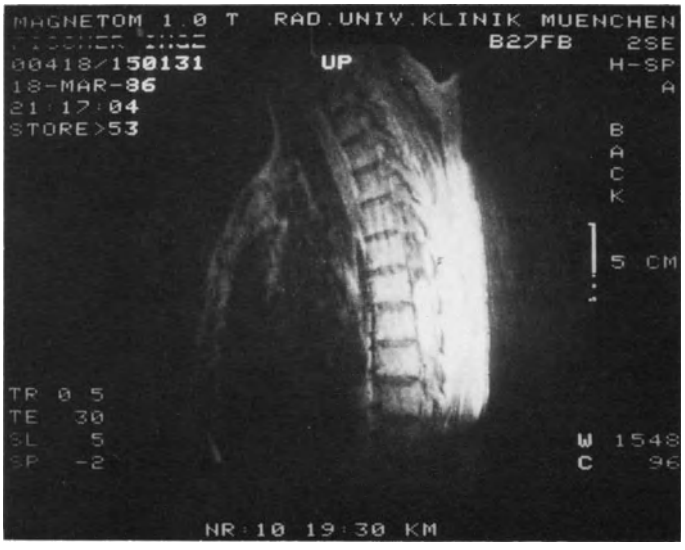

Fig. 3. MRT (Siemens 1.0 T) after gadolinium-DTPA shows an intramedullary contrast-enhancing tumor at the level T7/8

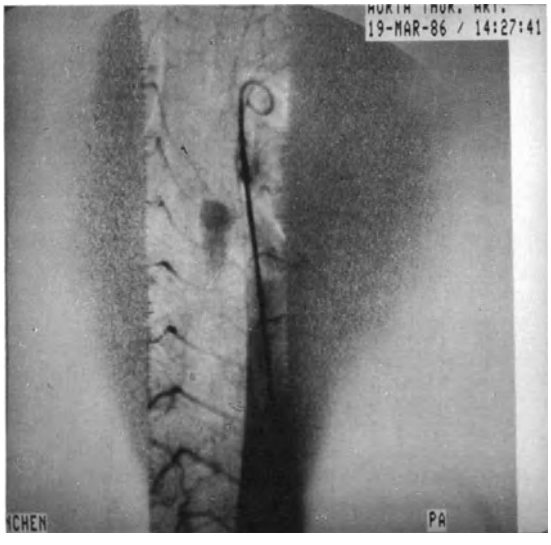

Fig. 4. Sequential DSA of the thoracic vessels clearly demonstrates a vascular tumor at the level T7/8

serum proteins in a normal concentration and a normal relation of the serum protein fractions to each other.

The patient did not improve significantly after this second operation and was transferred to Munich's University Neurosurgical Clinic, where we performed gadolinium-enhanced MRT of the thoracic spine (Fig. 3).

This demonstrated a contrast-enhancing intramedullary lesion which proved to be a vascular/capillary tumor in DSA of the thoracic aorta

(Fig. 4). Laminectomy of vertebral bodies T7 and T8 was performed and a capillary hemangioblastoma (Lindau tumor) was totally resected.

Discussion

A preoperative diagnosis in cases of secondary syringomyelia due to an underlying intramedullary spinal tumor cannot be achieved with conventional neuroradiological examinations. In general, the tumor is small and may be confined to only one or two spinal segments. The accompanying syringes are usually situated above the lesion, although – as is demonstrated in the above case – syrinx formation above and below the tumor may be present. The vascular abnormalities in this case most likely represent venous congestion rather than true angioma racemosum venosum. The secondary syringes in all of our cases showed no direct connection to the intramedullary tumors. Hence a biopsy from the edge of the syrinx revealed only gliotic changes. We should therefore be very reluctant to use the term "a tumor could be excluded" in these special cases.

How can we explain the nature of this complex form of syringomyelia? Obviously, there are no relations to the classical forms of hydrosyringomyelia, and in none of our patients could we detect any form of hindbrain abnormality, obstruction of the foramina of Luschka or Magendie, or dysraphic disorders. There was no clinical evidence of any influence of altered spinal hydrodynamic pressure on the natural course of the disease.

In our view, a key point of the biological nature of the syringes lies in the examination of the syrinx content. The fact that in the case presented above serum proteins in a concentration representing normal values were found, strongly suggests a transudation rather than an active secretion of the liquid. We believe that the underlying mechanism of the transudation of serum proteins into the spinal cord can be explained by the lack of a blood-cord barrier function of the underlying tumors. Therefore, it is no surprise that in most cases (six of eight) the medullary tumors were capillary hemangioblastomas, a tumor with an abundant network of pathological vessels. Once transudation due to a missing barrier has occurred, the liquid might show a simple mechanical distribution pattern and might ascend (or descend) along the spinal fibers and tracts, following the line of least mechanical resistance.

In summary, the condition of secondary syringomyelia due to an underlying intramedullary tumor represents a clinical entity that should not be confused with hydrosyringomyelia or cystic gliomas or other cystic tumors of the spinal cord.

Conclusion

Magnetic resonance tomography is the only diagnostic tool that enables us to differentiate between the various forms of syringomyelia and to demonstrate the underlying tumors in cases of secondary syringomyelia. In the near future, our knowledge of these conditions will be improved considerably by the new techniques of MR flow imaging and MR spectroscopy (1). Of course, the whole spinal cord has to be examined, and gadolinium-DTPA or gadolinium-DOTA (5) must be given to demonstrate small tumors. If we could have used these diagnostic possibilities in our patients earlier, a number of unnecessary operations – mostly shunting procedures – could have been avoided and earlier diagnosis could have been achieved.

In cases of an intramedullary tumor, sequential DSA of the thoracic vessels must follow to establish a preoperative diagnosis, which at least in cases of capillary hemangioblastoma should be possible with great diagnostic safety.

References

1. Axel L, Morton D (1987) MR flow imaging by velocity-compensated/uncompensated difference images. J Comput Assist Tomogr 11(1):31-34
2. Case Records of the Massachusetts General Hospital (1987) Case 3-1987. N Engl J Med 316:150-157
3. Gawehn J, Schroth G, Thron A (1986) The value of paraxial slices in MR-imaging of spinal cord disease. Neurorad 28:347-350
4. Kiwit JCW, Schober R, Vitzthum H, Wechsler W (1986) Neuropathological aspects of the syringomyelic complex. In: Voth D, Glees P, Lorber J (eds) Spina bifida - neural tube defects. de Gruyter, Berlin New York, pp 73-80
5. Knop RH, Frank JA, Dwyer AF, Girton ME, Naegele M, Schrader M, Cobb J, Gansow O, Maegerstadt M, Brechbiel M, Baltzer L, Doppman JL (1987) Gadolinium cryptelates as MR contrast agents. Comput Assist Tomogr 11(1):35-42
6. Masaryk TJ, Modic MT, Geisinger MA, Standefer J, Hardy RW, Boumphrey F, Duchesneau PM (1986) Cervical myelopathy: A comparison of magnetic resonance and myelography. J Comput Assist Tomogr 10(2):184-194
7. McComb J (1983) Recent research into the nature of cerebrospinal fluid formation and absorption. J Neurosurg 59:369-383
8. Pasto E, Rifkin MD, Rubenstein JB, Northrup BE, Cotler JM, Goldberg BB (1984) Real-time ultrasonography of the spinal cord: intraoperative and postoperative imaging. Neuroradiology 26:183-187
9. Sartor K (1986) Spinal tumors: Magnetic resonance imaging. In: Wenker H, Klinger M, Brock M, Reuter F (eds) Advances in neurosurgery, vol 14. Springer, Berlin Heidelberg New York, pp 72-80
10. Scotti G, Scialfa G, Colombo N, Landoni L (1987) Magnetic resonance diagnosis of intramedullary tumors of the spinal cord. Neuroradiology 29:130-135

Noninvasive Diagnosis of Lumbosacral Lesions with Special Reference to Magnetic Resonance Tomography

P. Gruß, R. Lindner, N. Obletter, and G. Rey

Neurochirurgische Abteilung des Krankenhauses der Barmherzigen Brüder, Prüfeninger Straße 86, D-8400 Regensburg 1

Introduction

Magnetic resonance tomography (MRT) has begun its victorious advance upon diagnosis of diseases of the central nervous system. Owing to the fact that the majority of neurosurgical operations in German hospitals are in the lumbosacral region, it is essential to understand how significant the new, illustrative method of diagnosis is in this region. As far as is known at present, the application of a magnetic field of the strength in normal use today is harmless, whereas the other procedures, X-ray and CT investigations, involve the use of ionizing rays. In our studies we were impressed by the excellent readings obtainable by the new method when applied to lumbosacral lesions. We can see sliced sections of the spinal column and its content in the various planes and can thus obtain a good overall pictorial representation. But at the same time details can be observed which not only provide localization but furnish the neurosurgeon with increasingly reliable data on the type of lesion concerned.

Patients, Methods, and Discussion

Malformations

For accurate study of lumbosacral malformations affecting the nervous system, good full-size X-rays have been required as well as CT scans and myelography using water nonsoluble contrast medium, but now astonishing MRT images show the lumen of the spinal canal in cases of lumbosacral malformations; they also enable assessments to be made of changes in wall formations and make visible the content of the spinal column (5), conus medullaris malformation, tumors, and the suchlike (Fig. 1a). It is in cases of lumbosacral malformation that there is an appreciable increase in diagnostic scope, in that the rectum and bladder can also be seen. Thus in addition to the morphological diagnosis, it is also possible to obtain positive information on functional disturbances which, in lumbosacral malformations, can also affect the bladder and the rectal area, so that the proper conclusion can now be drawn in cases where expansion or displacement of these organs is displayed (Fig. 1b). To a neurosurgeon who, up to only a few years ago, had to rely on the overall X-ray diagnosis procedure for assessing a possible ventrosacral meningocele (2), this opens up completely new avenues of approach.

Tumors

Spinal tumors can be rendered visible in one way or another by MRT. If we exploit the numerous possible variants and particularly the possi-

Ed. by W. Walter, M. Brandt, M. Brock, and M. Klinger

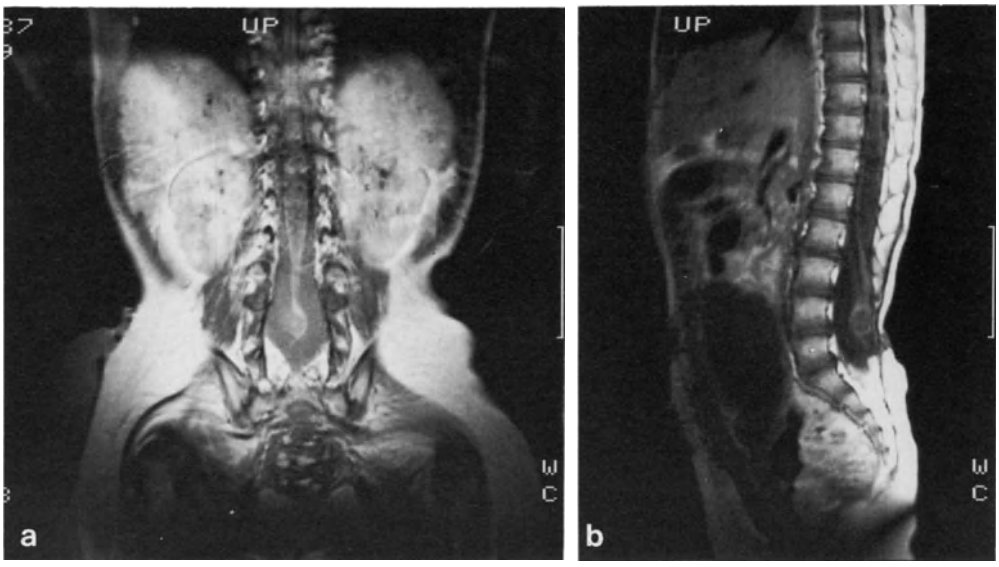

Fig. 1a,b. MRT carried out owing to persistent micturition disturbance in a 3-year-old child with hydrocephalus and an already operated spinal malformation. The topography of the cystic changes in the medulla is shown, with the filum terminale and lipomatous appendage (a) in the spinal canal, the lower section of which is expanded and malformed. Moreover, the images enable assessment of the rectum (considerably congested and bladder (displaced, b)

bilities of using images produced during differing "relaxation intervals" (6), correspondingly definite findings can be established: The spinal lesion can then be shown relative to its closer and more distant surroundings (Fig. 2a) – for instance the precise extent of an intradural tumor can be ascertained (Fig. 2b), and particularly its level in the spinal column. Extradural tumors may be recognized as having a connection with the bony structures of the spinal column and its surroundings, so that for therapeutic indications, MRT is often adequate, and it is indeed increasingly replacing myelography (1).

Inflammatory Changes

Magnetic resonance tomography does not rely on static display of organic material; rather it is the biological reactions of the substrated cell that create the image, and great things can therefore be expected of the new method in respect of inflammatory changes (9). We saw a 25-year-old man suffering from sciatic pain and considerable ischialgia. The lumbar spinal column X-ray pictures were already indicative of upper plate changes, and CT (8) revealed structural changes in the intervertebral space with a sprinkling of small hyperdensity foci and osteolysis at the upper plates (Fig. 3a). This was a finding which at this stage could no longer be attributed to a degenerative disease. It was shown in the MRT to be a change proceeding from the lumbar intervertebral space 4/5, attacking the neighborhood of the vertebral body but not going beyond the osseous structures (Fig. 3b). This was a tubercular diskitis which was verified by CT-controlled puncture of the intervertebral space.

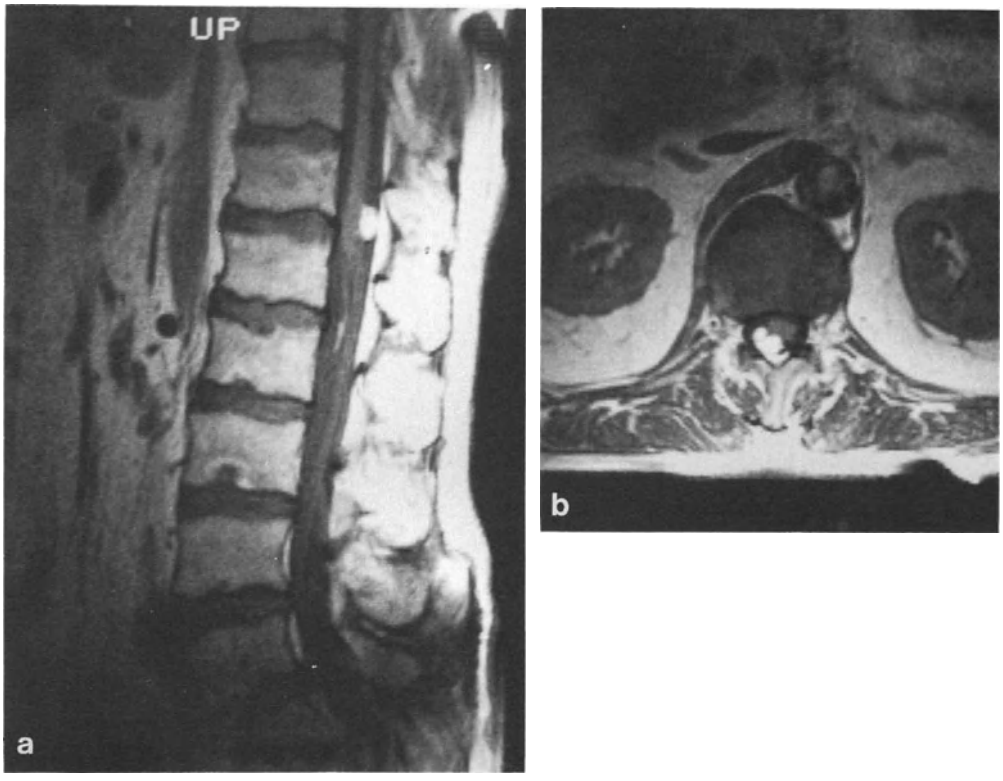

Fig. 2a,b. In this 50-year-old man, MRT proves that it is possible with accurate topographical representation of a small intradural tumor, to show the position of the tumor in relationship to the conus medullaris (a, b) and, by virtue of the signalling effect, enables a lipoma to be diagnosed (histology: lipoma with sarcomatous bone ridge degeneration). In this case, MRT renders CT and myelography superfluous

Degenerative Changes

Up to quite recently, myelography and CT were still superior to MRT procedures, but improved techniques and better image presentation in MRT combined with its clearly proven harmlessness have resulted in a constant increase in value and usefulness of the new method, including its use for degenerative processes in the lumbosacral region. In sagittal layers images are obtained giving a precise representation of the spinal column, its contents, and its surroundings (3). According to the degree of progress and the extent of spinal degeneration, the nature of the signals from a disk will vary, and this variation can be used to yield information about the "biological quality," which makes a valuable contribution to the choice of therapy (4). Arching of material forward into the spinal canal is normally detectable; this means that with the superior representation of the overall lumbosacral area, errors in height localization, e.g., in the case of a slipped disk, hardly ever occur. In the so-called T_2 contrast radiographs, CSF is very signal intensive, i.e., bright, like in myelograms (7). The effect of a sharp point in the bone edge formation on the lumbosacral subarachnoid space thus becomes detectable with appropriately careful tech-

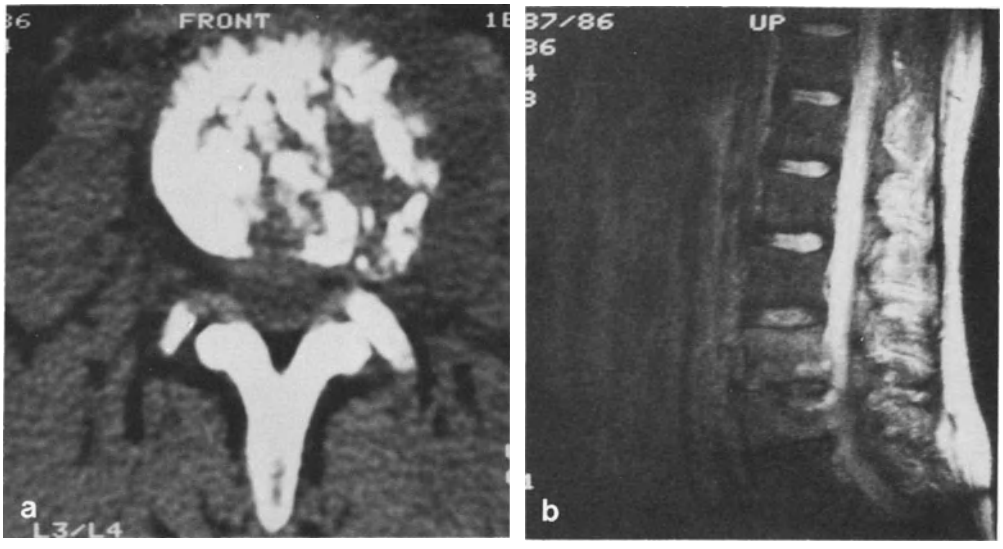

Fig. 3a,b. CT in the case of a 25-year-old man suffering from sciatic pain. Destruction of the intervertebral space and its immediate neighborhood is seen, the cause of which is not known (a). MRT (b) confirms the presence of changes in the intermediate vertebral space which, as opposed to the obviously sound disks, is low signalizing throughout but clearly evidences a higher degree of signal disturbance with small focal changes. In the T_2 contrast image an appreciably lower level of signal is noted in the thickened upper plates, especially in the dorsal area, whereas high signals are recorded in the neighboring spongiosa. (Diagnosis: tubercular spondylodiscitis)

niques, even if the sclerotic bone material itself does not convey a signal. The lumen of the spinal canal is easily assessable in the transversal layers (Fig. 4a): the dural envelope can be defined and the epidural fat is very signal-intensive in all its phases, so that axial differences in its representation can be easily assessed (Fig. 4b). It will probably be possible to assess defects in the sagittal ligament and thus to obtain very useful information for other possible therapeutic interventions (e.g., chemonucleolysis).

Finally, attention should be drawn to the possibility of postoperative control investigations (9). In unfavorable cases, the results obtained indicate possible inflammatory changes, relapses, or scarring in the neighborhood of the operation. In favorable cases the intervertebral space recovers and there is again a higher echo signal; the sagittal ligament, although incised, once again appears intact, and the subarachnoid space shows no indentations.

Conclusions and Summary

For the neurosurgeon, MRT constitutes a new and first-class method which gives information on the way in which nervous structures are affected where spinal lumbosacral lesions are present. The changes can be accurately localized because the images obtained represent the lumbosacral area, its surroundings, and its contents. Owing to the fact that

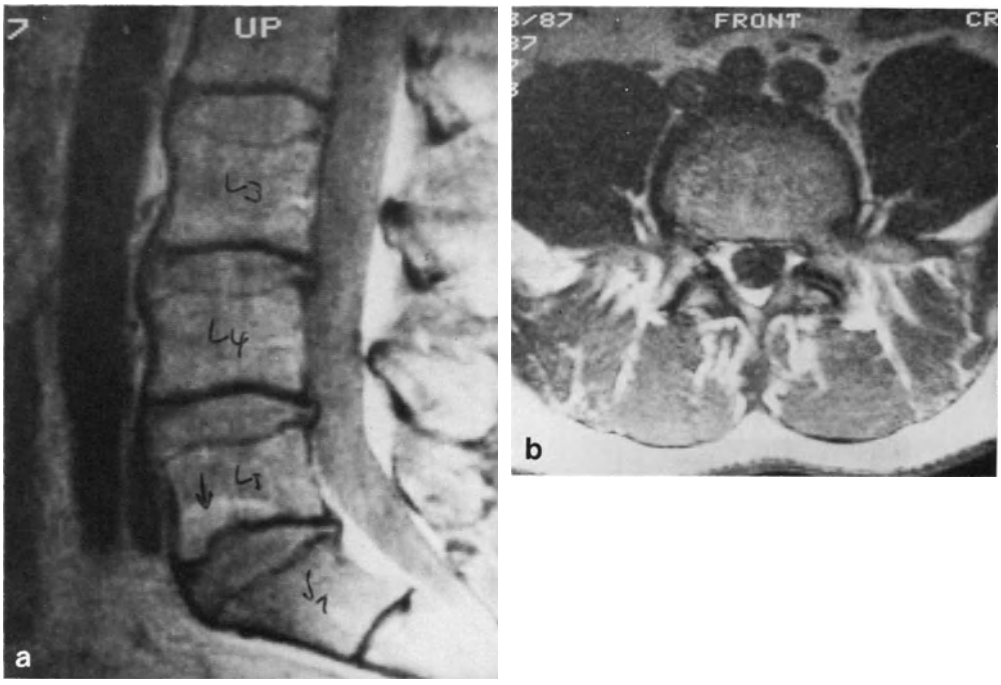

Fig. 4. In this 47-year-old man CT revealed a medium-degree symmetrical (!) protrusion between the 4th and 5th lumbar vertebrae similar to the one between the 3rd and 4th lumbar vertebrae and between the 5th lumbar and the 1st caudal vertebrae. The transverse tomogram clearly demonstrates the absence of any epidural tissue on the left side; a mass of tissue, gray in appearance and equal in signal intensity to the disk itself, is protruding into the intervertebral foramen. (Diagnosis: slipped disk between the 4th and 5th lumbar vertebrae, but still covered by thinned-down sagittal ligament)

the biological substrate is itself represented in the picture, it is often possible to obtain evidence of the type of lesion concerned. The fact that compact bony structures are "nonsignalling" can scarcely be regarded as a disadvantage.

This article outlines and demonstrates the diagnostic limits of neurosurgical methods by appropriate examples of lumbosacral malformation, tumor, inflammatory disorders, and degenerative changes. The MRT findings are compared as far as possible and where necessary with the other diagnostic procedures, as well as with operative findings, and are discussed on the basis of recent literature.

References

1. Einsiedel HGv, Stephan R (1985) Magnetic resonance imaging of spinal cord syndromes. Eur J Radiol 5:127-132
2. Gruß P (1982) Neurochirurgische Operationen an der Wirbelsäule. Hippokrates, Stuttgart
3. Heller H, Braitinger S, Petsch R, Dornenmann H (1986) Disk processes im MR. Eur J Radiol 6:59-64

4. Hickey DS, Aspden RM, Hukins DW, Jenkins JP, Isherwood J (1986) Analysis of magnetic resonance images from normal and degenerate lumbar intervertebral discs. Spine 11:702-708

5. Huk W, Heindel W, Deimling M, Stetter E (1983) Nuclear magnetic resonance (NMR) tomography of the central nervous system. Comparison of two imaging sequences. J Comput Assist Tomogr 7:468-475

6. Lissner J, Seiderer M (1987) Klinische Kernspintomographie. Enke, Stuttgart

7. Modic TM, Paylicek W, Weinstein MA, Boumphrey F, Ngo F, Hardy R, Duchesnau PM (1984) Magnetic resonance imaging of intervertebral disk disease. Radiology 152:103-111

8. Schubiger O (1984) Die Computertomographie der Wirbelsäule. Hippokrates, Stuttgart

9. Weisz GM, Kitchener PN (1987) The use of magnetic resonance imaging in the diagnosis of postoperative lumbar condition. Med J Aust 146: 99-101

MRI in Complications of Neurosurgical Spine Surgery

W. E. Braunsdorf, F. Koschorek, and H.-P. Jensen

Neurochirurgische Universitätsklinik, Weimarer Straße 8, D-2300 Kiel 1

Introduction

Until now the neuroradiologic diagnostic tools for differentiation of complications in lumbar disk surgery have been poor. Myelography did not differentiate scars from disk herniations. The diagnosis of inflammation was difficult. CT improved the diagnostic workup, but MRI seems to overcome many of the unsolved problems in the differentiation of complications in spine surgery (1).

Material and Method

Seventy-seven patients with complaints after lumbar disk surgery were studied by MRI from 1984 through 1987 – first at the Radiologic Institute Oldenburg, at 0.35 T and later at 0.5 T, and since January 1987 in the Dept. of Radiology, University of Kiel, at 1.5 T. Both in Oldenburg and in Kiel a superconducting magnet was used. In Oldenburg the operating parameters were: matrix 256 × 512, slice thickness from 5 to 10 mm, spin-echo technique with TR 400 ms/1600 ms and TE 35 ms/140 ms. In Kiel the matrix was 256 × 256, slice thickness 5 mm, TR 500 ms/1700 ms, and TE 30 ms/100 ms. All patients were studied by CT and in 44 patients myelography had to be performed. Forty-eight patients had to be treated surgically again.

MR Signs

1. *Normal disk:* high signal intensity on long TR/long TE image (4).
2. *Disk degeneration:* decrease of signal intensity on long TR/long TE image due to decrease of water content in the disk, sometimes in line with disk space lowering (1,2,4-7).
3. *Disk herniation:* decrease of signal intensity on long TR/long TE image, bulging or protruding/prolapsing disk material on short TR/short TE, long TR/short TE, and long TR/long TE images. The relation to the diameter of the spinal canal and the nerve root canal and to nervous structures is visible. Thus the extent of a disk herniation and the severity of this finding can be rated (1,5,6).
4. *Postoperative scar formation* (Fig. 1): slight to moderate decrease of signal intensity. Sometimes evidence of fibrosis and extradural scar strings (3).
5. *The postoperative disk:* low signal intensity of the disk space. Higher signal intensity gives evidence of residual disk material (5,6).
6. *Inflammation:* low signal intensity on short TR/short TE images and increase of signal intensity on long TR/long TE images of both disk space and adjacent parts of the vertebral body (1).

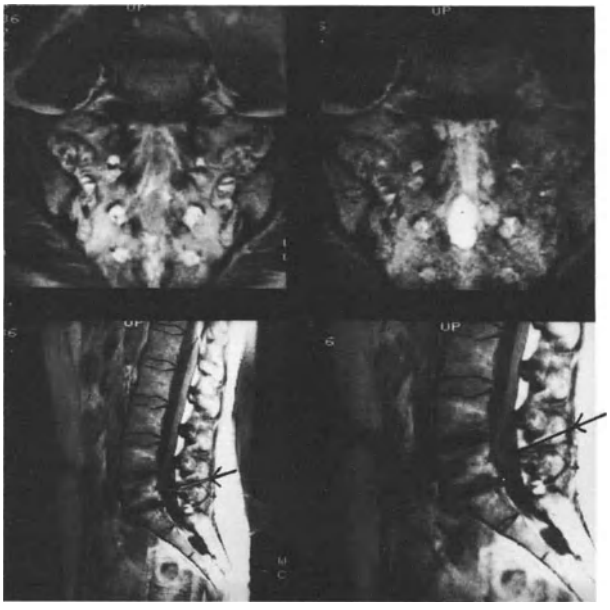

Fig. 1. Postoperative scar formation. Intradural cystic adhesions are demonstrated *(arrow)*. There is cystic dilatation of sacral root S4 and an irregular shape of neighboring vertebral bodies (spondylitis)

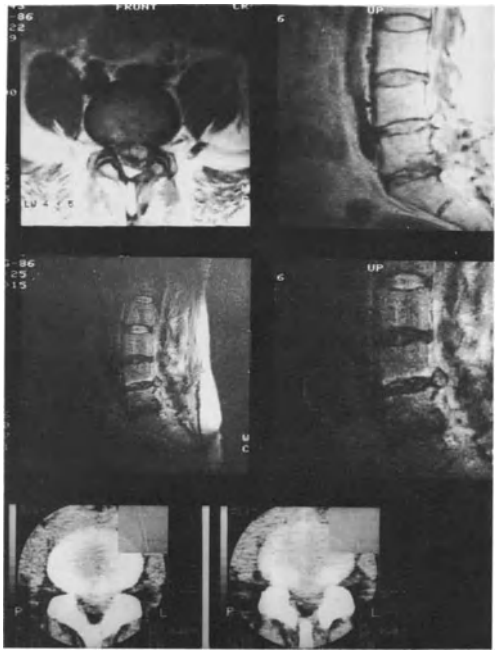

Fig. 2. Disk recurrence at L4/5 is excellently visualized by MRI; CT (performed by Radiological Institute Dres. Kaesbach/Wierer, Kiel) failed to differentiate between scar and disk herniation

Based on these MRI signs in 10 of the 77 patients the MR study was said to be normal; in 30 patients MRI gave evidence of disk recurrence (Fig. 2), and in 18 patients it gave evidence of scar formation. In two cases a nerve root or dural sac anomaly could be demonstrated, whereas in five cases spinal stenosis was visualized. As in CT – depending on the

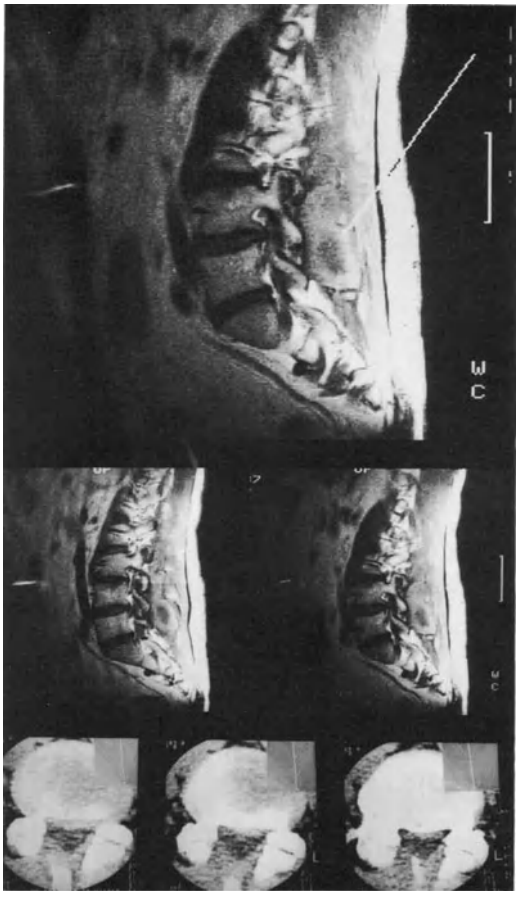

Fig. 3. Nonmetallic foreign body within the muscles after lumbar disk surgery. MRI demonstrates the foreign body, whereas CT (performed by Radiological Institute Dres. Kaesbach/Wierer, Kiel) failed to do so

field of view – in two cases a malignant tumor which grew from the pelvis into the vertebral canal could be demonstrated by MRI. In one case (Fig. 3) MRI revealed a foreign body after spine surgery in an external clinic; in this case CT and myelography were negative. Postoperative inflammation could be shown in 9 of 77 cases.

Discussion

In this series the advantages of myelography were: a so-called familiar image, good demonstration of spinal stenosis and pathology of the arachnoid membrane, localization of height, and CSF study. The disadvantages were: necessity of contrast material, poor demonstration of lateral processes, and poor differentiation between scar and relapse. Further, cases of large caudal sac pathologies may be missed, and there is no visualization of soft tissue structures.

Both myelography and CT need ionizing radiation. In CT beam hardening with subsequent artifacts occurs in edge structures. Pathology of the arachnoid membrane is not demonstrable, and no relation to segments is seen in cases of developmental disturbances in the lumbosacral junction. The problem of gantry angulation has not yet been overcome.

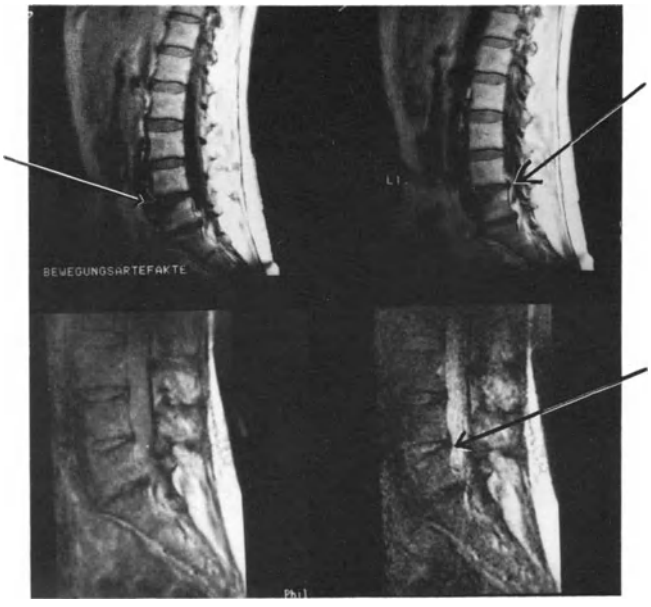

Fig. 4. Spondylodiskitis at L4/5 *(arrow). Above:* 11 days after the onset of symptoms. *Below:* 4 weeks after immobilization

MRI is not available everywhere and is expensive. Bone disorders are difficult to read and may be misleading.

With regard to postoperative scar formation, in all 18 cases MRI was in line with the surgical findings, whereas CT was in 15. Myelography failed in 14 cases. In nine cases of inflammation, MRI was positive within two weeks after onset of clinical signs, i.e., at a time when plain X-ray films and CT usually fail to demonstrate spondylitis or diskitis (Fig. 4). Spinal stenosis is demonstrable both with MRI and with myelography. Pathology of the arachnoid membrane is well visualized in myelography, but MRI may be superior to it as intradural disorders may be better visible.

Conclusions

In this series MRI was in many respects superior to myelography and/or CT. But the price is long examination times and high costs. With fast field echo imaging (FFE) an excellent T_2 contrast is achievable within a shorter time. Regarding the differentiation between scar tissue and disk recurrence, FFE can overcome the shortcomings of common spin-echo sequences without time dissipation (3).

References

1. Braundsdorf WE, Larkamp U, Kuhlendahl D (1987) Erste Erfahrungen mit der Kernspintomographie in der Differentialdiagnose von Bandscheinbenrezidivvorfällen gegenüber der postoperativen Narbenbildung. Tg. der Arbeitsgruppe "Wirbelsäule" der Dtsch. Gesellschaft für Neurochirurgie, Bochum, 22.1.-23.1.1987
2. Chafez NI, Gernant HK, Moon KL, Helms LA, Morris JA (1983) Recognition of lumbar disk herniation with NMR. AJR 141:1153-1156

3. Koschorek F et al. (in preparation) Fast field echo (FFE) imaging for lumbar disk recurrence.

4. Modic MT, Weinstein MA, Pavlicek W, Starnes DL, Duchesneau PM, Boumphrey F, Hardy R (1983) Nuclear magnetic resonance imaging of the spine. Radiology 148:757-762

5. Modic MT, Pavlicek W, Weinstein MA, Boumphrey F, Hardy R, Duchesneau PM (1984) Magnetic resonance imaging of intervertebral disk disease. Radiology 152:103-111

6. Mikhael MA, Ciric IS, Kudrna JC, Hindo WA (1985) Recognition of lumbar disk disease with magnetic resonance imaging. Computerized Radiology 9/4:213-222

7. Steiner HH, Kunze ST (1986) Kernspinresonanztomographische Befunde beim cervikalen Bandscheibenvorfall. Neurochirurgia 29:186-188

Computer Tomography

Brain Edema-Tumor Quotient in Cranial Computer Tomography as a Preoperative Factor in Histological Prognosis

U. Wildförster, Th. Schneider, and W. Delank

Neurochirurgische Universitätsklinik, Knappschaftskrankenhaus Bochum-Langendreer, In der Schornau 23-25, D-4630 Bochum 7

Introduction

Cranial computer tomography (CT) directly shows the perifocal edema surrounding intracerebral space-occupying lesions. LANGE et al. (4) reported in *Zerebrale Computertomographie* on this possibility. AMUNDSEN et al. (1) examined the diminution of absorption by the peritumoral structure in different groups of brain tumors. KAZNER et al. (3) worked out the relation of perifocal edema to the histological classification of brain tumors. WENDE et al. (5) studied 3750 patients with brain tumors in evaluating the differential diagnostic value of cranial CT, without especially focusing on the importance of the perifocal edema. ITO et al. (2) reported on this problem in 1986, without comparing the histological aspects. The question we posed is whether any further information relevant to preoperative histological diagnosis can be gained from the relation of brain edema to tumor in cranial CT.

Method

In a retrospective study covering the 3 years from October 1984 to September 1986 we examined the relation of peritumoral edema to tumor in cranial CT. All patients were divided into different groups according to the histological findings: metastases, meningiomas, low-grade gliomas (WHO grades I and II), and malignant gliomas (WHO grades III and IV). All of the operations performed were primary extirpations of supratentorial brain tumors. In every case we evaluated a preoperative contrast-enhanced cranial CT scan performed in our hospital. Patients who underwent antiedema therapy were not included in the investigation.

The study included 83 patients, 41 male and 42 female, with an average age of 54.8 years (Table 1). The histological differentiation showed 27 patients with metastases (average age 50.9 years), 16 with meningiomas (average age 61.3 years), 14 with low-grade gliomas (average age 48.3 years), and 25 with malignant gliomas (average age 52.6 years). The heterogeneous group of metastases showed the following distribution of primary tumors: 11 pulmonary carcinomas, 3 melanomas, 2 adenocarcinomas of colon, 2 hypernephrotic adenocarcinomas, 2 thyroid carcinomas, 2 non-Hodgkin lymphomas, 1 cancer of the breast, and 4 cases of unknown or unproved primary tumor.

In these 83 patients the preoperative contrast-enhanced cranial CT scans were examined as follows: By planimetry the maximum tumor expansion was measured as well as the peritumoral edema. For exact evaluation of the areas, the medium density was compared with the density of white matter and CSF as a point of reference. In addition the standard deviation of the medium density was controlled (Fig. 1).

Advances in Neurosurgery, Vol. 16
Ed. by W. Walter, M. Brandt, M. Brock, and M. Klinger

Table 1. Distribution of patients according to histology, sex, and age

	No.	Males	Females	Average age
Metastases	27	18	9	50.9
Meningiomas	16	4	12	61.3
Gliomas I/II	14	8	6	48.3
Gliomas III/IV	26	11	15	52.6
Total number	83	41	52	
Medium age				54.8

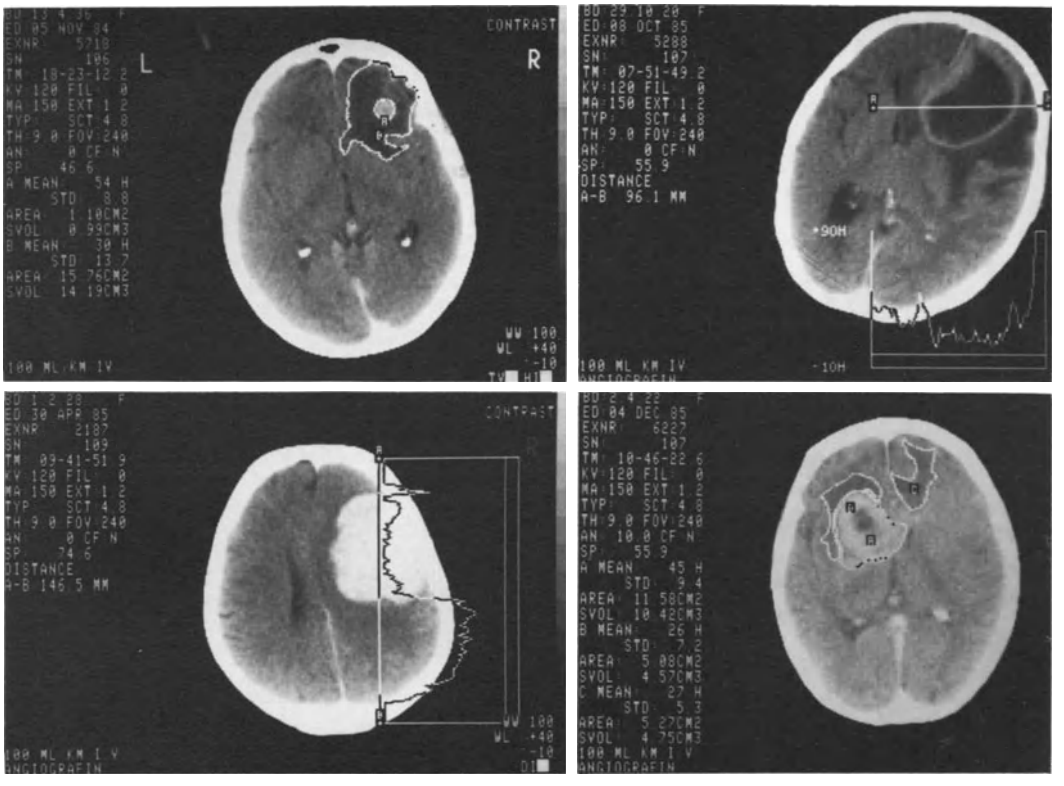

Fig. 1. Planimetric measurement of brain edema and tumor in cranial CT. *Top left:* metastasis; *top right:* low-grade glioma; *bottom left:* meningioma; *bottom right:* malignant glioma

Results (Figs. 2,3)

In the group of patients with metastases the edema-tumor relation was 2.87 on average. The average value in all other groups was considerably lower. In the group of meningiomas it was 1.29 and in the group of malignant gliomas, 1.53. The inhomogeneous group of low-grade

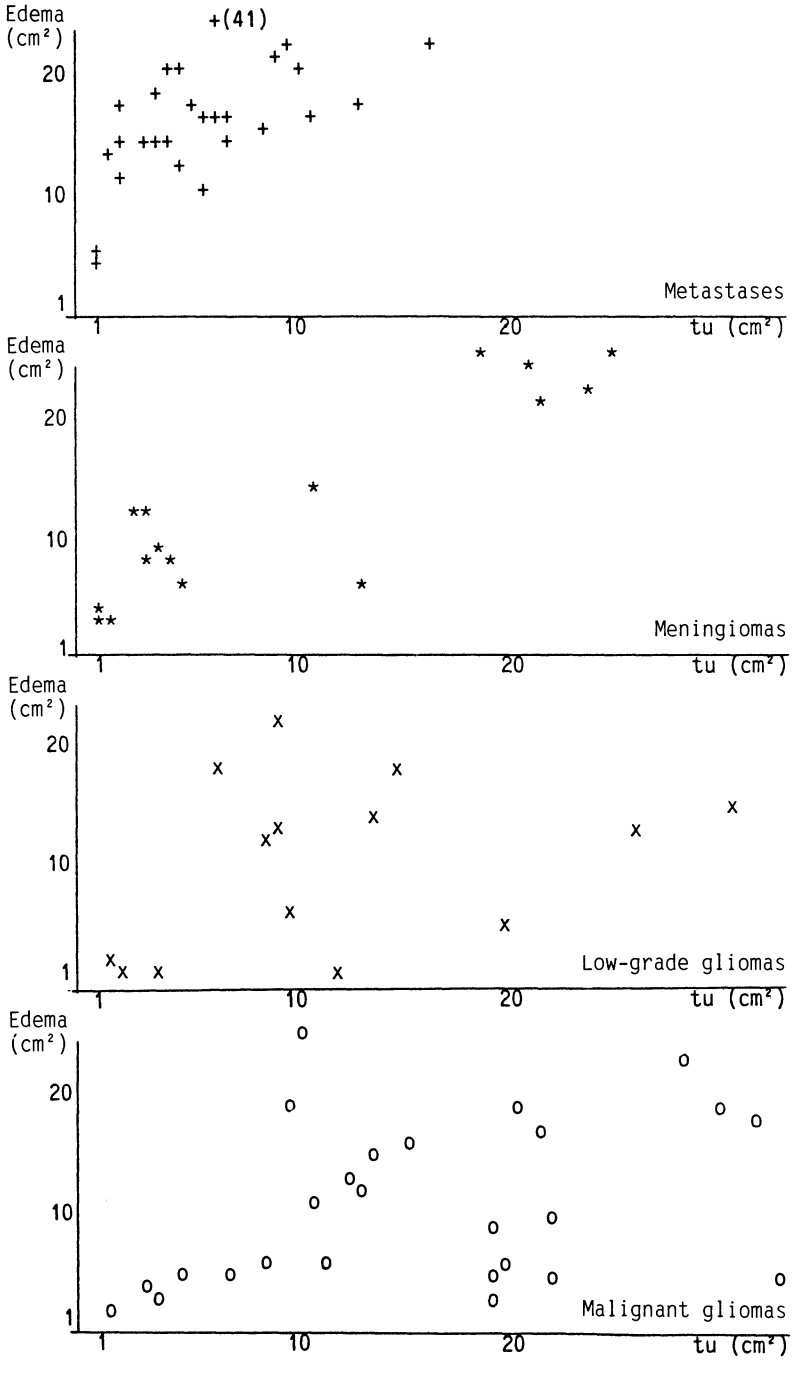

Fig. 2. Brain edema-tumor relation

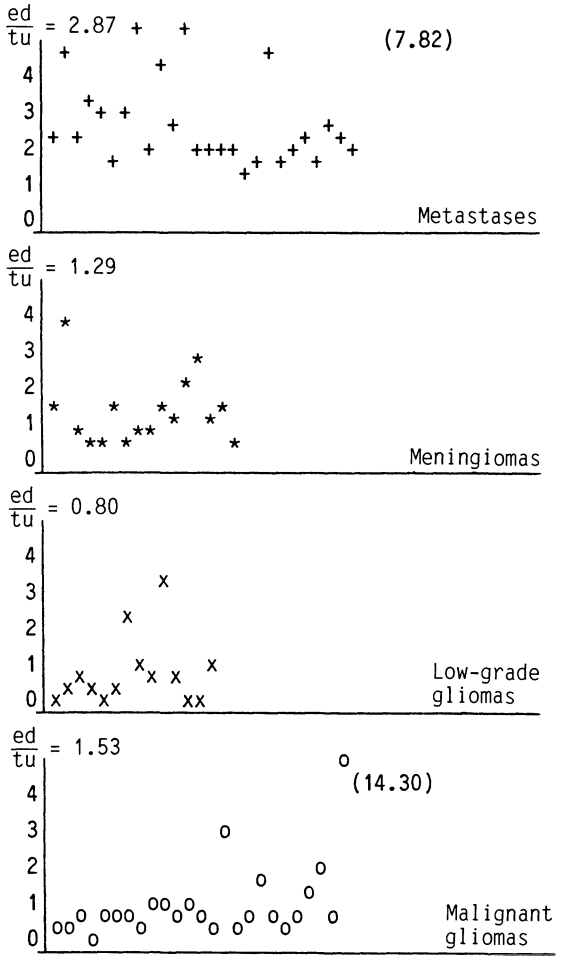

Fig. 3. Brain edema-tumor quotient: average value of histological groups

gliomas deserves special mention; here the average value was 0.80, including three pilocytic astrocytomas without any perifocal edema.

The location of the space-occupying lesion within the hemisphere had no influence on the edema-tumor relation, nor even on the distance of the tumor to the surface of the brain.

Discussion

In the literature only a few investigations have been reported on the relation of peritumoral edema to intracerebral tumor in cranial CT, especially regarding the value of histological differentiation. Our examination shows that the surrounding edema is larger than the tumor itself in most cases; the only exception is the group of low-grade gliomas. The results prove that the space-occupying effect is essentially caused by the perifocal edema.

The quantification of the relation of edema and tumor will help in preoperative evaluation of the histological diagnosis. We could show that the coefficient increases with the anaplasia of the tumor. This fact seems to be independent of the patient's age.

The delimitation of metastases from meningiomas and gliomas is exactly possible, but there is no chance of differentiating the metastases themselves in relation to their primary tumors.

Two aspects concerning the validity of our results should be discussed. Of course, we could not exactly demarcate the real microscopic spreading of edema and tumor; we could only do our measurements macroscopically in accordance with the technical possibilities of our CT equipment. Further, we only did planimetric measurements in the slice showing the maximum tumor expansion. The first examinations at the beginning of our series evaluated the real volume of tumor and edema in all slices; the results controlled the correctness of the relations found by planimetric measurement.

Conclusion

Quantitative measurement of the edema-tumor relation provides greater preoperative certainty regarding the histological diagnosis of intracerebral tumors.

References

1. Amundsen P, Dugstad G, Syvertsen AH (1978) The reliability of computer tomography for the diagnosis and differential diagnosis of meningiomas, gliomas, and brain metastases. Acta Neurochirurgica 41:177-190
2. Ito U, Reulen HJ, Huber P (1986) Spatial and quantitative distribution of human peritumoural brain oedema in computerized tomography. Acta Neurochirurgica 81:53-60
3. Kazner E, Wende S, Grumme Th, Lanksch W, Stochdorph O (1981) Computertomographie der Hirngeschwülste. In: Computertomographie intrakranieller Tumoren aus klinischer Sicht. Springer, Berlin Heidelberg New York, pp 22-25
4. Lange S, Grumme Th, Meese W (1977) Kap. 8: Neoplasmen. In: Zerebrale Computertomographie. Schering AG, Berlin Bergkamen, pp 81-110
5. Wende S, Kretzschmar K, Kishikawa T, Kazner E, Grumme Th, Lanksch W (1982) Der Wert der Computertomographie für die Differentialdiagnose der Hirntumoren. (2. Grazer CT-Symposium, Nr. 44) CT-Sonographie 2:54

Ergometric Achievement Tests in Young Hydrocephalus Patients

U. Szuwart, H. Bennefeld, and Th. Herter

Neurochirurgische Klinik der Westfälischen Wilhelms-Universität, Albert-Schweitzer-Straße 33, D-4400 Münster

Introduction

The participation of children with hydrocephalus in sporting activities has often given rise to discussion between doctors and guardians. For this reason the physical load-bearing capacity of children and young people with shunt-supplied hydrocephalus has been investigated.

Investigated Persons and Method

Thirty-one boys and girls between 5 and 25 years of age with shunt-supplied hydrocephalus from the Neurosurgical Department of the Univeristy Clinic of Münster were chosen for the study. The conditions for participation were adequate cooperation and the exclusion of severe CNS malformations with distinct cerebral and physical weaknesses. Besides the general medical and neurological/neurosurgical case histories, a detailed sporting history was ascertained. Physical investigations from general medical, neurological, and sport medical viewpoints were followed-up by an ECC, a spirometry recording, and a total blood count. In addition bicycle and treadmill ergometry achievement tests were performed; the usual sport medical procedure and criteria for breaking-off after attaining the achievement maximum were applied. The achievements were compared to other medical literature, and advice on training was given.

Results

According to the sporting histories of the patients, a broad spectrum of sport is practised. Swimming, cycling, tennis, dancing, and football were the favorite sports. However, the physical load achieved during these sports cannot be objectivized as it involves individual evaluation.

The weekly length of sporting activity seen in relation to the physical efficiency data revealed marked differences in performance. Patients who did sport more frequently also showed higher achievements during the investigations (Tables 1, 2).

The achievement comparison followed according to the "physical work capacity" (PWC) at a physical load heart rate of 170/min. This result indicates the achievement per kg/body weight on the bicycle ergometer at a defined lead level of the cardiopulmonary system (3). The high heart rate was chosen because children and young people generally have a higher rate than adults. As a second comparative result the

 Advances in Neurosurgery, Vol. 16
Ed. by W. Walter, M. Brandt, M. Brock, and M. Klinger

Table 1. Maximum efficiency of boys investigated

Pt.No.	Age (yrs)	Sporting history: Sporting activity (h/wk)	Sporting history: Sport prohibited	Maximum efficiency: Bicycle (W/kg)	Maximum efficiency: Treadmill (km/h)
1	18.5	6-8		3.7	14
2	17.7	6-16	Total proh.	3.57	12
3	17.0	-	Total proh.	0.91	-
4	16.7	6	Part. proh.	3.25	-
5	16.6	4		2.07	12
6	16.3	6-20		2.72	14
7	15.5	2-3		2.35	12
8	14.0	4-10		2.16	12
9	13.8	6-8	Part. proh.	3.3	14
10	11.6	5		2.43	12
11	10.9	5-10		3.5	12
12	10.5	2	Part. proh.	2.4	6
13	10.5	5-10		3.42	10
14	8.7	3-4		2.86	12
15	8.5	4-6		3.68	12
16	8.4	3-4		3.62	12

Table 2. Maximum efficiency of girls investigated

Pt.No.	Age (yrs)	Sporting history: Sporting activity (h/wk)	Sporting history: Sport prohibited	Maximum efficiency: Bicycle (W/kg)	Maximum efficiency: Treadmill (km/h)
F1	24.4	4-5	Part. proh.	3.02	10
F2	17.2	6-10	Part. proh.	2.38	12
F3	16.1	2	Part. proh.	1.21	10
F4	15.9	2	Total proh.	1.98	8
F5	15.3	5	Total proh.	1.51	8
F6	15.0	4-6	Part. proh.	2.38	10
F7	13.0	5-6		3.09	10
F8	11.1	6-10		3.47	12
F9	10.9	3-5		3.13	-
F10	8.6	4		-	8
F11	7.7	3		3.37	10
F12	7.1	6		2.94	8
F13	6.2	3		-	8
F14	5.9	3	Part. proh.	-	7
F15	5.8	2		-	8

body weight-related achievement with a lactate level of 3 mmol/l of capillary blood was chosen. This result shows the achievement at the lower threshold of the aerobic to anaerobic muscular work, which in children and young people is lower than in adults due to a reduced lactate production. Figures 1 and 2 show the results of our study in comparison to the results of untrained persons in medical literature (5, 6). The results of ergometry correlate to a high degree with the anthropometric data. Consequently, the investigated group of patients does not differ greatly from healthy persons of the same age. The results of our patients were low in comparison with healthy persons (with the exception of seven experimentees). There was a close correlation between maximum achievement and the achievement in the area of the anaerobic threshold. Here, no deviation from the norm was also to be noted.

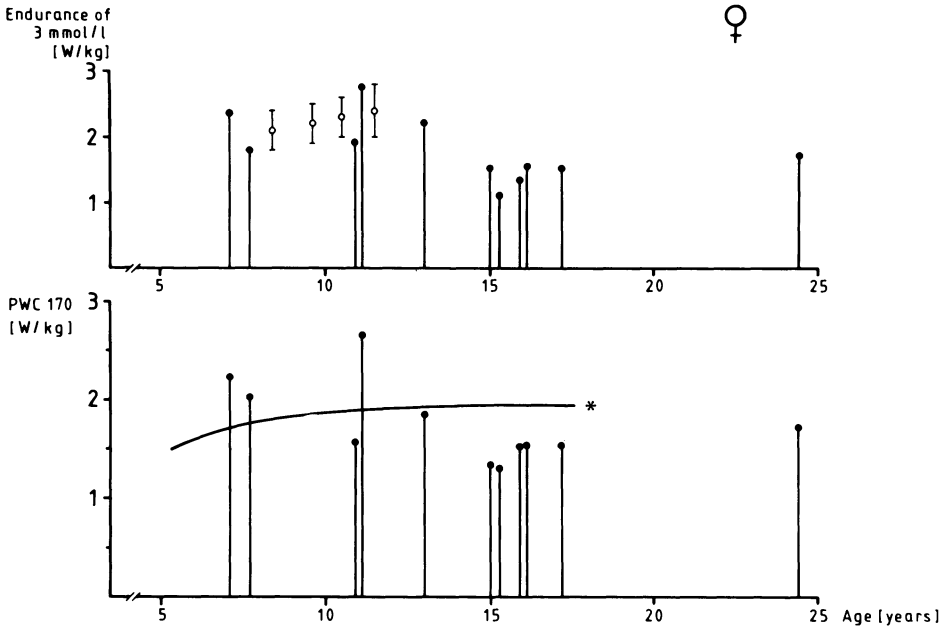

Fig. 1. PWC 170 results and relative achievements with lactate levels of 3 mmol/l in *female* patients with hydrocephalus, in comparison with written results of healthy experimentees on the bicycle ergometer. *, Normal levels according to ROST (6). ♀, Mean levels with standard deviation according to PROKOP (5)

Difficulties arising in connection with sporting activities did not differ in healthy experimentees of the same age. In most cases the cause lay in lack of stamina as a result of too little training, incorrect breathing and running techniques, or previous slight general medical defects.

Discussion

Physiological considerations allow the assumption of large variations in functional pressure difference between the ends of the valve system

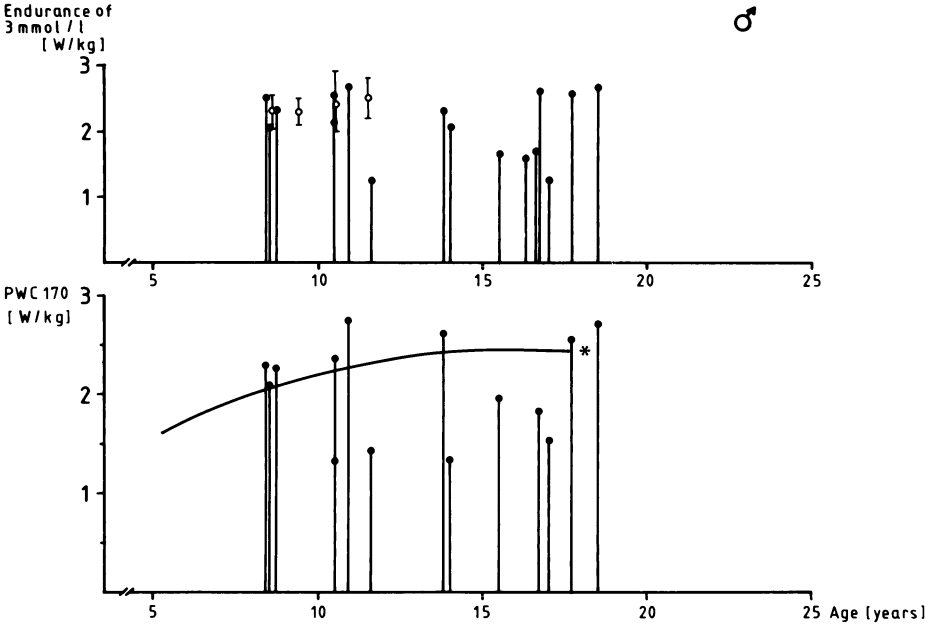

Fig. 2. PWC 170 results and relative achievements with lactate levels of 3 mmol/l in *male* patients with hydrocephalus, in comparison with written results of healthy experimentees on the bicycle ergometry. *, Normal levels according to ROST (6). ⊖, Mean levels with standard deviation according to PROKOP (5)

at greater physical effort (1, 2). Valve complications were to be expected. VOTH (7, 8) reported, however, that he had not observed any valve complications during physical activity. Even in this chosen form of physical loading, which brought the experimentees to their maximum physical load threshold, no valve system complications were noted. Slight neurological damage, like a slight unilateral hemispastic or congenital coordination disturbance, did not mean a limitation. The condition of training alone was important for the achievement.

We were able to prove in our study that children with a drained hydrocephalus are fully able to cope with normal physical loads. In our opinion, regular sport suited to individual needs is necessary for the development of the child patient. According to our results, the prohibition of sport for medical reasons is not justified even if slight physical complaints arise. A better solution for the children concerned would be to carefully choose the type of sport and sport apparatus used as well as regular training. The implanted shunt system does not necessitate a limitation of sporting activity. The inclusion of patients in sports lessons and active participation in sports clubs should be encouraged.

References

1. Gruber R (1983) Zur Pathophysiologie des Slit Ventrikel Syndroms (SVS), seiner Therapie und Prophylaxe. In: Voth D (ed) Hydrocephalus im frühen Kindesalter. Enke, Stuttgart, pp 237-243
2. Gusmao S (1979) Etude experimentale de l'hydrodynamic des valves et son application clinic. Monographie de l'Université Louis. Pasteur, Strasbourgh
3. Hollmann W, Hettinger Th (1980) Sportmedizin - Arbeits- und Trainingsgrundlagen. Schattauer, New York
4. Mader A, Liesen H, Heck H, Phillippi H, Rost R, Schürch P, Hollmann W (1976) Zur Beurteilung der sportmedizinischen Ausdauerleistung im Labor. Sportarzt und Sportmedizin 4/80:5-109
5. Prokop L (1987) Kinder-Sportmedizin. Fischer, Stuttgart
6. Rost R, Hollmann W (1982) Belastungsuntersuchungen in der Praxis. Thieme, Stuttgart
7. Voth D (1982) Über die körperliche Belastbarkeit von Kindern mit einem Shunt-System zur Behandlung des Hydrozephalus internus. Sozialpädiatrie 4:315-320
8. Voth D, Haberstock K, Held J (1983) Therapieziel der Hydrozephalusbehandlung und Definition. Zeitwahl, Ergebnisse. In: Voth D (ed) Hydrozephalus im frühen Kindesalter. Enke, Stuttgart, pp 324-331

New Research

Biophysical Differences in Cells of Brain Tumors, Brain Edema, and Normal Glial Tissue

H. G. Kollmann, W. Heidegger, and H. E. Diemath

Neurochirurgische Abteilung der Landesnervenklinik, Ignaz-Harrer-Straße 79, A-5020 Salzburg

Basic Considerations

The most important problem in modern cell biology and cancer research is the explanation of irregular cell growth. In recent years scientific research has concentrated more on the biochemical processes in the cell nucleus than on phenomena in the cell membrane. However, studies have shown that there is an interaction between cell membrane and nucleus, in particular a flow of information from the membrane to the nucleus via the adenylcyclase/cAMP system (3). Therefore studies of biochemical and biophysical parameters in the cell membrane are becoming more important, in addition to morphological and serological diagnostic procedures.

The normal cell membrane is composed of phospholipids and globular proteins in a so-called fluid mosaic model (2, 5). The ratio is 100:1, in the molecular weight 1:1. Normally there is a difference in electrical potential between the intra- and extracellular compartments, the so-called transmembrane potential (TMP). Depending on the kind of cells, the TMP is between 10 and 100 mV. Measurements in vitro of cell cultures (FL cells, HeLa cells) have shown a TMP between 10 and 25 mV, while in cells of muscles and the nervous system the TMP is between 80 and 100 (or even 200) mV (4). If the specific morphological structure of the membrane and its ionic permeability are altered, by viral or chemical factor for example, the TMP will change; thus it is reduced under the influence of cytostatics such as amethopterin. It is well known, too (1), that the TMP depends on the state of the cell cycle. During mitosis the TMP is lower than in the state of synthesis G1 and G2. But it is not known whether increased mitosis induces a lower TMP or vice versa. Nevertheless, the TMP is a good and very sensitive indicator of alterations in structure or function, and changes in TMP occur quite a lot earlier than the morphological abnorlities can be seen.

Intracellular pH Measurements

While biophysical phenomena in the cell membrane, like TMP and surface potential (zeta potential), have been extensively studied, intracellular pH measurements with microelectrodes in brain tumor cells have not been performed until now. In our study we investigated 22 cases of brain tumors (14 gliomas, 5 meningiomas, and 3 brain metastases).

For the measurements we used as an electrochemical sensor, micro antimony pH electrodes and mini reference electrodes of the silver/silver chloride type; a high input impedance electrometer amplifier was

Advances in Neurosurgery, Vol. 16
Ed. by W. Walter, M. Brandt, M. Brock, and M. Klinger

used as the electrochemical analyzer. The measurements were carried out in cells of normal glial tissue, brain edema, tumor, and tumor surface. On average the pH was 7.05 (± 0.28) in the normal glial tissue, 7.10 (± 0.45) in brain edema, 7.01 (± 0.40) in the tumor center, and 6.96 (± 0.34) at the tumor surface.

Conclusion

The above measurements show that intracellular pH in brain tumors was lower (particularly at the surface) than in normal glial tissue and brain edema. This is in line with the TMP measurements. Further experimental studies will be necessary to establish the relation between these biophysical and biochemical phenomena and those of the morphological structure, protein synthesis, and cell cycle. Maybe in the future the reported procedures will be used not only as an indicator of cell alterations but also to initiate new steps in tumor research.

References

1. Cone CD (1969) Electroosmotic interactions accompanying mitotic initiation in sarcoma cells in vitro. Trans NY Acad Sci 31:404
2. Green DE (ed) (1972) Membrane structure and its biological applications. Ann NY Acad Sci 195
3. Hardeland R (1971) Das zyklische Adenosin-3',5'-monophosphat als regulatorische Mittlersubstanz. Naturwiss Rdsch 24:199
4. Redmann K (1971) Messungen elektrischer Membranpotentiale kultivierter Einzelzellen mittels Mikroelektroden. Acta Biol Med Germ 28:55-68
5. Singer SJ (1972) A fluid lipid-globular protein mosaic model of membrane structure. Ann NY Acad Sci 195:16-23

Prostaglandins $F_{2\alpha}$ and E_2 as Possible Mediators of Peritumoral Brain Edema

J. Anagnostopoulos-Schleep, W. Schlegel, K. H. Krähling, and H.-J. König

Neurochirurgische Klinik der Westfälischen Wilhelms-Universität, Albert-Schweitzer-Straße 33, D-4400 Münster

Introduction

Cerebral edema, a common secondary form of brain damage in patients with intracranial neoplasms, is a potential cause of morbidity and mortality. Despite the fact that our knowledge of its pathogenesis has advanced considerably, questions regarding the mechanisms of its formation, expansion, and maintenance remain unanswered.

Many etiological factors are involved in the evolution of perifocal edema. Recent studies have demonstrated a correlation between edema and damage to the blood-brain barrier (15), abnormalities in the tumor vessels (13), a pressure effect exerted on the surrounding tissues (8), cellular secretory activity (9), cerebral hypoxia (1), and tumor cellularity and vascularity (13). The size, histology, and location of the primary brain lesion do not always correlate with edematous expansion (6, 13). The possibility of a diffusible humoral factor, derived from alternated cerebral (1) or neoplastic cells, or taken up from extravasation through leaky tumor vessels (1), also appears promising.

Prostaglandins (PGs), important intermediates of the arachidonic acid cascade, are strong favorites as possible mediators of perifocal brain edema. Central nervous tissue has a complete system for their endogenous biosynthesis (14) and high prostaglandin $F_{2\alpha}$ ($PGF_{2\alpha}$) and prostaglandin E_2 (PGE_2) synthesis is known to be a feature of neoplastic cell growth (5). Both PGs are biologically active compounds, are potent constrictors of the cerebral vessels (10, 14), have been postulated to play an important role in the regulation of cerebral microcirculation (10, 14), are released by membrane disruption, and are involved in the development of ischemic edema (2, 4, 7).

In the present report tumor, edematous, and normal brain tissue from patients with cerebral neoplasms was examined for the presence of $PGF_{2\alpha}$ and PGE_2 to evaluate whether an overproduction of these substances might be associated with the pathogenetic mechanism underlying peritumoral edema.

Material and Methods

Twenty patients with primary brain tumors and metastases were selected initially for the present study. Factors such as sex, age, and tumor location were not used as selection criteria. The group with primary neoplasms included 15 patients (8 females, 7 males), with a mean age of 45 and a range of 23-66 years. Histological examination revealed

Advances in Neurosurgery, Vol. 16
Ed. by W. Walter, M. Brandt, M. Brock, and M. Klinger

five meningiomas, six astrocytomas graded I-II, two astrocytomas graded III-IV, one oligodendroglioma, and one ependymoma. The mean age of the group with metastases (1 female, 4 males) was 52 years with a range of 24-67 years. Two squamous cell carcinomas, one malignant melanoma, one adenocarcinoma, and one mesothelioma were diagnosed histologically. All subjects were free of medication or conditions known to affect PG biosynthesis for at least 1 week prior to surgery.

During surgery samples of tumor, edematous, and adjacent brain tissue (normal) were obtained. All tissues were removed as atraumatically as possible, collected in chilled glass tubes containing EDTA, and frozen to -40°C until analysis. Concentrations of PG were measured by the radioimmunoassay technique developed by SCHLEGEL et al. (12).

The volumes of the tumor and the perifocal edema were estimated on the preoperative CT scan. Tumor size was approximated by measuring the greatest diameter (d) of the enhanced mass in any tomographic section. The sizes were arbitrarily grouped into small (d<2 cm), medium (2 cm<d<5 cm), and large (5 cm<d). The expanse of perifocal brain edema was estimated according to the classification of Kazner et al. (6) as mild (degree I), moderate (II), or extensive (III).

The results were statistically analyzed after testing for normal distribution using the Wilcoxon matched-pairs rank test.

Results

Higher levels of PG were found in tumor and edematous tissue than in the corresponding adjacent brain samples. Table 1 summarizes our findings in a total of 52 samples examined for $PGF_{2\alpha}$ and PGE_2 content. In normal samples, $PGF_{2\alpha}$ concentrations averaged 0.18±0.01 ng/mg with a range of 0.01-0.48 ng/mg. PGE_2 levels averaged 0.22±0.07 ng/mg with a range of 0.02-1.17 ng/mg. No differences were found among various regions of the brain.

In edematous tissue mean concentrations of both PGs were similar. $PGF_{2\alpha}$ levels averaged 0.74 ng/mg (0.02-3.15 ng/mg) while those of PGE_2 averaged 0.74 ng/mg (0.04-2.60 ng/mg). In four cases (1, 8, 10, 12) with mild edema formation, the direction and removal of edematous tissue for analysis was not possible. The increases in PG concentrations compared with normal tissue were significant. These apparently higher levels did not correlate with the size of the primary brain lesion.

Tumor samples showed significantly higher levels of both PGs. $PGF_{2\alpha}$ concentrations averaged 2.32 ng/mg (0.01-16.68 ng/mg), while those of PGE_2 averaged 2.59 ng/mg (0.07-16.35 ng/mg). The amounts of PGE_2 extracted were slightly higher than those of $PGF_{2\alpha}$. As indicated in Table 1, no correlation was found between PG levels, tumor size, and degree of histological differentiation. The mean values of the group with primary brain neoplasm were 2.80 ng/mg (0.01-16.68 ng/mg) for $PGF_{2\alpha}$ and 2.76 ng/mg (0.07-16.35 ng/mg) for PGE_2. Those of the group with metastases were 0.87 ng/mg (0.30-1.25 ng/mg) for $PGF_{2\alpha}$ and 2.08 ng/mg (0.61-4.29 ng/mg) for PGE_2. The lower concentrations in the metastases were evaluated as statistically not significant.

Peritumoral brain edema was estimated as mild in 11 cases (55%), moderate in 6 (30%), and extensive in 3 (15%). In mild perifocal edema (degree I) tumorous $PGF_{2\alpha}$ concentrations averaged 1.87 ng/mg (0.01-16.68 ng/mg) and those of PGE_2 2.11 ng/mg (0.07-16.35 ng/mg). In edema samples $PGF_{2\alpha}$ showed a mean value of 0.23 ng/mg and PGE_2 0.35 ng/mg (0.04-0.84 ng/mg). In the group with moderate edema (degree II) $PGF_{2\alpha}$

Table 1. Prostaglandin concentrations in normal, edematous, and tumorous tissue removed at operation from 20 patients

Patient			Tumor characteristics				Normal		Edema		Tumor	
Case	Sex	Age	Size	Histology	Location	Edema	$PGF_{2\alpha}$	PGE_2	$PGF_{2\alpha}$	PGE_2	$PGF_{2\alpha}$	PGE_2
1	m	58	m	Olig	p	I	0.42	1.17	-	-	0.70	2.19
2	m	27	m	Astro I	t	I	0.48	0.16	0.83	0.84	16.68	16.35
3	m	34	l	Astro I	t	III	0.11	0.08	1.30	2.60	2.98	8.50
4	f	24	s	Melan M	o	II	0.24	0.15	0.76	0.82	1.25	2.51
5	m	57	m	Ad M	p	III	0.14	0.07	0.16	0.41	0.58	0.16
6	m	48	s	Astro III	f	II	0.08	0.09	0.22	0.27	0.44	1.32
7	f	61	l	Mening	t	I	0.01	0.05	0.02	0.04	0.01	0.07
8	f	45	m	Mening	t	I	0.16	0.09	-	-	0.50	0.56
9	f	66	m	Astro IV	o	III	0.20	0.12	3.15	2.09	8.10	7.11
10	m	25	l	Epend	p	I	0.16	0.46	-	-	0.31	0.51
11	f	23	m	Astro II	p	I	0.06	0.06	0.18	0.19	0.51	0.25
12	f	32	m	Mening	p	I	0.19	0.02	-	-	0.65	1.12
13	m	54	l	Astro II	t	I	0.10	0.23	0.13	0.48	0.30	0.82
14	f	55	m	Astro I	f	I	0.03	0.05	0.03	0.06	0.54	0.18
15	m	56	m	Sq M	f	II	0.45	0.30	0.98	1.02	1.23	2.12
16	m	67	m	Sq M	o	I	0.21	0.53	0.22	0.77	0.30	0.87
17	m	43	l	Astro II	o	I	0.08	0.06	0.25	0.09	0.17	0.35
18	m	56	m	Mesoth M	t	II	0.18	0.55	0.36	1.17	1.01	4.29
19	f	38	l	Mening	f	II	0.02	0.04	0.06	0.16	0.22	0.22
20	f	62	m	Mening	o	II	0.30	0.08	3.12	0.80	9.94	1.86
Mean values:							0.18	0.22	0.74	0.74	2.32	2.59

Abbreviations: *Sex:* f, female; m, male. *Size:* s, small (d<2 cm); m, medium (2 cm<d<5 cm); l, large (5 cm<d). *Histology:* Olig, oligodendroglioma; Astro, astrocytoma; Melan, melanoma; Ad, adenocarcinoma; Mening, meningioma; Epend, ependymoma; Sq, squamous cell carcinoma; Mesoth, mesothelioma; M, metastasis. *Location:* p, parietal; t, temporal; o, occipital; f, frontal. The expanse of brain edema is classified according to KAZNER et al. (6). Results of PG concentrations are given as ng/mg

levels in tumor tissue averaged 2.34 ng/mg (0.22-9.94 ng/mg) and PGE_2 levels 2.05 ng/mg (0.22-2.51 ng/mg). In edematous samples $PGF_{2\alpha}$ averaged 0.91 ng/mg (0.06-3.12 ng/mg) and PGE_2 0.70 ng/mg (0.16-1.17 ng/mg). Cases with extensive edema (degree III) almost always demonstrated markedly higher concentrations of prostaglandins in neoplastic and edematous tissue. The mean value of $PGF_{2\alpha}$ in tumor was 3.80 ng/mg (0.58-2.98 ng/mg) and that of PGE_2 5.4 ng/mg (0.61-8.50 ng/mg). In edema extracts $PGF_{2\alpha}$ concentrations averaged 1.53 ng/mg (0.16-3.15 ng/mg) and PGE_2 1.70 ng/mg (0.41-2.60 ng/mg). There was a significant correlation between edema expansion and prostaglandin concentrations in tumorous and edematous samples. Edema expansion did not correlate with the size and localization of the primary lesion.

Discussion

Brain tissue has a high lipid content, mainly phospholipids, as the major structural component of cellular membranes. It has been confirmed that ischemia and hypoxia stimulate decomposition of membrane-bound phospholipids and release arachidonic acid, the precursor of PGs. (11). Once biosynthesized, PGs produce an effect in situ and since brain has low activities of PG-metabolizing enzymes (14), they are primarily cleared into the general circulation through choroidal and extrachoroidal transport mechanisms (3). Under physiological, "basal" conditions the endogenous biosynthesis of PGs is exceedingly reduced (10, 14). In our series the PG levels in the control samples of adjacent brain were very low, though they did not demonstrate the real tissue content owing to the nonphysiological disruption of cellular barriers during dissection. Concentrations of PGE_2 were slightly higher than those of $PGF_{2\alpha}$ and no differences were found among various regions of the brain.

Our hypothesis is that excessive production and release of PGs by neoplastic cells alter the peritumoral environment, inducing microcirculatory disturbances (10, 14), decreasing cerebral blood flow (10), disrupting the blood-brain barrier, and revealing perifocal ischemia and edema (2, 4, 7). In addition, local hypoxia may enhance the PG synthesis rate of the surrounding cells (4) and maintain edema expansion (Fig. 1). The premise that PGs are exceedingly produced by tumor cells (5) has been strengthened by our observations. Primary and metastatic tumor samples have been shown to contain significantly increased levels of both PGs as compared with normal cerebral tissue. In agreement with previous reports (5), PGE_2 concentrations in neoplastic samples were higher than those of $PGF_{2\alpha}$. PG levels did not correlate with tumor size and degree of histological differentiation. Since slow-growing cells release more PG in vitro than do fast-growing cells (5), an explanation for missing histological correlation could be tumor inhomogeneity (variations in amount of necrosis or malignant differentiation) and the fact that samples for extraction and histological examination were different.

Our results indicate that expansion of peritumoral brain edema was associated with increased PG levels in neoplastic and edematous tissue (Fig. 2). The significant increase of PG concentrations in edematous samples may have been primarily mediated via the excessive production, release, and diffusion of PGs by the tumor mass. In vitro studies demonstrated that the majority of PG synthesized by cell cultures was secreted into the culture medium (5), as evidence of cells' incapability to store these substances (14). A secondary mechanism may be the enhancement of PG formation by the peritumoral neural cells, due to local hypoxia (2, 4, 7) induced by the vasoconstrictive effect of

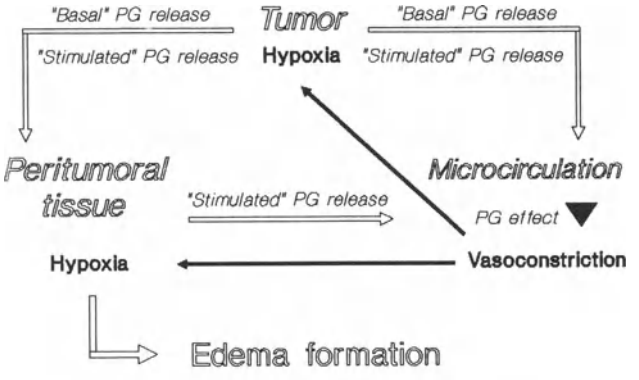

Fig. 1. Hypothesis: $PGF_{2\alpha}$ and PGE_2 involvement in the pathogenesis of peritumoral brain edema

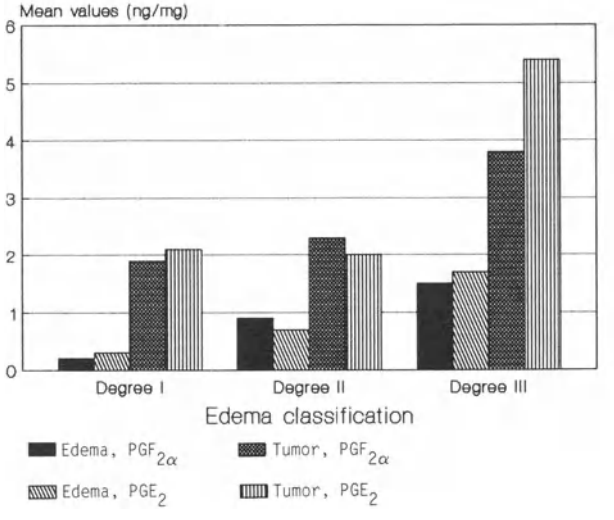

Fig. 2. Expansion of peritumoral brain edema in relation to PG levels in neoplastic and edematous tissue

PGs (10). Since brain has a reduced capability for local degrading of PGs (14), regional accumulation due to PG-mediated peritumoral microcirculatory disturbances (10, 14), and consequently decreased clearance and transport of material from the cerebral parenchyma to the draining vascular lumina (3), is also possible. In agreement with earlier reports (6), we found no dependence of edema extension on the size and localization of the primary brain lesion (Fig. 3).

Conclusions

Peritumoral brain edema is a multifactorial phenomenon. Prostaglandins $F_{2\alpha}$ and E_2 synthesized and released by neoplastic cells may, in addition to other previously reported factors, alter the local environment of a brain tumor. In our study, expansion of perifocal edema correlated with increased PG concentrations in neoplastic and edematous tissue and not with other characteristics of the primary brain lesion.

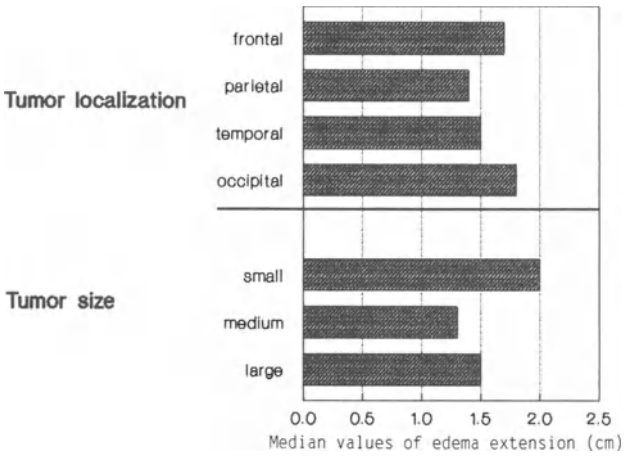

Fig. 3. Extension of perifocal edema in relation to the tumor localization and size

References

1. Baethmann A (1978) Pathophysiological and pathochemical aspects of cerebral edema. Neurosurg Rev 1:85-100
2. Bhakoo KK, Crockard HA, Lascelles PC, Avery SF (1984) Prostaglandin synthesis and oedema formation during reperfusion following experimental brain ischemia in the gerbil. Stroke 15:891-895
3. Bito LZ, Davson H, Hollingsworth JR (1976) Facilitated transport of prostaglandins across the blood-cerebrospinal fluid and blood-brain barriers. J Physiol 256:273-285
4. Iannotti F, Crockard A, Ladds G, Symon L (1981) Are prostaglandins involved in experimental ischemic edema in gerbils? Stroke 12:301-306
5. Jaffe BM (1974) Prostaglandins and cancer: an update. Prostaglandins 6:453-460
6. Kazner E, Lanksch W, Steinhoff H, Wilske J (1975) Die axiale Computer-Tomographie des Gehirnschädels - Anwendungsmöglichkeiten und klinische Ergebnisse. Fortschr Neurol Psychiatr 43:487-574
7. Koide T, Gotoh O, Asano T, Takakura K (1985) Alterations of the eicosanoid synthetic capacity of rat brain microvessels following ischemia: relevance to ischemic brain edema. J Neurochem 44:85-93
8. Kuhn C, Rosai J (1969) Tumors arising from pericytes. Arch Pathol Lab Med 88:653-663
9. Philippon J, Foncin JF, Grob R, Srour A, Poisson M, Pertuiset B (1984) Cerebral edema associated with meningiomas: possible role of a secretory-excretory phenomenon. Neurosurg 14:295-301
10. Pickard JD (1981) Role of prostaglandin and arachidonic acid derivatives in the coupling of cerebral blood flow to cerebral metabolism. J Cereb Blood Flow Metabol 1:361-384
11. Rehncrona S, Westerberg E, Akesson B, Siesjö BK (1982) Brain cortical fatty acids and phospholipids during and following complete and severe incomplete ischemia. J Neurochem 38:84-93

12. Schlegel W, Wenk K, Dollinger HC, Raptis S (1977) Concentrations of prostaglandin A-, E-, F-like substances in gastric mucosa of normal subjects and of patients with various gastric diseases. Clin Sci Molec Med 52:255-258

13. Smith HP, Challa VR, Moody DM, Kelly DL Jr (1981) Biological features of meningiomas that determine the production of cerebral edema. Neurosurg 8:428-433

14. Wolfe L (1982) Eicosanoids: prostaglandins, thromboxanes, leucotrienes, and other derivates of carbon-20 unsaturated fatty acids. J Neurochem 38:1-14

15. Yamada K, Ushio Y, Hayakawa T, Kato A, Yamada N, Mogami H (1982) Quantitative autoradiographic measurements of blood-brain barrier permeability in the rat glioma model. J Neurosurg 57:394-398

Interferon-Beta Therapy for Malignant Gliomas (Systemic and Intralesional Administration): First Results of an Ongoing Clinical Study

F. K. Albert, V. Tronnier, A. Hoch, P. Oldenkott, and E. Sigmund

Neurochirurgische Abteilung, Bundeswehrkrankenhaus, Oberer Eselsberg 40, D-7900 Ulm

Introduction

Although different modalities of brain tumor therapy have been introduced during recent years, the poor prognosis of malignant gliomas has not improved substantially. Controlled clinical trials have shown that the prolongation of median survival times achieved is only some months greater than with surgical treatment or steroid therapy alone (6, 17, 19). As well as grade III gliomas, gliobastomas continue to have a regularly fatal outcome.

Current investigations aiming to improve this unsatisfactory state of affairs include the use of "biological response modifiers." Interferon (IFN) is one of the best-known of these (1, 8, 13, 14). Up to now, by far the greatest experience with IFN therapy for high-grade gliomas has been reported from Japan, where both experimental and clinical trials have been performed to examine the properties of this therapeutic approach since 1979 (9, 11, 13, 15, 18). Fibroblast-derived interferon (IFN-ß) proved to be more effective than other types (2, 11). Administered intravenously, IFN-ß only reaches a minimal concentration within the CSF, owing to its high affinity to serum protein and its low capacity to pass through the blood-brain barrier (10, 13). Because of this, some Japanese authors have recommended local administration of the drug, e.g., intrathecally or intralesionally (10, 12). The rates of responders attained by local and systemic regimens (complete and partial response together) are reported by some Japanese authors to be from 25% (7, 9, 13) to 40% (11). Hitherto, there has been a deficit of experience in clinical centers outside Japan, with regard both to the number of patients and the reproducibility of these favorable results.

Materials and Methods

From March 1985 through March 1987, a total of eight patients were treated with human fibroblast interferon (HuIFN-ß) for malignant supratentorial gliomas in the Neurosurgical Department of the Federal Armed Forces Hospital, Ulm. This preliminary study was designed to assess the antitumor efficacy of IFN-ß, when applied in addition to surgery and radiotherapy. There were two grade III astrocytomas (WHO) and six glioblastomas, three of the latter representing recurrent growths. HuIFN-ß was administered intravenously in six patients, and intralesionally in four patients, using an Ommaya reservoir implanted into the cavity after tumor removal. The local therapy was given additionally to the i.v. route in two patients, and administered intralesionally alone in two other patients (for details, see Fig. 1).

 Advances in Neurosurgery, Vol. 16
Ed. by W. Walter, M. Brandt, M. Brock, and M. Klinger

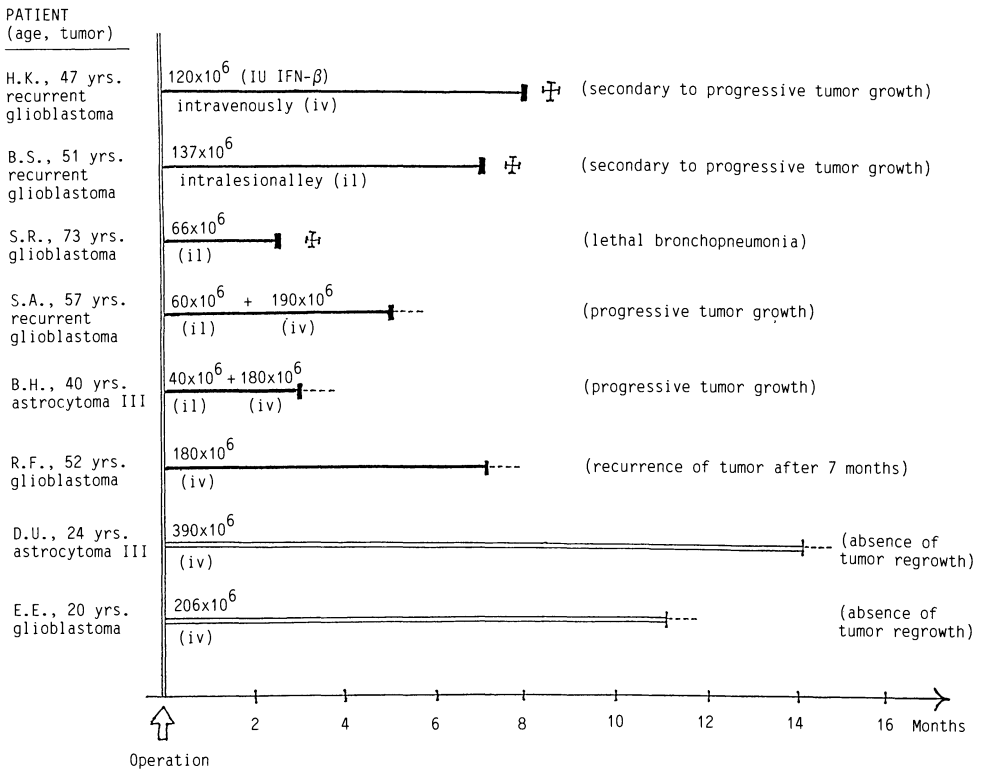

Fig. 1. Clinical courses in eight patients with high-grade gliomas who were treated with IFN-ß

The systemic (i.v.) therapy was routinely given three times a week, administering $5x10^6$ IU each time, over a period of 2-6 months. The intralesional administrations were performed with single doses of $1x10^6$ to $5x10^6$ IU given every day at first, and three times a week thereafter. The total doses administered intravenously were from $120x10^6$ to $390x10^6$ IU, and $137x10^6$ IU intralesionally.

The patients' courses were checked by routine examinations, including clinical findings, computed tomography, and assessment of the Karnofsky score. We also performed serial determinations of deoxythymidine kinase (dTK) activity of fluid samples derived from the tumor cavity, obtained by puncture of the Ommaya reservoir. DTK has been demonstrated to be a marker for the biological activity of neoplastic lesions and other disorders within the CNS (4, 5).

To determine an additional parameter of the antitumor activity of HuIFN-ß, we recently started investigations of the in vitro sensitivity of tumor tissue specimens obtained during surgery. This procedure is regarded as an important screening test in the evaluation of IFN therapy (9).

Results

Patients' Courses

Our study did not reveal any recognizable antitumor activity in five patients: in the meantime, two of them have died of recurrent glioblastomas, and progressive tumor growth is visible in the other three. As shown by serial CT examinations, the ongoing IFN therapy did not have any effect on the dynamics of tumor growth in these cases (for example, see Fig. 2). A 73-year-old patient died from intercurrent bronchopneumonia 10 weeks after surgery, obviously independent of the IFN therapy. Two patients, operated on for a glioblastoma and a grade III astrocytoma at the ages of 20 years and 24 years, respectively, with subsequent radiotherapy and systemic IFN treatment, were recently found to show no tumor relapse, as demonstrated by clinical examination and computed tomography (Fig. 3). In these cases, the recurrence-free periods are 11 months and 14 months, respectively. For a summary of our results, see Fig. 1.

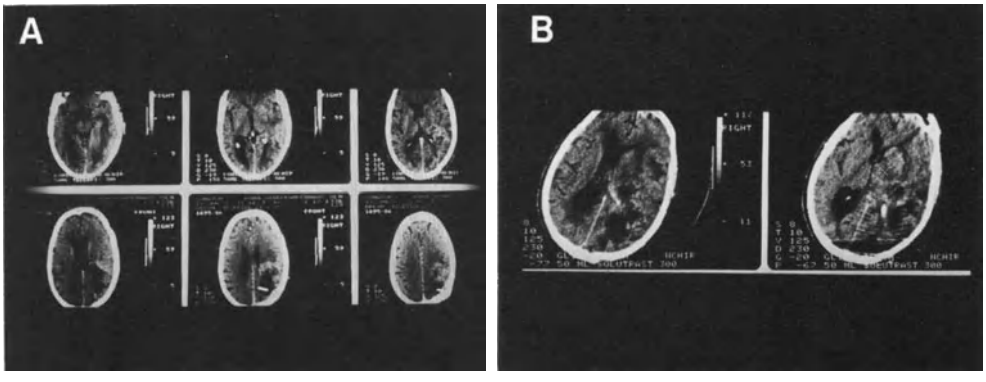

Fig.2A,B. Recurrent glioblastoma, unaffected by IFN therapy. A CT scan at the 9th week of intralesional IFN-ß administration. B Three months thereafter. (patient B.S.)

Side-effects

Serious leukopenia was observed in one patient undergoing intravenous IFN therapy, necessitating both a dose reduction and a shortening of the overall duration of therapy. Repeated epileptic seizures were observed in two patients with intralesional treatment, occurring immediately after IFN administration. In one case we were forced to replace this local therapy by an intravenous application. In another patient, the intralesional treatment gave rise to a bacterial infection of both the Ommaya reservoir and the intracerebral cavity. This bacterial infection was later controlled by local and systemic antibiotic therapy.

Additional difficulties resulted from the long-term therapy, IFN regularly being administered three times a week for several months. Usually, this not only imposed a heavy physical strain on the patient and required the family doctor's cooperation, but also caused problems concerning the readiness of the health insurance companies to pay the high costs.

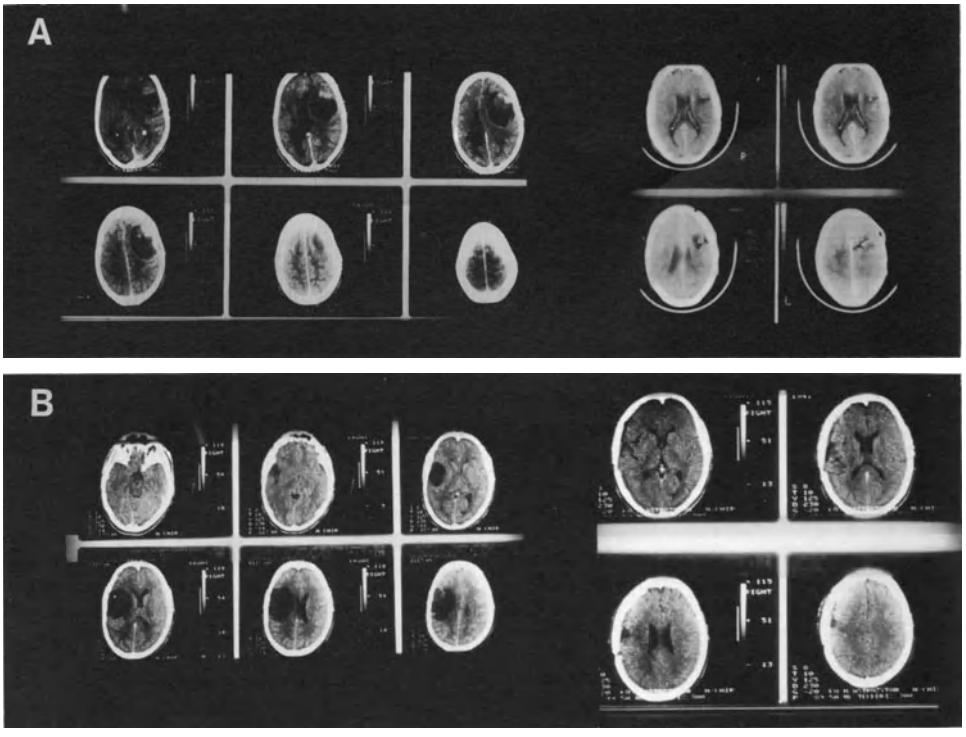

Fig. 3. CT scans in two patients with absence of tumor regrowth after A 11 months, and B 14 months. A Glioblastoma, preoperative scan (*upper left*) and 11 months after operation (*upper right*). B Grade III astrocytoma, preoperative scan (*lower left*) and 14 months after operation (*lower right*)

Deoxythymidine Kinase Activity

Serial dTK activities could be determined in two patients with progressive tumor growth despite IFN therapy (patients B.S. and B.H.), and for a period of 11 months in another patient revealing absence of relapse till now (E.E.). In the latter case (Fig. 4B), the activities clearly ranged below the values determined in the samples of the two other individuals (Fig. 4A). An interpretation of the absolute values given in Fig. 4 is not possible. Up to now, very little knowledge exists concerning this biological marker derived from brain tumor cavities. PERSSON et al. report an investigation comparable to our own, in which they determined dTK activities as a method for control of intralesional brain tumor therapy with BCNU (16). The practical application of this special investigation cannot be assessed definitely. It might be possible that an increase of dTK activity could be observed in cases of tumor regrowth. Some critical remarks will be given later.

In Vitro Study

Determination of the in vitro sensitivity of tumor tissue exposed to HuIFN-ß in cell culture has only recently been started. We therefore

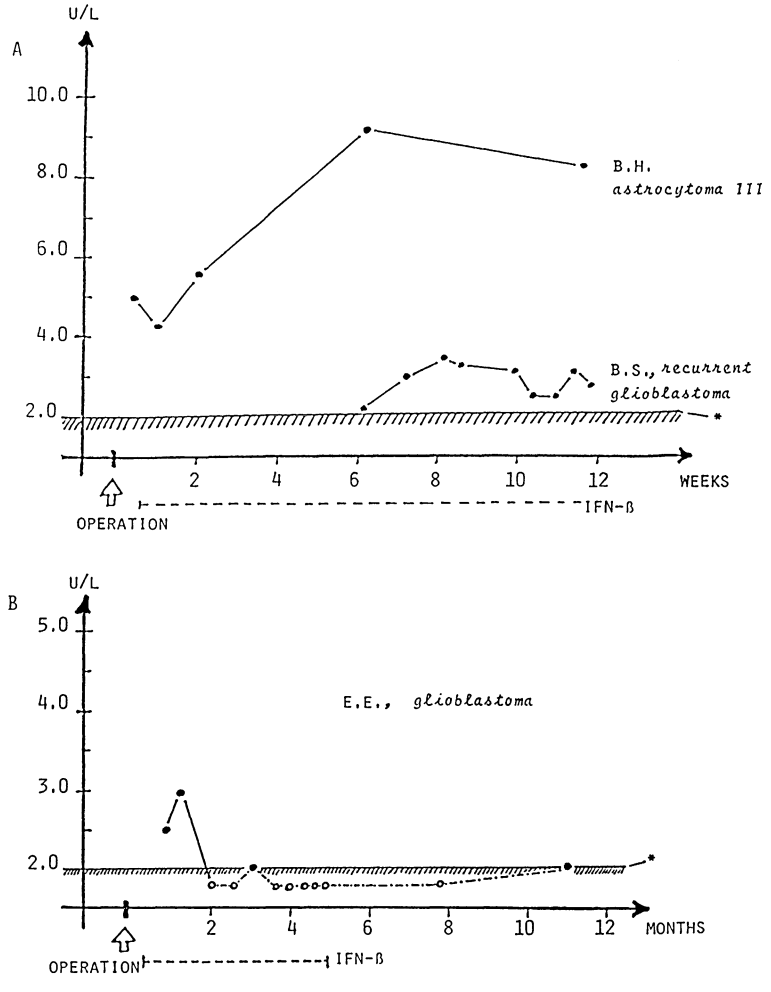

Fig. 4A,B. Thymidine kinase activity (determinations of samples derived from Ommaya reservoir). A Two cases of progressive tumor growth despite IFN therapy. B One case with absence of recurrent tumor through 11 months. *, lower limit of dTK detection

were able to have tumor specimens investigated from one patient only (S.A.). In this case, we could not observe any influence of IFN therapy on the patient's poor course, nor was there any recognizable antitumor activity of HuIFN-ß in the cell culture.

Conclusions

Both the number of our patients and the observation period are very limited. Our ongoing study is therefore not suitable for providing a reliable assessment of the antitumor efficacy of HuIFN-ß monotherapy for malignant gliomas. Our initial 2-year experience, however, does not justify great optimism and also does not seem to confirm the fa-

vorable rates of remission reported from Japan:

1. In five patients there was no recognizable influence of IFN therapy on the progressive tumor growth. Partly, this may be attributable to the recurrences representing one-half of our glioblastomas. DUFF et al. reported complete therapeutic failure, too, when applying IFN treatment to recurrent glioblastomas (3). In one patient who had died from intercurrent pneumonia, the observation period was too short for evaluation.
2. Both cases of young patients with absence of relapse after 11 months and 14 months, respectively, do not justify assessment either: recurrence-free intervals of more than 1 year are not unusual, particularly in young people, even under conventional treatment.
3. The usefulness of the intralesional administration has to be regarded critically because of the gradual development of a glial-mesenchymal membrane lining the walls of the cavity after tumor removal, presumably preventing IFN from penetrating into the adjacent area. The same presumably holds true for dTK, which is supposed to be kept back beyond this barrier.

In spite of this rather negative appraisal, we do not consider a complete rejection of IFN therapy for malignant gliomas to be warranted. The antitumor activity of IFN-ß may be greater when it is combined with cytostatic drugs, e.g., nitrosourea compounds. Additionally, more specific routes of administration should be investigated, particularly aimed at the variable pool of glioma cells revealing distinct degrees of differentiation and cell cycle behavior (e.g., carrier techniques; increase of the effective concentration of IFN within the tumor tissue and marginal areas, the latter representing the presumed site of origin of recurrent growth). Both controlled clinical studies and further basic research are necessary, also concerning the immunological mechanisms of IFN used therapeutically in gliomas.

Acknowledgment. We are indebted to Dr. D.H. Meier, Neurological Clinic, University of Tübingen, for performing the in vitro assay.

References

1. Boëthius J, Blomgren H, Collins VP, Greitz T, Strander H (1983) The effect of systemic human interferon-alpha administration to patients with glioblastoma multiforme. Acta Neurochir 68:239-251
2. Cook AW, Carter WA, Nidzgorski F, Akhtar L (1983) Human brain tumor-derived cell lines: growth rate reduced by human fibroblast interferon. Science 219:881-883
3. Duff TA, Borden E, Bay J, Piepmeier J, Sielaff K (1986) Phase II trial of interferon-ß for treatment of recurrent glioblastoma multiforme. J Neurosurg 64:408-413
4. Gronowitz JS, Källander CFR, Diderholm H, Hagberg H, Pettersson U (1984) Application of an in-vitro assay for serum thymidine kinase: results on viral disease and malignancies in humans. Int J Cancer 33:5-12
5. Gronowitz JS, Källander CFR, Hagberg H, Persson L (1984) Deoxythymidine-kinase in cerebrospinal fluid: a new potential "marker" for brain tumours. Acta Neurochir 73:1-12
6. Jellinger K, Kothbauer P, Vollmer R et al. (1979) Combination chemotherapy (COMP Protocol) and ratiotherapy of anaplastic supratentorial gliomas. Acta Neurochir 51:1ff

7. Koyama Y (1984) Pharmacokinetics and clinical trials of Hu-IFN-ß in malignant tumors. In: Kishida T (ed) Interferons. Kyoto, pp 1-7

8. Mahaley MS Jr, Gillespie GY (1984) Immunotherapy of patients with glioma: fact, fancy, and future. In: Rosenblum ML, Wilson CB (eds) Prog Exp Tumor Res, vol 28. Karger, Basel

9. Nagai M, Arai T, Kohno S, Kohase M (1982) Interferon therapy for malignant brain tumors. In: Kono R, Vilcek J (eds) The clinical potential of interferons. Treatment of viral diseases and malignant tumors. Jap Med Res Found, Publ No 15, Univ of Tokyo Press

10. Nagai M, Arai T (1983) Treatment of malignant brain tumors with interferon. In: Kishida T (ed) Interferons. Kyoto

11. Nagai M, Arai T (1984) Clinical effect of interferon in malignant brain tumours. Neurosurg Rev 7:55-64

12. Nakagawa Y, Hirakawa K, Ueda S, Suzuki K, Fukuma S, Kishida T (1983) Local administration of interferons for malignant brain tumors. Cancer Treat Rep 67:833-835

13. Nakamura O, Takakura K, Kobayashi S (1982) Effect of human interferon-ß in the treatment of malignant brain tumors (abstract). UCLA Symp Molec Cellul Biol XXV:465-477

14. Obbens E, Feun LG, Leavens ME, Savaraj N, Stewart DJ, Guttermann JU (1985) Phase I clinical trial of intralesional or intraventricular leukocyte interferon for intracranial malignancies. J Neuro-Oncol 3:61-67

15. Otsuka SH, Handa H, Yamashita J, Suda K, Takeuchi J (1984) Single agent therapy of interferon for brain tumours: correlation between natural killer activity and clinical course. Acta Neurochir 73:13-23

16. Persson L, Boëthius J, Gronowitz JS, Källander CFR, Lindgren L (1985) Thymidine kinase in brain-tumor cysts. J Neurosurg 63:568-572

17. Seiler RW (1982) Die undifferenzierten Astrozytome des Großhirn. Springer, Berlin Heidelberg New York

18. Ueda S, Hirakawa K, Suzuki K, Nakagawa Y, Ibayashi N, Kishida T (1982) Interferon therapy of brain tumor patients. Neurol Surg 10: 149-154

19. Walker MD, BTSG (1978) Evaluation of BCNU and/or radiotherapy in the treatment of anaplastic gliomas. J Neurosurg 49:333ff

Morphological Findings in Malignant Gliomas Before and After Interferon Therapy

G. Ebhardt and Th. Rommel

Pathologisches Institut, Sektion Neuropathologie, Krankenhaus Merheim, Ostmerheimer Straße 200, D-5000 Köln 91

Introduction

Interferons represent a group of proteins and glycoproteins present in the body which - due to their antigenic, biological, and chemical properties - are divided into subgroups: alpha-interferon (IFN-α), beta-interferon (IFN-β), and gamma-interferon (IFN-γ). The various types of interferon differ in their biological range of effects, but they all show antiviral, immunomodulating, and antiproliferative activities. With the two last properties mentioned, therapeutic possibilities for tumors have become apparent. Up to now a great many results for interferon drugs in the treatment of tumors have been described: they range from the disappearance of the tumor to lack of response. Japanese teams have reported on initial, good clinical experience with interferon therapy in the case of malignant gliomas (11). In this study (12) it was shown that with malignant gliomas, therapy involving IFN-β was superior to the other forms of interferon. In keeping with its strong linkage to serum protein, IFN-β cannot pass the intact blood-brain barrier easily, with the result that the concentration in the fluid is low if there is intravenous injection. The therapeutically effective minimum concentration of IFN-β that is known from in vitro experiments is not achieved through systemic application (12). For this reason an attempt was made to obtain an effective titer by means of local application, that is to say, by injecting the drug intrathecally or by putting it directly into the operating cavity (11).

Material and Method

Five patients with malignant gliomas or glioblastomas were treated with IFN-β. After the tumor had been extirpated, 500 000 IFN-β was put into the resection cavity and at the same time a Rickham reservoir was installed. The combined therapy began 1 week after the operation. Three times per week for 1 month 500 000 IU IFN-β was applied to the tumor cavity, each time through the Rickham reservoir. At the same time - but every other day for 3 months - 500 000 IU IFN-β was added systemically. In the case of two patients the tumor relapses were removed by means of an operation. All of the tumors were immersed in paraffin and investigated using conventional staining methods and immunohistochemical reactions, in order to produce macrophages (vimentine) and lymphocytes (LCA).

Results

The five patients involved were three men and two women aged between 48 and 82. The histological findings were: three glioblastomas - two

Advances in Neurosurgery, Vol. 16
Ed. by W. Walter, M. Brandt, M. Brock, and M. Klinger

small-celled tumors and one mix-celled tumor; one mixed glioma, grade III; and one mixed glioma, grade III/IV (Table 1). In two glioblastomas and in the mixed glioma, grade III/IV, the round-cell infiltration was at a very low level. One glioblastoma showed low-grade round cell infiltration and the mixed glioma, grade III, showed medium-grade round cell infiltration (Table 2). In the case of all the patients receiving interferon therapy, tumor relapses occurred within 1-6 months. In two patients (cases 2 and 3 in the tables) after 10 and after 3 months the tumor relapses were operated on. The morphological diagnoses had not increased in either case (Table 2). The formation of capsules around the tumors after interferon therapy could not be observed (Fig. 1). In the case of the 48-year-old woman (case 3), approximately 7 months after the first and 3 months after the second operation a relapse occurred once again which was not tackled with an operation. All of the patients died. The intervals between the first operation and the patients' death was between 3 and 14 months (Table 3).

Table 1. Clinical data and morphological diagnoses for the five patients before commencement of the interferon therapy

Case No.	Sex	Age (years)	Anamnesis, duration (weeks)	Localization	Histological diagnosis
1	m	66	Approx. 7	Right-hand side, temporoparietal	Small-celled glioblastoma
2	m	54	Approx. 2	Right-hand side, temporoparietal-occipital	Mix-celled glioblastoma
3	f	48	Approx. 4	Left-hand side, temporal	Mixed glioma, grade III; transition glioblastoma
4	f	73	Approx. 6 months	Right-hand side, temporo-occipital	Predominantly small-celled glioblastoma
5	m	82	10 months? or 4 weeks	Right-hand side, frontal	Mixed glioma, grade III

Discussion

With malignant gliomas interferon therapy is meant to have two mechanisms of action. On the one hand, an antiproliferative or antitumoral effect is meant to occur, and on the other hand interferon is meant to have not only stimulating but also inhibitory effects on immunological reactions, as follows from the extensive, predominantly Japanese studies. In fact, the effect of interferon on malignant glious brain tumors remains difficult to assess, since with the majority of these investigations a combined treatment involving an operation, radiation, and/or cytostatics was carried out using interferon (1, 4, 5, 8, 9). This study was carried out in order to test isolated dosing with interferon. The systemic and local application of interferon resulted in tumor relapses in the case of all five patients within 1-6 months of the therapy being started. All of the patients died within 3-4 months after the first operation. These survival times with malignant gliomas or glioblastomas can freely be compared with large statistics, in which individual glioblastoma patients survive even up to 5 years (21, 22). Even today the average life expectancy of glioblastoma pa-

Table 2. Extent of round cell infiltration in the five tumors before the interferon therapy and in the two tumor relapses after the interferon therapy

Case No.	1st histological diagnosis	Round cell infiltration	2nd histological diagnosis	Round cell infiltration
1	Small-celled glioblastoma	Very low grade		
2	Mix-celled glioblastoma	Low grade	Mix-celled glioblastoma	Quite sporadic, perivascular
3	Mixed glioma grade III/IV	Very low grade	Mixed glioma, grade III/IV	Very low grade
4	Predominantly small-celled glioblastoma	Very low grade		
5	Mixed glioma, grade III	Medium grade		

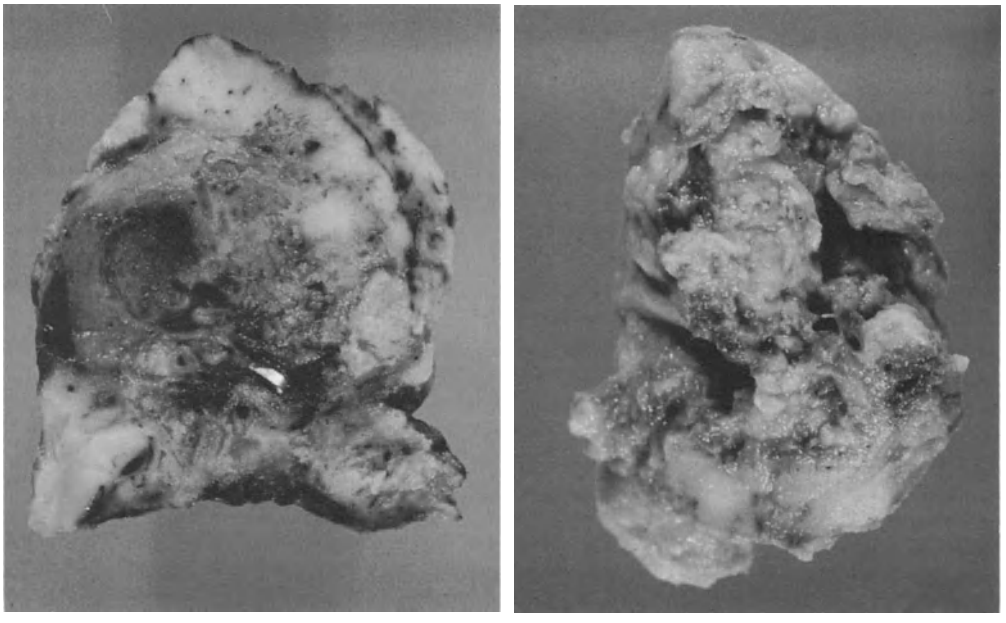

Fig. 1. Case No. 2, mix-celled glioblastoma. On the *left* is the surgical specimen obtained before the interferon therapy; on the *right* is the relapsed tumor after the interferon therapy

tients is still between 9 and 15 months. In vitro experiments have shown that interferon drugs inhibit the growth of glioma cells in naked mice (13, 19). Owing to his in vitro experiments, MEIER (10) pointed out that the dosage that would be necessary for an effective inhibition of growth in tumor cells in the brain was very high and, consequently, dangerous and not usable for human beings. Even with a combined therapy involving interferon and radiation after the opera-

Table 3. Occurrence of relapses in the malignant gliomas and glioblastomas after the interferon therapy. Interval between the 1st operation and the deaths of the five patients

Case No.	1st operation	1st relapse CT	2nd operation	2nd relapse CT	Death	Interval between 1st op. and death
1	22.01. 1985	18.03. 1985			May 1985	4 months
2	07.06. 1985	30.12. 1985	01.04.1986		Aug. 1986	14 months
3	08.07. 1985	02.08. 1985	09.10.1985	Jan. 1986	Sept.1986	14 months
4	14.04. 1986				July 1986	3 months
5	24.04. 1985	17.07. 1986			Sept.1986	4 months

tion, HEISS and RIOS-NOGALES (6) did not seen any improved results compared with the absence of additional interferon therapy, since the relapses occurred within a short space of time and the side-effects were serious. This means that the authors do not see any indication for applying interferon in the case of glioblastoma patients at the present time. There appears to be agreement that, with relapses of glioblastomas, interferon therapy does not produce any improvement in the medium survival time (1, 5).

The activation of macrophages and natural killer cells is meant to be one of the stimulating effects of interferon on the immune system. The cells in the central nervous system that have been made capable of phagocystosis develop in two ways. On the one hand, monocytes come with the flowing blood to the brain and wander through the walls of the blood vessels into the tissue. On the other hand, the adventitial cells of the blood vessels can become larger and also take over from one another. In the tissue both cell forms are converted into the mobile, so-called rod-shaped, microglia cells or macrophages. The proliferation of the vascular wall cells is a characteristic of the malignant gliomas and also of the glioblastomas, and they must be viewed more as reactive than as blastomatous (18).

As a result of the traumatic damage caused to the tissue during the operation, a stimulus for proliferating macrophages is already given; the same applies to postoperative radiation. When there was a comparison of the two tumors that could be examined before and after the interferon therapy, an increase in the rate of macrophages could not be proven. With the two relapses the immunostimulating effect of interferon could not be verified either. The morphological correlate of an immunological reaction in the brain would be an increase in the level of lymphocytes. The existence of these cells can be proven not only inside the tumor tissue but also in the tumor marginal zone right into the leptomeninges. What is particularly impressive is the lymphocytic infiltration in the marginal area of brain metastases. With respect to the strength and frequency of the infiltrate, the details in the literature vary. While BÖKER and his staff (2, 3) are of the opinion that glioblastomas have a lower level of lymphocytes than malignant gliomas and better differentiated gliomas, REINCKE (15) found that

gliomas with increased malignancy have a higher level of round cells. The mixed gliomas, grade III, show the highest rate. In the case of the glioblastomas, SIEBER (17) found round cell infiltration in 78% of 396 cases; this is distinctly higher than was observed by BÖKER (2), PALMA et al. (14), and RIDLEY and CAVANAGH (16). The polymorphic-celled glioblastomas had the highest strength of infiltrate. The fact that in none of our cases was there a polymorphic-celled glioblastoma would thus be an explanation for our findings of only low-grade infiltrations before therapy, except for the mixed glioma, grade III, where there was medium-grade infiltration. Up to the present day, the significance of the immunological position of defence in patients with malignant gliomas has not been definitely resolved. A possible connection between the frequency and strength of the lymphocyte content inside and around the tumor tissue in the brain and the length of survival is controversial (7).

Conclusions

In the five patients who were treated for morphologically protected, malignant gliomas or glioblastomas only with IFN-β that was applied locally for over 1 month and systemically for over 3 months, antitumoral and/or immunostimulating effects could not be proven. The relapses occurred between periods of 1 month and 6 months. The patients died between 3 and 14 months later. The findings expected morphologically, such as the formation of capsules around the tumors and increased content of macrophages and lymphocytes, could not be confirmed in the two tumors which could be examined after therapy. (A dissection was not carried out in any case.) The number of cases is only small, but the bad results did not make it appear justified to continue the isolated interferon therapy. Further examinations with a combination of interferon, radiation, and chemotherapy should clear up the question as to whether in this way better results can be obtained regarding the survival time and the quality of life of glioblastoma patients.

References

1. Alber FK (to be published) Erste Erfahrungen mit β-Interferon bei malignen Gliomen (systemische und intraläsionale Applikation)
2. Böker D-K (1982) Lymphocytic infiltration in human intracranial tumors - morphologic evidence for a host-immune reaction and comparison with the leukocyte migration inhibition (LMI test). Clin Neuropathol 1:113-120
3. Böker D-K, Kalff R, Gullotta F, Weekes-Seifert S, Möhrer U (1984) Mononuclear infiltrates in human intracranial tumors as a prognostic factor. Influence of preoperative steroid treatment I. Glioblastoma. Clin Neuropathol 3:143-147
4. Boëthius J, Blomgren H, Collins VP, Greitz T, Strander H (1983) The effect of systemic human interferon-alpha administration of patients with glioblastoma multiforme. Acta Neurochirurgica 68: 239-251
5. Duff TA, Borden E, Bay J, Piepmeier J, Sielaff K (1986) Phase II trial of interferon-β for treatment of recurrent glioblastoma multiforme. J Neurosurg 64:408-413
6. Heiß E Rios-Nogales L (1987) Interferon bei Glioblastomen? In: Symposium: Therapie primärer Hirntumoren. Essen, 26.-28.3., p 48

7. Jellinger K (1987) Pathology of human intracranial neoplasia. In: Jellinger K (ed) Therapy of malignant brain tumors. Springer, Wien New York, pp 1-90

8. Mahaley Jr. MS, Urso M, Whaley RA, Williams TE, Guaspari A (1984) Interferon as adjuvant therapy with initial radiotherapy of patients with anaplastic gliomas. J Neurosurg 61:1069-1071

9. Mahaley Jr. MS (1985) Treatment of recurrent gliomas with interferon. In: Kirchner H, Schellekens H (eds) The biology of the interferon system. Elsevier, pp 529-533

10. Meier DH (1987) In-vitro sensitivity of primary brain tumors to interferon alpha, beta and gamma. In: Symposium: Therapie primärer Hirntumouren, Essen 26.-28.3., p 15

11. Nagai M, Arai T, Kohno S, Kohase M (1982) Interferon therapy for malignant brain tumors. In: Kono R, Vilcek J (eds) The clinical potential of interferons. University of Tokyo Press, Tokyo, pp 257-273

12. Nagai M, Arai T (1984) Treatment of malignant brain tumors with interferon. In: Kishida T (ed) Interferons. Jpn Convention Services, Osaka, pp 208-216

13. Otsuka S Handa H, Yamashita J, Suda K, Takeuchi J (1984) Single agent therapy of interferon for brain tumours: correlation between natural killer activity and clinical course. Acta Neurochirurgica 73:13-23

14. Palma L, Di Lorenzo N, Guidetti B (1978) Lymphocytic infiltrates in primary glioblastomas and recidivous gliomas. J Neurosurg 49: 854-861

15. Reincke M (1986) Die lymphozytäre Infiltration von astrocytären Tumoren, Oligodendrogliomen und oligo-astrocytären Mischgliomen. Inaugural-Dissertation, Universität Köln

16. Ridley A, Cavanagh JB (1971) Lymphocytic infiltration in glioma: evidence of possible host resistance. Brain 94:117-124

17. Sieber B (1985) Lymphocytäre Infiltrationen im Glioblastom. Inaugural-Dissertation, Universität Köln

18. Stoltenburg-Didinger G, Cervós-Navarro J (1976) Ultrastruktur der Gefäße im Glioblastom. Deutsche Gesellschaft für Neuropathologie und Neuroanatomie, Jahrestagung, 8.-11.10., Berlin, p 44

19. Tanaka N, Nagao S, Tohgo A, Sekiguchi F, Kohno M, Ogawa H, Matsui T, Matsutani M (1983) Effects of human fibroblastic interferon on human gliomas transplanted into nude mice. Gann 74:308-316

20. Ueda S, Hirakawa K, Nakagawa Y, Suzuki K, Kishida T (1983) Brain tumors. In: Sikora K (ed) Interferon and cancer. New York, pp 129-139

21. Wüllenweber R, Kuhlendahl H, Miltz H (1973) Astrocytomas of the cerebral hemisperes. A review on 1500 cases. Proc German Society Neurosurg 3:100-107

22. Wüllenweber R, Kuhlendahl H, Miltz H, Grunert V, Sunder-Plassmann M (1973) Astrocytomas and glioblastomas: a comparative review of 2500 cases. Excerpta Medica 293:36-37

Electroretinographic Recordings After Intra-arterial Infusion of the Rabbit's Retina with 1,3-bis(2-chloroethyl)-1-nitrosurea (BCNU) Suggesting Retinal Toxicity of BCNU

N. Roosen, S. Schreiner, U. Weber, H. Baseler, M. Schirmer, and W. J. Bock

Neurochirurgische Universitätsklinik, Moorenstraße 5, D-4000 Düsseldorf 1

Introduction

The current therapeutic management of patients harboring malignant gliomas comprises surgery, radiotherapy, and chemotherapy (28). The results with adjuvant chemotherapy using intravenous BCNU, as reported by WALKER et al. in 1978 (29), have demonstrated a small but significant advantage in comparison with conventional surgery followed by radiation therapy. Since severe toxicity, particularly hematologic toxicity, is the dose-limiting factor in BCNU chemotherapy (27), the intra-arterial [i.a.] route of administration has been preferred by several investigators to achieve a higher tumoricidal effect without additional systemic complications (6, 7, 10, 13, 26, 30). Accumulating experience with this approach revealed a rather high incidence of local adverse effects such as leukencephalopathy (10-12, 14, 17) and ophthalmological complications (8, 10-12, 16, 18, 25, 31). The pathophysiology of the retinal effects of BCNU has been studied only occasionally (4, 5). A useful tool to study alteration of retinal function is electroretinography [ERG] (1). We used this technique to investigate subacute and chronic toxicity of the rabbit's retina after i.a. BCNU. Preliminary results of these studies have been presented (23) and in the present paper further details are provided.

Methods

Sixteen adult Bastard Chinchilla rabbits of either sex, each weighing between 3.0 and 3.5 kg, were studied. The ERG was recorded during anesthesia with Ketanes/Rompun[1], and Hypnorm/Valium[1] was used for surgery.

Short (10-μs) white xenon flashes illuminating a central field of 35°, with a frequency of 30 flashes/min and a variable flash intensity (I to V on the scale of the Knott Light Stimulator LT 1001), were used to elicit the ERG. Henkes' corneal electrodes were used. Both photopic (room lights, ±450 cd/m^2) and scotopic (after 3, 10, and 15 min of dark adaptation) ERG recordings were obtained. The mean and the standard deviation of the mean of the various components in preinfusion ERGs were determined in each study group. Thereafter sequential postinfusion ERGs were registered on postinfusion days 1, 2, 7, 18, 28 and 60. The standard amplitude at the lowest flash intensity [SA], the maximal amplitude of the a- and b-waves [A(a_{max}) and A(b_{max})], the a- and b-wave latencies [L(a_{max}) and L(b_{max})], and the b- to a-wave ratio [b_{max}/a_{max} ratio] were calculated.

[1] 15 mg/kg Ketanest (ketamine); 6 mg/kg Rompun (xylazine); 0.5 ml/kg Hypnorm (100 mg fluanisone and 2 mg fetanyl/10 ml); 1.5 mg/kg Valium (diazepam)

Advances in Neurosurgery, Vol. 16
Ed. by W. Walter, M. Brandt, M. Brock, and M. Klinger

For i.a. BCNU infusion the left external carotid artery was catheterized using microsurgical techniques. The retina receives its major blood supply from the external carotid artery by way of the internal maxillary and external ophthalmic arteries (22), which can be demonstrated by angiography (23). We infused 10 ml of several solutions [either 5% glucose in H_2O (5% glucose), 0.3% ethanol in 5% glucose in H_2O (0.3% ethanol), or 100 mg/200 mg BCNU in 0.3% ethanol in 5% glucose in H_2O (100 mg BCNU/200 mg BCNU)]. At the end of the infusion, the arteriotomy was sutured so as to ensure patency of the vessel. Then, the wound was closed.

Results

SA. 100 mg and 200 mg BCNU caused a slight decrease of photopic and scotopic SA.

A(a_{max}) (Fig. 1). 5% glucose was followed by hypernormal a-waves. A discrete and transient increase of photopic A(a_{max}) was seen on days 7, 18, and 28 after 0.3% ethanol. Small but definite changes in photopic and scotopic A(a_{max}) were noted following infusion of 100 mg BCNU: there was an increase in amplitude after 28 and 60 days. At the higher dose of 200 mg BCNU there seemed to be a reduction of A(a_{max}) towards subnormal values, especially in the photopic recordings.

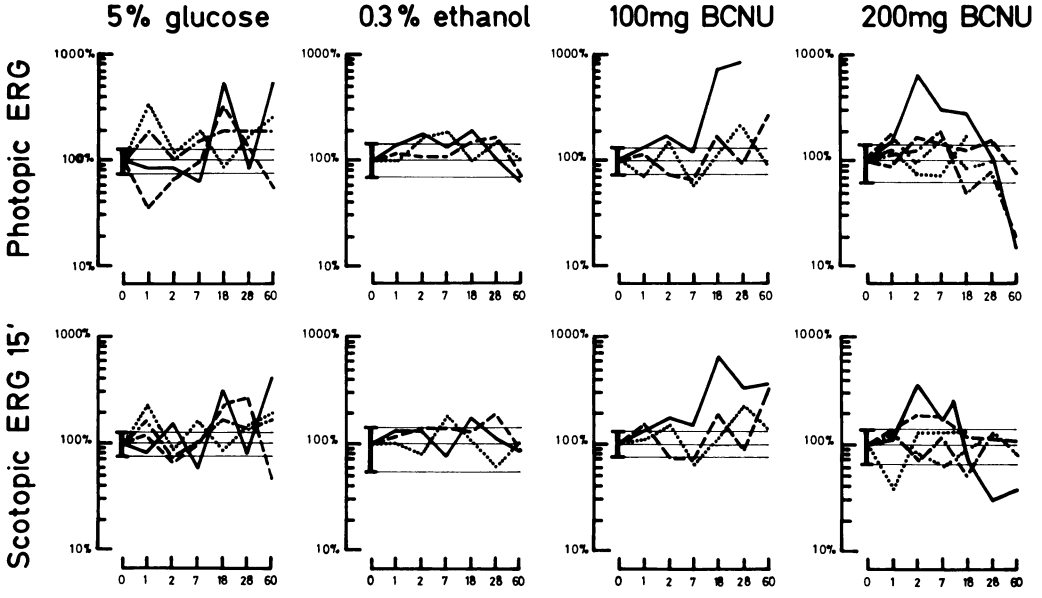

Fig. 1. The maximal amplitude of the a-wave of the photopic and the 15-min scotopic ERG is depicted after infusion of 5% glucose, 0.3% ethanol, 100 mg BCNU, and 200 mg BCNU. Further details: see text

A(b_{max}). A parallelism between A(b_{max}) and A(a_{max}) recordings could be noted.

[b_{max}/a_{max}] *ratio* (Fig. 2). The mean values did not differ significantly from 1.0, which demonstrates the similarities between A(b_{max}) and A (a_{max}).

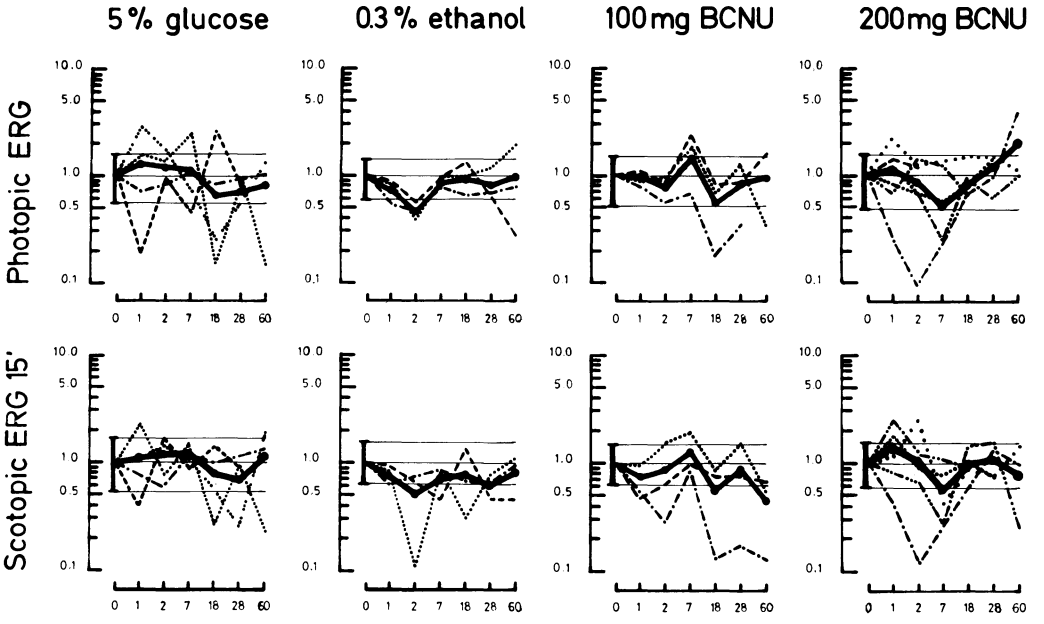

Fig. 2. After infusion of several solutions (5% glucose, 0.3% ethanol, 100 mg BCNU, and 200 mg BCNU) there is no significant change in b_{max}/a_{max} ratio

L (a_{max}) and L(b_{max}) (Fig. 3). There was a slight increase in scotopic L(a_{max}) after 200 mg BCNU. Scotopic L(b_{max}), however, was clearly increased following 200 mg BCNU.

Discussion

The a-wave of the ERG is generated by the photoreceptors of the retina (9, 20), whereas the inner nuclear layer (2, 3, 9) with its MÜLLER (glial) (15, 19) and amacrine cells (21) causes the b-wave. The ganglion cells do not have an effect on the signals obtained in flash ERG (9).

The slight changes in A(a_{max}) and L(a_{max}) suggest a possible dose-dependent, toxic effect of BCNU upon the photoreceptors. The infusion of 0.3% ethanol did not cause an appreciable alteration of the electrophysiologic function of the retinal receptors. As evidenced by the b_{max}/a_{max} ratio, there was no clear selective vulnerability of the inner as compared to the outer retinal layers. However, scotopic L(a_{max}) and in particular L(b_{max}) were increased 28-60 days after 200 mg BCNU, suggesting a definite retinotoxicity with some preference for the inner retinal layers.

Vascular lesions of the retina cause changes of the b-wave (1, 24). Therefore, our findings could be interpreted as resulting from retinal ischemia. An ischemic retinopathy is suggested by several clinical and experimental findings too (5, 8, 11, 18, 25). However, ERG in i.a. BCNU-related amaurosis did not show a-waves nor b-waves, probably because the retinopathy was much too advanced in these patients (25).

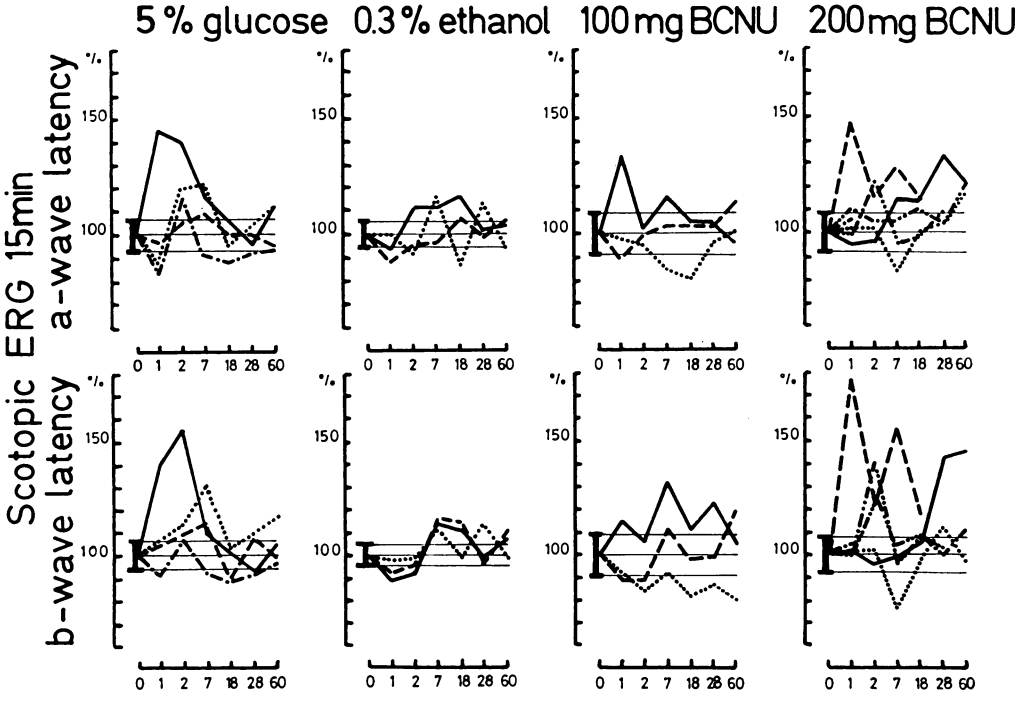

Fig. 3. Infusion of 200 mg BCNU causes an increase in L(b_{max}) and a slight increase in L(a_{max}), both in the 15-min scotopic ERG

Conclusions

Our study did not show frank ERG abnormalities due to i.a. BCNU. We did find, however, some evidence of b-wave alterations, which are suggestive of inner nuclear layer dysfunction as seen in ischemic retinopathy. We hope that further studies, especially electrophysiologic-histopathologic correlations, will further elucidate the pathogenesis and pathophysiology of i.a. BCNU-related retinopathy.

References

1. Babel J, Stangos N, Korol S, Spiritus M (1977) Ocular electrophysiology - a clinical and experimental study of electroretinogram, electrooculogram, visual evoked response. Thieme, Stuttgart
2. Brown KT (1968) The electroretinogram: its components and their origin. Vision Res 8:633-677
3. Brown KT, Wiesel TN (1961) Localisation of origins of the electroretinogram components by intraretinal recording in the intact cat eye. J Physiol 158:257-280
4. Crafts DC, Levin VA, Nielsen S (1976) Intracarotid BCNU (NSC-409962): a toxicity study in six rhesus monkeys. Cancer Treat Rep 60:541-545
5. De Wys WD, Fowler EH (1973) Reports of vasculitis and blindness after intracarotid injection of 1,3-bis(2-chloroethyl)-1-nitrosurea (BCNU; NSC-409962) in dogs. Cancer Treat Rep 57:33-40

6. Feun LG, Wallace S, Young WKA, Lee YY, Leavens ME, Moser R, Svaraj N, Burgess MA, Plager C, Benjamin RS, Tang RA, Mavligit GM, Fields WS (1984) Phase-I trial of intracarotid BCNU and cisplatin in patients with malignant intracerebral tumors. Cancer Drug Delivery 1:239-245

7. Foo SH, Choi IS, Berenstein A, Wise A, Ransohoff J, Koslow M, George A, Lin J, Feigin I, Budzilovich G, Kupersmith M, Hanson R, Lequerica S, Aleksic S, Kricheff I (1986) Supraophthalmic intracarotid infusion of BCNU for malignant glioma. Neurology 36:1437-1444

8. Gebarski SS, Greenberg HS, Gabrielsen TO, Vine AK (1984) Orbital angiographic changes after intracarotid BCNU chemotherapy. AJNR 5:55-58

9. Granit R (1947) Sensory mechanisms of the retina. Oxford University Press, London

10. Greenberg HS, Ensminger WD, Chandler WF, Layton PB, Junck L, Knake J, Vine AK (1984) Intra-arterial BCNU chemotherapy for treatment of malignant gliomas of the central nervous system. J Neurosurg 61:423-429

11. Grimson BS, Mahaley MS Jr, Dubey HD, Dudka L (1981) Ophthalmic and central nervous system complications following intracarotid BCNU (carmustine). J Clin Neuro-Ophthalmol 1:261-264

12. Kapp J, Vance R, Parker JL, Smith RR (1982) Limitations of high dose intra-arterial 1,3-bis(2-chloroethyl)-1-nitrosurea (BCNU) chemotherapy for malignant gliomas. Neurosurgery 10:715-719

13. Kapp JP, Vance RB (1985) Supraophthalmic carotid infusion for recurrent glioma: rationale, technique, and preliminary results for cisplatin and BCNU. J Neuro-Oncol 3:5-11

14. Kleinschmidt-DeMasters BK (1986) Intracarotid BCNU leukencephalopathy. Cancer 57:1276-1280

15. Kline RP, Ripps H, Dowling JE (1978) Generation of b-wave currents in the skate retina. Proc Natl Acad Sci USA 75:5727-5731

16. Madajewicz S, West CR, Park HC, Ghoorah J, Avellanosa AM, Takita H, Karakousis C, Vincent R, Caracandas J, Jennings E: Phase II study - intra-arterial BCNU therapy for metastatic brain tumors. Cancer 47:653-657

17. Mahaley MS jr, Whaley RA, Blue M, Bertsch L (1986) Central neurotoxicity following intracarotid BCNU chemotherapy for malignant gliomas. J Neuro-Oncol 3:297-314

18. Miller DF, Bay JW, Lederman RJ, Purvis JD, Rogers LR, Tomsak RL (1985) Ocular and orbital toxicity following intracarotid injection of BCNU (carmustine) and cisplatinum for malignant gliomas. Ophthalmology 92:402-406

19. Miller RF, Dowling JE (1970) Intracellular responses of the Müller (glial) cells of mudpuppy retina: their relation to b-wave of the electroretinogram. J Neurophysiol 33:323-341

20. Murakami M, Kaneko A (1966) Subcomponents of P III in cold-blooded vertebrate retina. Nature 210:103-104

21. Nakatsuka K, Hamasaki DI (1985) Destruction of the indoleamine-accumulating amacrine cells alters the ERG of rabbits. Invest Ophthalmol Vis Sci 26:1109-1116

22. Prince JH (1964) The rabbit in eye research. Thomas, Springfield

23. Roosen N, Schreiner S, Schirmer M, Weber U (in press) Effects of intra-arterially administered 1,3-bis(2-chloroethyl)-1-nitrosurea (BCNU) on the electroretinogram of the rabbit. A study on the retinal toxicity of BCNU. In: Brain oncology - biology, diagnosis and therapy. Proceedings of the International Meeting on Brain Oncology, Rennes, September 4th & 5th, 1986. Nijhoff, Boston

24. Sabates R, Hirose T, McMeel JW (1983) Electroretinography in the prognosis and classification of central retinal vein occlusion. Arch Ophthalmol 101:232-235

25. Shingleton BJ, Bienfang DC, Albert DM, Ensminger WD, Chandler WF, Greenberg HS (1982) Ocular toxicity associated with high-dose carmustine. Arch Ophthalmol 100:1766-1772

26. Stewart DJ, Grahovac Z, Benoit B, Addison D, Richard MT, Dennery J, Hugenholtz H, Russell N, Peterson E, Maroun JA, Vandenberg T, Hopkins HS (1984) Intracarotid chemotherapy with a combination of 1,3-bis(2-chloroethyl)-1-nitrosurea (BCNU), cis-diaminedichloroplatinum (cisplatin), and 4'-O-demethyl-1-O-(4,6-O-2-thenylidene-β-D-glucopyranosyl)epipodophyllotoxin (VM-26) in the treatment of primary and metastatic brain tumors. Neurosurgery 15:828-832

27. Takvorian T, Hochberg F, Canellos G, Parker L, Zervas N, Frei E (1981) The toxicity of high-dose BCNU with autologous marrow support. In: Prestayko AW, Baker LH, Crooke ST, Carter SK, Schein PS (eds) Nitrosureas. Current status and new developments. Academic Press, New York, pp 155-169

28. Vick NA, Wilson CB (1985) Total care of the patient with a brain tumor. Neurol Clin 3:705-710

29. Walker MD, Alexander E jr, Hunt WE, MacCarty CS, Mahaley MS jr, Mealey J jr, Norrell HA, Owens G, Ransohoff J, Wilson CB, Gehan EH, Strike TA (1978) Evaluation of BCNU and/or radiotherapy in the treatment of anaplastic gliomas. A cooperative clinical trial. J Neurosurg 49:333-349

30. West CR, Avellanosa AM, Barua NR, Patel A, Hong CI (1983) Intra-arterial 1,3-bis(2-chloroethyl)-1-nitrosurea (BCNU) and systemic chemotherapy for malignant gliomas: a follow-up study. Neurosurgery 13:420-426

31. Yamada K, Bremer AM, West CR, Ghoorah J, Park HC, Takita H (1979) Intra-arterial BCNU therapy in the treatment of metastatic brain tumor from lung carcinoma. Cancer 44:2000-2007

Problems of Fibrin Adhesion to Nerves

Th. Herter, W. Walter, M. Brandt, and U. Szuwart

Neurochirurgische Klinik der Westfälischen Wilhelms-Universität, Albert-Schweitzer-Straße 33, D-4400 Münster

Although fibrin adhesion is very successfully employed in many surgical areas and especially in neurosurgery, there are still considerable problems in using it as a nerve adhesive. Special advantages were expected of this field of application in particular, namely, simplification of the operative technique but also avoidance of inconvenient suture granuloma. Hence, it is frequently employed even to date, all the more so as no comparative study has unequivocally verified the inferiority of nerve anastomosis with fibrin adhesive in relation to suture technique.

In analyzing the problems with nerve adhesion one must take at least three time periods into account:

1. The immediate maximum strain
2. The maximum strain in the following period up to recovery
3. The late result

The problems of immediate maximum stress were compiled by MATRAS et al. (8).

The maximum strain in the following period was investigated by DUSPIVA (4), whose nerve anastomosis achieved with adhesive exhibited a marked fall-off in stability after 24 h. With the help of fibrinolysis inhibitors he was able to suppress this reaction to a large extent. This was confirmed in clinical trials by KUDERNA (7). However, very poor late results then occurred through fibrosis, which, of course, represents a serious complication in nerve surgery. On the one hand the structure and composition of the nerve encourages such a reaction; on the other, good functional regeneration is dependent on the intactness of the relatively fine structures and is therefore very prone to interference. We have therefore attempted, in an extensive study, to discover the factors that considerably affect the success of fibrin adhesion.

We examined five factors for their influence on fibrosis:
1. Thrombin
2. Factor XIII
3. Cold inhibited globulin (CIG) = fibronectin
4. Aprotinin
5. The influence of ischemia caused by the adhesive cuff

Material and Method

The investigations were carried out on Wistar rats. The sciatic nerve was isolated bilaterally, whereby one side was used as a transplant

Advances in Neurosurgery, Vol. 16
Ed. by W. Walter, M. Brandt, M. Brock, and M. Klinger

for the other. The evaluation was done histologically by means of Goldner sections, histometrically using a projection technique, and electrophysiologically by means of computed measurement of the integral of the area of maximal motor cumulative action potential. By means of intensive preliminary experiments a collateral innervation was eliminated, MATRAS et al. having failed on this previously. The results were statistically substantiated using the Wilcoxon, Mann, Whitney U-test.

Results

It appeared (see Fig. 1) that certain concentrations of thrombin, factor XIII, and CIG have a fibrosis-promoting effect, whereas with aprotinin and the fibrin adhesive cuff no additional fibrosis was observed. The examination of the CIG also led to a comparison of both the fibrin adhesives at present available. It was shown that one fibrin adhesive also containing CIG with an aprotinin concentration of 100 KIU is unequivocally inferior to the other, not only in relation to the collagen content but also electrophysiologically. On using the normal aprotinin concentration there were no statistically significant differences.

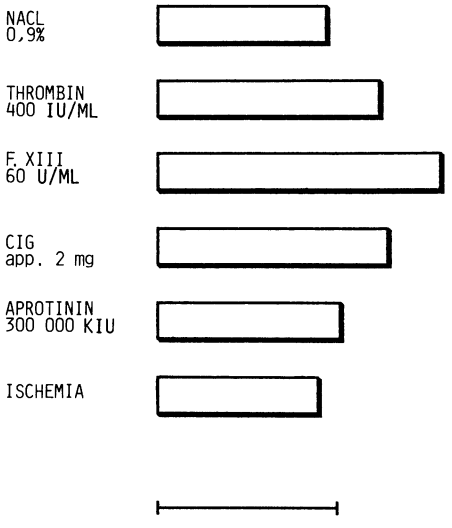

Fig. 1. The influence of various factors on the fibrosis of nerve anastomosis

Discussion

Thrombin

Thrombin can have not only an inhibiting but also a promoting influence on cell proliferation, depending on the point of time of its addition to fibroblast cultures (1, 2, 3, 9, 10). The fibrosing effect demonstrated in our investigations could develop directly on special cell receptors (5). An additional indirect influence through the involution of the proliferative effect of certain serum components has also been reported (12). Thrombin is incorporated into the fibrin clot. To what extent the further induction of fibroblasts is thereby

inactivated, or whether via this process even longer action times ensue, remains open. On the basis of our results we propose a further reduction of thrombin to approximately 1.5 U per ml adhesive.

Factor XIII

Our results suggest that high concentrations have a fibrolytic effect. This was also described, among others, by KNOCHE and SCHMIDT (6), who noted an additional connective tissue promoting effect of higher factor XIII doses in other tissues too.

CIG/Fibronectin

As CIG was not available as a pure substance, both fibrin adhesives available on the market were compared, as only one of the preparations contains CIG. By means of a multifactorial experimental trial design it was shown that the adhesive strength was reduced by CIG and it probably plays an important role in the dissolution of the clot. We attribute the fibrosis-promoting effect to the premature decline of the adhesive strength and resulting microdehiscence caused by this. CIG should not be added to adhesives.

Aprotinin

The effect of aprotinin on the absolute collagen content is controversial. Not only increases in neutral influences but also decreases are described in the literature, usually after examination of the gastrointestinal tract. According to our results, aprotinin is in all probability not directly responsible for fibrosis of nerve anastomoses. At most, KUDERNA's (7) results can be explained by the longer fibrin clot persistence achieved by higher doses of aprotinin. By virtue of our trials we see no need to change to any other fibrinolytic inhibitor than aprotinin.

Ischemia

RÖTTGEN and WÜLLENWEBER (11) attribute the fibrotic changes in autoplastic transplants mainly to unsatisfactory nutrition caused by the fibrin clots. There are also reports of poor microvascularization of transplants by fibrin clots. Our results show, however, that such grave nutritive deficits are not caused by fibrin clots, so that functionally and histologically no influence was observed. This could be attributable to the diffusion through the fibrin layer being barely obstructed, or the diffusion routes in the nerve's longitudinal direction being short enough to guarantee nutrition of the transplant to a certain extent in the first few days.

Altogether, the results give rise to the desire for an improvement of adhesive for nerve anastomosis. Fears of a nutritional barrier being formed by the fibrin adhesive seem inopportune following our investigations.

References

1. Bernsmeier R, Holzgrebe E, Lück P, Bruhn HD, Zurborn KH (1983) Thrombin, Faktor XIII und Fibronectin als Regulatoren der Proliferation von Tumorzellen und Gefäßwandzellen. Onkologie 6:4-7
2. Bruhn HD, Christophers E, Pohl J, Schoel G (1981) Regulation der Fibroblasten- und Endothelzellproliferation durch Thrombin. Faktor XIII und Fibronectin. In: Blümel G, Haas S (eds) Mikrozirkulation und Prostaglandinstoffwechsel - Neues über Fibrinogen und Fibrinkleber. Schattauer, Stuttgart New York, pp 257-265
3. Chen LB, Buchanan JM (1975) Mitogenic activity of blood components. I. Thrombin and Prothrombin. Proc Natl Acad Sci 72:131-135
4. Duspiva W (1978) Neue Erkenntnisse zur Anastomosierung durchtrennter peripherer Nerven. Fortschr Med 96:2214-2218
5. Hall WM, Ganguly P (1980) Binding of thrombin to cultured human fibroblasts: evidence for receptor modulation. J Cell Biol 87:601-610
6. Knoche H, Schmitt G (1976) Autoradiographische Untersuchungen über den Einfluß des Faktor XIII auf die Wundheilung im Tierexperiment. Arzneim-Forsch 26:547-551
7. Kuderna H (1979) Nervenklebung. Dtsch Z Mund-Kiefer-Gesichts-Chir 3:325-355
8. Matras H, Dinges HP, Lassmann H, Mamoli B: Zur nahtlosen interfaszikulären Nerventransplantation im Tierexperiment. Wien Med Wochenschr 37:517-522
9. Pohjanpelto P (1977) Proteases stimulate proliferation of human fibroblasts. J Cell Physiol 91:387-392
10. Pohl J, Bruhn HD, Christophers E (1979) Thrombin and fibrin-induced growth of fibroblasts: role in wound repair and thrombus organization. Klin Wochenschr 57:273-277
11. Röttgen P, Wüllenweber R (1974) Die Chirurgie der peripheren Nerven. In: Olivecrona H, Tönnis W, Krenkel W (eds) Handbuch der Neurochirurgie, vol 7/3. Springer, Berlin Heidelberg New York, p 269
12. Zetter BR, Sun TT, Chen LB, Buchanan JB (1977) Thrombin potentiates the mitogenic response of cultured fibroblasts to serum and other growth promoting agents. J Cell Physiol 92:233-240

Neurosurgical Operations

Meningioma of the Tentorium

R. A. Frowein, W. Köning, G. Friedmann, and F. Thun

Neurochirurgische Universitätsklinik, Joseph-Stelzmann-Straße 9, D-5000 Köln 41

At our Bochum conference in 1974, isotope diagnosis achieved the best results, with 23 diagnoses of location out of a total of 24 cases (95%) and 16 correct diagnoses of the kind of tumor out of the 24 cases. The mortality rate at that time was 36%. In Hannover in 1984 we demonstrated that even fairly small tumors in the middle cranial fossa could be diagnosed with the help of CT. Up till now, six MR tomograms have made it possible to locate meningiomas in relation to the tentorium and, with gadolinium, to arrive at a reliable diagnosis.

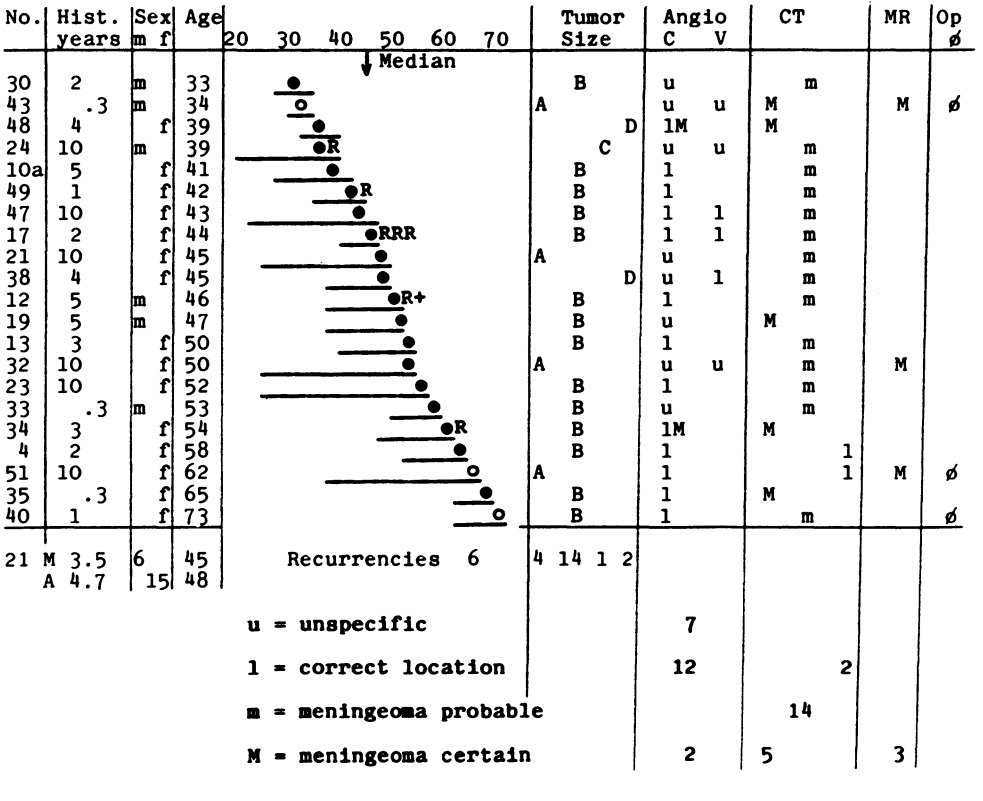

Fig. 1. Twenty-one petroclinoidal tentorial meningiomas

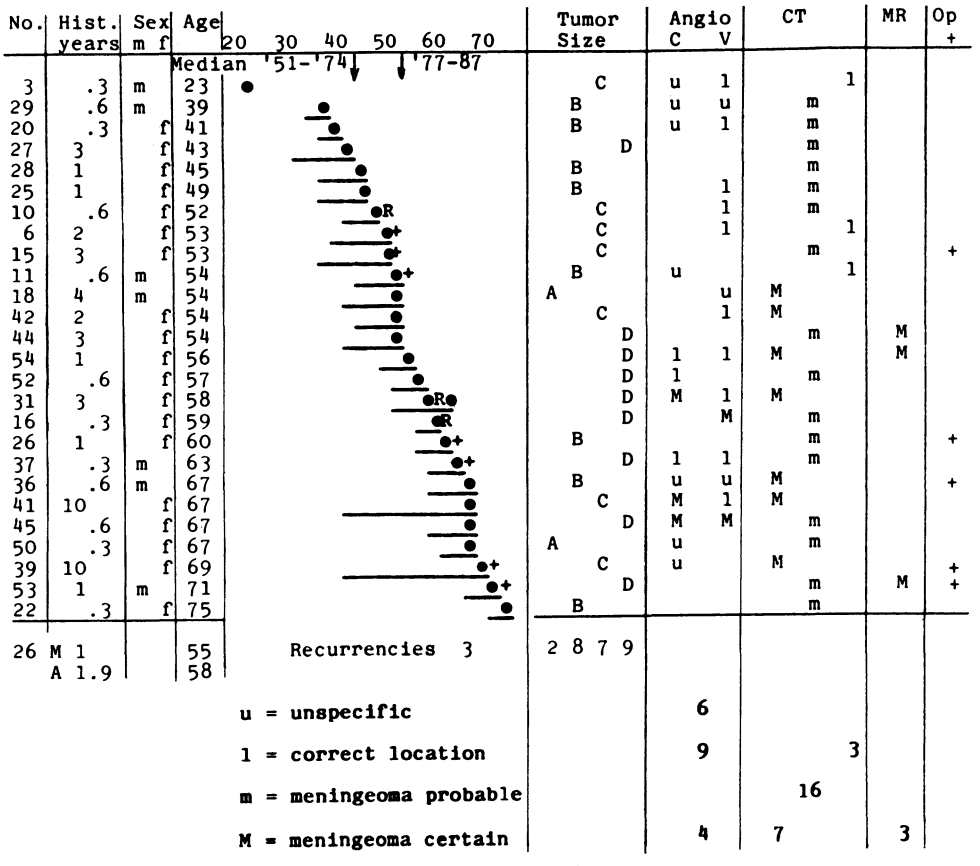

Fig. 2. Twenty-six occipital/suboccipital tentorial meningiomas

Further Cases in Cologne

Since 1977 21 petroclinoidal and 26 occipital/suboccipital supratentorial and infratentorial meningiomas have been diagnosed in Cologne (Figs. 1, 2). With normal or DSA angiography, 14 of the 21 meningiomas of the middle cranial fossa could be localized: in two cases the specific kind of tumor was identified. As to the occipital and suboccipital tumors, the location was identified correctly 19 times, the specific kind of tumor 4 times.

Computed tomography with contrast medium showed the correct location in 19 out of 21 petroclinoidal cases; in 23 out of 26 occipital/suboccipital cases it led to the suspicion or to the certainty of a meningioma. In only one case was a medulloblastoma in the upper vermis mistakenly identified as a meningioma, and in one case a purely infratentorial meningioma in the ascending segment of the tentorium was mistakenly taken to be supratentorial.

The six correct *MR examinations* have already been cited. Thus the *accuracy of the radiological diagnosis* of tentorial meningioma has risen to 48 out of 53 (i.e., 90%).

The following *clinical problems*, on the other hand, remain: The mean age of patients at the time of diagnosis of occipital supratentorial and infratentorial meningiomas has increased from the earlier figure of 45 by 10 years to 55 years. The average duration of the anamnesis has gone down in half of these cases from 4 years to 1 year (the arithmetic mean is 1.9 years); thus the short anamneses which mistakenly suggest malignancy have risen dangerously. The preoperative size of the tumor in the middle cranial fossa is 20 cm^3 in half the cases; above and beneath the occipital tentorium it is 31 - 33 cm^3. However, there is no correlation with the length of anamnesis.

With CT and MR we are able to keep track of the time during which the tumor doubles in size, which is on average 1 year. For this reason three small tumors in the middle cranial fossa have not yet been operated on.

The mortality for operations in the occipital area, both supratentorial and infratentorial, is now 5 out of 26 cases; thus the rate has gone down from 36% to 19%. A relatively large number of patients over 60 years old who had large tumors are to be found among the lethal cases.

Cases of recurrence had to be operated on again in 3 out of 26 occipital and 6 out of 21 petroclinoidal tumors; in some cases several operations were carried out.

Summary

With our present optimal radiological diagnosis it should be possible in at least half of all such cases to achieve a reduction in the age at operation, in the size of the tumor, and in the rates of mortality.

CSF Fistula Occlusion by Ethibloc: Clinical Experiences with 62 Surgically Treated Cases

K. H. Krähling, J. Anagnostopoulos-Schleep, and H.-J. König

Neurochirurgische Klinik der Westfälischen Wilhelms-Universität, Albert-Schweitzer-Straße 33, D-4400 Münster

CSF fistulas following fractures of the base of the skull have been occluded using muscle, duraplasty, or fibrin glue. A new method was developed 4 1/2 years ago that is suitable for frontal and otogenous CSF fistulas. An alcoholic solution of zein derived from maize is introduced into the bony clefts. Ethibloc (Table 1) has been used for several years to occlude the duct of Wirsung (1-7,10,11,12,13,15).

Table 1. Contents of 1 ml Ethibloc (manufactured by Ethicon, Hamburg-Norderstedt)

210 mg	zein
162 mg	natrium amidotrizoate tetrahydrate
145 mg	oleum papaveris
6 mg	propylene glycol

The adhesive is of viscous consistence, hardening to a mass like chewing gum within minutes when mixed with air or water. The process of total hardening will last for hours. Within 40 - 90 days the agglutinant is replaced by connective tissue without voluminal change. Pulverized antibiotics may be added (14). Using a transfrontal approach the bony clefts have been occluded by fascia or duraplasty. Depending on the surface of the frontal skull base water seal could not always be achieved. The danger of meningitis was not eliminated. Careful and skilled handling of the cover material was required.

Application of Ethibloc has proved much easier, safer, and less time consuming. This makes it superior to former procedures. By a small frontal osteoplastic trepanation the frontal skull base is approached intradurally using the operating microscope. The dural defect and the bony cleft are to be demonstrated and the Ethibloc applied using a bulbous cannula. In the beginning the fluid solution will easily extend through the bony clefts. Volumes between 0.5 and 1.0 ml are usually sufficient. A second depot is placed between bony structures and dura mater. A third depot is used to cover the dura defect intradurally (8,9). The fistula is closed intrathecally and the bony clefts are filled up with adhesive.

There is no interaction of Ethibloc with brain tissue except soft adhesions in the case of focal contusion. This has been confirmed by an animal study. In rabbits it could be impressively demonstrated that

Table 2. Clinical experiences with Ethibloc in the closure of frontobasal CSF fistulas (Neurochirurgische Universitätsklinik Münster, 1983 - April 1987)

Localization		Liquorrhea		Meningitis		Surgically treated before
		preop.	postop.	preop.	postop.	
Dorsal wall of frontal sinus	31	27	0	7	0	3
Lamina cribrosa	29	25	0	9	0	4
Roof of sphenoid sinus	2	2	0	0	0	0
	62	54	0	16	0	7

Table 3. Application of Ethibloc in other indications (Neurochirurgische Universitätsklinik Münster, 1983 - April 1987)

Closure of opened frontol sinuses	23 cases
Closure of small dura defects	58 cases
Filling of burr holes and saw lines	40 cases
Great traumatic defects of the frontal skull base	6 cases
Malformations of the frontal skull base	4 cases
Wrapping of aneurysms	7 cases
Wrapping of aneurysm clips	8 cases

there is neither early nor late interaction between Ethibloc and the undamaged brain nor any other side-effects.

Since 1983 62 CSF fistulas have been occluded by Ethibloc (Table 2). The defect was located in the posterior wall of the frontal sinus in 31 cases, in the area of the lamina cribrosa in 29 cases, and at the roof of the sphenoid sinus in two cases. All except eight patients had liquorrhea preoperatively. Sixteen had been treated for meningitis and seven had been surgically treated for CSF fistula before.

No adverse effects have been observed. In all cases the fistulas have been occluded safely. Postoperative survival was uneventful up to 4 1/2 years. Application of Ethibloc is favored by a remarkable reduction of operation time including the compression of the frontal lobe by self-retaining retractors. The solution is applicable within a few minutes without any time-consuming preparation. Composed with fibrin glue or duraplasty Ethibloc is less costly.

In addition Ethibloc may be used to close opened frontal sinuses, small dural defects, or burr holes (Table 3). In closing of malformations and great traumatic defects of the frontal skull base, Ethibloc was successful. In some cases we wrapped unclippable aneurysms with Ethibloc; in some others the clip was supplied with a drop of Ethibloc to prevent clip sliding.

References

1. Bücheler EW, Hupe W, Klosterhalfen H, Altenähr E, Erbe W (1978) Neue Substanz zur therapeutischen Embolisation von Nierentumoren. Fortschr Röntgenstr 128:599-603
2. Dahlke H, Dociu N, Muxfeldt H, Thurau K, Treppl M-E (1982) Experimental pancreatic duct obstruction with an alcoholic prolamine solution producing a pancreatic exocrine atrophy. In: Winter GD, Gibbons DF, Plenks H (eds) Biomaterials 1980. Wiley
3. Gall FP, Gebhardt CH (1979) Ein neues Konzept in der Chirurgie der chronischen Pankreatitis. Rezidivverhütung durch Gangokklusion und Erhaltung des Magens. Dtsch Med Wochenschr 104:1003-1006
4. Gebhardt CH, Gall FP (1980) Partielle Duodenpankreatektomie mit intraoperativer Pankreasschwanzverödung bei chronischer Pankreatitis. Langenbecks Arch Chir 353:157-162
5. Gebhardt CH, Gall FP, Mühe E, Lauterwald A (1979) Ist die totale Pankreatektomie zur Behandlung der chronischen Pankreatitis noch zu verantworten? Langenbecks Arch Chir 350:129-137
6. Gebhardt CH, Gall FP, Zirngibl H (1983) Chirurgische Behandlung der chronischen Pankreatitis. Deutsches Ärzteblatt 80/8:17-22
7. Gebhard CH, Stolte M (1978) Pankreasgang-Okklusion durch Injektion einer schnellhärtenden Aminosäurenlösung. Experimentelle Studie. Langenbecks Arch Chir 346:149-166
8. Krähling KH, König, H-J (1984) Eine neue Technik zum Verschluß der frontobasalen Liquorfistel. Erfahrungen mit einer aushärtenden alkoholischen Prolaminlösung. Fortschr Med 102/40:55-56
9. Krähling KH, König H-J (1984) Ein neuer Werkstoff in der Neurochirurgie. Neurochirurgie 27:166-169
10. Land W, v. Liebe S, Höpp H, Jocham D (1980) Simultantransplantation von Pankreas und Niere. Verwendung eines neuen Pankreasgangokklusionsgels. Chir Praxis 27:15-25
11. Rassweiler J, Kaufmann GW, Rohrbach R, Richter B (1980) Kapilläre Embolisation. Teil I: Verschluß des gesamten arteriellen Gefäßsystems der gesunden Rattenniere. Fortschr Röntgenstr 133:644-653
12. Rettinger G, Stolte M, Bäumler C (1981) Ausschaltung von Speicheldrüsen durch temporäre Okklusion des Gangsystems mit einer Aminosäurenlösung. HNO 29:294-299
13. Richter G, Rohrbach R, Kauffmann GW, Rassweiler J (1981) Kapilläre Embolisation. Teil II: Verschluß des gesamten arteriellen Gefäßsystems experimentell erzeugter Nierentumoren. Forschr Röntgenstr 135:85-97
14. Schultheis K-H, Schulz A, Schiefer H (1981) Schnellhärtende Aminosäurenlösung als mögliche Chemotherapeutika-Trägersubstanz zur Behandlung der chronischen Osteomyelitis. Unfallchirurgie 7/6:324-333
15. Wittrin G, Jost JO, Clemens M, Arndt M (1981) Pankreasgangokklusion nach partieller Duodenopankreatektomie in der Karzinomchirurgie. Chirurg 52:157-159

Tumor Growth of Recurrent Meningiomas

W. Köning and R. A. Frowein

Neurochirurgische Universitätsklinik, Joseph-Stelzmann-Straße 9, D-5000 Köln 41

Systematic measurements of the volume of tumors or examinations of the growth of meningiomas are reported by some authors (2,3,6,9). In this study the distribution of tumor volume and the growth rate of meningiomas, based on the measurement of volume, were determined.

Materials and Methods

Between 1979 and 1986 the preoperative tumor volume of 111 patients with intracranial meningiomas was measured. In 43 patients with recurrent meningiomas, the speed of growth was determined by calculating the tumor doubling time (Td). The area of tumor in each scan was measured by planimetry. The volume of the tumor was calculated as the sum of the products of the area of tumor multipled by the slice of thickness. The Tds were determined by the exponential equation $Td = t \times \log 2/\log (Vm/Vn)$ (2,6), Vm being the volume after t month and Vn the initial volume. For the first postoperative measurements the initial volume was taken to be, in the case of a macroscopic total excision (Simpson's grade III) (10), a theoretical remaining volume of 0.5 ccm, and in the case of incomplete excision (grade IV), a theoretical remaining volume of 1.0 ccm.

Results

Tumor volumes: The distribution frequency of the volume of the 111 meningiomas was revealed as approximately normal in a semilogarithmic scale, with a size span of 3.0 - 260 ccm (Fig. 1). Tumors with a volume of less than 3 ccm were less frequent. The diameters varied between 0.7 cm and 8.0 cm. In allocating tumor volumes to individual locations, a location-specific distribution of size is revealed in three areas (Fig. 2).

Group A: The median values of the tumor volumes of the meningiomas of the orbit, sphenoid wing en plaque, and suprasellar region lay between 4 and 8 ccm. With one exception all meningiomas in these locations remained below a maximum size of 20 ccm, with a corresponding diameter of 3.5 cm.

Group B: The meningiomas of the central and tentorial regions were of a medium size, with median values of 25 - 32 ccm. In only one case was a maximum size of 80 ccm reached, with a corresponding diameter of 5.3 cm.

Group C: The largest tumors were produced by meningiomas of the olfactory groove and the sphenoid wing en globe, and by parasagittal and

Advances in Neurosurgery, Vol. 16
Ed. by W. Walter, M. Brandt, M. Brock, and M. Klinger

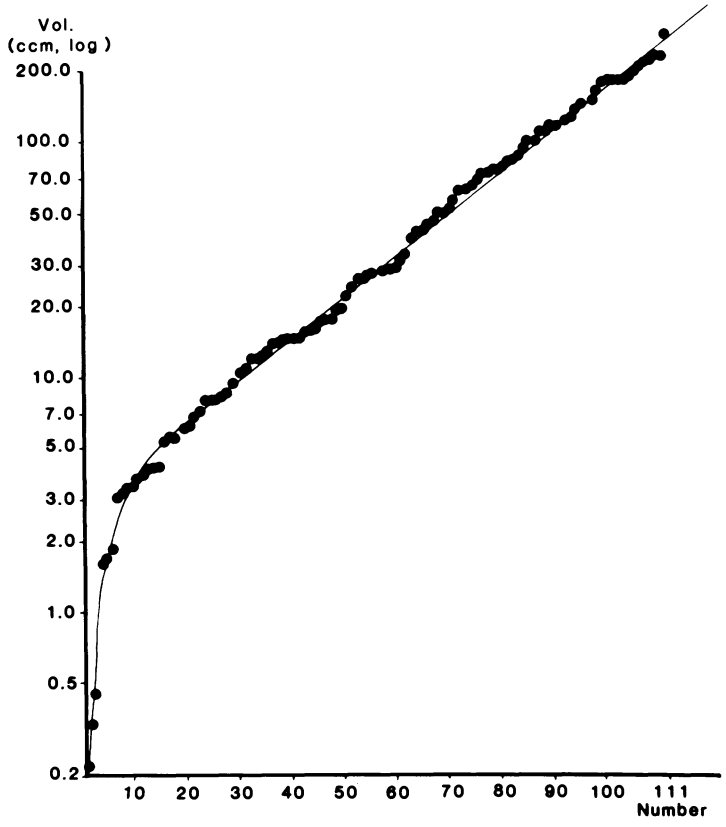

Fig. 1. Frequency of the preoperative tumor volumes of 111 intracranial meningiomas

convexity meningiomas. Median values of 78 - 95 ccm and a maximum size of up to 260 ccm with a corresponding diameter of 8 cm were noted.

Most of the meningiomas had no obvious correlation between tumor volume and duration of first symptoms. Only in meningiomas of the convexity and parasagittal region, outside of the central region, was there an appreciable indirect relationship (Fig. 3). Whilst the smallest tumors in this group had an average duration of symptoms of 30 months, in the case of the biggest tumors the duration shrank progressively down to 5.6 months. This paradoxical relationship was also reported by TÖNNIS in 1962 (12). Thus the duration of symptoms is an inappropriate means of judging the tumor growth.

Tumor Doubling Time (Td)

In 92% of the 43 recurrent meningiomas the Td ranged between 0.5 and 48 months (Fig. 4). In 8% of the cases the Td was longer, which in some cases meant a virtual halt in growth. Predictably, the malignant and angioblastic meningiomas exhibited the shortest time, with an average Td of 2.8 months. The Td did not appear to be dependent on the usual histological subtypes of meningiomas. However, there were clear dif-

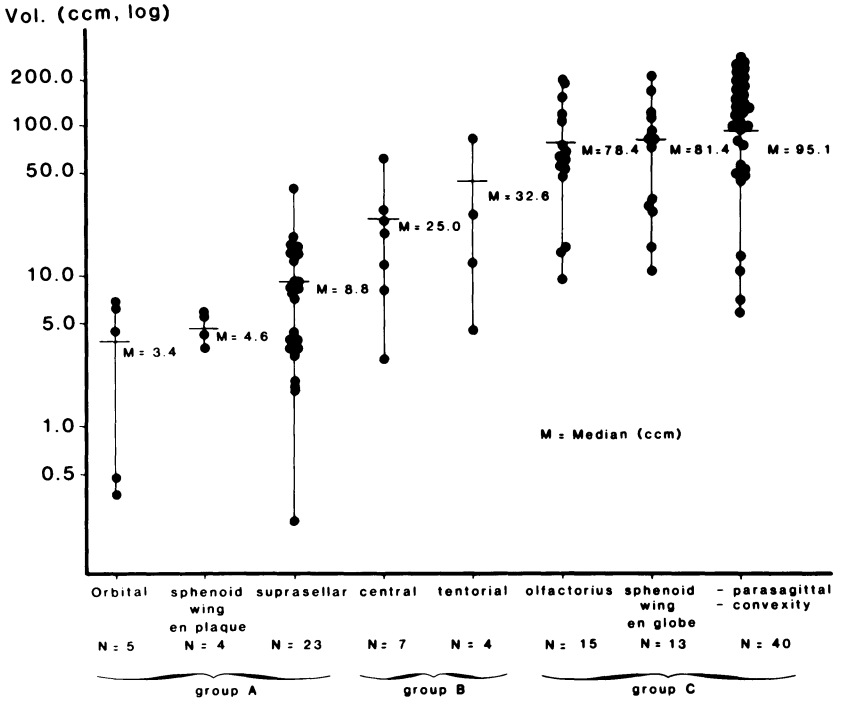

Fig. 2. Distribution of 111 tumor volumes at different locations

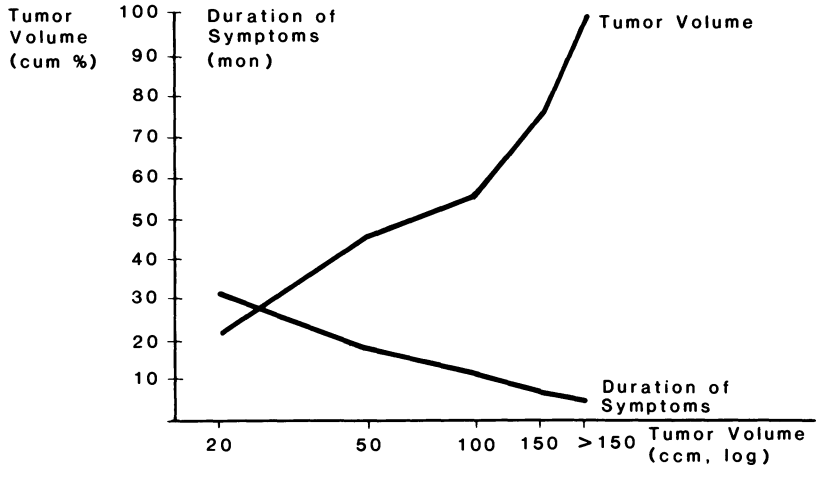

Fig. 3. Cumulative frequency of the preoperative tumor volumes and average duration of symptoms of 31 meningiomas of the convexity and parasagittal region

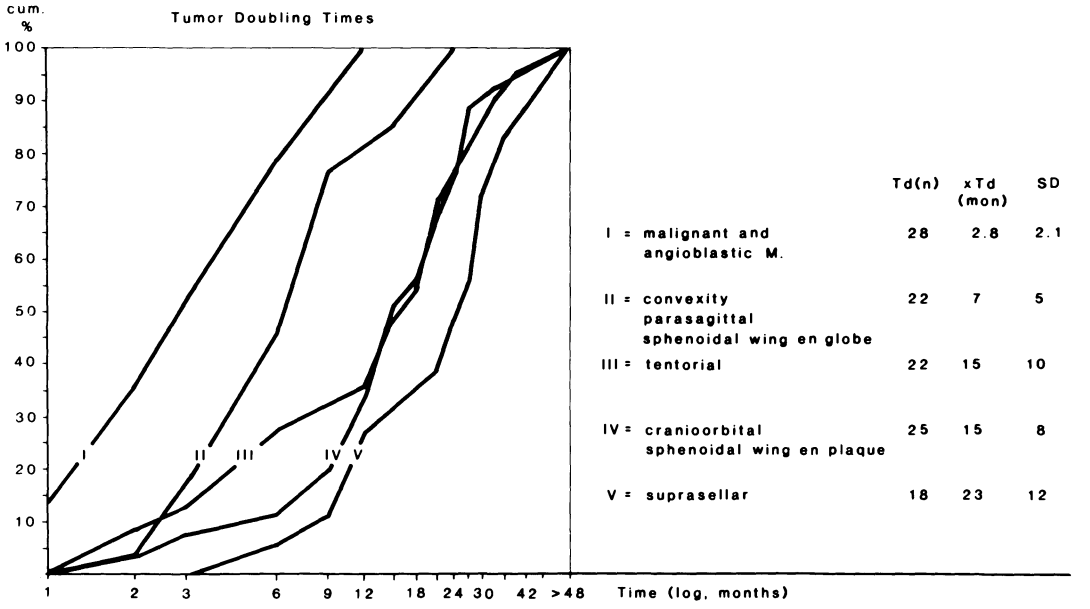

Fig. 4. Cumulative frequency of the tumor doubling times according to malignancy and tumor location. *Td*, tumor doubling time; $\bar{x}Td$, median of Td; *SD*, standard deviation

ferences in the average Tds of the various locations. The majority of the suprasellar meningiomas grew very slowly, with an average Td of 23 months. Next came the meningiomas of the sphenoid wing en plaque and of the orbital and tentorial region, with Tds of 15 months, while meningiomas of the sphenoid wing en globe and of the parasagittal and convexity region were clearly faster growing, with a Td of 7 months. Individual times were very variable.

Discussion

The prognosis for patients with intracranial meningiomas depends on the location, the size of the tumor, the extent of surgical excision, and, in the case of malignant and angioblastic meningiomas, the histology (4,5,7,10,11). The overall rate of recurrence is 21% - 29%. In cases of incomplete excision and difficult localization, the rate rises to 40% (1,8,10). If clinical symptoms are lacking the decision for surgical treatment is difficult. CHO examined two benign, two angioblastic, and four malignant meningiomas and found a good correlation between the inverval before recurrence and the "in vivo labeling" of tumor cells with bromodeoxyuridine (2). First results with Ki 67 labeling suggest a quicker growth in recurrent meningiomas (9). Our Td figures based on the measurements of tumor volumes confirm the predictably short times for malignant and angioblastic meningiomas. Within the large group of benign meningiomas notable differences occurred according to the localization of the meningiomas, irrespective of their further more extensive histological subtype. The Td of basal, suprasellar, and cranioorbital meningiomas and of meningiomas of the tentoral region was almost twice as long as the Td of meningiomas in other locations. Thus, in individual cases the calculation of the current Td,

taking into account the location and size of the tumor, is of prognostic importance in the treatment of patients with recurrent meningiomas.

References

1. Chan RC, Thompson GD (1984) Morbidity, mortality and quality of life following surgery for intracranial meningiomas. J Neurosurg 60:52-60
2. Cho GK, Hoshino T, Nagashima T, Murovic JA, Wilson CB (1986) Prediction of tumor doubling time in recurrent meningiomas. J Neurosurg 65:790-794
3. Christensen D, Laursen H, Klinken L (1983) Prediction of recurrence in meningiomas after surgical treatment. Acta Neuropathol 61:130-134
4. Crompton RM, Gauthier-Smith PC (1970) The prediction of recurrence in meningiomas. J Neurol Neurosurg Psychiatr 33:80-87
5. Cushing H, Eisenhardt L (1938) Meningiomas. Hafner, New York, 1962, reprint, vols 1,2
6. Hoshino T, Nagashima T, Murovic JA (1986) Proliferative potential of human meningiomas of brain: a cell kinetics study with bromodeoxyuridine. Cancer 58:1466-1472
7. Melamed SH, Sarhar A, Beller AJ (1979) The recurrence of intracranial meningiomas. Neurochirurgia 22:47-51
8. Mirimanoff RO, Dosoretz DE, Lingood RM, Ojemann RG (1983) Meningioma: analysis of recurrence and progression following neurosurgical resection. J Neurosurg 62:18-24
9. Roggendorf W, Schuster TH, Pfeiffer J (1987) Charakterisierung des unterschiedlichen Wachstums der Meningiome mit dem Proliferationsmarker Ki 67. Symposium Therapie primärer Hirntumoren, Vortrag, Essen
10. Simpson D (1957) The recurrence of intracranial meningiomas after surgical treatment. Neurol Neurosurg Psychiatr 20:22-39
11. Skullerud U, Löken AC (1974) The prognosis in meningiomas. Acta Neuropathol (Berl) 29:337-344
12. Tönnis W (1962) Diagnostik der intrakraniellen Geschwülste, Meningiome. In: Olivecrona H, Tönnis W (eds) Handbuch der Neurochirurgie, vol 3. Springer, Berlin

Transpeduncular Stabilization with the Fixateur Interne in Cases of Spinal Instability

B. Kaden, M. Faensen, and M. Brock

Neurochirurgische Klinik, Universitätsklinikum Steglitz, Hindenburgdamm 30, D-1000 Berlin 45

Introduction

Spinal trauma, disk surgery, pathological fractures, and congenital anomalies can lead to static and neurological alterations caused by an unstable spine. The surgical procedures usually applied to date, such as laminated endoprostheses (6), Harrington rods (2), their modification (3), dorsal plates (7), and Luque's instrumentarium (4), have failed to fulfill therapeutic demands. The principle of transpeduncular reinforcement of a vertebral body with the aid of Schanz screws, introduced by MAGERL (5) when describing the fixateur externe, was further developed and applied by DICK (1) to the fixateur interne. This system has the advantage that segmental immobilization can be limited to only one movement segment and must not be extended beyond the affected segments. The Schanz screws are screwed into the peduncles under X-ray control parallel to the upper plate and in a slightly convergent manner. Connection between the upper and lower Schanz screws on each side is achieved by means of threaded rods and appropriate clamping devices, the angulation of which remains stable (Fig. 1). Distraction or compression can also be achieved with the aid of the rods. Repositioning can be accomplished by direct manipulation of the Schanz screws.

Material and Methods

The fixateur interne was applied in 17 patients from the middle of the thoracic spine to the sacrum (Table 1). The age of the patients ranged from 15 to 70 years (mean 42 years). There were nine women and eight men. In ten cases, the fixateur interne was combined with a dorsal spondylodesis using autologous spongiosa.

Vertebral Body Fractures

Seven patients with traumatic vertebral body fractures, kyphosing, and constriction of the spinal canal were treated with a fixateur interne. The mean age of the patients was 37 years. There were progressive cauda equina symptoms in four cases, while one patient had paraplegia resulting from a crushed spinal cord. Laminectomy was performed and dural lesions were treated in four cases. In one patient, the fixateur interne had to be prematurely removed due to infection. Following laminectomy, in this case, a fixateur externe had been initially used and later substituted by a fixateur interne, which had to be removed because of infection. After its healing, ventral spondylodesis was performed with autologous spongiosa. A vertebral body contraction was performed in four cases (Fig. 2).

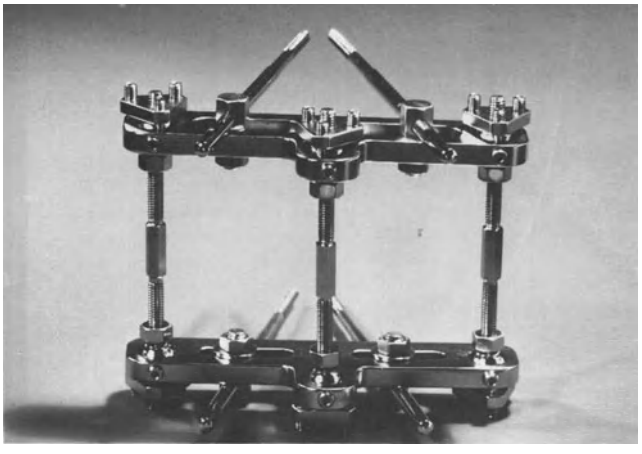

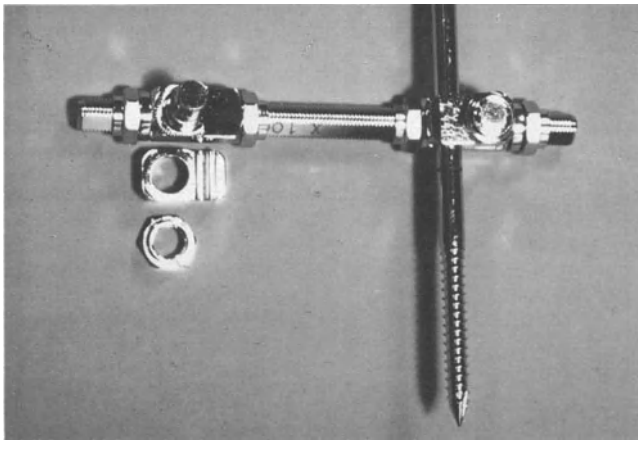

Fig. 1. *Above:* fixateur externe (MAGERL). *Below:* fixateur interne (DICK), combined with Schanz screws

Table 1. Bridged levels

No. of patients	Levels
2	T3 - T6
1	T4 - T10
2	T11 - L1
1	L1 - L4
3	L1 - L3
1	L2 - L4
3	L4 - L5
4	L4 - S1

Pathological Vertebral Body Fractures

A fixateur interne was applied in three patients with vertebral body metastases, instability, and neurological symptoms. In one case, a

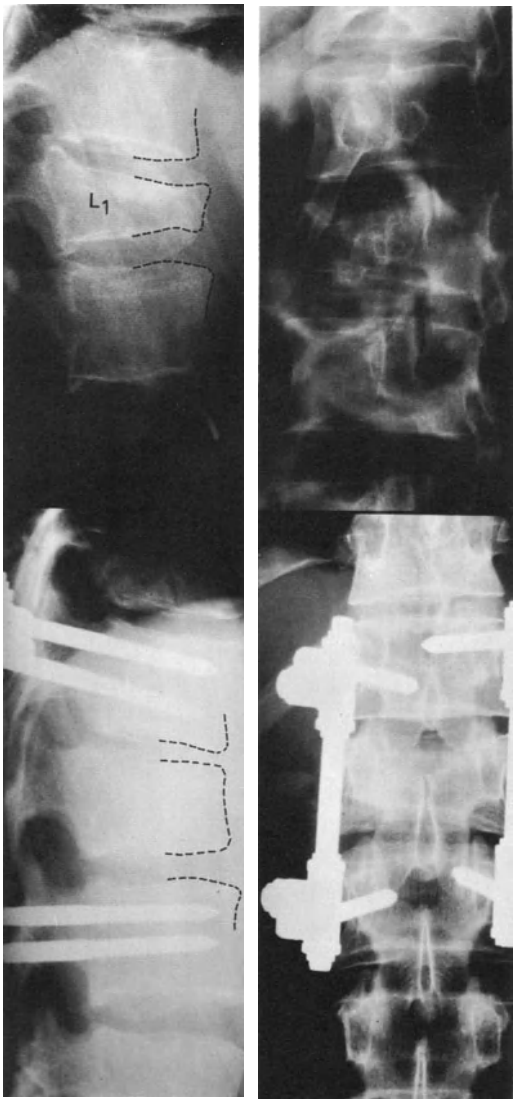

Fig. 2. 28-year-old man after a fall from a tree. Compression fracture, kyphosing, no neurological symptoms. Fixation of T12 - L2; vertebral grafting with autologous spongiosa. Mobilization on 7th postoperative day. Discharged symptom-free on 10th postoperative day

laminated endoprosthesis which had been implanted 5 years previously and had lost its stabilizing function had to be replaced by the fixateur interne, because the patient was complaining of strong back pain and difficulty in walking. The pain was relieved, and the ability to walk was regained. The second patient had a contrast medium stop and was submitted to a laminectomy of T5 and T6. The fixateur interne was implanted from T4 to T7. The patient could be mobilized with little pain; care was markedly facilitated, but neurological symptoms did not improve. In the third case, a 73-year-old woman with a known melanoma metastasis, the paraparesis diminished after implantation of the fixateur interne from T6 to T10 to bridge the vertebral body destruction in T8.

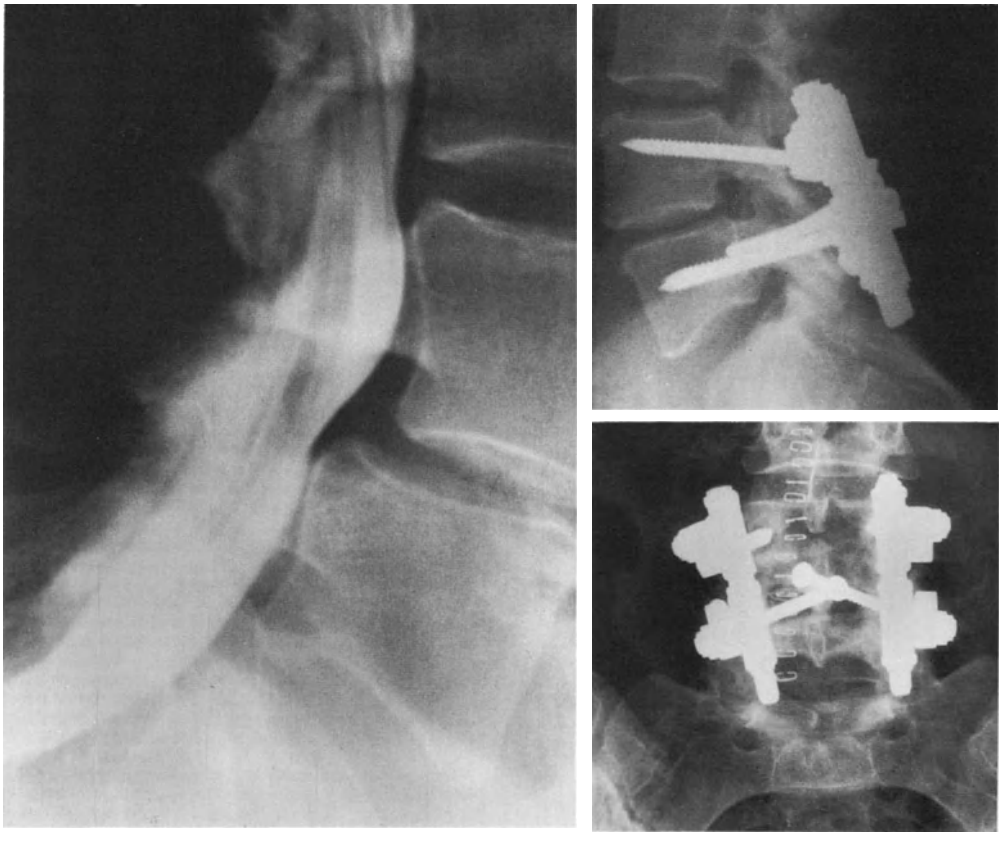

Fig. 3. 45-year-old female patient following repeated disk surgery. Severe bilateral load-dependent lumboischialgia. Stabilization at L4/5 with the fixateur interne and dorsal spondylodesis. Considerable clinical improvement was achieved, and the patient was able to work as a housewife

Degenerative Spondylopathies

Four patients had a postdiskotomy syndrome with load-dependent lumboischialgia. Clinical and radiological findings showed instability at L4/L5 in three cases and at L4/S1 in one. These segments were immobilized by means of the fixateur interne. A dorsal spondylodesis with autologous spongiosa was performed in all cases. Subjective improvement was achieved in two cases (Fig. 3), but the result was unsatisfactory in the other two. The latter patients, however, had psychic alterations and degenerative changes in other spinal segments.

Spondylolisthesis

In three patients, fixation of L4/L5 and S1 was carried out in combination with dorsal spondylodesis. A two-session procedure was used in two patients. First, the fixateur externe was implanted percutaneously under fluoroscopic control, and repositioning was achieved by stepwise distraction. In a second session, the fixateur externe was replaced by

a fixateur interne. In one case, an infection led to premature removal of the fixateur interne. The other patients showed a definite subjective improvement as well as a marked objective increase in stability.

Conclusions

The fixateur interne constitutes a new device for simple and efficient spinal stabilization in cases of vertebral instability of varying etiology (including inflammatory alterations of the vertebral column). Its implantation was uncomplicated in 17 cases. The occurrence of infections has led us to abandon the two-session procedure. Repositioning and reinforcement of the vertebra following fractures was less satisfactory in the initial cases. Long-term observations are still necessary to determine any loss of correction after removal of the fixateur interne. Our results, however, indicate that it seems unnecessary to carry out a dorsal and ventral procedure in order to avoid late loss of the achieved correction.

Summary

Traumatic, tumoral, degenerative, and congenital instability of the vertebral column can be repositioned and stabilized by transpeduncular reinforcement even when under load. In contrast to what occurs when using the Harrington instrumentarium (including the modification according to Jacobs), the Luque procedure, and the spinal plates, only the affected movement segments are stiffened by the fixateur interne. The fixateur interne constitutes a further development of the fixateur externe. The indication for its application, also in combination with spongiosa grafts, is described based on the favorable results obtained in 17 patients.

References

1. Dick W (1984) Innere Fixation von Brust- und Lendenwirbelfrakturen. Huber, Bern Stuttgart Toronto
2. Flesch JR, Leider LL, Erickson DL, Chou SN, Bradford DS (1977) Harrington instrumentation and spine fusion for unstable fracture and fracture dislocation of the thoracic and lumbar spine. J Bone Joint Surg 59A:143-153
3. Jacobs RR, Casey MP (1984) Surgical management of thoracolumbar spinal injuries. General principles and controversial considerations. Clin Orthop 189:22-35
4. Luque ER (1982) Segmental spinal instrumentation in treatment of fractures of the spine. Orthop Trans 6:22
5. Magerl F (1982) External skeletal fixation of the lower thoracic and the lumbar spine. In: Uhthoff HK (ed) Current concepts of external fixation of fractures. Springer, Berlin Heidelberg New York
6. Oppel F, Kunft HD (1977) Akutversorgung von Wirbelfrakturen durch laminierte Endoprothesen: Indikation, Technik, bisherige Erfahrungen. Hefte Unfallheilkd 132:343
7. Roy-Camille R, Saillant G, Marie-Anne S, Mamoudy P (1980) Behandlung von Wirbelfrakturen und -luxationen am thorako-lumbalen Übergang. Orthopäde 9:63-68

States of Psychomotor Epilepsy Following Different Kinds of Brain Disease and Trauma

R. Mewe, H.-J. König, K. H. Krähling, C. E. Elger, and W. Wiesmann

Neurochirurgische Klinik der Westfälischen Wilhelms-Universität, Albert-Schweitzer-Straße 33, D-4400 Münster

The transitional syndrome usually occurs after head injury or after states of unconsciousness following cerebral surgical intervention (1). Typical signs are well-known and include disturbances of consciousness and thinking, drive, and emotions (Table 1). Nevertheless there is no strong correlation between clinical signs and the underlying event at any time. As stated above, signs of transitional syndrome tend to appear after severe craniocerebral trauma. We have also observed phenomena of this kind after clipping an aneurysm and after operating on a cerebral abscess, for example. The EEG showed characteristic features of epileptic state. Because of the clinical symptoms and the EEG results we classified them as psychomotor epilepsy (2).

Table 1. Clinical signs of transitional syndrome and psychomotor epileptic state

Lack of drive and agitation
Affective instability
Amnesia
Hallucination – dreamy state
Blocking of thought processes

Case Reports

In the last 3 years we have observed seven patients with clinical symptoms of the transitional syndrome and and the above-mentioned EEG changes (Table 2; Fig. 1). The ages of four male and three female patients ranged between 18 and 68 years. In four patients we found craniocerebral trauma. In one case a large epidural hematoma was operated on. An aneurysm of the anterior communicating artery was operated on in a 45-year-old patient. Postoperatively he showed symptoms of transitional syndrome, with signs of psychosis by hallucinating. A meningioma of the medial sphenoid bone on the right was operated on in a 53-year-old man. Transitional syndrome appeared postoperatively for about 5 days. A left-sided temporal abscess was totally removed in a 23-year-old female patient.

In all these patients EEG was recorded after admission to hospital and postoperatively. Pathological EEG findings were seen until the 5th day. Amnesia was a main symptom during the epileptic state.

Advances in Neurosurgery, Vol. 16
Ed. by W. Walter, M. Brandt, M. Brock, and M. Klinger

Table 2. Details of the seven patients with transitional syndrome

No. of case	Preexisting epilepsy	Sex/age	Brain disease
1	No	M/42	Craniocerebral trauma III Epidural hematoma
2	No	M/53	Meningioma of medial sphenoid bone
3	No	M/18	Craniocerebral trauma II
4	No	M/45	Aneurysm of the anterior communicating artery
5	No	F/68	Craniocerebral trauma II
6	No	F/34	Craniocerebral trauma II
7	No	F/23	Abscess of temporal lobe

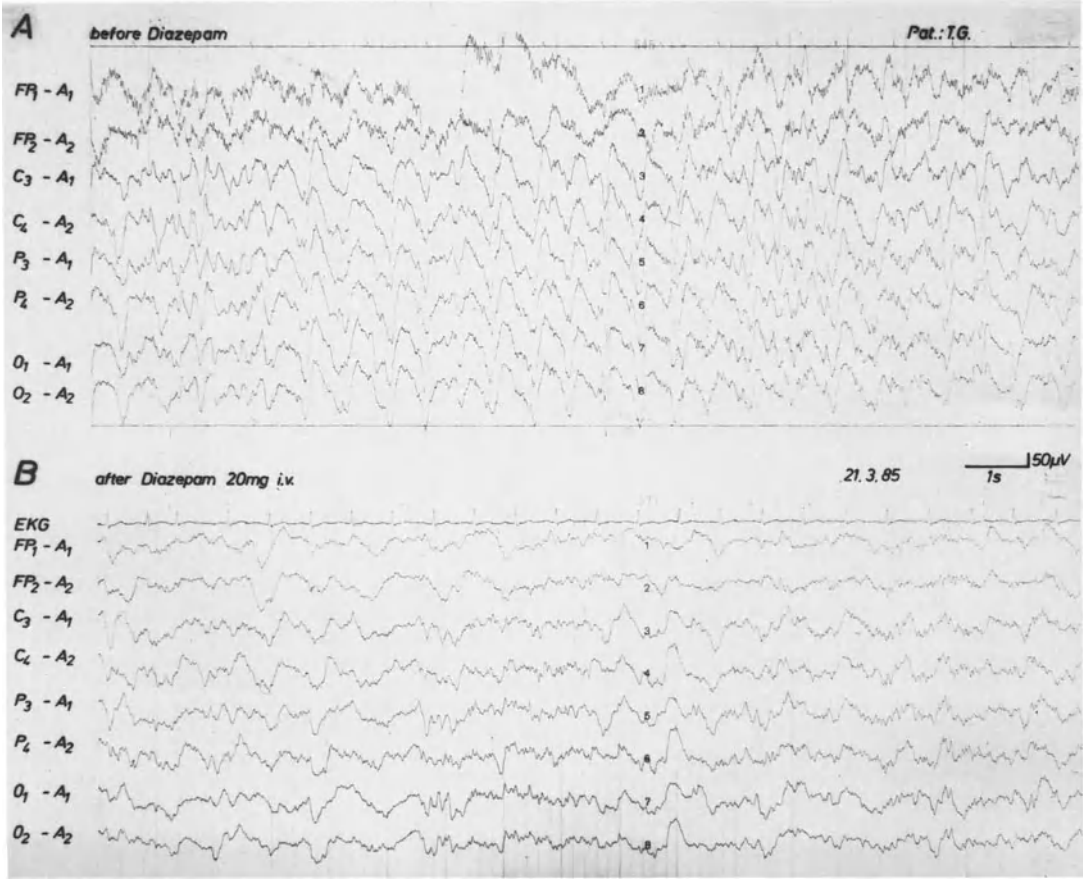

Fig. 1A,B. EEG pattern of the 68-year-old female patient (No. 5) before and after diazepam therapy

Table 3. Diagnosis and therapy of psychomotor epileptic state

1. Result of clinical research	
2. EEG	
3. Infusion therapy	Diazepam or clonazepam and/or phenytoin
4. Control of EEG and clinical research	

We started anticonvulsive therapy by giving 1 or 2 mg clonazepam and continued by giving high dose phenytoin. The clinical symptoms of the transitional syndrome disappeared after between 12 and 36 h.

Discussion

Nonconvulsive epileptic states pass for rare events. In the literature they are usually described as single cases (1,2). In the nonconvulsive epileptic state, typical EEG patterns demonstrate the epileptic event; patients demonstrate no signs of ictal activity like tonic-clonic movements. The only uncharacteristic alterations are to be seen in some psychic changes and behavioral abnormalities (4) that may last for hours to years (3).

The clinical distinction between transitional syndrome and psychomotor epileptic state is difficult because symptoms may be nearly identical. The necessary diagnostic instrument is the EEG (Table 3).

Until today there have been no signs of an ictal event in any of these patients. The anticonvulsive therapy with phenytoin was continued for 4 weeks.

From the point of view of differential diagnoses, these cases have to be set apart from other types of psychosis such as delirium or other forms which have to be evaluated differently in terms of both their development and their therapy.

References

1. Hendrikson GF (1973) Status epilepticus partialis with fear as clinical expression. Epilepsia 14:39-46
2. Hofmann WE, Przuntek H (1986) Status partieller Anfälle mit komplexer Symptomatologie. Nervenarzt 57:61-63
3. Gökyigit A, Apak S, Caliskan A (1986) Electrical status epilepticus lasting for 17 months without behavioural changes. Electroencephalogr Clin Neurophysiol 63:32-34
4. Drake J, Coffey CE (1983) Complex partial status epilepticus simulating psychogenic unresponsiveness. Am J Psychiatr 140:800-801

Subject Index

Abscess of temporal lobe 292
Acoustic evoked brain stem potentials, *see* Brain stem auditory evoked potentials
- neurinomas 49
--, intraoperative derivation at root entry zone 92
Action potential, intraoperative derivation of 91
--, prolongation in latency 93
-- of trigeminal nerve 90
Adenomas, sella 166
Adhesive for nerve anastomosis 271
Adjuvant chemotherapy 263
AEPs, *see* Auditory evoked potentials
Afferent single unit potentials 98
Anastomosis, laser assisted 34
Aneurysm 67, 291, 292
-, flow pattern of 59
-, - velocieties 60
-, giant 60, 117
-,-, balloon 118
-, shrinkage 11
--, laser-assisted 11
- surgery 57
--, central conduction time 87
--, delayed 71
--, Doppler system for 57
--,--, microvascular 57
-, unclippable 279
Angioblastic meningiomas 282
Angiogram, selective 115
Angiographic findings, cavernous angioma 188
--, cerebral vascular malformation 184
Angiographically occult vascular malformations 191
Angiography, selective of spinal angioma 116
-, superselective 114, 116
Angiomas 116
Angioplasty 114
-, percutaneous transluminal 114
Antitumor activity of interferon 252
Arachidonic acid 246
Arachnoid membrane 224
Argon laser 3, 7
Articular nerve supply 127
Astrocytomas, removal by CUSA 44, 45
Auditory evoked potentials (AEPs) 108
---, 40-Hz 110, 111
-- middle and long latency, prognostic usefulness 111
AVM, MRI examination 183
-,- identification 185
Axonal sprouting activity 24

Baclofen
-, intrathecal administration 135, 136
-,- therapy 137
-, muscle relaxant 135
BAEPs, *see* Brain stem auditory evoked potentials
Balloon 115, 118
Basilar artery 65
BCNU [1,3-bis (2-chloroethyl)-1-nitrosurea]
- chemotherapy 263
-, retinal effects 263
-, toxic effect 265
BCNU-related amaurosis 265
- retinopathy 266
BEAM, *see* Brain electrical activity mapping
Benign meningiomas 284
Biological activity of neoplastic lesions 251
- marker 253
Biopsy of brain tumors, endoscopic 53

---, stereotaxic 55
Blood-brain barrier 257
Blood flow velocity 68
Brain damage 243
- death, use of TCD 66
- edema 229
- electrical activity mapping (BEAM) 105
---- of event-related potentials in coma 105
- metastases 260
- necroses by Nd:YAG laser 11
- stem auditory evoked potentials (BAEPs) 83, 102, 108, 110, 111
----- and prognosis 102
-- ependymomas 153
-- gliomas 153
---, postoperative survival 154
-- tumors 152
---, advantages of MRI in surgery 152
- tumor surgery 47
-- therapy 250
- tumors 44
--, detection of, by CT 147
--,-, by MRI 147
--, removal by CUSA 48
--, surgical ultrasonic aspiration 45

Calibrated leak balloon 116
Cancer research 241
Carbon dioxide laser, *see* CO_2 laser
Carotid artery-cavernous sinus fistulas 118, 119
Carotid artery, recanalization 7
- siphon, use of TCD 66
Cauda equina disorders 98
Caudal sac pathologies 224
Cavernomas, angiographic confirmation 187
-, CT examination 187, 188, 190
-, histological examination 189
-, MRI examtination 183, 187, 188, 190
-, neuropathology 190
Cavernous angioma, angiographic findings 188, 190
--, intracerebral, MRI findings 191
--,-, neuropathological investigations 190
--,-, neuroradiological investigations 190
Cavitron 13
- ultrasonic aspirator, *see* CUSA
CCT, *see* Central conduction time *and* Somatosensory central conduction time

Cell infiltration 261
- membrane 241
Central conduction time, *see also* Somatosensory central conduction time
--- in aneurysm surgery 87
Cerebral abscess 291
- endoscopy 5
- microcirculation, regulation of 243
- RARE hydrography 176
Cerebrovascular insufficiency 62
- malformations (CVMs) 183
--, angiographic findings 184
--, CT findings 184
--, MRI findings 184
--, surgery, cerebral angiography 185
--, value of MRI 183
- occlusive lesions 62
Cervical meningioma, RARE scans 177
- radiculopathy 94
--, electrophysiologic localization 94
- syrinx, MRT 212
Chordotomy 126
Circulatory abnormalities, TCD study 65
CO_2 laser 11, 13, 14, 23
--, pituitary adenoma 16
Coagulated collagen 33
Coagulation properties 3
Coma grade 108
- grading, CCT 100
--, ICP 100
Comatose patient 105, 111
Combined therapy 259
Communicating syringomyelia 207
Computer tomography (CT) in children 156
--, coronal, microadenoma 170
--, delineation of tumors 158
--, demonstration of tumors 156
--, detection of tumors 147, 158
--, diagnostic value for lesions of sella turcica 162
--, findings, acromegaly 168
--,-, cerebral vascular malformations 184
--,-, empty sella 168
--,-, spinal space-occupying lesions 196
--, low-grade gliomas 148
--, meningiomas 164
--, pituitary adenomas 162
--,- lesions, findings 168
--,- tumors 166, 172
Conduction in nerve fibers 98
Continuous infusion pump 137
Contrast enhancement 147
Coronal CT, microadenomas 170

Cortical evoked potentials 91
--- of trigeminal nerve 91
Craniocerebral trauma 292
Craniopharyngiomas, cystic, endoscopic aspect 55
-, MRI 164
Craniospinal junction, MRI parameters 207
CSF fistulas, frontal 278
--, otogenous 278
CT, *see* Computer tomography
- myelography 177
CUSA (Cavitron ultrasonic aspirator) 13, 15, 39, 40, 44, 45
-, astrocytomas 44
-, brain tumors 48
-, efficiency 45
-, glial tumors 13
-, glioblastomas 44
-, handpiece 42
-, meningiomas 44
-, metastases 44
-, neurinomas 44
- in neurosurgery 13, 14
-, pituitary adenoma 16
- for tumor operations 14
-, vibration waves 41
CVM, *see* Cerebrovascular malformations
Cytostatics 241

Degenerative spondylopathies 289
Delayed aneurysm surgery 71
- ischemic deficits 70
Deoxythymidine kinase (dTK) activity 251
Dermatomal patterns 97
- stimulation 94
DIDID, *see* Doppler index of delayed ischemic deficits
Differentiation of tumor tissue from edema 149
Disk degeneration 222
- herniations 222
- recurrence 223, 225
- surgery 286
Diskitis 225
Disseminated metastases 133
Doppler, extracranial stenosis 63
- findings 59, 69
--, vasospasm 68
- index of delayed ischemic deficits (DIDID) 70
- sonography, intraoperative 73
--, transcranial, *see* Transcranial Doppler sonography
- system 57, 61, 62
-- for aneurysm surgery 57, 61
--, miniaturized probes 61
--, transcranial pulsed 62
Drained hydrocephalus 237
Dura defect 278

EC/IC bypass surgery 63
---, flow values 63
Edema extension 247
Edema-tumor relation 230
Electrophysiologic localization 94
-- in cervical radioculopathy 94
Electroretinography (ERG) 263
-, a-wave 265
Electrostimulation 123
Embolization 116, 117
Empty sella syndrome, MRI 164, 165
Endogenous components, P3 105
--, P300 105
Endoneural fiber density 33
- regeneration 33
Endoscope with Nd: YAG laser 52
Endoscopic biopsy of brain tumors 53
Endoscopy, craniopharyngiomas, cystic 55
-, intracerebral hemorrhages 55
-, ventricular tumors 55
Ependymomas, out of brain stem 153
-, MRT 202
Epidural stimulation 126
ERG, *see* Electroretinography
Evoked potentials (EPs) 105, 109
--, acoustic evoked brain stem potentials 83, 102, 108
--, auditory 110, 111
--,-, brain stem 83, 102, 108
--, cortical 91
--,-, of trigeminal nerve 91
--, disappearance of wave 87
--, false-negative cases 88
--, grades 110
-, impairment 87
--, influence on surgical planning 87
--, intraoperative monitoring 83
--, 40-Hz middle latency auditory 108
--, late components, prognostic value 106
--, perioperative functional loss 85
-- and prognosis 102, 103
--, sensory 94, 87
--, somatosensory 83
--, visual 83
Evoked responses 110
Excitatory amino acids 135
Expansion of peritumoral brain edema 246
Experimental nerve anastomosis 31

Extracranial Doppler sonography 63
- stenosis, Doppler 63
Extradural tumors, MRT 204, 217

Facet denervation 127
--, long-term results 128
Fibrin adhesives 270
Fibrinolytic therapy 114
Fibrosis of nerve anastomosis 270, 271
Fistulas, carotid artery-cavernous sinus 118, 119
Fixateur externe 287
- interne 287
--, implantation 288
Flow pattern of an aneurysm 59
- values after EC/IC bypass surgery 63
- velocities 63
-- in aneurysm 60
-- of blood 68
Fractures of the base of the skull 278
Frequency changes after early aneurysm surgery 68
-- after SAH 68

Gadolinium-DTPA 143, 148, 150, 213
Giant aneurysm 60, 117
--, balloon 118
-- of MCA, MRI examination 183
Glasgow Coma Score 101
- Outcome Scale 100, 102, 106
Glial tumors, surgery by CUSA 13
Glioblastoma 149
-, life expectancy of patients 258
-, CT, edema/brain tissue 149
-,-, tumor/edema 149
-, MRI, edema/brain tissue 149
-,-, tumor/edema 149
-, recurrent 255
-, removal by CUSA 44, 45
Glioma 233
- cells, growth 259
Growth rate of meningiomas 281
- in recurrent mengingiomas 284

Halo effect 5
Handpiece 42
Hangman's fracture 76
Head injury 291
--, treatment 100
High-flow compartment 117
Highly vascular meningiomas, treatment with Nd:YAG laser 12
Hormone-producing tumors 166
Human cognitive information processing 105
----, P3 105
Hydrocephalus 234, 236
-, drained 237
Hyperhidrosis 8

ICP monitoring 100
Idiopathic trigeminal neuralgia 90
IFN therapy, *see* Interferon therapy
Immunological mechanisms of interferon 255
Index finger stimulation 95
- of primary brain damage 102
Infratentorial neoplasms, RARE scan 176
Interferon (IFN), antitumoral effects 261
- drugs 257
-, effect on malignant glious brain tumors 258
-, immunological mechanisms 255
-, immunostimulating effects 261
-, stimulating effects 260
- therapy 252, 258, 260
--, intralesional 252, 255
--, intravenous 252
Interventional neuroradiology 114
Intracellular pH in brain tumors 242
Intracerebral cavernous angiomas, MRI findings 191
---, neuropathological investigations 190
---, neuroradiological investigations 190
---, neuroradiology 190
- hemorrhages, spontaneous, endoscopic evacuation 55
- tumor 232
Intracranial cavernous angiomas, neuropathological findings 187
Intracranial circulatory arrest 66
- meningiomas 281
--, prognosis for patients 284
- tumors 46
--, localization 46
--, postoperative clinical course 46
Intradural tumor, MRT 218
Intradural-extramedullary tumor, MRT 203
Intramedullary tumors 206
--, gadolinium-DTPA 213
Intraoperative application of lasers 13

- derivation of the action potential 91, 92
- Doppler sonography 73
---, cervical spine 73
---,--, indications for 73
---,--,- luxation and compression fractures 73
---,--,- osteosynthesis 73
---,--,- tumor resection 73
---,--,- vascular surgery 73
---, compression fractures 77
---, metastases 78
---, tumors 74, 77
---, vertebral artery 76, 77, 79
- monitoring of evoked potentials 83
- single unit potential recording 98
- ultrasound examination, position of artery 73
Intraspinal space-occupying lesions, MRT 201
Intrathecal administration of baclofen 135, 136, 137
Intraventricular opiate application 130, 133
Ischemic deficits, delayed 70
--, neurological 70
- edema 243
Isolated interferon therapy 261
Isotope diagnosis 275

Lactate level 236
LANA, *see* Laser-assisted nerve anastomoses
Laser focal diameter 11
- nerve anastomosis 21
- neurosurgery 7, 14
- operations 4
--, astrocytomas 4
--, glioblastomas 4
--, meningiomas 4
--, metastases 4
-- with Nd:YAG 10
--, tumors 14
- penetration into brain 11
- wavelength 11
Laser-assisted anastomoses 34
- aneurysm shrinkage 11
- microanastomoses 28, 29
- nerve anastomoses (LANA) 28, 29, 34
- vascular anastomoses (LAVA) 11, 20, 28, 29
Lasers 3, 29
-, argon 3, 7
-, CO_2, *see* CO_2 laser
-, intraoperative application 13
-, Nd:YAG, *see* Nd:YAG laser
- in neurosurgery 13, 14
- for tumor operations 14
Late EP components, prognostic value 106
LAVA, *see* Laser-assisted vascular anastomoses
Lesions of sella turcica 162
Life expectancy of glioblastoma patients 258
Localization of spinal tumors 177
Lumbosacral junction 224
- lesions 216
--, malformations 216
--, MRT 216
--, noninvasive diagnosis 216
--, tumors 216
- malformations 216

Macroadenomas, MRI 163
Magnetic resonance in diagnosis 145
-- imaging 147, 170, 220, 222
---, anatomy of sellar region 165
---, brain tumors 147, 152
--- of cerebrovascular malformations 183
---, cervical syrinx 212
--- in children 156, 159, 160
---, craniopharyngiomas 164
---, delineation of tumors 158
---, demonstration of tumors 156
---, detection of tumors 158
---, diagnostic value for lesions of sella turcica 162
---, differentiation of tumor tissue from edema 149
---, empty sella syndrome 164, 165
---, ependymoma 202
---, extradural tumors 204, 217
---, findings, cerebro-vascular malformations 184
---,-, intracerebral cavernous angiomas 191
---,-, macroadenomas 168
---,-, microadenomas 168
---,-, spinal space-occupying lesions 196
---,-, with and without syringosubarachnoid shunt 209
---, glioblastoma 149
---, identification of AVMs 185
---, intradural tumors 218
---, intradural-extramedullary tumors 203
---, intraspinal space-occupying lesions 201
---, low-grade gliomas 148

Magnetic resonance imaging, lumbosacral lesions 216
---, macroadenomas 163
---, microadenomas, focal pathological signal alterations 171
---, meningiomas 150, 164
--- of metastases 150
---, pituitary adenomas 162
---,- lesions, findings 168
---,- tumors 166, 172
---, solid spinal cord tumors 211
---, spinal lumbosacral lesions 219
---, spontaneous transverse lesions 204
---, superiority 159
---, syringomyelia 206
---, tubercular spondylodiscitis 219
-- tomography, *see* Magnetic resonance imaging
Magnetostrictive transducer 39
Malformations, cerebrovascular 183
- of frontal skull base 279
-, lumbosacral 216
Malignant gliomas, monotherapy 254
--, prognosis 250
- meningiomas 282
- parotid tumors, treatment with CO_2 laser 17
---,- with CUSA 17
- supratentorial gliomas 250
Medulloblastoma 48
Meningiomas 49, 233, 292
-, angioblastic 282
-, benign 284
-, CT 164
-,-, edema/brain tissue 149, 150
-, tumor/edema 149
-, growth rate 281
-, highly vascular, treatment with Nd:YAG laser 12
-, intracranial 281, 284
-,- prognosis for patients 284
-, malignant 282
- of the middle cranial fossa 276
-, MRI 164
-,-, edema/brain tissue 149, 150
-,-, tumor/edema 149
-, recurrent 281
-,-, growth 284
-, removal by CUSA 44, 45
-,- by Nd:YAG laser 18
-, suprasellar 284
Meningitis 279
Metastases 233, 260
-, CT 150
-, CUSA 44, 45
-, Doppler sonography 78
-, MRI 150
Microadenomas, coronal CT 170
-, direct CT signs 163
-, indirect CT signs 163
-, MRT , focal pathological signal alterations 171
- of pituitary 162
Microanastomoses 29
-, laser-assisted 28, 29
Microdehiscence 271
Microprobes for intraoperative use 58
Microsurgical tissue welding 20
Microvascular decompression 90
- Doppler system 57, 58
--- for aneurysm surgery 57
Middle finger stimulation 95
Monotherapy for malignant gliomas 254
Morphine 131
-, intraventricular administration 130, 133
Mortality for operations in occipital area 277
MR, *see* Magnetic resonance
- contrast agent 143
---, gadolinium-DTPA 143, 148, 150
- examinations, head 144
--, spinal region 144, 145
- myelography 177
MRI, *see* Magnetic resonance imaging
- examination of AVMs 183
-- of cavernoma 183
-- of giant aneurysm of MCA 183
- parameters of craniospinal junction 207
- stereotaxy 179
-- for intracerebral lesions 179
MRI-compatible stereotactic ring 181
MRI/CT-stereotactic surgery 180
MRT, *see* Magnetic resonance tomography 166
Multipeak potential 92
Myelography 224

Nd:YAG fiberoptic tube 52
- laser 3, 5, 7, 12, 13, 14, 24
--, 1.32 µm 31, 34
--, action 24
--, brain necroses 11
-- endoscope 52
--, meningiomas 18
--,-, highly vascular 12

-- operations 10
--, tissue welding 12
-- transection 23, 25
Neoplastic cells, release of prostaglandins 246
Nerve adhesion 269
- anastomoses 29, 269
--, adhesive for 271
--, experimental 31
--, fibrosis 270, 271
--, laser-assisted 11, 21, 28, 29
--, sciatic 33
- bonding 21
- fibers, conduction in 98
- regeneration 23
- root filaments, efferent 98
-- function 98
-- potentials 95, 96
- surgery 269
Neurinomas, removal by CUSA 44, 45
Neuroendoscope 52
Neuroendoscopy 52
Neurological ischemic deficits 70
Neuroma formation 24
-- after scalpel division 25
Neuromatous neurotization 33, 34
Neuromonitoring 83, 88
Neurophysiological investigations 100
Neurosurgery Cavitron 13, 14
-, lasers 13, 14
Nimodipine 67, 69
Nonconvulsive epileptic state 293
Nuclear magnetic resonance (NMR) imaging 143
Nucleus pulposus, vaporization 8

Occlusive vascular disease, examination by TCD 63
Oligodendrogliomas, removal by CUSA 45
Opiate administration, technique 131
- receptors 130
OPMILAS YAG 10, 12
--, optic nerve tumors 12
-- micromanipulator 11
Optic nerve tumors 12

P3 method 106
Paraneoplastic pain 133
-- syndrome 130, 131, 133
Parotid tumor, malignant, treatment with CO_2 laser 17
--,-,- with CUSA 17
Percutaneous technique 127
- transluminal angioplasty 114
Perifocal edema 229
--, evolution of 243
Peripheral nerves, regeneration 23
Peritumoral brain edema 244
---, expansion 246
---, pathogenesis 247
- edema 229, 232
Piezoelectric crystal 39
Pituitary adenoma, CT 162
--, MRI 162
--, treatment with CO_2 laser 16
--,- with CUSA 16
- lesions, CT findings 168
--, MRT findings 168
- microadenomas 162
- tumors, CT 166, 172
--, MRT 166, 172
Poles of the tumor, MRI 199
Post-rior fossa, tumors 156
Postherpetic neuralgia 123
Postoperative radiation 260
- scar formation 225
Preoperative examinations 174
- identification of kind of tumor 198
- localization of tumor 198
- size of tumor 277
- tumor volume 281
Prevertebral stimulation 126
Primary brain damage, index of 102
Procaine, reduction of single unit potential activity 99
Prognosis of malignant gliomas 250
Prostaglandin levels 244
-- in neoplastic and edematous tissue 247
Prostaglandins, release by neoplastic cells 246
Psychomotor epilepsy 291
Pump, continuous infusion 137
- reservoir 131
- system 130

Radiological diagnosis 277
-- of tentorial meningioma 276
Rapid acquisition with relaxation enhancement (RARE) 174
RARE, *see* Rapid acquisition with relaxation enahncement
- hydrography 174
--, cerebral 176
- scan, cervical meningioma 177
--, infratentorial neoplasms 176
Rat sciatic nerve 23

Recanalization of carotid artery 7
Recurrence 277
Recurrent glioblastomas 255
- meningiomas 281
--, growth 284
- tumors 254
Regenerating units 23
Regeneration, endoneurial 33
- of peripheral nerves 23
Regenerative activity 23
Regulation of cerebral microcirculation 243
Respiratory depression, central 133
Retinal effects, of BCNU 263

SAH, *see* Subarachnoid hemorrhage
Scalpel transection 24
Scar formation 222, 225
Sciatic nerve, rat 23
-- anastomosis 33
Secondary syringomyelia 211
Selective angiogram 115
- angiography of spinal angioma 116
Sella, adenomas in 166
Sensory distribution for C7 96
- evoked potentials (SEPs) 94, 97
SEPs, *see* Somatosensory evoked potentials *and* Sensory evoked potentials
Sequential DSA 215
-- showing vascular tumor 213
- finger stimulation 95, 96, 97
Single unit potential activity 99
----, reduction by procaine 99
-- potentials, afferent 98
---, recording during spinal operation 99
Skull base, tumors 156
Solid spinal cord tumors, MRT 211
Somatosensory central conduction time (CCT), *see also* Central conduction time 100, 101
- evoked potentials (SEPs) 83, 85, 90, 102
---, median nerve 101
--- of trigeminal nerve 90
Sonotec 39, 40
-, handpiece 42
-, vibration waves 41
Space-occupying lesions of the spinal canal, CT 199
----, MRI 199
Spasticity 135
-, spinal 137
-, supraspinal 137
-, treatment of 135
Spinal analgesia 130
- angiomas 116
- lumbosacral lesions, MRT 219
- space-occupying lesions 196
---, CT findings 196
---, MRI findings 196
- spasticity 137
- stabilization 290
- trauma 286
Spondylitis 223
Spondylodesis 289
Spondylolisthesis 289
Spontaneous transverse lesions, MRT 204
Sporting activity, hydrocephalus 234
Sprouting activity, axonal 24
Stellate ganglion 5
Stereotaxic biopsy 55
Stimulation, dermatomal 94
-, epidural 126
-, index finger 95
-, middle finger 95
-, prevertebral 126
- rate 108, 109
-, sequential finger 95, 96, 97
- of sympathetic trunk 123
-, thumb 95
Subarachnoid cysts, cerebral RARE hydrography 176
- hemorrhage (SAH) 67
--, end of third week after 71
-- frequency changes 68
Subclavian steal syndrome 115
Superselective angiography 114, 116
Suprasellar meningiomas 284
Supraspinal spasticity 137
Surface coils 204
Surgical ultrasonic aspiration 44
---, acoustic neurinoma 49
--- of brain tumors 44, 45, 49
-----, application mode 50
-----,- time 50
-----, efficiency 47
---, meningioma 49
Sympathetic trunk 123, 125
--, stimulation 123
Sympathectomy 5, 8, 123
-, transthoracic 8
Syringomyelia (SM) 201, 202, 214
-, MRI 206
-, pathogenesis 206
-, secondary 211, 214
Syringosubarachnoid shunt 212
--, MRI findings 209

TCD, *see* Transcranial Doppler sonography
Tentorial meningioma, radiological diagnosis 276
Thumb stimulation 95
Time course, of vasospasm 69, 71
Tissue welding 20
--, microsurgical 20
--,-, by CO_2 laser 20
-- by Nd:YAG laser 12
Transarticular dorsal C 1/2 screw fixation 73
Transcranial Doppler sonography (TCD) 62, 66, 67, 71
---, brain death 66
---, carotid siphon 66
---, circulatory abnormalities 65
---, occlusive vascular disease 63
---, vascular malformations 65
---, vertebral artery occlusion 64
- pulsed Doppler device 62
Transitional syndrome 291
Transmembrane potential 241
Transpedicular C2 screw fixation 74
---, osteosynthesis 76
Transpeduncular reinforcement 290
Transthoracic sympathectomies 8
Traumatic defects of frontal skull base 279
Treatment of head injury 100
- of tumors 257
Trigeminal nerve, action potential 90
--, cortical evoked potentials 91
--, damage 93
--, SEPs 90
- neuralgia 91
Tubercular spondylodiscitis, MRT 219
Tumor cells 246
- delineation, CT 158
--, MRI 158
- detection, CT 158
--, MRI 158
- doubling time 282
- operations by CUSA 14
-- by laser 14
- regrowth 253
- relapses 258
- research 242
- tissue, consistency 45
-, in vitro sensitivity 251, 253
--, vascularization 45
Tumors, hormone-producing
- of posterior fossa 156
- of skull base 156

Ultrasonic aspiration, *see* Surgical ultrasonic aspiration
- surgical aspirator 39
---, *see also* CUSA, Sonotec.
Ultrasound guidance 52
- imaging 52
Unclippable aneurysms 279
Unstable spine 286

Valve complications 237
Vaporization of the nucleus pulposus 8
Vascular anastomoses, laser-assisted 11, 20, 28, 29
- malformations, TCD 65
- tumors, sequential DSA 213
Vasospasm 67, 69
-, angiographically demonstrated 68
-, Doppler findings 68, 69
-, time course 69, 71
Ventricular tumors, endoscopic techniques 55
VEPS, *see* Visual evoked potentials
Vertebral artery, intraoperative Doppler sonography 76, 79
-- occlusion, TCD 64
- body fractures 286
-- metastases 287
- instability 290
- metastases 203
Vibration energy 42
- waves of CUSA 41
-- of Sonotec 41
Visual evoked potentials (VEPs) 83

WADA test 117

Zoster neuralgia 123, 125

M. Samii, Hannover; **W. Draf,** Fulda

Surgery of the Skull Base

1989. Approx. 250 illustrations. Approx. 500 pages.
ISBN 3-540-18448-1. In preparation

Contents: Surgery of the Anterior Skull Base: Surgery of Malformations of the Anterior Skull Base. - Surgery for Trauma to the Anterior Skull Base. - Surgery for Inflammatory Complications in the Region of the Anterior Skull Base. - Surgery of Space-Occupying Lesions of the Anterior Skull Base. - Surgery of Tumors of the Orbit and Adjacent Skull Base. - Special Operative Techniques. - Surgery of the Middle Skull Base: Surgery of Traumatic Lesions of the Middle Skull Base. - Surgery of Inflammatory Disorders of the Middle Skull Base. - Surgery of Space-Occupying Lesions of the Middle Skull Base. - Surgery of the Posterior Skull Base: Surgery of the Internal Auditory Canal and Cerebellopontine Angle. - Surgery of Tumors of the Lateral Posterior Skull Base and Petrous Bone. - On the Problem of Paralytic Dysphagia Caused by Posterior Skull Base Tumors. - Surgery of the Clivus: Introductory Remarks. - General Operative Techniques. - Surgery of the Craniocervical Junction: Introductory Remarks. - Operative Technique. - Surgery of the Facial Nerve and Skull Base: Introductory Remarks. - General Operative Techniques. - Special Operative Techniques.

This is the first text to consider the skull base as a whole and from an interdisciplinary point of view. It analyzes the wide spectrum of pathological entities which can affect this crossroad region, including anomalies, traumatology, tumors and infectious processes.
The book considers general as well as specific surgical aspects and offers a wealth of excellent drawings and pictures to complement the text.
The reader will find himself equipped with a complete textbook on skull base surgery that emphasizes clinical applications and reflects valuable relevant experience from the fields of both ENT and neurosurgery.

Springer-Verlag
Berlin Heidelberg New York
London Paris Tokyo

K. Sugita, Shinshu University

Microneurosurgical Atlas

With the Assistance of S. Kobayashi

1985. 456 figures (including 202 colored illustrations by the author). XI, 274 pages. ISBN 3-540-15110-9

Y. Keravel, Paris-Créteil; **M. Sindou,** Lyon, France

Giant Intracranial Aneurysms

Therapeutic Approaches

With contributions by numerous experts

With a Foreword by M. G. Yasargil

1988. 123 figures. 163 pages. ISBN 3-540-18131-8

Original French edition by Masson, Paris 1984

F. Pluchino, G. Broggi, Milano, Italy (Eds.)

Advanced Technology in Neurosurgery

With the assistance of C. L. Solero, M. Fornari

1988. 152 figures. XII, 240 pages. ISBN 3-540-17918-6

K. Tabuchi, Saga, Japan; **A. Nishimoto,** Okayama University, Okayama, Japan

Atlas of Brain Tumors

Light- and Electron-Microscopic Features

1988. 258 figures. XVI, 247 pages. ISBN 3-540-70024-2

J. Schramm, Erlangen; **S. J. Jones,** London (Eds.)

Spinal Cord Monitoring

1985. 139 figures, 63 tables. XII, 329 pages. ISBN 3-540-15774-3

R. P. Sengupta, V. L. McAllister, Newcastle-upon-Tyne

Subarachnoid Haemorrhage

Foreword by Professor Sir John Walton

1986. 243 figures, 130 tables. 378 pages. ISBN 3-540-15534-1

Springer-Verlag
Berlin Heidelberg New York
London Paris Tokyo